

University of Warwick institutional repository: <http://go.warwick.ac.uk/wrap>

**A Thesis Submitted for the Degree of PhD at the University of Warwick**

<http://go.warwick.ac.uk/wrap/56272>

This thesis is made available online and is protected by original copyright.

Please scroll down to view the document itself.

Please refer to the repository record for this item for information to help you to cite it. Our policy information is available from the repository home page.

## Library Declaration and Deposit Agreement

### 1. STUDENT DETAILS

*Please complete the following:*

Full name: .....

University ID number: .....

### 2. THESIS DEPOSIT

2.1 I understand that under my registration at the University, I am required to deposit my thesis with the University in BOTH hard copy and in digital format. The digital version should normally be saved as a single pdf file.

2.2 The hard copy will be housed in the University Library. The digital version will be deposited in the University's Institutional Repository (WRAP). Unless otherwise indicated (see 2.3 below) this will be made openly accessible on the Internet and will be supplied to the British Library to be made available online via its Electronic Theses Online Service (EThOS) service.

[At present, theses submitted for a Master's degree by Research (MA, MSc, LL.M, MS or MMedSci) are not being deposited in WRAP and not being made available via EThOS. This may change in future.]

2.3 In exceptional circumstances, the Chair of the Board of Graduate Studies may grant permission for an embargo to be placed on public access to the hard copy thesis for a limited period. It is also possible to apply separately for an embargo on the digital version. (Further information is available in the *Guide to Examinations for Higher Degrees by Research*.)

2.4 If you are depositing a thesis for a Master's degree by Research, please complete section (a) below. For all other research degrees, please complete both sections (a) and (b) below:

#### (a) Hard Copy

I hereby deposit a hard copy of my thesis in the University Library to be made publicly available to readers (please delete as appropriate) EITHER immediately OR after an embargo period of ..... months/years as agreed by the Chair of the Board of Graduate Studies.

I agree that my thesis may be photocopied. YES / NO (Please delete as appropriate)

#### (b) Digital Copy

I hereby deposit a digital copy of my thesis to be held in WRAP and made available via EThOS.

Please choose one of the following options:

EITHER My thesis can be made publicly available online. YES / NO (Please delete as appropriate)

OR My thesis can be made publicly available only after.....[date] (Please give date)  
YES / NO (Please delete as appropriate)

OR My full thesis cannot be made publicly available online but I am submitting a separately identified additional, abridged version that can be made available online.  
YES / NO (Please delete as appropriate)

OR My thesis cannot be made publicly available online. YES / NO (Please delete as appropriate)

---

3. GRANTING OF NON-EXCLUSIVE RIGHTS

Whether I deposit my Work personally or through an assistant or other agent, I agree to the following:

Rights granted to the University of Warwick and the British Library and the user of the thesis through this agreement are non-exclusive. I retain all rights in the thesis in its present version or future versions. I agree that the institutional repository administrators and the British Library or their agents may, without changing content, digitise and migrate the thesis to any medium or format for the purpose of future preservation and accessibility.

4. DECLARATIONS

(a) I DECLARE THAT:

- I am the author and owner of the copyright in the thesis and/or I have the authority of the authors and owners of the copyright in the thesis to make this agreement. Reproduction of any part of this thesis for teaching or in academic or other forms of publication is subject to the normal limitations on the use of copyrighted materials and to the proper and full acknowledgement of its source.
- The digital version of the thesis I am supplying is the same version as the final, hard-bound copy submitted in completion of my degree, once any minor corrections have been completed.
- I have exercised reasonable care to ensure that the thesis is original, and does not to the best of my knowledge break any UK law or other Intellectual Property Right, or contain any confidential material.
- I understand that, through the medium of the Internet, files will be available to automated agents, and may be searched and copied by, for example, text mining and plagiarism detection software.

(b) IF I HAVE AGREED (in Section 2 above) TO MAKE MY THESIS PUBLICLY AVAILABLE DIGITALLY, I ALSO DECLARE THAT:

- I grant the University of Warwick and the British Library a licence to make available on the Internet the thesis in digitised format through the Institutional Repository and through the British Library via the EThOS service.
- If my thesis does include any substantial subsidiary material owned by third-party copyright holders, I have sought and obtained permission to include it in any version of my thesis available in digital format and that this permission encompasses the rights that I have granted to the University of Warwick and to the British Library.

5. LEGAL INFRINGEMENTS

I understand that neither the University of Warwick nor the British Library have any obligation to take legal action on behalf of myself, or other rights holders, in the event of infringement of intellectual property rights, breach of contract or of any other right, in the thesis.

---

*Please sign this agreement and return it to the Graduate School Office when you submit your thesis.*

Student's signature: ..... Date: .....

# **Amino-Containing Polymers for Catalysis Using RAFT Polymerization**

---

*Submitted for the degree of Doctor of Philosophy*

September 2012

**Maria José Cotanda Santapau, MSc.**

Department of Chemistry

THE UNIVERSITY OF  
**WARWICK**



To my niece Pepa Cotanda II,

who was born the day I submitted this thesis.

# Table of Contents

Table of Contents .....	I
Declaration of authorship .....	I
Acknowledgements:.....	II
List of Publications .....	III
Abbreviations .....	IV
Summary .....	VIII
<b>Chapter 1: Introduction .....</b>	<b>1</b>
1.1 Polymerization techniques.....	2
1.1.1 Living polymerization.....	2
1.1.2 Controlled radical polymerization .....	3
1.2 Self-Assembly of amphiphilic block copolymers .....	16
1.3 Stimuli responsive polymers .....	20
1.3.1 Temperature responsive polymers.....	20
1.3.2 pH responsive.....	23
1.4 Catalytic polymeric particles .....	26
1.4.1 Hydrophobic pockets for organic synthesis in aqueous media.....	28
1.4.2 Site isolation .....	34
1.5 Conclusions .....	40
1.6 References .....	41
<b>Chapter 2: Synthesis of DMAP-Functionalized Organocatalytic Nanoreactors.....</b>	<b>51</b>

2.1	Abstract:.....	52
2.2	Introduction.....	52
2.3	Results and discussion.....	56
2.3.1	Monomer synthesis.....	56
2.3.2	Copolymerization with styrene.....	58
2.3.3	Formation of amphiphilic block copolymer.....	74
2.3.4	Micelle formation .....	89
2.4	Conclusions .....	91
2.5	Experimental Section.....	93
2.5.1	Materials: .....	93
2.5.2	Instrumentation:.....	93
2.5.3	Monomer synthesis.....	94
2.5.4	Synthesis of the CTA <b>2.3</b> <sup>57</sup> .....	95
2.5.5	Polymer synthesis.....	96
2.5.6	Formation of micelles <b>2.12</b> .....	100
2.6	References .....	102
<b>Chapter 3: Molecular recognition driven catalysis using polymeric nanoreactors...</b>		<b>108</b>
3.1	Abstract:.....	109
3.2	Introduction.....	109
3.3	Results and discussion.....	115
3.3.1	Acylation Reactions: .....	115
3.3.2	Effect of substituents on the equilibrium position: .....	117
3.3.3	Comparison with organic solvents and bulk: .....	119
3.3.4	Catalyst loading: .....	122
3.3.5	Recycling experiments:.....	124

3.3.6	Molecular recognition: .....	125
3.4	Conclusions .....	130
3.5	Experimental Section.....	131
3.5.1	Materials: .....	131
3.5.2	Instrumentation:.....	131
3.5.3	Polymers synthesis .....	133
3.5.4	Formation of micelles 3.2.....	135
3.5.5	Formation of DMAP containing micelles <b>3.4</b> .....	136
3.5.6	General protocol for the acylation reaction of 1 alcohol with 1 anhydride: .....	137
3.5.7	Recycling experiments.....	142
3.5.8	General protocol for the selective acylation reaction of 1-phenylpropanol .....	142
3.5.9	One pot selective acylation of different alcohols with butyric anhydride:.....	143
3.6	References .....	146

## **Chapter 4: Design of amino polymers via RAFT polymerization for the synthesis of polyurethane foams ..... 149**

4.1	Abstract .....	150
4.2	Introduction.....	150
4.3	Results .....	156
4.3.1	Synthesis of multidentate amino monomers.....	156
4.3.2	Direct homopolymerization by RAFT .....	162
1.1.1	Copolymerization.....	172
1.1.2	Polyurethane foam tests .....	181
1.1.3	Particle formation (Future work).....	185
4.4	Conclusions .....	186
4.5	Experimental.....	188

4.5.1	Materials.....	188
4.5.2	Instrumentation:.....	188
4.5.3	Synthesis of S-1-dodecyl-S'-( $\alpha,\alpha'$ -dimethyl- $\alpha''$ -methyl acetate) trithiocarbonate ( <b>4.5</b> , DDMEAT).....	188
4.5.4	Monomer synthesis.....	189
4.5.5	Polymer Synthesis .....	192
4.6	References .....	196

## **Chapter 5: Stimuli-responsive properties of DMAEA containing polymers ..... 199**

5.1	Abstract .....	200
5.2	Introduction.....	200
5.3	Results and discussion.....	202
5.3.1	Homopolymerization of DMAEA.....	202
5.3.2	Copolymerizations.....	210
5.3.3	Copolymerization of DMAEA with MA.....	211
5.3.4	pH-responsive dilute solution behavior .....	217
5.3.5	Temperature responsive properties .....	221
5.3.6	Self-catalyzed hydrolysis in water <sup>25</sup> .....	226
5.4	Conclusions .....	232
5.5	Experimental.....	233
5.5.1	Materials.....	233
5.5.2	Instrumentation:.....	233
5.5.3	Hydrogen ion titration .....	233
5.5.4	General procedure for homopolymerization of DMAEA: .....	234
5.5.5	General procedure for copolymerization of MA with DMAEA .....	234
5.6	References .....	236
	Conclusions.....	240

## **Declaration of authorship**

This thesis is submitted in partial fulfillment of the requirements for the degree of Doctor of Philosophy. It describes work carried out from January 2009 to September 2012. Unless otherwise indicated, the research described is my own and not the product of a collaboration. No part of this thesis has been submitted to any other university, or as any part of any other submission to the University of Warwick.

Signed,

Date:

## **Acknowledgements:**

First, I would like to thank Rachel O'Reilly for giving me the opportunity to work in her group and for her support throughout my PhD with her patience and knowledge whilst giving me the freedom to work in my own way.

I must thank the Department of Chemistry for providing the support and equipment I have needed to produce and complete my thesis and AWE for funding my studies.

I am also very thankful to all the O'Reilly group members, without their help and criticism it would have been impossible to write this thesis. Especially I must thank Nikos for all the support, advice and useful and productive discussions. I am also particularly grateful to Jared and Helen for patiently teaching me everything during my first year.

And of course a very big thank you goes to all the nice people I met during my PhD, those who were there when I just needed to have a laugh and a drink. It would have been impossible to carry out this research without those breaks.

Finally and most importantly of all I must thank my parents and my talented brothers for standing my schizophrenic behavior all these years. Thank you for reminding me that my life was not just my PhD.

## List of Publications

- Pepa Cotanda, Rachel K O'Reilly: 'Design of DMAP Containing Polymers Via RAFT Polymerization' ACS polymers preprint, 2011. (**Chapter 2**)
- Pepa Cotanda, Annehelen Lu, Joseph Patterson, Nikos Petzetakis, Rachel K. O'Reilly. "Functionalized organocatalytic nanoreactors: hydrophobic pockets for acylation reactions in water". *Macromolecules*, 2012, 5, 2377–2384. (**Chapter 3**)
- Annhelen Lu, Pepa Cotanda, Joseph P. Patterson, Deborah A. Longbottom and Rachel K. O'Reilly "Aldol Reactions Catalyzed by L-Proline Functionalized Polymeric Nanoreactors in Water". *Chem. Commun.*, 2012, DOI: 10.1039/C2CC35170F.
- Pepa Cotanda, Rachel K. O'Reilly. "Molecular recognition driven catalysis using polymeric nanoreactors". *Chem. Commun.* 2012, DOI: 10.1039/C2CC35655D. (**Chapter 3**)
- Pepa Cotanda, Nikos Petzetakis, Rachel O'Reilly. "Catalytic polymeric nanoreactors: more than a solid supported catalyst". 2012, *MRS Communications*, accepted for publication. (**Chapter 1**)
- Nikos Petzetakis, Mathew Robin, Joseph Patterson, Elizabeth G. Kelley, Pepa Cotanda, Paul H. H. Bomans, Nico A. J. M. Sommerdijk, Andrew P. Dove Thomas H. Epps, III, and Rachel K. O'Reilly "Hollow block copolymer nanoparticles through spontaneous one step structural reorganization". 2012, Manuscript Submitted.
- Pepa Cotanda, Rachel O'Reilly, Karen Pocket, Colin Warriner "One pot formulation for polyurethane foams formation" Patent in preparation. (**Chapter 4**)



## Abbreviations

$\delta$	chemical shift
aq	aqueous
AIBN	2,2'-azo-bis(isobutyronitrile)
ATRP	Atom Transfer Radical Polymerisation
Bn	benzyl
br	broad
CRP	Controlled Radical Polymerisation
CTA	Chain Transfer Agent
d	doublet
Da	Daltons ( $\text{g mol}^{-1}$ )
DCM	dichloromethane
CMT	critical micellar temperature
DDMAT	S-1-dodecyl-S'-( $\alpha,\alpha'$ -dimethyl- $\alpha''$ -acetic acid)trithiocarbonate

DDMEAT	S-1-dodecyl-S'-( $\alpha,\alpha'$ -dimethyl- $\alpha''$ -ethyl acetate)trithiocarbonate
DMAEA	diethylaminoethyl acrylate
DMAEMA	diethylaminoethyl methacrylate
DMAP	dimethylaminopyridine
DMF	dimethyl formamide
DMSO	dimethyl sulfoxide
DP	Degree of Polymerization
EDCI	N-Ethyl-N'-(3-dimethylaminopropyl)carbodiimide hydrochloride
eq	equivalents
GPC	Gel Permeation Chromatography
IR	Infra Red
$K_a$	acid dissociation constant
LCST	lower critical solution temperature
[M]	monomer concentration

m	multiplet
MA	methyl acrylate
MADIX	MAcromolecular Design by Interchange of Xanthates
MMA	methyl methacrylate
$M_n$	number average molecular weight
$M_w$	weight average molecular weight
MW	molecular weight
NEM	N-ethylmorpholine
NIPAM	N-isopropylacrylamide
NMP	Nitroxide Mediated Polymerisation
NMR	Nuclear Magnetic Resonance
$p$	packing parameter
PDI	Polydispersity Index
PMA	pentamethyl dipropylenetriamine
PS/PSt	polystyrene

PU/PUR	polyurethane
RAFT	Reversible Addition Fragmentation chain Transfer
RBF	round bottomed flask
RT	room temperature
s	singlet
SG1	<i>N</i> -(2-methylpropyl)- <i>N</i> -(1-diethylphosphono-2-dimethylpropyl)- <i>N</i> -oxyl
t	time
T <sub>g</sub>	glass transition temperature
TMPDA	Tetramethylpropylenediamine
TEMPO	(2,2,6,6-Tetramethylpiperidin-1-yl)oxyl
THF	tetrahydrofuran
TRIS	tris(hydroxymethyl)aminomethane
UV	ultraviolet
UCST	upper critical solution temperature
X	halide

## Summary

Chapter 1 is a general introduction of the whole thesis and it features the main concepts of this project.

Chapter 2 reports the synthesis and self- assembly of a temperature-responsive DMAP containing nanoreactor. The DMAP motif is incorporated in to a monomer and polymerized by RAFT with styrene in order to form the hydrophobic block of a polymeric micelle. The shell of the micelle is formed by chain extension of the styrenic block with NIPAM, which provides temperature responsive properties to the system.

In Chapter 3, the concept of using polymeric micelles to catalyze organic reactions in water is presented and compared to surfactant based micelles in the context of molecular recognition, achieving enzyme-like specific catalysis by tethering the catalyst in the well-defined hydrophobic core of a polymeric micelle

In Chapter 4, the incorporation of different catalytic amino motifs into a polymer backbone is investigated by RAFT polymerization in order to catalyze the reaction between polyalcohols and polyisocyanates in the formation of polyurethane foams.

In the final chapter, the stimuli-responsive properties of DMAEA containing polymers are investigated. DMAEA is copolymerized by RAFT with the non-responsive MA at different loadings in order to study how the distance between amine motifs affects the polymer LCST and  $pK_a$  values

## **Chapter 1:Introduction**

## 1.1 Polymerization techniques

### 1.1.1 *Living polymerization*

Up until the mid 90's, the only viable way to produce polymers with low-polydispersity (PDI) and well-defined molecular weight (MW) was to use living polymerization techniques, such as anionic or cationic procedures.<sup>1</sup>

Anionic polymerization was first reported in Nature by Szwarc<sup>2</sup> when he discussed the living polymerization of styrene in THF solution of sodium naphthalenide, in a system that was completely devoid of oxygen and water.<sup>3</sup> In this work they showed that if, after the polymerization had finished, more monomer or different monomer was added the process of polymerization continued, hence the term “living” was coined.

For a polymerization to be defined as living there are seven criteria that it must meet:<sup>4</sup>

- Reaction must go to 100% conversion and if more monomer is added the reaction must continue
- Molecular weight is directly proportional to the conversion of the monomer
- Each initiator makes one chain so number of active chains is constant
- Molecular weight can be controlled by stoichiometry
- Narrow polydispersity (PDI)
- Block copolymers can be made by sequential addition of a second monomer species
- Polymers can be chain end functionalized.

Living polymerization is a popular method for synthesizing block copolymers since the polymer scaffold can be made in steps, each stage containing a different monomer with the

additional advantages of predetermined molar mass and control over end-groups. However, the methodology is unsuitable for large scale industrial applications due to extremely stringent reaction conditions and high monomer purity, hence conventional radical chemistry is often employed in industry.

### 1.1.2 *Controlled radical polymerization*

Although radical techniques avoid the need for stringent reaction conditions they also lack the high degree of control that a living polymerization offers. Thus the development of new “living” controlled radical polymerization processes was necessary and has been an area of great research interest over the last decade.<sup>5,6</sup> There are various controlled radical polymerization (CRP) techniques of interest, which all allow for the polymerization of vinyl monomers to be carried out in a controlled manner to obtain polymers with predictable molecular weights (MWs) and relatively low polydispersity indexes (PDIs). In fact, polydispersities obtained for CRPs can approach the values typically obtained for living procedures (*ca.* 1.1)<sup>6</sup> and are often tolerant to trace impurities in the reaction media.

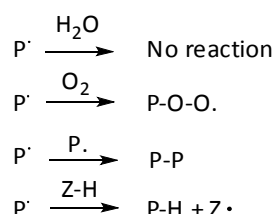
A typical CRP procedure consists of three steps:

1. Initiation to create a reactive radical vinyl monomer.
2. Propagation resulting in polymer chain growth by successive addition of monomer units to the chain end radical.
3. Termination between polymer chain ends, or the recombination of any remaining reactive radicals.

In an uncontrolled radical polymerization process the reaction rates of these steps are not controlled. Due to the highly reactive nature of radicals, the fastest step is termination, which



means that many chains terminate before complete conversion. Furthermore, the propagation step is faster than initiation, so that as the reaction progresses, some chains have grown significantly while others are still initiating. Finally, control is further hindered in free radical polymerizations by chain transfer events such as disproportionation, which can move growing radical sites between and within polymer chains (Scheme 1.1).



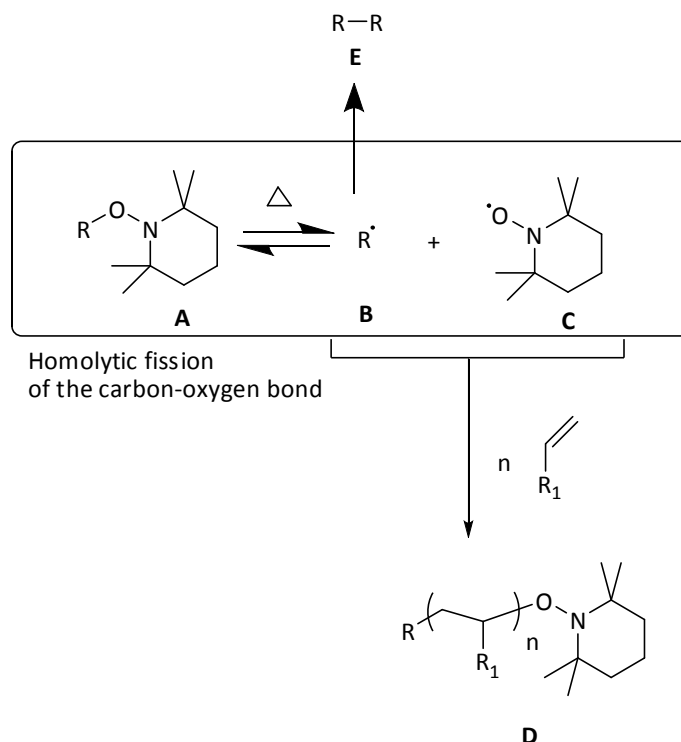
Scheme 1.1: Possible side reactions for radicals.

In order to gain control over a radical polymerization, firstly the reaction needs to be completely free from oxygen; however trace amounts of water are tolerable, unlike anionic/cationic polymerizations. The concentration of the propagating radical needs to be kept low since inter-chain termination is more likely with an increased concentration of propagating radical chain ends relative to initiator concentration. The final possible side reaction in a radical polymerization is the reaction of the propagating radical,  $\text{P}^\bullet$  with Z-H and subsequent chain transfer of the radical to a group, Z. This is a potential solution to the problem of chain termination since Z could be an inactive or dormant species. This method can therefore be used to inhibit the rate of polymerization reaction, decreasing the concentration of propagating radicals and preventing inter-chain termination events. Thus controls the MW and PDI and forms the principle on which CRP techniques operate.

CRPs are based on the establishment of a dynamic equilibrium in solution between active (propagating) and deactivated (dormant) species. The dynamic equilibrium can be achieved by two general mechanistic approaches: the first one involves the reversible deactivation of propagating chains that subsequently can be reactivated, either catalytically as in atom transfer radical polymerization (ATRP)<sup>7</sup> or spontaneously like in nitroxide mediated polymerization (NMP).<sup>8</sup> The second approach relies on the degenerative transfer between propagating chains and dormant species with a typical example of this kind being reversible addition-fragmentation chain transfer polymerization (RAFT).<sup>9-13</sup>

– *Nitroxide Mediated Polymerization (NMP)*

The first of the CRP mechanisms to be proposed was a polymerization that proceeds with reversible termination by end-coupling. Nitroxide Mediated Polymerization (NMP) was first reported by Georges in 1993.<sup>14</sup> The main features of a nitroxide-mediated radical polymerization (Scheme 1.2) are that the carbon-oxygen bond of a dormant, or inactive, alkoxyamine species (A) is homolytically unstable and undergoes thermal fragmentation at *ca.* 125 °C to give a stable, or persistent nitroxide radical (C) and a polymeric radical (B).<sup>15</sup>



Scheme 1.2: Schematic representation of the NMP persistent radical effect. Species C is the persistent radical 2,2,6,6-tetramethylpiperidiny-1-oxy (TEMPO).

The free nitroxide radical C does not initiate the polymerization, but caps the growing polymer to create a dormant (unreactive) species (D). The radical C does not react with itself due to its sterically bulky substituents, therefore the cycle of fragmentation and monomer addition is then repeated to achieve controlled polymerization in which termination events have been minimized. At the beginning of the polymerization (the reaction medium is not viscous) when alkoxyamine A decomposes, a fraction of the initiating radical B undergoes radical coupling, resulting in terminated oligomer E. This removes two initiating radicals from the reaction mixture, giving an increase in the concentration of C relative to B, which leads to the “persistent radical effect”, a self-limiting process as it results in a more efficient formation of D

and decreases the formation of E. The persistent radical effect is what enables control over polymerization processes.<sup>16</sup>

The Hawker group has contributed significantly to advances in this field and has now developed a universal initiator (Figure 1.1) that can be readily modified to allow for chain end functionalized polymers.<sup>15,17,18</sup> This has proved to be superior to 2,2,6,6-tetramethylpiperidiny-1-oxy (TEMPO) and has enabled the polymerization of a wide range of monomers such as acrylates, acrylamides and styrenes.

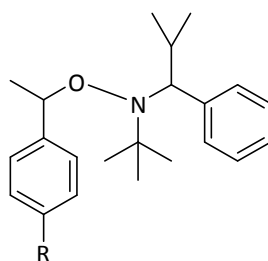


Figure 1.1: Structure of Hawker's universal NMP initiator.

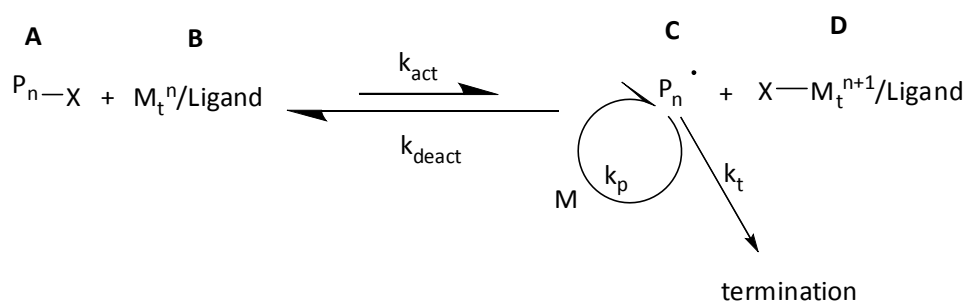
Nitroxide-mediated processes do not require an added metal complex, leading to a high functional group tolerance and facile purification without metal contamination.

The major limitations of NMP are the high temperature needed (*ca.* 125°C) and its incompatibility with a number of vinyl monomer families. Typically, the use of NMP has been limited to styrene-based systems, as the level of control afforded to homopolymerization of acrylate/methacrylates random copolymers with high acrylates/methacrylate levels is poor.<sup>19</sup> However, Charleux *et al.* recently reported a well-controlled and living copolymerization of acrylate/methacrylates using (*N*-*tert*-butyl-*N*-(1-diethyl phosphono-2,2-dimethylpropyl) nitroxide (SG1) as the initiator,<sup>20,21</sup> despite this the NMP of methacrylates is still regarded as

problematic.<sup>22</sup> Moreover, recent work from Charleux *et al.* allows for the controlled polymerization of methacrylates *via* SG1 in the presence of styrene at temperatures typically in the 70–90 °C range.<sup>21,23,24</sup> This approach was believed to be universal as it has been successfully applied to numerous methacrylates such as methylmethacrylate (MMA), methacrylic acid (MAA), *n*-butyl methacrylate (*n*BMA), *tert*-butyl methacrylate (*t*BMA), methacryloyl galactose (AcGalEMA) and poly(ethylene glycol) methyl ether methacrylate (MePEGMA). However, the conditions for the homopolymerization of styrenes still need to be optimized.

– Atom Transfer Radical Polymerization (ATRP)

This technique was developed by Matyjaszewski<sup>7</sup> and Sawamoto,<sup>25</sup> independently, at the same time and was coined Atom Transfer Radical Polymerization or ATRP. ATRP is a radical polymerization that proceeds *via* reversible termination by a halide (X) and transfer to a metal complex (B) (normally a transition metal, usually Cu or Fe).<sup>26,27</sup> The generalized mechanism can be seen in Scheme 1.3.<sup>7,28</sup>



Scheme 1.3: Schematic mechanism for ATRP polymerization.

Initiation occurs *via* homolytic fission of a P-X bond (A) in the presence of the transition metal (B) in a low oxidation state. At the propagation step the transition metal ion is oxidized (D)

and an organic radical (C) is generated that can react with a monomer M to produce a new radical species. Polymerization control is maintained as a result of the dynamic equilibrium ( $k_{\text{act}}/k_{\text{deact}}$ ) between the dormant (A) and active chain (C) by electron exchange between the active chain and the transition metal complex (B). Termination occurs by combination of two radical species ( $k_t$ ).

ATRP allows polymerization of a variety of monomers (styrenics, acrylates, methacrylates, and acrylonitrile) and is largely unaffected by the presence of oxygen and other inhibitors. An advantage of the alkyl halide end group is that it can be easily transformed into various functionalities.<sup>29</sup> A disadvantage of this method is that the metal catalyst used in the polymerization often needs to be removed from the polymer, especially for biomedical and catalytic applications. The development of higher activity catalysts and polymerization procedures involving continuous regeneration of the deactivator has reduced the amount of copper required down to ppm levels;<sup>30</sup> however, for electronic and biomedical applications it may be necessary to further reduce the catalyst concentration to below 1 ppm. In addition, the use of a metal catalyst such as Cu can be incompatible with some monomers such as those containing amino functionalities, especially tertiary amines. The polymerization of tertiary amines can be achieved with the use of polydentate ligands in order to avoid the displacement of the ligand on the copper complex by the polymer chain.<sup>31</sup> Although all these problems may sometimes be mitigated by appropriate selection of the reagents and reaction conditions, there is, nonetheless, a clear need for a more versatile process.

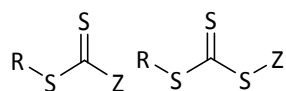
– *Reversible Addition Fragmentation Chain Transfer (RAFT) Polymerization*

The final CRP mechanism which has been elucidated is polymerization *via* reversible chain transfer. The RAFT process was developed by Moad, Thang, Rizzardo and co-workers at the Commonwealth Scientific and Industrial Research Organization (CSIRO) in Australia and was reported in 1998 so is the newest of the three CRP mechanisms.<sup>9</sup> Six months prior to this a similar technique had been reported by Rhodia Chimie, a French chemical company, that they coined MACromolecular Design by Interchange of Xanthates (MADIX).<sup>32</sup> The two processes operate using the same mechanism so MADIX can be considered a specific type of RAFT polymerization.

Over the last 10 years, RAFT polymerization has evolved into an extremely powerful synthetic tool for polymer synthesis.<sup>11</sup> The versatility of RAFT, with respect to reaction conditions and monomer class, facilitates the preparation of materials with well-defined molecular characteristics. One particularly advantageous feature of RAFT is its applicability to the synthesis of water-soluble copolymers both directly in aqueous media under homogeneous conditions as well as in organic media.<sup>10</sup> The ease of access to an almost infinite number of RAFT mediating agents now affords the ability to polymerize virtually any activated, and some non-activated, hydrophilic and hydrophobic monomers.<sup>11</sup> Using RAFT there is no need for a catalytic metal center as in ATRP, thus RAFT has the potential to be used in the synthesis of biocompatible polymers where trace elements of transition metals may prove toxic. There is also no need for the elevated temperature required for NMP, and polymerizations can often be performed at temperatures around 60 °C.

In a RAFT polymerization a chain transfer agent (CTA) is introduced along with a conventional radical initiator (often AIBN) and the monomer. There are four types of RAFT CTAs (Figure 1.2).

dithioester      trithiocarbonate



dithiocarbamate      xanthate

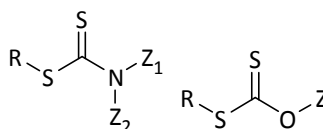


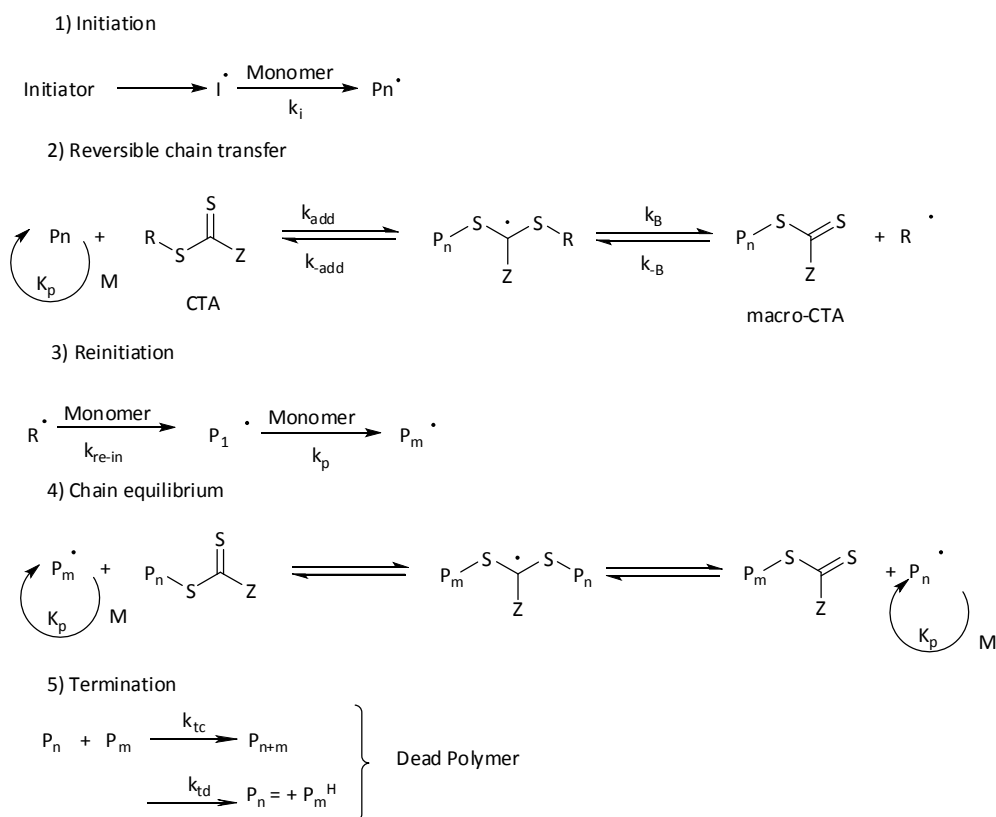
Figure 1.2: Chain transfer agents

Each of these CTAs are able to polymerize a variety of types of monomers with good control over molecular weight and PDI.<sup>11</sup>

- Dithioesters and trithiocarbonates: styrenes, acrylates, methacrylates, acrylamides and methacrylamides.
- Dithiocarbamates: styrenes, methacrylates and methacrylamides
- Xanthates : Vinyl acetates and N-Vinylcarbazole.

The transfer of the CTA between growing radical chains, present at a very low concentration, and dormant polymeric chains, present at a higher concentration, regulates the growth of the polymer molecular weight and limits termination reactions.



*Mechanism of RAFT polymerization:*<sup>33</sup>

Scheme 1.4: Mechanism of RAFT polymerization

The radical species produced from the decomposition of the radical initiator reacts with the monomer (Step 1, rate constant  $k_i$ ), as shown in Scheme 1.4. This growing polymer chain rapidly adds to the reactive CS bond of the CTA ( $k_{\text{add}}$ ) to form a radical intermediate (the radical initiator may add directly onto the CTA, before reacting with the monomer). Step 2 shows the fragmentation of the intermediate occurring reversibly either toward the initial growing chain ( $k_{\text{add}}$ ) or to free the re-initiating group (R) and a macro chain-transfer agent (macro-CTA) ( $k_B$ ). The R group can then re-initiate polymerization ( $k_{\text{re-in}}$ ) by reacting with the monomer and starts the growth of a new polymer chain, which will propagate ( $k_p$ ) (step 3)

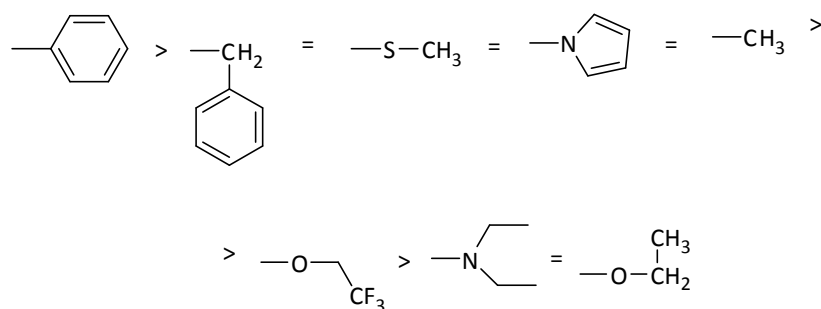
or react back on the macro-CTA ( $k_{\text{B}}$ ). Once the initial CTA has been entirely consumed, the macro-CTA agent is solely present in the reaction medium and enters equilibrium (step 4). This equilibrium is considered the *main equilibrium*, and a rapid exchange between active and dormant chains ensures equal probability for all chains to grow ( $P_{\text{n}}$  and  $P_{\text{m}}$ ), therefore leading to the production of polymers of narrow molecular weight distribution.

For a controlled RAFT polymerization:<sup>34</sup>

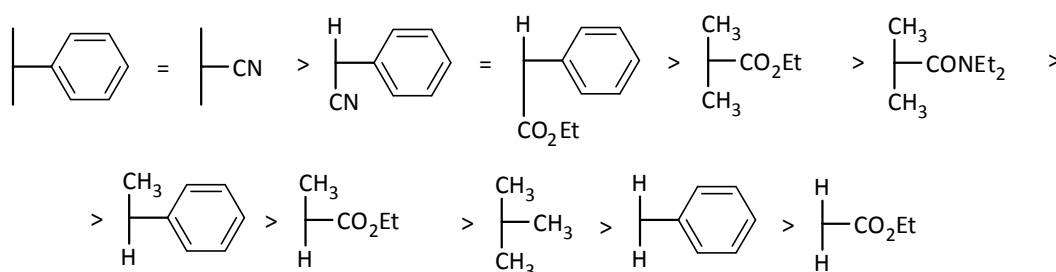
- $\text{R}\cdot$  must be able to be a persistent radical, and should readily reinitiate polymerization.
- $k_{\text{B}}$  must be high so that the intermediate radicals fragment rapidly due to weak S-R bonds.
- Radical intermediate should readily fragment in favor of products.
- CTAs must have a reactive thiocarbonyl double bond (high  $k_{\text{add}}$ ).
- R-capped initiators and polymer chains must be unreactive.
- The equilibrium constant ( $k_{\text{B}}/k_{\text{add}}$ ) for the fragmentation step must lie far to the left (i.e. much less than one) to keep the steady state concentration of  $\text{R}\cdot$  low.

The stability of the thiocarbonyl-thio radical intermediate formed depends on the attached Z group and its ability to help stabilize the radical species (Scheme 1.5). An effective CTA has a stabilizing Z group that is not too stable that it will not fragment to produce the initiating radical R which is the second part of the reversible addition/fragmentation process.

The main function of the R group in a CTA is to initiate polymerization and to stabilize the thiocarbonyl-thio radical (Scheme 1.6). The initiating R group must be a good leaving group with respect to the growing polymer chain but also a good initiating species with respect to the monomer unit.



Scheme 1.5: Selection of Z groups for a RAFT CTA.<sup>11</sup> Addition rate decreases while fragmentation rate increases from left to right.



Scheme 1.6: Relative stability/ability to reinitiate R group for a RAFT CTA.<sup>11</sup> Fragmentation rates decrease from left to right.

RAFT polymerization has been proposed to be the most versatile controlled polymerization method due to its compatibility with a wide variety of monomers and reaction conditions.<sup>9,11-13</sup>

One of the major redeeming features of RAFT is the wide range of functional and non-functional monomers which can be polymerized in a controlled fashion *via* this technique. To date, RAFT has been successfully employed in the polymerization of nonionic, cationic, anionic, zwitterionic and other hydrophilic/water-soluble monomers from a range of monomer families in both aqueous and organic media.<sup>10,35</sup>

The RAFT process is generally not compatible with unprotected primary or secondary amine groups since the thiocarbonylthio group reacts rapidly by aminolysis to form, in the first

instance, a thiol and a dithiocarbamate. However, tertiary amines can be polymerized by RAFT with very good control without the need for any special conditions (Figure 1.3).<sup>36</sup>

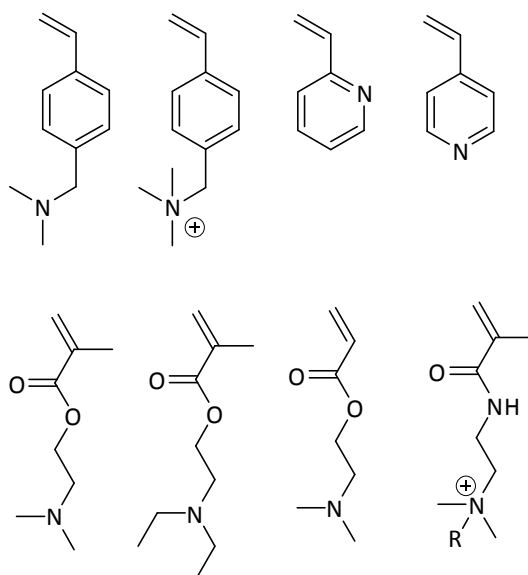
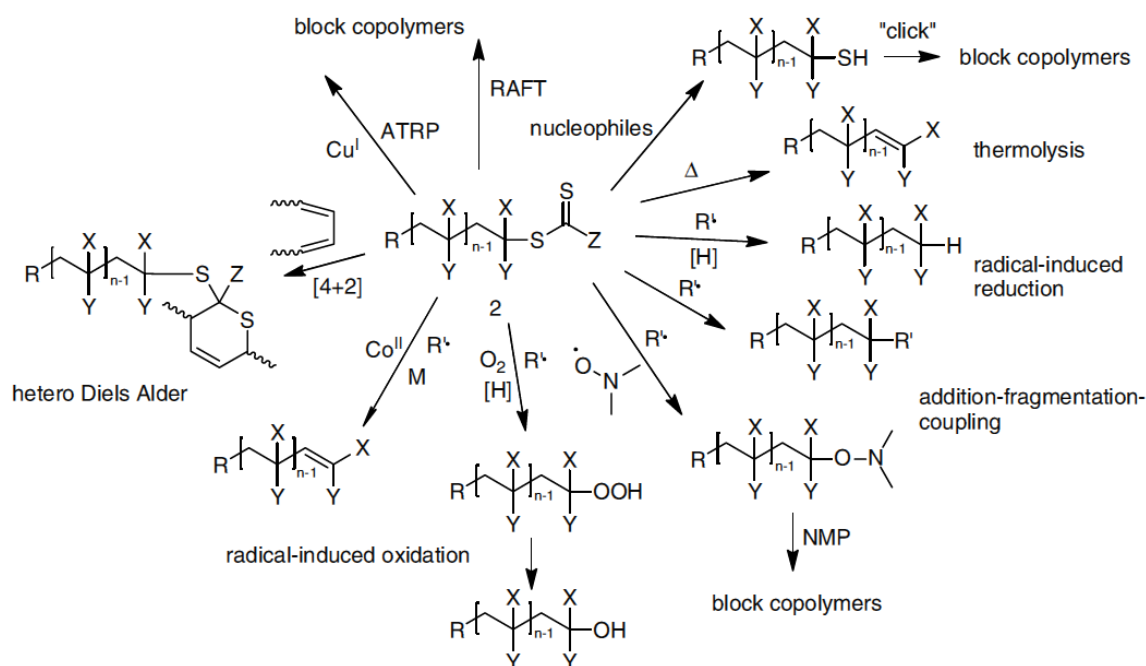


Figure 1.3: Examples of amine-containing monomers which have been polymerized under RAFT conditions.<sup>10</sup>

The major disadvantage of using RAFT is that CTAs are often prepared from toxic materials such as carbon disulfide and tailoring of the CTA structure is required to mediate the polymerization of a range of monomer classes. Significant work in the area of RAFT initiator synthesis has been reported, most notably by Perrier and Rannard who have reported a method to produce RAFT CTAs that avoids the use of toxic materials.<sup>37</sup> Another potential drawback of RAFT is that the polymers are usually colored due to the thiocarbonyl CTA and most commercial applications may require white polymers. Although this issue can be controlled with an appropriate design of the initial RAFT agent or by end group removal, there has been increasing interest in development of methods for the modification or removal of the thiocarbonylthio end group post-polymerization (Scheme 1.7).<sup>38-42</sup>



Scheme 1.7: Processes for RAFT end-group transformation ( $R' \cdot$  = radical;  $[H]$  = hydrogen donor;  $M$  = monomer).<sup>42</sup>

A further drawback is the often complex synthetic route to different CTAs and that no one CTA is applicable to all monomer systems. In order to polymerize multiple monomers, this may mean that a variety of CTAs need to be prepared and explored. In 2009 the CSIRO group developed a switchable CTA that, by changes in pH, was able to polymerize a wide range of monomers including styrene and vinyl acetate.<sup>43</sup> However, polymerization conditions still need to be optimized in order to achieve chain extension of these homopolymers with control.<sup>44</sup>

## 1.2 Self-Assembly of amphiphilic block copolymers

Supramolecular self assembly techniques have provided a versatile means by which to selectively assemble polymer molecules into well-defined three dimensional core-shell nanostructures (among others). These polymeric materials have potential applications as drug

delivery vehicles,<sup>45</sup> molecular imaging agents,<sup>46</sup> precursors to nano-sized microelectronic devices and catalysts.<sup>47</sup> These supramolecular structures can be formed by the spontaneous self-assembly of well-defined amphiphilic diblock copolymers in selective solvents in order to minimize energetically unfavourable hydrophobic-hydrophilic interactions, and can be stabilized and functionalized using a range of chemistries to afford robust functional polymeric nanoparticles.<sup>48,49</sup>

The morphology obtained through polymer self assembly is generally dictated by the free energy of the aggregates, which in turn depends on three components; the free energy of the core, which relates to the stretching of the core-forming block; the free energy of the corona, to which steric or electrostatic interactions of the coronal blocks contribute; and the free energy of the interface, which depends on the interactions between the core forming block and the solvent.<sup>47</sup> The various reported morphologies are primarily a result of the inherent molecular curvature and how this influences the packing of the copolymer chains: specific self-assembled nanostructures can be targeted according to a dimensionless “packing parameter”,  $p$  (Equation 1.1):<sup>50</sup>

$$p = \frac{v}{a_o l_c}$$

Equation 1.1: Definition of the packing parameter  $p$

where  $v$  is the volume of the hydrophobic chains,  $a_o$  is the optimal area of the head group, and  $l_c$  is the length of the hydrophobic tail. As a general rule, spherical micelles are favored when  $p \leq \frac{1}{3}$ , cylindrical micelles when  $\frac{1}{3} \leq p \leq \frac{1}{2}$  and vesicles (also known as polymersomes) when  $\frac{1}{2} \leq p \leq 1$  (Figure 1.4).

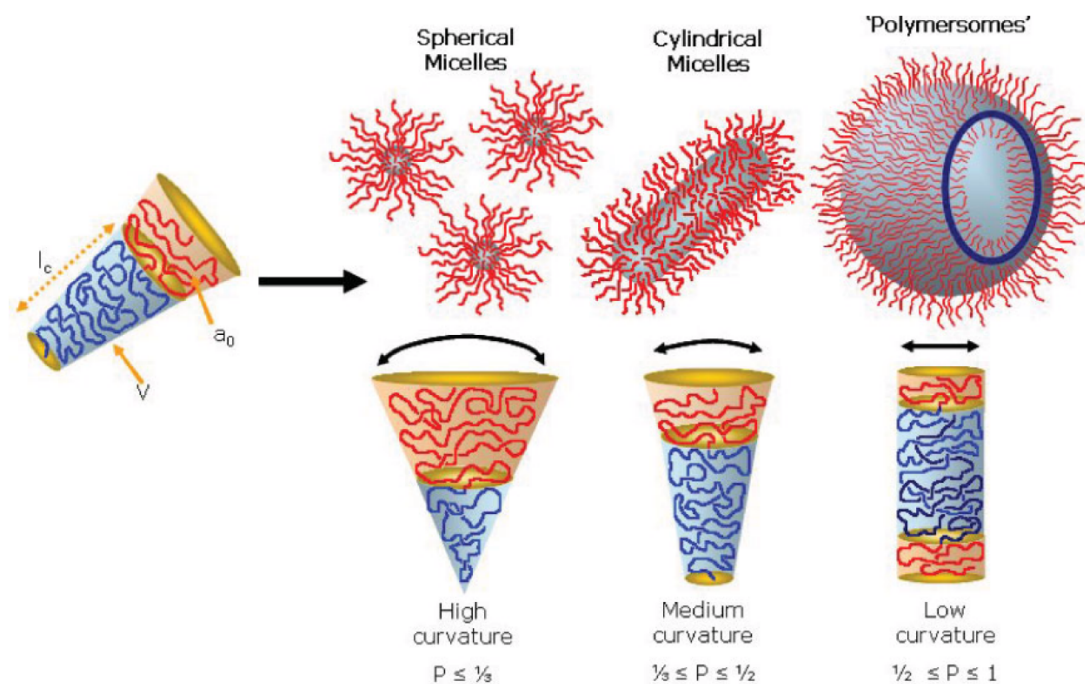


Figure 1.4: Self-assembled structures depending on the inherent curvature of the molecule, defined by  $p$ .<sup>48</sup>

The simplest method for the assembly of synthetic polymer chains into nanoparticles is the formation of spherical polymer micelles in solution. Conventional micelles based on hydrophilic-hydrophobic diblock copolymers have been extensively reported.<sup>47,48,51,52</sup>

The major driving force behind the self-assembly of amphiphilic copolymers is the decrease in free energy of the system due to the removal of the hydrophobic fragments from the incompatible aqueous environment by the formation of a micelle core which is stabilized and 'protected' from the surrounding aqueous media by the hydrophilic blocks. Amphiphilic micelles are formed spontaneously *via* the solution-state self assembly of amphiphilic multi-block copolymers, which consist of hydrophobic and hydrophilic chain segments (Figure 1.5). The self-assembly process is usually achieved by the so-called "solvent switch" method which involves dissolving the amphiphilic copolymer in a good solvent for all of the blocks and then gradually adding a non-solvent for one of the blocks (selective solvent) at a concentration

above its critical micelle concentration (cmc). Then *via* dialysis or evaporation, the complete replacement of the good solvent by the non-solvent is achieved and well-defined aggregates (micelles) are prepared. Furthermore, depending on the combination of polymer and solvent, the final system can be kinetically trapped, where no unimer exchange is observed (frozen micelles), or dynamic, when fast intermicellar polymer chain exchange is allowed and the solvent, to a certain extent, penetrates the solvophobic core.<sup>53</sup>

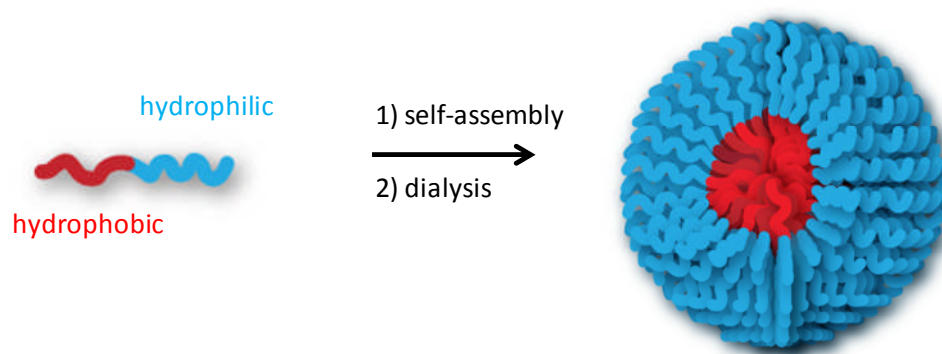


Figure 1.5: Self-assembled spherical micelles from amphiphilic block copolymers in water.

These structures are not stable to drastic changes in concentration and temperature and stabilization through shell or core cross-linking can be performed in order to obtain stable robust particles.<sup>51,54,55</sup> Many examples of the stabilization and functionalization of these nanoparticles have been reported in the literature however in this work we will look at developing both responsive and functional polymeric particles for specific applications such as in supported catalysis.



### 1.3 Stimuli responsive polymers

Stimuli-responsive polymers and copolymers have attracted considerable interest for decades, due their potential applications in a wide range of fields, such as detergency, surface coating, waste-water treatment, oil recovery, drug-release, and nanotechnology.<sup>56-60</sup>

In this direction, some systems have been studied in order to obtain “smart” materials, the behavior of which depends intrinsically on structural parameters and experimental conditions. The association behavior of stimuli-responsive block copolymers in solution can be responsive to a wide range of stimuli including temperature, pH, salt or light.<sup>61-64</sup> These polymers that exhibit large changes in their physical state or properties in response to small changes in environmental stimuli are also called 'smart' polymers. pH- and temperature-responsive polymers are the two most studied 'smart' polymer systems.

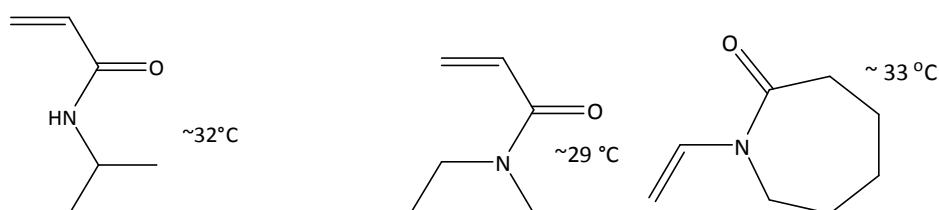
#### 1.3.1 *Temperature responsive polymers*

Temperature is the most widely used stimulus in responsive polymer systems. A change of temperature is not only relatively easy to control, but also practically very easily to employ. Most synthetic macromolecules become more soluble when heated, but some polymers separate from solution upon heating (coil-to-globule transition). This unusual property, referred to as inverse temperature-dependent solubility, is characteristic of polymers which dissolve when cooled and phase separate when heated above the phase transition temperature, known as a lower critical solution temperature (LCST). At this temperature, the enthalpic contribution of the solvent hydrogen bonded to the polymer chain ( $\Delta H$ ) becomes less than the entropic gain of the system as a whole ( $\Delta S$ ). The LCST is largely dependent on the hydrogen-bonding capabilities of the constituent monomer units. The dissolution enthalpy

$\Delta H$  due to the hydrogen bonding of the basic sites on the polymer with the solvent favors dissolution and the entropic organization  $\Delta S$  of the solvent required to achieve this hydrogen bonding is unfavorable. Since the free energy of dissolution is equal to  $\Delta H - T \Delta S$ , it can change from negative (favorable) to positive (unfavorable) as the temperature increases. Thus, some polymers are known to exhibit LCST behavior in strongly interacting solvents such as water.

Polymers bearing amide groups form the largest group of thermosensitive polymers (Figure 1.6). These polymers are biocompatible and display temperature-dependent phase behavior in aqueous solution. In addition, statistical, block, or brush copolymers, based on these and other thermo-responsive polymers have been widely studied.<sup>65</sup>

*N*-isopropylacrylamide *N,N*-diethylacrylamide *N*-vinylcaprolactam



2-isopropyl-2-oxazoline vinyl methyl ether

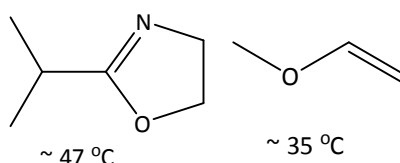


Figure 1.6: Structure of a range of thermo-responsive monomers and their LCST values

*N*-isopropylacrylamide (NIPAM) is an extremely important non-ionic acrylamide monomer and has been the subject of intensive research in recent years. It has been so widely studied

mainly because of the sharpness of its phase transition, the closeness of its LCST, about 32 °C, to physiologically relevant temperatures, and the easy of variation of its LCST by copolymerization, addition of salts or addition of surfactants to the polymer solution (Figure 1.7).<sup>66</sup>

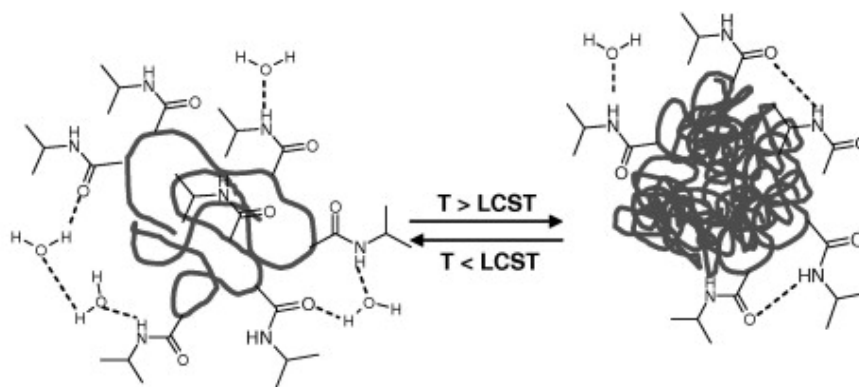


Figure 1.7: PNIPAM coil-to-globule transition<sup>67</sup>

The synthesis of block copolymers based on PNIPAM has received also tremendous attention.<sup>68,69</sup> Well defined block copolymers based on PNIPAM have been synthesized *via* RAFT to afford smart amphiphilic block copolymers with a switchable hydrophilic-hydrophobic segment of PNIPAM and a second responsive or non-responsive hydrophobic block. Through this combination, different types of water soluble block copolymers can be achieved: hydrophobic-hydrophilic, hydrophilic-hydrophobic, double hydrophilic or double hydrophobic.<sup>70-75</sup>

Applications of this switchable behavior include the dissolution of a double hydrophilic block copolymer in an aqueous medium and its reversible switching upon heating above 32 °C, to an amphiphilic block copolymer, which can then reversibly self-assemble in micelles or

aggregates, depending on the length of each block and the ratio of the hydrophilic/hydrophobic blocks in the copolymer.<sup>68</sup>

Alternatively, poly(oligo(ethyleneglycol)methacrylate) based polymers have attracted great attention in the last couple of years due to their tunable LCST behavior.<sup>36</sup> Copolymers of different poly(oligo(ethyleneglycol)methacrylate) monomer lengths exhibit thermoresponsive behavior comparable to PNIPAM and are considered as ideal structures, which combine both the properties of poly ethylene glycol (PEG) (i.e., nontoxicity, anti-immunogenicity) and PNIPAM (i.e., thermosensitivity almost independent of external conditions) in a single macromolecule.<sup>76</sup>

It is well known that the accuracy and the reproducibility of LCST transitions are highly dependent on the polydispersity of the polymer and, as mentioned above, the development of CRP techniques has enabled the synthesis of polymers and polymeric structures with well defined molecular weights.<sup>77</sup> Moreover, the architecture as well as the desired monomer composition and distribution along the backbone can be controlled in an excellent manner.<sup>78,79</sup>

### 1.3.2 *pH responsive*

Polymers having pH-responsive character are generally formed from ionizable monomers having a hydrophilic nature. In such polymers, a change in pH induces a change in the net charge which causes a phase change around the pK value of the ionizable groups (Figure 1.8). As an example, the copolymers of methyl methacrylate (MMA) with dimethylamino ethyl methacrylate (DMAEMA), which is hydrophilic at low pH, when amino groups are protonated but more hydrophobic when amino groups are deprotonated. These copolymers are soluble at low pH but precipitate under slightly alkaline conditions.

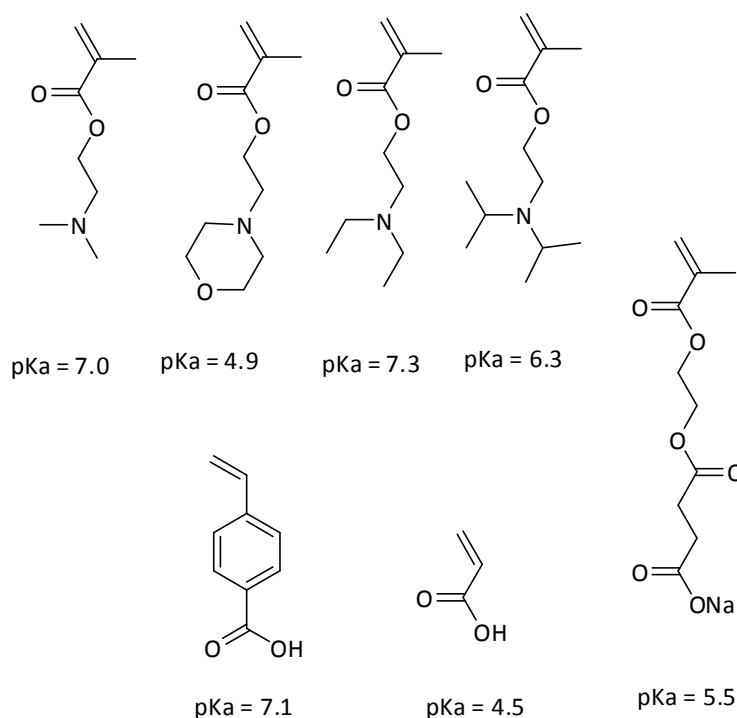


Figure 1.8: Chemical structures of different monomers whose homopolymers exhibit pH responsive properties

( $pK_a$  values reported for the homopolymers).<sup>80,81</sup>

Cationic polymers have been evaluated for a wide range of applications including antimicrobial coatings, additives for cosmetics, and gene vectoring.<sup>82-84</sup> Well defined cationic polymers have been prepared by several polymerization techniques including anionic, group transfer, NMP, ATRP, and ring opening metathesis polymerization.<sup>10</sup> Cationic, or protonable polymers have also been prepared via RAFT.<sup>78</sup>

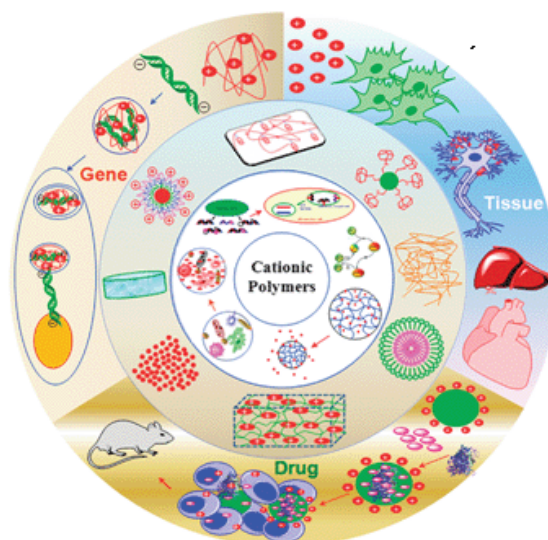


Figure 1.9: Schematic representation of the bioactive properties, architectures and therapeutic applications of cationic polymers.<sup>84</sup>

Polymeric amines have been used in many different industrial applications and play very important roles in some emerging areas of biotechnology, such as gene delivery and antibacterial coatings. For these applications, the usefulness of polyamines is related to their cationic charges due to the protonation of the amine nitrogens under low pH conditions. The capability to precisely predict the pH-dependent protonation property of a polyamine is a very difficult task, even when the information about the protonation behavior of the corresponding monomeric species in the unpolymerized state is precisely known since in a polymeric structure, the protonation reactions of the different amine groups within the polymer chain are highly intercorrelated among themselves due to the strong electrostatic repulsion between the protonated amine groups.<sup>85</sup> Small molecule amines are weak electrolytes, and therefore normally exhibit pH-dependent protonation behaviors in aqueous solutions. The protonation equilibrium can be modeled simply in terms of the characteristic  $pK_a$  (or  $pK_b$ ) value of the amine compound. However, when the amine molecules are covalently linked into a polymer

structure, the protonation behavior becomes far more complicated because of the strong intrachain electrostatic repulsion between adjacent charged groups and the conformational degree of freedom of the polymer.<sup>85</sup>

#### 1.4 Catalytic polymeric particles

In organic reactions the catalyst is often the most expensive component and usually very toxic. Its incorporation onto a solid support has been of great interest because of several advantages such as simplification of product work-up, separation, isolation, and reuse of the catalysts. In 1963 Merrifield introduced the concept of using supported species to overcome some of the physical and mechanical difficulties of completing long syntheses rapidly and efficiently.<sup>86</sup> Merrifield highlighted a solid-phase method for oligopeptide synthesis using polystyrene-based resins as a precursor. In this method, the synthesis of peptides is achieved by consecutive reactions involving supported protecting groups where the separation of the new supported species is not possible and hence the reactions must be clean and very high yielding. The use of polymer-supported reagents is less demanding. Over the last decade, polymer-supported catalysts have been extensively used in organic synthesis.<sup>87,88</sup> By attaching the catalyst into a polymer support it can be easily recovered after each reaction for recycling and not every site needs to be available for reaction.<sup>89</sup> However, these immobilized catalysts are sometimes less active than the corresponding original catalysts and the precursors can be expensive and hard to synthesize.<sup>90</sup>

During the last few years, the interest in developing novel polymeric nanostructures as scaffolds for catalysis has increased significantly.<sup>91-93</sup> Nanometric core-shell structured containers can be applied as catalytic nanoreactors where functionalities can be incorporated

on the surface, the shell or the well defined core of the polymeric support. The advantages of such nanostructures over traditional supports are numerous since they combine benefits from both homogeneous and heterogeneous catalysts creating a novel environment for reaction and improved recovery.

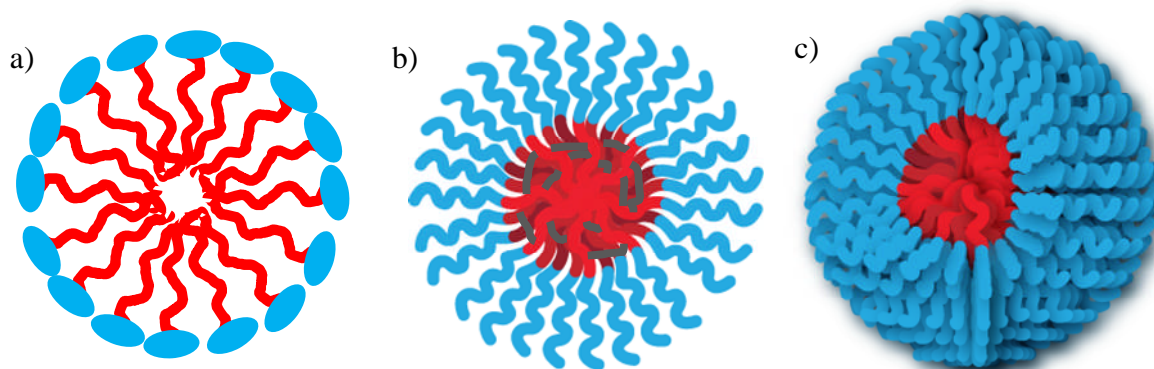


Figure 1.10: Different type of micelles and micelle analogous structures a) small molecule surfactants, b) star-like polymer, c) amphiphilic block copolymer micelle. (Red domain hydrophobic and blue domain hydrophilic)

With the introduction of CRP techniques the range of accessible polymer architectures, which have the capacity to act as nanoreactors for organic reactions, has now greatly increased.<sup>11,17,94</sup> Given the number of examples of catalytic polymeric nanoreactors in the literature, in this chapter we will focus in core-shell type polymeric nanoparticles, where the specific catalytic groups are tethered within the core domain and protected from degradation or side reactions by the surrounding corona, allowing the selective reaction of the reagents within this central domain in an overall homogeneous media (Figure 1.10). A few selected examples are discussed which illustrate the benefits of tethering the catalyst in the core of a polymeric nanoreactor.



#### 1.4.1 *Hydrophobic pockets for organic synthesis in aqueous media*

The use of organic solvents in chemical laboratories is considered a very important problem for the health and safety of workers and environmental pollution. Green Chemistry aims to change the use of toxic solvents with greener alternatives, with replacement and synthetic techniques, separation and purification which do not need the use of solvents.

Despite water being cheap, safe and the most abundant solvent on earth, its application in organic synthesis is restricted by the low solubility in water of organic compounds and the decomposition or deactivation of some substrates in aqueous conditions.<sup>95-97</sup> A good approach in order to overcome these challenges has been the introduction of surfactants and water soluble dendrimers as reaction pockets.<sup>98,99</sup> By carrying out organic reactions in the presence of surfactant-type micelles, enhancement of rates and/or specificity has been observed for different reactions based on hydrophobic forces.<sup>100</sup> The high concentration created in the hydrophobic core, enhances the reaction rates and induces selectivity in the same way as enzymes in biological systems (Figure 1.11). Unfortunately, problems with catalyst recovery and product isolation limit the scope of this approach. In the same way as surfactant-based micellar systems, polymeric micelles concentrate the reactants within a nanoenvironment and alter the selectivity of the product. However, a further advantage of polymeric self-assembled systems is their stability and proposed improved recovery over surfactant-based micelles.

Therefore, polymeric core-shell-type catalytic nanoreactors have been investigated in which the hydrophobic core provides a favorable confined environment for the hydrophobic starting materials, while the hydrophilic shell guarantees water-solubility. The simplest method for the

assembly of synthetic polymer chains into nanoparticles is solution self-assembly to allow for the formation of spherical polymer micelles.

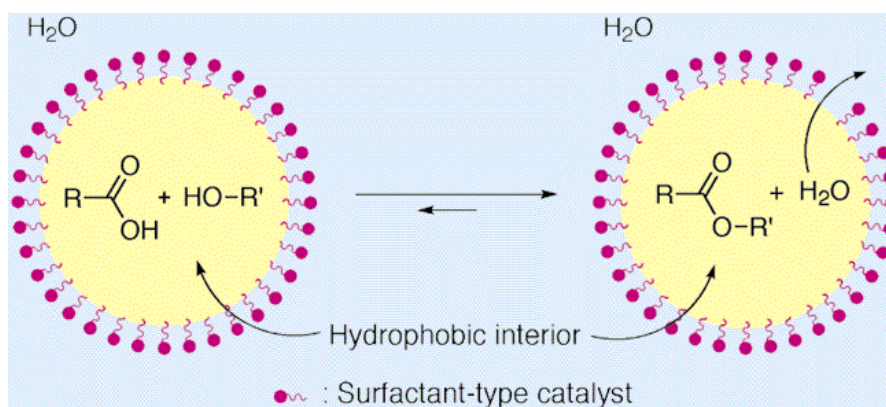


Figure 1.11: Surfactant-type brønsted acid-catalyzed direct esterification of carboxylic acids with alcohols in an emulsion system.<sup>101</sup>

The kinetically frozen nature of some polymeric micelles in water creates a confined hydrophobic pocket which avoids water permeability creating a stable environment for hydrolyzable substrates. Thayumanavan and Ramamurthy recently reported a comparative study of product selectivity using amphiphilic polymer versus surfactant based micelles in water (Figure 1.12).<sup>102</sup> Their studies revealed that the hydrophobic domains created by a kinetically frozen styrenic-based amphiphilic homopolymer stops hydrolysis of hydrophobic substrates and offers better control over selectivity than micelles formed from small molecule surfactants because of the more stable and confined hydrophobic pocket generated by the amphiphilic homopolymer.

Utilizing this unique environment for the reaction of hydrophobic substrates in aqueous media, functional amphiphilic block copolymers have been self-assembled into micelles in water with incorporation of functional groups within the core, enabling different reactions to

be performed in an overall hydrophobic environment. Nuyken and co-workers pioneered the development of a platform of amphiphilic, water-soluble block copolymers for metal catalysis in water.<sup>91</sup> The covalent immobilization of transition metal catalysts (Rh, Ir or Pd) within the hydrophobic core increases the local concentration of the catalyst in the reaction.<sup>103,104</sup> The hydrophobic substrates were dissolved in the micellar core, where the catalyst is also located; this allows for transformations to be carried out in an overall aqueous environment, increasing significantly the reaction rates over the water-soluble homopolymer counterparts.<sup>105</sup> However, the leaching of the catalyst could not be avoided therefore the recyclability of this polymeric system was limited.

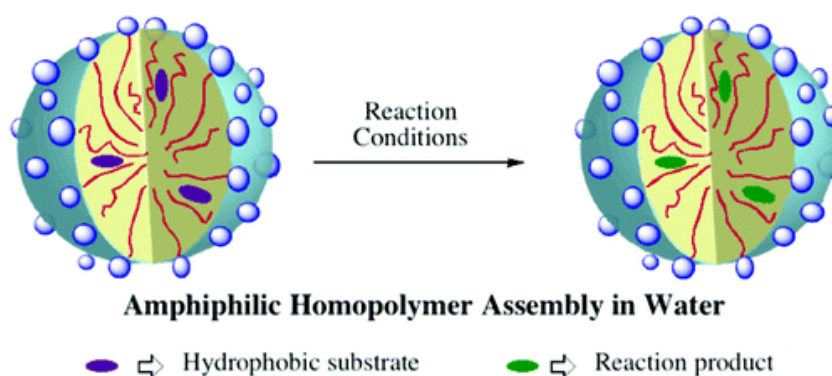


Figure 1.12: Schematic representation of a reaction within the homopolymer micelle-type nanocontainer.<sup>102</sup>

In Nuyken's work, unfunctionalized polymers were synthesized by the living cationic polymerization of 2-oxazoline monomers and the active catalyst was introduced by a post-functionalization method. Whilst this approach affords well-defined precursor polymers often the post-modification to introduce the active site can be inefficient. Hence, a new strategy has been developed which involves the synthesis of functionalized monomers, which can be incorporated selectively into a specific domain of a diblock copolymer *via* robust CRP techniques.<sup>100,106-109</sup> This approach allows for the synthesis of functional polymers without the

need of protecting groups or post-functionalization steps.<sup>110</sup> The choice of functional monomer provides the possibility of introducing a variety of functional groups into the micelle (core, shell or surface) which can tune the properties of the nanostructure for different applications. By introducing a stimuli-responsive block in the synthesis of block co-polymers, one block can be tuned to be hydrophilic or hydrophobic by applying an external stimulus, whereas the other block remains hydrophobic or hydrophilic offering convenient ways to control the self-assembly. Following this strategy, the concept of micelles as pseudo-homogeneous catalyst supports has been explored using recoverable and responsive polymers.<sup>108,111</sup>

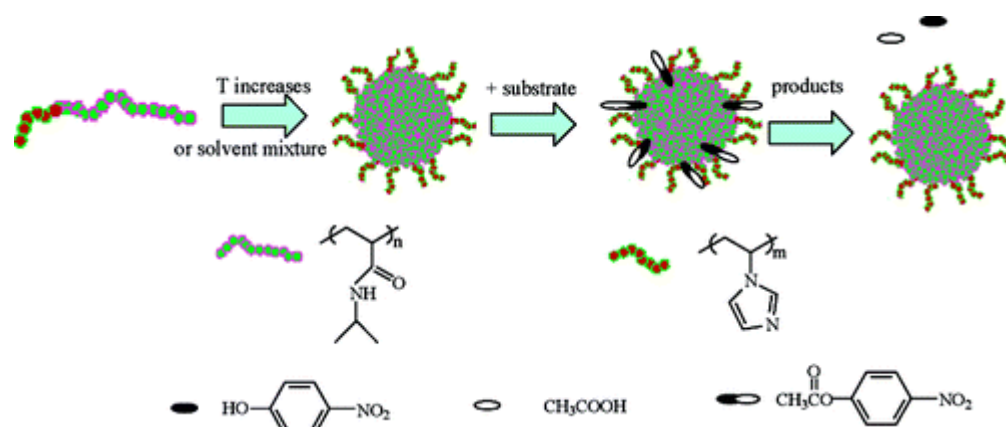


Figure 1.13: Stimuli-responsive double hydrophilic block copolymer micelles with switchable catalytic activity.<sup>108</sup>

Most significantly Liu and co-workers used RAFT to synthesize stimuli-responsive block copolymers, poly(N-isopropylacrylamide)-*b*-poly(N-vinylimidazole) (PNIPAM-*b*-PVim), which self-assembled above the LCST of NIPAM into micelles with the hydrophobic NIPAM constituting the core of the micelles.<sup>108</sup> Interestingly, the authors in this case incorporated the catalytic PVim functionality in the shell of the aggregates and studied the hydrolysis reaction of p-nitrophenyl acetate (NPA) at elevated temperatures, where the BCP is above its critical

micellization temperature (CMT), and thus formed micelles (Figure 1.13). They found that in the presence of the catalytic micelles the rate of ester hydrolysis increased up to 7 times, and they proposed that this was due to the hydrophobic affinity of the reactants for the hydrophobic NIPAM core which brought the reactants in close proximity to the catalytic shell and increased their local concentration. Although, in this example the authors left the catalyst “exposed” in the shell domain and the reaction did not take place in the core of the aggregates, the importance of selective localization of the starting materials *via* hydrophobic attractions was illustrated.

In 2009 Zhao et al. used ATRP to synthesize a poly(ethylene oxide)-*b*-poly(methoxydi(ethylene glycol) methacrylate-co-2-(N-methyl-N-(4-pyridyl)amino)ethyl methacrylate), (PEO-*b*-P(DEGMMA-co-MAPMA)) diblock copolymer.<sup>109</sup> In this case MAPMA, a 4-dimethylaminopyridine (DMAP) functionalized monomer, was copolymerized with the temperature-responsive DEGMMA monomer. The corresponding temperature-responsive block with the tethered DMAP functionality formed the hydrophobic core of the micelle upon heating to 30-48 °C.<sup>109</sup> They envisioned that hydrophobic substrates could be concentrated in the core of the micelle and proposed that this would result in an enhanced reaction rate. To explore this, the authors studied the hydrolysis of NPA at different temperatures always above the CMT of the aggregates. Disappointingly, the reaction rates did not increase with temperature as much as expected by the Arrhenius equation and the result was attributed to a poor partitioning of the starting materials to the hydrophobic core.

Although polymeric micelles can be more stable than surfactant-based micelles, these structures can be affected by drastic changes in concentration or temperature. The stabilization

of polymeric micelles through shell or core cross-linking (after self-assembly) in order to obtain stable robust particles has been extensively reported in the literature, although only a few examples of their application in catalysis have been reported.<sup>112</sup>

Catalytic shell cross-linked micelles have been synthesized by our group using NMP. In this case the core of the particles contained a terpyridine side group which could be utilized as a ligand to bind Cu(I) species.<sup>106</sup> The catalytic efficiency of these nanoparticles on mediating “click” reactions was confirmed by using a fluorogenic reaction between an azido coumarin and an alkynyl small molecule. Further, more recent work by Weck and co-workers used poly(2-oxazoline) based amphiphilic triblock copolymers with a salen functionalized hydrophobic block prepared by living cationic polymerization.<sup>100</sup> The polymers were self assembled into core-shell-corona micelles and stabilized them by photocrosslinking the mid-block. Subsequently, the catalytic sites were generated by adding Co (III) which produced Co(III)-salen complexes in the hydrophobic core of the particles.

The authors explored the kinetic resolution of a range of epoxides of different hydrophobicities. These nanoreactors exhibited substrate selectivity based on hydrophobic effects. However, at the same catalyst loading, the non-cross-linked catalyst showed a slightly higher catalytic activity due to the less permeable shell in the cross-linked particles. The same effect has been recently observed by Stenzel *et al.* when comparing the rate of release for a drug encapsulated in the core of a cross-linked and non-cross-linked micelle.<sup>45</sup> Despite its high stability, shell-cross-linked micelles lead to network formation, which can act as an obstacle for drug diffusion, leading to a reduced release rate.

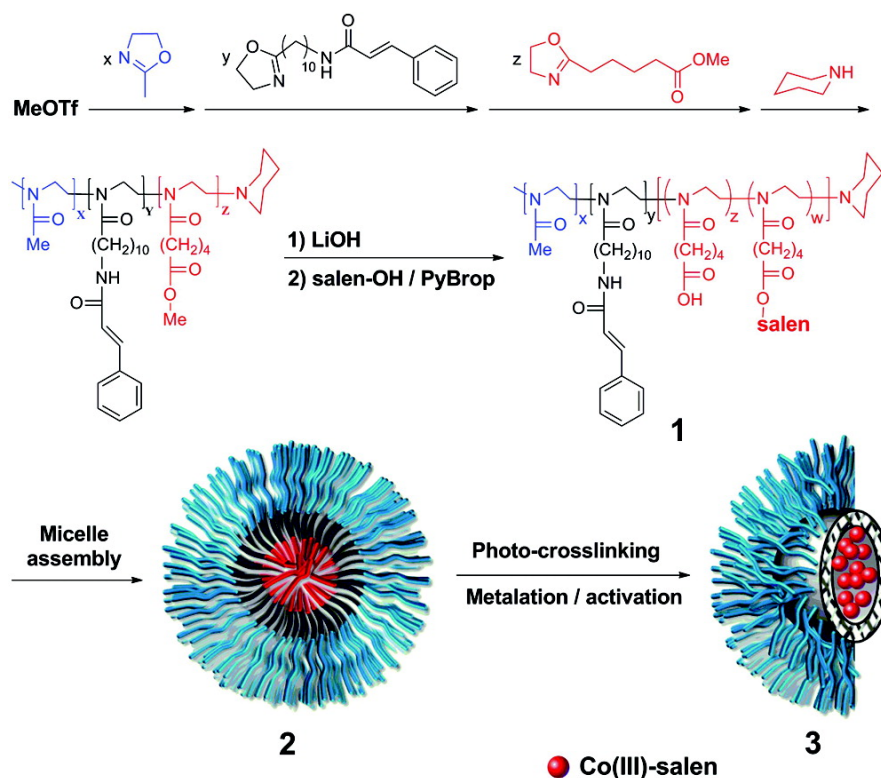


Figure 1.14: Schematic representation of the synthesis of poly(2-oxazoline) shell cross-linked micelles with Co(III)–salen-functionalized cores.<sup>100</sup>

#### 1.4.2 Site isolation

One-pot multistep reactions are effective at reducing the waste and the cost of a synthetic process because they decrease the number of work-ups and purification steps, as well as the volume of solvent used. These reactions are especially useful when multiple catalysts are used so that one traps an unstable intermediate formed by the other. Though a variety of these reactions have been reported, they are limited to a relatively small number of systems where the catalysts are compatible with each other.<sup>113,114</sup> The work of Patchornik in 1981 demonstrated that this limitation can be overcome by immobilizing incompatible catalysts on solid supports.<sup>115</sup> The principle of site isolation has been applied to catalysis making use of different supports. Several examples show how polymeric nanostructures render incompatible

catalysts compatible.<sup>93,116,117</sup> In recent years, soluble dendritic and other hyperbranched polymers have emerged as attractive systems for the encapsulation and isolation of various functional groups within the interior of the structure.<sup>99</sup> The placement of catalytic functionality at the interior of a globular dendritic structure protects the catalyst from deactivation and allows for the tuning of molecular properties and catalytic activity by modification of the periphery and the interior environment, respectively.<sup>99</sup> Such stable unimolecular supports can exist with high stability in different solvents and temperatures; however their synthetic difficulty limits their use.

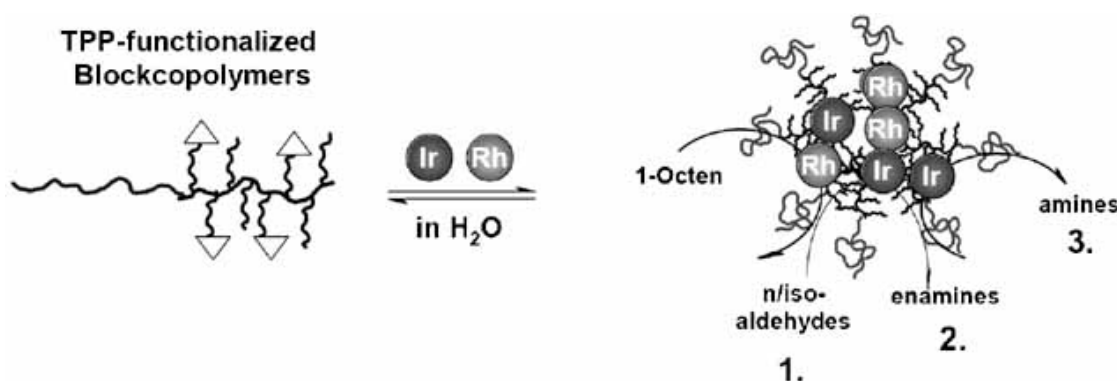


Figure 1.15: Attempted cascade reactions using mono and bimetallic micellar catalysis in the hydroaminomethylation of 1-octene.<sup>103</sup>

Cascade reactions in self-assembled polymeric nanoreactors have been explored by Weberskirch *et al.* for the mono (Rh) and bimetallic (Rh and Ir) micellar catalysis in the hydroaminomethylation of 1-octene. Unfortunately, conditions optimized for one reaction were not favorable for the next one, probably due to the competition of more than 1 substrate for the metal center and the deactivation of the catalyst.<sup>103</sup>



– *Polymeric stars*

A similar but simpler approach to obtain stable polymeric nanoreactors is to synthesize unimolecular micelles. The facile synthesis and tunable composition of star polymers makes them an attractive alternative to the widely studied dendritic systems or other cross-linked micelles. A polymeric star is a macromolecule containing a single branched core with multiple linear chains or arms forming a 3D globule. The use of CRP techniques allows the formation of unimolecular branched stars and the selection of initiators, monomers or cross-linkers allows for covalent incorporation of functionalities into the structure. The synthesis of polymeric stars is commonly carried out via three different strategies based on the sequence of formation of the core and the arms (Figure 1.16). In the “core-first” approach, polymeric arms are grown from a multifunctional cross-linked initiator, while in the “arm first” approach pre-synthesized linear polymers are cross-linked using difunctional compounds.<sup>118-121</sup> A third strategy, “coupling onto”, consists of attaching linear polymers onto a multifunctional core. The “arm first” method is the most commonly used strategy to synthesize stars by the most popular CRP techniques (NMP, RAFT and ATRP).

Although it has been already demonstrated that cross-linking the core or the shell domain reduces the micelle permeability, the introduction of the catalytic motif into the core of a polymeric star is a very simple way of protecting the catalyst from the environment and avoiding side reactions. Such structures share the recyclability of cross-linked micelles and have shown outstanding properties for site isolation.

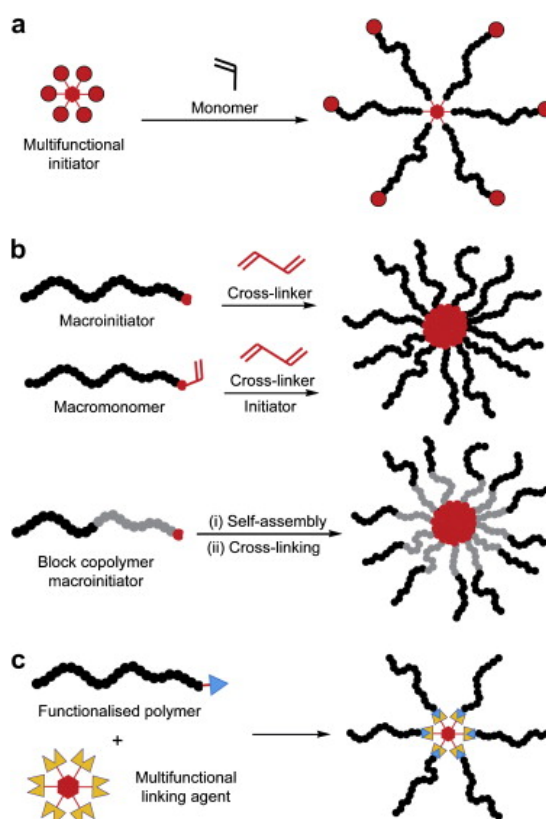


Figure 1.16: Synthetic approaches for the preparation of star polymers via controlled polymerization techniques;

(a) the core-first approach, (b) the arm-first approach and (c) grafting to-approach.<sup>122</sup>

The groups of Fréchet and Hawker have developed an effective method to synthesize star polymers with core confinement of functionalities by NMP using the arm first approach. In 2005 Fréchet *et al.* reported the synthetic utility of site isolation by carrying out a one pot cascade reaction using the otherwise incompatible acid and base catalysts (Figure 1.17).<sup>117</sup> They synthesize star polymers that contain acid (*para*-toluenesulfonic acid) or base (DMAP) catalysts in their cores to perform acid-catalyzed deprotection and the nucleophilic amine-catalyzed Baylis–Hillman reaction in the same pot. These star polymers can be recovered after reaction and yield higher activities in acylation reactions than linear polymers or other solid supports.

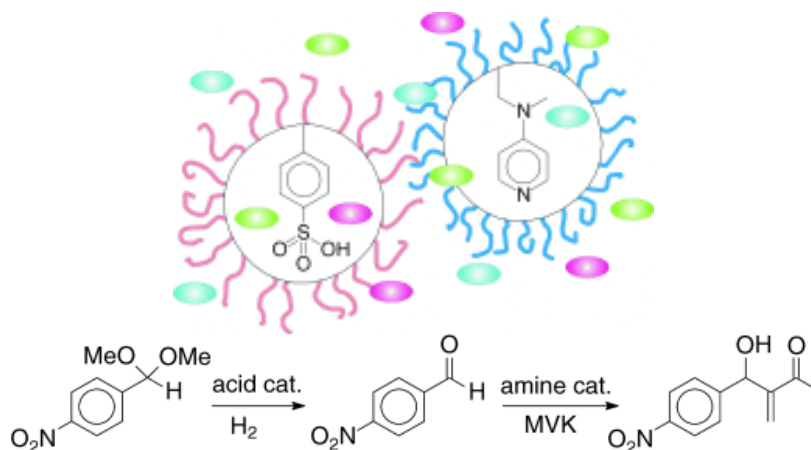


Figure 1.17: One-pot-reaction cascade involving sequential acid-catalyzed acetal hydrolysis followed by the amine-catalyzed Baylis-Hillman reaction.<sup>117</sup>

This ability to carry out an otherwise incompatible cascade of reactions is characteristic of biological systems where different enzymes are used consecutively to create a wide range of chemical transformations through the combination of simple steps. Further studies reported that site isolation with star polymers enables the combination of incompatible catalysts for more sophisticated asymmetric cascade reactions. This group have also published the design of non-interpenetrating star polymers to combine iminium, enamine, and hydrogen bond catalysis in one pot for asymmetric reactions that generate cascade products with more than one chiral centre.<sup>93</sup>

The groups of Sawamoto and Matyjaszewski have also extensively reported the formation of functional polymeric stars by ATRP.<sup>123-125</sup>

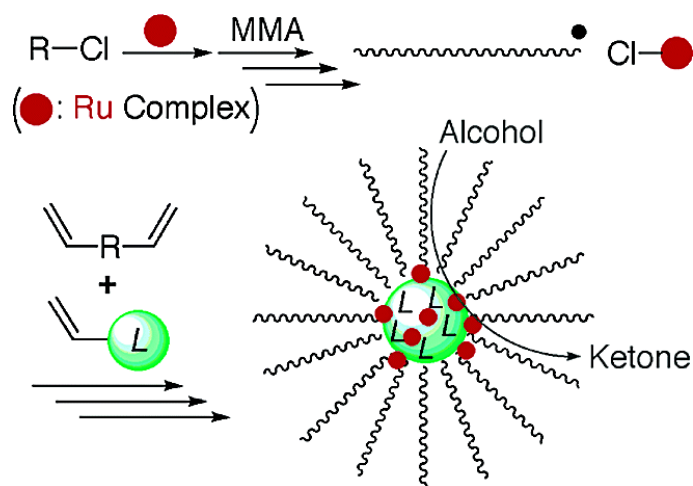


Figure 1.18: Direct encapsulation of metal catalyst into star polymer core during metal-catalyzed living radical polymerization.<sup>124</sup>

In 2003 Sawamoto reported an interesting procedure to synthesize catalytic stars whereby a ruthenium complex was incorporated into the core using ruthenium-catalyzed living radical polymerization. A ruthenium catalyst was encapsulated by cross-linking poly (methylmethacrylate) “arms” using ethylene glycol dimethylacrylate in the presence of diphenyl-4-styrylphosphine as a ligand to form the catalytic core. The ruthenium-containing star polymers were then employed as a catalyst for the oxidation of alcohols into ketones (Figure 1.18). However, they observed that the activity of the stars was lower than the unsupported complex in solution, probably due to overloading of catalyst in the core of the star. Sawamoto and co-workers cleverly use a cited “drawback” of ATRP (difficult removal of the metal catalyst) to synthesize a very efficient and highly recyclable nanoreactor. In this case, the residual metal catalyst used to synthesize the nanoreactor by ATRP and is encapsulated and employed as a catalyst for organic reactions. Furthermore, the same star polymer catalysts show high activity, versatility, functionality tolerance, and recyclability as a catalyst in ATRP.

## 1.5 Conclusions

In Chapter I, several research topics relevant to this dissertation have been reviewed. This began with a review of the history and mechanistic aspects of CRP techniques such as RAFT, which is utilized for polymer synthesis throughout all chapters. The application of CRP techniques for the synthesis of self-assembled polymeric nanoreactors has been briefly reviewed.

The stimuli responsive properties that can be introduced in such nanoscale polymeric architectures has also been covered, since this chemistry is utilized in Chapters 2, 3 and 4.

Chapter I conclude with a literature review on catalytic polymeric particles, which provides a relevant introduction to the overall themes of this thesis.

## 1.6 References

- (1) Thurmond, K. B.; Kowalewski, T.; Wooley, K. L. *J. Am. Chem. Soc.* **1996**, 118, 7239.
- (2) Szwarc, M. *Nature*. **1956**, 178, 1168.
- (3) Szwarc, M. *J. Polym. Sci., Part A: Polym. Chem.* **1998**, 36, IX.
- (4) Quirk, R. P.; Lee, B. *Polym. Int.* **1992**, 27, 359.
- (5) Hawker, C. J. *J. Am. Chem. Soc.* **1994**, 116, 11185.
- (6) Hawker, C. J. *Acc. Chem. Res.* **1997**, 30, 373.
- (7) Wang, J. S.; Matyjaszewski, K. *Macromolecules* **1995**, 28, 7901.
- (8) Hawker, C. J.; Barclay, G. G.; Orellana, A.; Dao, J.; Devonport, W. *Macromolecules* **1996**, 29, 5245.
- (9) Chiefari, J.; Chong, Y. K.; Ercole, F.; Krstina, J.; Jeffery, J.; Le, T. P. T.; Mayadunne, R. T. A.; Meijs, G. F.; Moad, C. L.; Moad, G.; Rizzardo, E.; Thang, S. H. *Macromolecules* **1998**, 31, 5559.
- (10) Lowe, A. B.; McCormick, C. L. *Prog. Polym. Sci.* **2007**, 32, 283.
- (11) Perrier, S.; Takolpuckdee, P. *J. Polym. Sci., Part A: Polym. Chem.* **2005**, 43, 5347.
- (12) Moad, G.; Rizzardo, E.; Thang, S. H. *Aust. J. Chem.* **2006**, 59, 669.
- (13) Moad, G.; Rizzardo, E.; Thang, S. H. *Polymer* **2008**, 49, 1079.

- (14) Georges, M. K.; Veregin, R. P. N.; Kazmaier, P. M.; Hamer, G. K. *Macromolecules* **1993**, 26, 2987.
- (15) Hawker, C. J.; Bosman, A. W.; Harth, E. *Chem. Rev.* **2001**, 101, 3661.
- (16) Fischer, H. *Macromolecules* **1997**, 30, 5666.
- (17) Benoit, D.; Chaplinski, V.; Braslau, R.; Hawker, C. J. *J. Am. Chem. Soc.* **1999**, 121, 3904.
- (18) Hawker, C. J.; Hedrick, J. L. *Macromolecules* **1995**, 28, 2993.
- (19) Listigovers, N. A.; Georges, M. K.; Odell, P. G.; Keoshkerian, B. *Macromolecules* **1996**, 29, 8992.
- (20) Couvreur, L.; Lefay, C.; Belleney, J.; Charleux, B.; Guerret, O.; Magnet, S. *Macromolecules* **2003**, 36, 8260.
- (21) Nicolas, J.; Mueller, L.; Dire, C.; Matyjaszewski, K.; Charleux, B. *Macromolecules* **2009**, 42, 4470.
- (22) McHale, R.; Aldabbagh, F.; Zetterlund, P. B. *J. Polym. Sci., Part A: Polym. Chem.* **2007**, 45, 2194.
- (23) Nicolas, J.; Dire, C.; Mueller, L.; Belleney, J.; Charleux, B.; Marque, S. R. A.; Bertin, D.; Magnet, S.; Couvreur, L. *Macromolecules* **2006**, 39, 8274.
- (24) Nicolas, J.; Guillaneuf, Y.; Lefay, C.; Bertin, D.; Gigmes, D.; Charleux, B. *Prog. Polym. Sci.* **2012**. DOI: 10.1016/j.progpolymsci.2012.06.002
- (25) Kato, M.; Kamigaito, M.; Sawamoto, M.; Higashimura, T. *Macromolecules* **1995**, 28, 1721.

- (26) Jakubowski, W.; Min, K.; Matyjaszewski, K. *Macromolecules* **2006**, 39, 39.
- (27) Cao, J.; Chen, J.; Zhang, K. D.; Shen, Q.; Zhang, Y. *Appl. Catal., A* **2006**, 311, 76.
- (28) Sawamoto, M.; Kamigaito, M. *Macromol. Symp.* **1995**, 98, 153.
- (29) Jankova, K.; Chem, X.; Kops, J.; Batsberg, W. *Macromolecules* **1998**, 31, 538.
- (30) Matyjaszewski, K. *Macromolecules* **2012**, 45, 4015.
- (31) Zhang, X.; Xia, J.; Matyjaszewski, K. *Macromolecules* **1998**, 31, 5167.
- (32) Charmot, D. *Polymeric Dispersions: Principles and Applications* **1997**, 335, 79.
- (33) Convertine, A. J.; Ayres, N.; Scales, C. W.; Lowe, A. B.; McCormick, C. L. *Biomacromolecules* **2004**, 5, 1177.
- (34) Moad, B.; Chong, Y. K.; Postma, A.; Rizzardo, E.; Thang, S. H. *Polymer* **2005**, 46, 8458.
- (35) Moad, G.; Rizzardo, E.; Thang, S. H. *Aust. J. Chem.* **2012**, 65, 985.
- (36) Fournier, D.; Hoogenboom, R.; Thijs, H. M. L.; Paulus, R. M.; Schubert, U. S. *Macromolecules* **2007**, 40, 915.
- (37) Wood, M. R.; Duncalf, D. J.; Rannard, S. P.; Perrier, S. *Org. Lett.* **2006**, 8, 553.
- (38) Chong, B.; Moad, G.; Rizzardo, E.; Skidmore, M.; Thang, S. H. *Aust. J. Chem.* **2006**, 59, 755.
- (39) Chong, Y. K.; Moad, G.; Rizzardo, E.; Thang, S. H. *Macromolecules* **2007**, 40, 4446.



- (40) Moughton, A. O.; Stubenrauch, K.; O'Reilly, R. K. *Soft Matter* **2009**, 5, 2361.
- (41) Postma, A.; Davis, T. P.; Moad, G.; O'Shea, M. S. *Macromolecules* **2005**, 38, 5371.
- (42) Moad, G.; Rizzardo, E.; Thang, S. H. *Polym. Int.* **2011**, 60, 9.
- (43) Benaglia, M.; Chiefari, J.; Chong, Y. K.; Moad, G.; Rizzardo, E.; Thang, S. H. *J. Am. Chem. Soc.* **2009**, 131, 6914.
- (44) Benaglia, M.; Chen, M.; Chong, Y. K.; Moad, G.; Rizzardo, E.; Thang, S. H. *Macromolecules* **2009**, 42, 9384.
- (45) Kim, Y.; Liemmawal, E. D.; Pourgholami, M. H.; Morris, D. L.; Stenzel, M. H. *Macromolecules* **2012**, 45, 5451.
- (46) Torchilin, V. P. *J. Control. Release* **2001**, 73, 137.
- (47) Mai, Y.; Eisenberg, A. *Chem. Soc. Rev.* **2012**, 41, 5969.
- (48) Blanz, A.; Armes, S. P.; Ryan, A. J. *Macromol. Rapid Commun.* **2009**, 30, 267.
- (49) Read, E. S.; Armes, S. P. *Chem. Commun.* **2007**, 3021.
- (50) Israelachvili, J. N.; Mitchell, D. J.; Ninham, B. W. *J. Chem. Soc., Faraday Trans.* **1976**, 72, 1525.
- (51) Wooley, K. L. *J. Polym. Sci., Part A: Polym. Chem.* **2000**, 38, 1397.
- (52) Zhang, L. F.; Eisenberg, A. *Science* **1995**, 268, 1728.
- (53) Nicolai, T.; Colombani, O.; Chassenieux, C. *Soft Matter* **2010**, 6.

- (54)Liu, S. Y.; Weaver, J. V. M.; Tang, Y. Q.; Billingham, N. C.; Armes, S. P.; Tribe, K. *Macromolecules* **2002**, 35, 6121.
- (55)Stenzel, M. H. *Macromol. Rapid Commun.* **2009**, 30, 1603.
- (56)Jeong, B.; Gutowska, A. *Trends Biotechnol.* **2002**, 20, 305.
- (57)Forster, S.; Antonietti, M. *Adv. Mater.* **1998**, 10, 195.
- (58)Kasgoz, H.; Ozgumus, S.; Orbay, M. *Polymer* **2003**, 44, 1785.
- (59)Haag, R. *Angew. Chem., Int. Ed.* **2004**, 43, 278.
- (60)Lutz, J. F. *Polym. Int.* **2006**, 55, 979.
- (61)Jiang, J. Q.; Tong, X.; Morris, D.; Zhao, Y. *Macromolecules* **2006**, 39, 4633.
- (62)Dai, S.; Ravi, P.; Tam, K. C. *Soft Matter* **2008**, 4, 435.
- (63)Andre, X.; Zhang, M. F.; Muller, A. H. E. *Macromol. Rapid Commun.* **2005**, 26, 558.
- (64)Wang, D.; Wu, T.; Wan, X. J.; Wang, X. F.; Liu, S. Y. *Langmuir* **2007**, 23, 11866.
- (65)Dimitrov, I.; Trzebicka, B.; Muller, A. H. E.; Dworak, A.; Tsvetanov, C. B. *Prog. Polym. Sci.* **2007**, 32, 1275.
- (66)Schild, H. G. *Prog. Polym. Sci.* **1992**, 17, 163.
- (67)Housni, A.; Narain, R. *Eur. Polym. J.* **2007**, 43, 4344.
- (68)Liu, B.; Perrier, S. *J. Polym. Sci., Part A: Polym. Chem.* **2005**, 43, 3643.

- (69)Eeckman, F.; Moes, A. J.; Amighi, K. *Int. J. Pharm.* **2004**, 273, 109.
- (70)Schilli, C. M.; Zhang, M. F.; Rizzardo, E.; Thang, S. H.; Chong, Y. K.; Edwards, K.; Karlsson, G.; Muller, A. H. E. *Macromolecules* **2004**, 37, 7861.
- (71)Arotcarena, M.; Heise, B.; Ishaya, S.; Laschewsky, A. *J. Am. Chem. Soc.* **2002**, 124, 3787.
- (72)Virtanen, J.; Arotcarena, M.; Heise, B.; Ishaya, S.; Laschewsky, A.; Tenhu, H. *Langmuir* **2002**, 18, 5360.
- (73)Nuopponen, M.; Ojala, J.; Tenhu, H. *Polymer* **2004**, 45, 3643.
- (74)Hong, C. Y.; You, Y. Z.; Pan, C. Y. *J. Polym. Sci., Part A: Polym. Chem.* **2004**, 42, 4873.
- (75)Hales, M.; Barner-Kowollik, C.; Davis, T. P.; Stenzel, M. H. *Langmuir* **2004**, 20, 10809.
- (76)Lutz, J.-F.; Akdemir, Ö.; Hoth, A. *J. Am. Chem. Soc.* **2006**, 128, 13046.
- (77)Fujishige, S.; Kubota, K.; Ando, I. *J. Phys. Chem.* **1989**, 93, 3311.
- (78)Chong, Y. K.; Le, T. P. T.; Moad, G.; Rizzardo, E.; Thang, S. H. *Macromolecules* **1999**, 32, 2071.
- (79)Zhong, M.; Matyjaszewski, K. *Macromolecules* **2011**, null.
- (80)Bories-Azeau, X.; Armes, S. P.; van den Haak, H. J. W. *Macromolecules* **2004**, 37, 2348.
- (81)Butun, V.; Liu, S.; Weaver, J. V. M.; Bories-Azeau, X.; Cai, Y.; Armes, S. P. *React. Funct. Polym.* **2006**, 66, 157.
- (82)Pfau, A.; Hössel, P.; Vogt, S.; Sander, R.; Schrepp, W. *Macromol. Symp.* **1998**, 126, 241.

- (83) Dincer, S.; Turk, M.; Piskin, E. *Gene Ther.* **2005**, *12*, 139.
- (84) Samal, S. K.; Dash, M.; Van Vlierberghe, S.; Kaplan, D. L.; Chiellini, E.; van Blitterswijk, C.; Moroni, L.; Dubruel, P. *Chem. Soc. Rev.* **2012**.
- (85) Lee, H.; Son, S. H.; Sharma, R.; Won, Y.-Y. *J. Phys. Chem. B* **2011**, *115*, 844.
- (86) Merrifield, R. B. *J. Am. Chem. Soc.* **1963**, *85*, 2149.
- (87) Madhavan, N.; Jones, C. W.; Weck, M. *Acc. Chem. Res.* **2008**, *41*, 1153.
- (88) Clapham, B.; Reger, T. S.; Janda, K. D. *Tetrahedron* **2001**, *57*, 4637.
- (89) Hodge, P. *Chem. Soc. Rev.* **1997**, *26*, 417.
- (90) Sherrington, D. C. *J. Polym. Sci., Part A: Polym. Chem.* **2001**, *39*, 2364.
- (91) Nuyken, O.; Persigehl, P.; Weberskirch, R. *Macromol. Symp.* **2002**, *177*, 163.
- (92) Mason, B. P.; Hira, S. M.; Strouse, G. F.; McQuade, D. T. *Org. Lett.* **2009**, *11*, 1479.
- (93) Chi, Y. G.; Scroggins, S. T.; Frechet, J. M. J. *J. Am. Chem. Soc.* **2008**, *130*, 6322.
- (94) Matyjaszewski, K.; Xia, J. H. *Chem. Rev.* **2001**, *101*, 2921.
- (95) Gruttadauria, M.; Giacalone, F.; Noto, R. *Adv. Synth. Catal.* **2009**, *351*, 33.
- (96) Shapiro, N.; Vigalok, A. *Angew. Chem., Int. Ed.* **2008**, *47*, 2849.
- (97) Narayan, S.; Muldoon, J.; Finn, M. G.; Fokin, V. V.; Kolb, H. C.; Sharpless, K. B. *Angew. Chem., Int. Ed.* **2005**, *44*, 3275.

- (98)Vriezema, D. M.; Aragonés, M. C.; Elemans, J.; Cornelissen, J.; Rowan, A. E.; Nolte, R. J. *M. Chem. Rev.* **2005**, *105*, 1445.
- (99)Helms, B.; Fréchet, J. M. J. *Adv. Synth. Catal.* **2006**, *348*, 1125.
- (100)Liu, Y.; Wang, Y.; Wang, Y.; Lu, J.; Piñón, V.; Weck, M. J. *Am. Chem. Soc.* **2011**, *133*, 14260.
- (101)Manabe, K.; Iimura, S.; Sun, X.-M.; Kobayashi, S. *J. Am. Chem. Soc.* **2002**, *124*, 11971.
- (102)Arumugam, S.; Vutukuri, D. R.; Thayumanavan, S.; Ramamurthy, V. *J. Am. Chem. Soc.* **2005**, *127*, 13200.
- (103)Gall, B.; Bortenschlager, M.; Nuyken, O.; Weberskirch, R. *Macromol. Chem. Phys.* **2008**, *209*, 1152.
- (104)Persigehl, P.; Jordan, R.; Nuyken, O. *Macromolecules* **2000**, *33*, 6977.
- (105)Zarka, M. T.; Nuyken, O.; Weberskirch, R. *Chem. Eur. J.* **2003**, *9*, 3228.
- (106)Ievins, A. D.; Wang, X. F.; Moughton, A. O.; Skey, J.; O'Reilly, R. K. *Macromolecules* **2008**, *41*, 2998.
- (107)Rossbach, B. M.; Leopold, K.; Weberskirch, R. *Angew. Chem., Int. Ed.* **2006**, *45*, 1309.
- (108)Ge, Z. S.; Xie, D.; Chen, D. Y.; Jiang, X. Z.; Zhang, Y. F.; Liu, H. W.; Liu, S. Y. *Macromolecules* **2007**, *40*, 3538.
- (109)O'Lenick, T. G.; Jiang, X.; Zhao, B. *Polymer* **2009**, *50*, 4363.

- (110) Lu, A.; Smart, T. P.; Epps, T. H.; Longbottom, D. A.; O'Reilly, R. K. *Macromolecules* **2011**, *44*, 7233.
- (111) Wang, Y.; Wei, G. W.; Zhang, W. Q.; Jiang, X. W.; Zheng, P. W.; Shi, L. Q.; Dong, A. J. *J. Mol. Catal. A: Chem.* **2007**, *266*, 233.
- (112) O'Reilly, R. K.; Hawker, C. J.; Wooley, K. L. *Chem. Soc. Rev.* **2006**, *35*, 1068.
- (113) Broadwater, S. J.; Roth, S. L.; Price, K. E.; Kobaslija, M.; McQuade, D. T. *Org. Biomol. Chem.* **2005**, *3*, 2899.
- (114) Tietze, L. F. *Chem. Rev.* **1996**, *96*, 115.
- (115) Cohen, B. J.; Kraus, M. A.; Patchornik, A. J. *Am. Chem. Soc.* **1981**, *103*, 7620.
- (116) Scroggins, S. T.; Chi, Y.; Fréchet, J. M. J. *Angew. Chem., Int. Ed.* **2010**, *49*, 2393.
- (117) Helms, B.; Guillaudeu, S. J.; Xie, Y.; McMurdo, M.; Hawker, C. J.; Frechet, J. M. J. *Angew. Chem., Int. Ed.* **2005**, *44*, 6384.
- (118) Gao, H. *Macromol. Rapid Commun.* **2012**, *33*, 722.
- (119) Bosman, A. W.; Vestberg, R.; Heumann, A.; Fréchet, J. M. J.; Hawker, C. J. *J. Am. Chem. Soc.* **2002**, *125*, 715.
- (120) Gregory, A.; Stenzel, M. H. *Prog. Polym. Sci.* **2012**, *37*, 38.
- (121) Matyjaszewski, K.; Tsarevsky, N. V. *Nature Chem.* **2009**, *1*, 276.
- (122) Blencowe, A.; Tan, J. F.; Goh, T. K.; Qiao, G. G. *Polymer* **2009**, *50*, 5.

(123)Baek, K.-Y.; Kamigaito, M.; Sawamoto, M. *Macromolecules* **2002**, 35, 1493.

(124)Terashima, T.; Kamigaito, M.; Baek, K.-Y.; Ando, T.; Sawamoto, M. *J. Am. Chem. Soc.* **2003**, 125, 5288.

(125)Terashima, T.; Ouchi, M.; Ando, T.; Sawamoto, M. *J. Polym. Sci., Part A: Polym. Chem.* **2010**, 48, 373.

## **Chapter 2: Synthesis of DMAP-Functionalized Organocatalytic Nanoreactors**



## 2.1 Abstract:

Novel core-reactive spherical polymeric micelles have been synthesized using Reversible Addition-Fragmentation Chain Transfer (RAFT) techniques. These nanostructures have 4-dimethylaminopyridine (DMAP) functionality selectively located within their hydrophobic domain to afford base catalysis of small molecules. Two DMAP monomers have been explored for copolymerization with styrene by RAFT. One of these monomers has been successfully copolymerized with styrene with very good control over the molecular weight and polydispersity index. The chain extension of this random copolymer with NIPAM has been studied to form DMAP functionalized thermo responsive amphiphilic block copolymers and self-assembled in solution to form the targeted micelles.

The new synthetic methodologies developed will provide the basis for the further development of a range of polymeric stimuli-responsive supported catalysts for utilization in organic and/or polymer synthesis.

## 2.2 Introduction

Supramolecular self-assembly techniques have provided a versatile means by which to selectively assemble polymer molecules into well-defined three dimensional core-shell nanostructures.<sup>1-4</sup> The simplest method for the assembly of synthetic polymer chains into nanoparticles is the solution formation of spherical polymer micelles. Conventional micelles based on hydrophilic-hydrophobic diblock copolymers have been extensively reported.<sup>5-8</sup>

The synthesis of block copolymers based on poly(N-isopropylacrylamide) (PNIPAM) has received tremendous attention.<sup>9,10</sup> It has been so widely studied mainly because of the sharpness of its phase transition, the closeness of its lower critical solution temperature (LCST), about 32 °C, to physiological temperature, and the ease by which its LCST is varied by copolymerization, addition of salts or surfactants to the polymer solution.<sup>11</sup> Well defined block copolymers based on PNIPAM have been synthesized to afford smart amphiphilic block copolymers with a switchable hydrophilic-hydrophobic segment of PNIPAM and a second responsive or non-responsive hydrophobic block. Through this combination, different types of water soluble block copolymers can be achieved: hydrophobic-hydrophilic, hydrophilic-hydrophobic, double hydrophilic or double hydrophobic.<sup>12-17</sup>

The development of novel catalytic functional polymeric nanostructures is of great interest and application to many different aspects of chemistry.<sup>18-23</sup> The advantages of such nanostructures over traditional supports are numerous. The specific groups within the hydrophobic core, which can be protected from hydrolysis or degradation by the surrounding hydrophilic corona, allows for the selective reaction of the reagents within this central domain in an overall hydrophilic or aqueous environment.<sup>24-26</sup> These assemblies have been suggested to combine the advantages of heterogeneous and homogeneous catalysis because of their solubility and facile catalyst recovery using ultrafiltration or precipitation processes.<sup>27,28</sup>

A strategy that has successfully been employed is the synthesis of functionalized monomers, which can be incorporated selectively into the hydrophobic domain *via* copolymerization to allow for the placement of reactive handles throughout the core region.<sup>29</sup> Amphiphilic block copolymers were self-assembled into micelles and shell cross-linked nanoparticles with

incorporation of acetylene functional groups within the core, enabling click chemistry to be performed in the core domain. The functionality embedded and dispersed throughout the core of polymeric micelles has been demonstrated to be available and reactive toward further chemical modification.<sup>29</sup>

An alternative approach recently reported uses a single site active catalyst generated inside the polymeric microcapsule.<sup>30</sup> Ievins *et al.* reported the synthesis of novel core reactive spherical micelles and nanoparticles with terpyridine functionality within the hydrophobic core and further modification by metal complexation within this domain to afford metal functionalized polymer nanostructures. The reactivity of this metal complex within the nanostructures was found to be an active catalyst for the “click” reaction of azido and alkynyl functionalized small molecules and demonstrate a higher activity than resin-supported catalysts.

DMAP (Figure 2.1) is a useful nucleophilic catalyst which can be used in a variety of reactions such as esterifications with anhydrides, the Baylis-Hillman reaction, hydrosilylations, tritylation, the Steglich rearrangement, Staudinger synthesis of  $\beta$ -lactams and many more.<sup>31-34</sup>

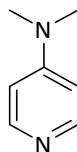


Figure 2.1: Structure of DMAP

In 2005 Frechet *et al.* demonstrated that DMAP modified monomers can be copolymerized, assembled and encapsulated for applications in heterogeneous catalysis.<sup>35</sup> These capsules can be recovered after reaction and yield higher activities in acylation reactions than linear polymers or other solid supports. In this work, the authors report a one-pot reaction cascade

performed with two different star polymers (unimolecular micelles), each containing a different catalytic group confined in its core. To demonstrate the synthetic utility of site isolation they explore the otherwise incompatible cascade reaction of acid and base catalysts.

In 2006 the group of McQuade published the first example of catalysis using encapsulated linear polymer-catalyst conjugates. The copolymerization of a DMAP modified monomer with styrene and encapsulation by interfacial polymerization gives a DMAP functionalized microcapsule that shows higher activity for DMAP-catalyzed acylation than that supported on cross-linked polystyrene.<sup>36</sup> Further work by McQuade's group reported the successful encapsulation of an amino catalyst *via* interfacial polymerization of an oil-in-water emulsion. The encapsulated amino catalyst showed greater activity than a comparable solid-supported catalyst, and its utility was demonstrated by applying it to a tandem reaction sequence involving an otherwise incompatible Lewis acid catalyst and nickel catalyst.<sup>36-38</sup>

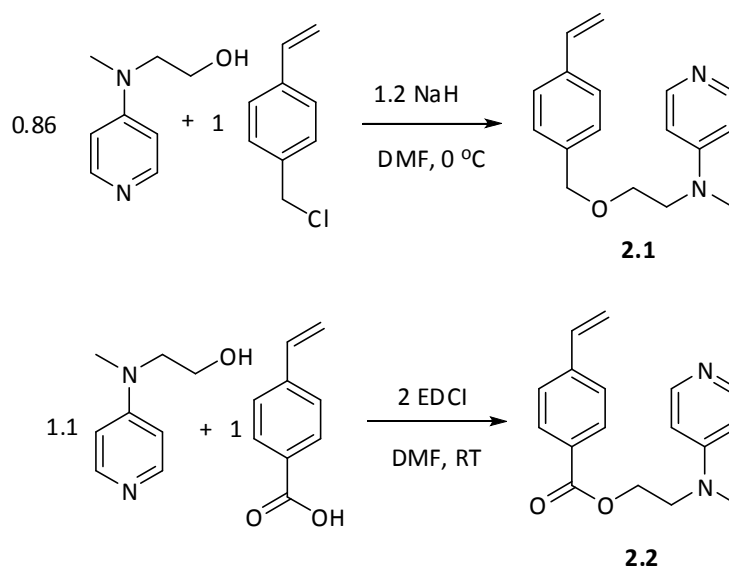
The concept of micelles as *pseudo* homogeneous catalyst supports has been explored using recoverable and responsive polymers such as PNIPAM.<sup>39,40</sup> By embedding catalytic functionality within the core domain it is protected and removed from the surrounding reactive environment. Upon application of an external stimulus, such nanospheres will allow for the selective and controlled release of the catalytic functionality. Over the last 10 years, RAFT polymerization has evolved into an extremely powerful synthetic tool for polymer synthesis.<sup>41</sup> The versatility of RAFT, with respect to reaction conditions and monomer class, facilitates the preparation of materials with well-defined molecular characteristics.<sup>41-44</sup>

The overall objective of our work is to synthesize new polymer supported catalytic micelles with stimuli-responsive properties, where DMAP is selectively supported in the hydrophobic

core. These micelles will act as nanoreactors to carry out catalysis of hydrophobic organic molecules in aqueous media. The temperature responsive PNIPAM shell is envisioned to facilitate the recovery of the catalyst without the need for organic solvents.<sup>18</sup>

## 2.3 Results and discussion

### 2.3.1 Monomer synthesis



Scheme 2.1: Synthesis of DMAP functionalized monomers **2.1** and **2.2**

Styrene based polymers chain extended with a water-soluble block are known to form kinetically frozen micelles in water.<sup>45,46</sup> We hypothesize that the confinement of the catalytic moiety in a completely hydrophobic glassy core will create a water-free environment and mimic non polar hydrophobic conditions for efficient catalysis reactions.

In order to obtain stable micelles with the catalytic functionality locked into the hydrophobic core, two styrenic monomers containing DMAP were synthesized, **2.1** and **2.2** (Scheme 2.1).

The synthesis of **2.1** has been reported previously.<sup>47</sup> Using a similar strategy, to that reported in

the literature, **2.1** was synthesized by the reaction of commercially available vinylbenzyl chloride and 4-(*N*-methyl-*N*-(2-hydroxyethyl)amino)pyridine (which was prepared by a literature procedure)<sup>48</sup> with NaH. Monomer **2.1** was isolated after column chromatography (CHCl<sub>3</sub> with 10 % MeOH) as a dark yellow liquid in a 50% yield (Figure 2.2).

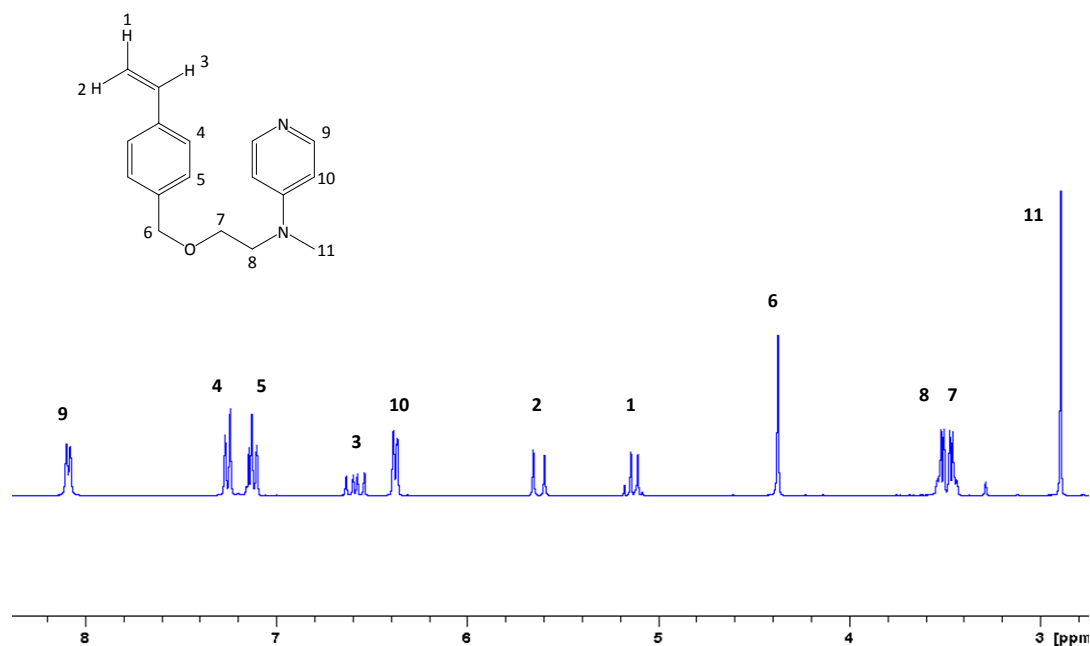


Figure 2.2: <sup>1</sup>H NMR spectrum of monomer **2.1** in CDCl<sub>3</sub>

This synthesis requires the use of pyrophoric NaH and the reaction success was found to depend strongly on the concentration of the reactive mixture. When adding the vinylbenzyl chloride solution under nitrogen to the reaction, the mixture became black forming undesirable side products due to the high reactivity of the vinylbenzyl chloride. This effect can be minimized by using a highly diluted solution (2 mL of CHCl<sub>3</sub> per 1 mL of vinylbenzyl chloride) and cooling the reaction with an ice bath. In addition, because of the pyrophoric properties of the NaH, anhydrous conditions were required. Given these difficulties, the synthesis of a second new DMAP functionalized monomer **2.2** was investigated.

Monomer **2.2** was synthesized from commercially available vinyl benzoic acid and 4-(*N*-methyl-*N*-(2-hydroxyethyl)amino)pyridine at room temperature by established procedures using Steglich esterification route.<sup>49</sup> After 2 days reaction, the mixture was washed with brine and dried over MgSO<sub>4</sub>. The product was isolated as a white powder in a 60% yield. The monomer **2.2** was fully characterized by <sup>13</sup>C and <sup>1</sup>H NMR spectroscopy (Figure 2.3), UV and mass spectrometry.

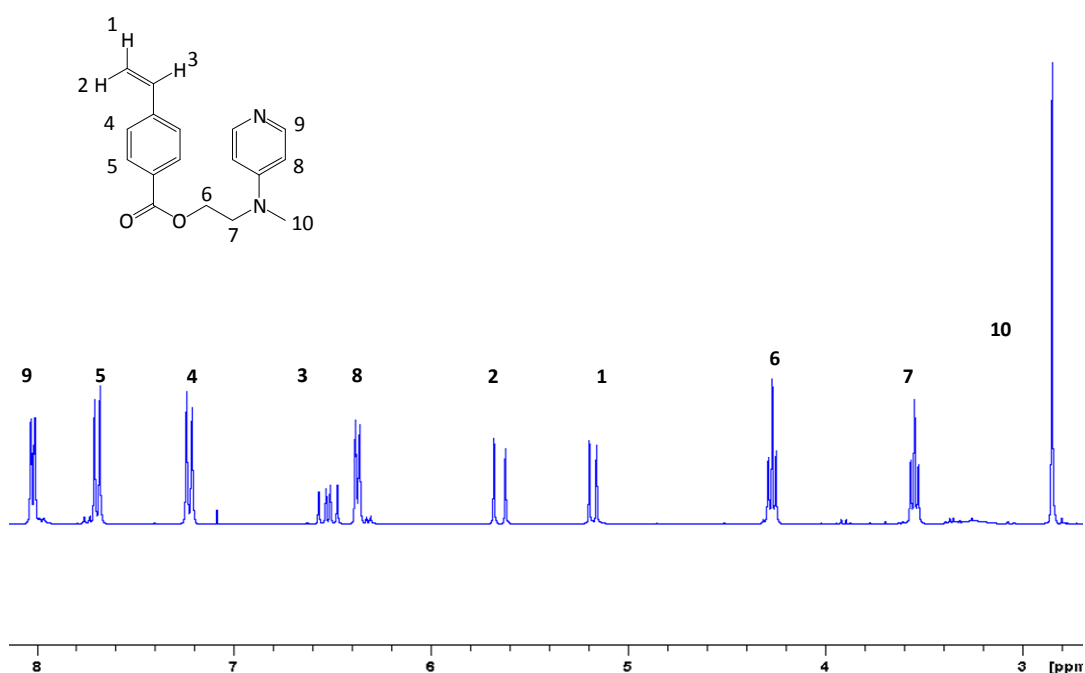


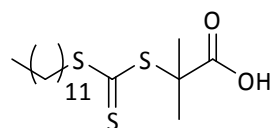
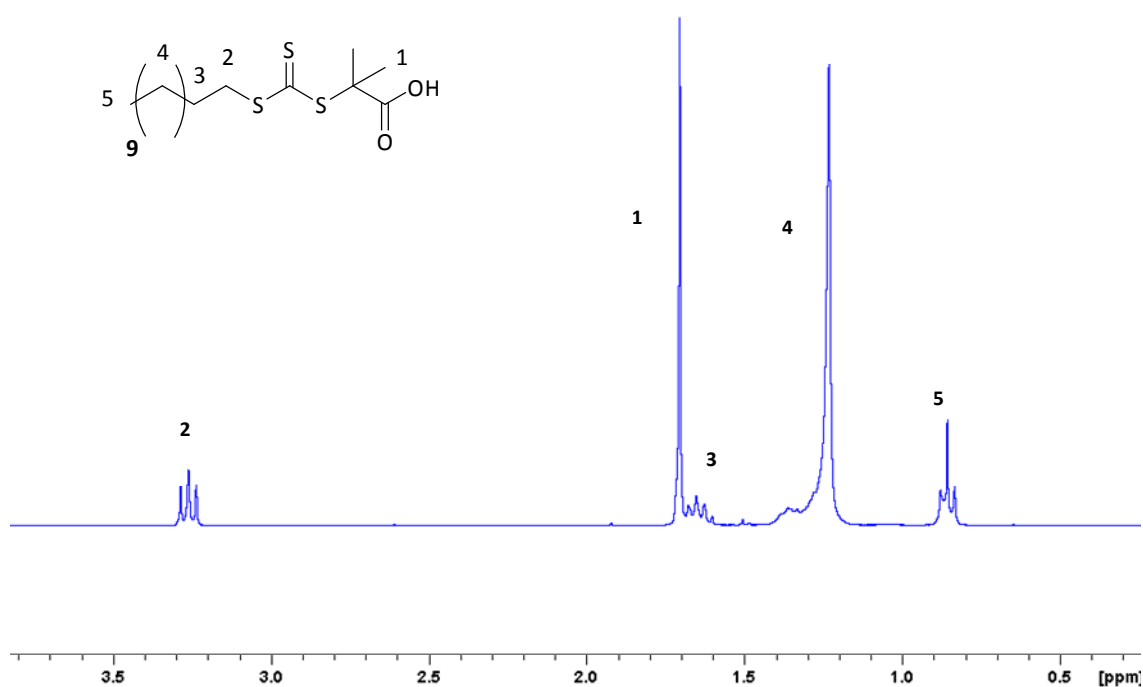
Figure 2.3: <sup>1</sup>H NMR spectrum of **2.2** in CDCl<sub>3</sub>

### 2.3.2 Copolymerization with styrene

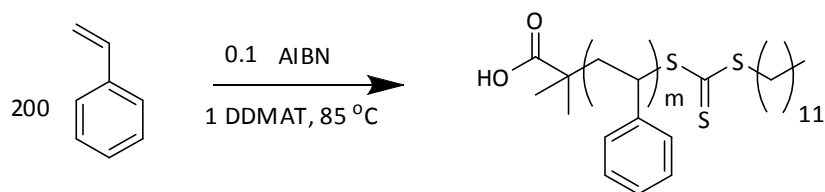
The copolymerization of monomers **2.1** and **2.2** with styrene was explored by RAFT using S-1-dodecyl-S'-( $\alpha,\alpha'$ -dimethyl- $\alpha''$ -acetic acid)trithiocarbonate DDMAT (**2.3**,

Figure 2.4) as a chain transfer agent (CTA). DDMAT is a commonly used RAFT agent, easy to synthesize, which has been demonstrated to mediate the polymerization of a wide range of

monomers including acrylates and styrenes.<sup>50-56</sup> CTA **2.3** was synthesized according with a literature procedure by reaction of dodecanethiol, CS<sub>2</sub>, 2-bromoisobutyric acid and K<sub>3</sub>PO<sub>4</sub> in acetone at room temperature for 1 day.<sup>57</sup> The clean product was isolated in a 62% yield after column chromatography, and characterized by <sup>1</sup>H and <sup>13</sup>C NMR spectroscopy (Figure 2.5).

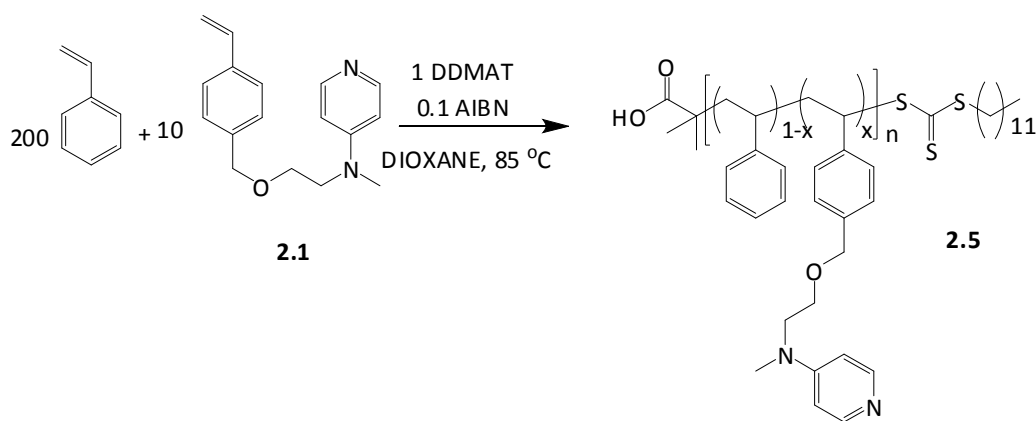
Figure 2.4: Structure of DDMAT (**2.3**)Figure 2.5: <sup>1</sup>H NMR spectrum of **2.3** in CDCl<sub>3</sub>



Scheme 2.2: Synthesis of polystyrene **2.4** using DDMAT

CTA **2.3** was used in the RAFT polymerization of styrene. After 24 hours at 85 °C the reaction achieve 50 % conversion, calculated by  $^1\text{H}$  NMR comparing the vinyl peaks from the monomer at *ca.* 6 ppm (3x1H) with the backbone peaks from the polymer at *ca.* 1.5 ppm (3H). After purification by precipitation in MeOH, the polymer obtained **2.4** had a DP of 107 ( $M_n = 11$  kDa), calculated by long acquisition  $^1\text{H}$  NMR in  $\text{CDCl}_3$  comparing the integration of the CTA protons (3H at 0.85 ppm) to the integration of the polystyrene protons (5H from 6.3 to 7.4 ppm). The polydispersity of the resultant polymer was 1.17 and the molecular weight was 10.2 kDa by THF SEC calibrated with PS standards.

Using similar conditions as reported for **2.4**, the copolymerizations of **2.1** and **2.2** with styrene were explored in detail. A kinetic study of the copolymerizations using DDMAT was performed in order to gain further polymerization data regarding the degree of living behavior and rate of polymerization. In this case, dioxane was used as a solvent in order to dissolve monomer **2.1**. This kinetic study was done using an intended 5 % incorporation of **2.1** or **2.2**, with a view towards an overall target DP of *ca.*100.

Scheme 2.3: Preparation of the random copolymer **2.5***Copolymerization of **2.1** with Styrene:*

To explore the kinetics of this reaction, different samples were taken under nitrogen at different times and analyzed by THF SEC and conversion  $^1\text{H}$  NMR in  $\text{CDCl}_3$ . The results are shown in Table 2.1. The conversion of the monomers was determined by  $^1\text{H}$  NMR spectroscopy by comparing the signals from both monomers with the signals from the resultant polymer as shown in Figure 2.6. Given the close proximity of the monomer signals and the new broad peaks of the polymer formed, values given for the conversion of the monomers at different times using this method has an associated error. This error will increase with the degree of polymerization hence the values given for the kinetic measurements are only a close estimation of the real conversion of the monomer.

The degree of incorporation of the functional monomer could be very easily determined by examination of the long acquisition  $^1\text{H}$  NMR spectrum of the resultant polymer and comparison of the signals attributable to the monomer **2.1** moiety at *ca.* 4.4 ppm (2H) and 3.7

ppm (2H), and the aromatic signals for the polystyrene at *ca.* 7 ppm with those for the DDMAT at 0.85 ppm (CH<sub>3</sub>) (Figure 2.7).

<b>t (h)</b>	<b>% conv St</b>	<b>% incorp 2.1</b>	<b>M<sub>n</sub> NMR (kDa)</b>	<b>M<sub>n</sub> SEC (kDa)</b>	<b>M<sub>w</sub>/M<sub>n</sub></b>
1.5	12	5	3.1	3.7	1.21
3.5	22	5	5.4	7.3	1.18
5.5	28	5	6.9	9.7	1.20
7.5	31	5	7.6	11.0	1.22
9.5	32	5	8.0	11.3	1.24
12	34	4	8.3	11.2	1.29
36	43	5	10.4	14.8	1.38
46	43	5	10.5	16.0	1.40
60	47	5	11.4	16.6	1.45
92	52	5	12.5	19.4	1.54
116	56	5	13.5	21.5	1.75

Table 2.1: Data of polymerization kinetics for **2.5**. Polymerization carried out in dioxane. Ratio of [Styrene]:[2.1]:[CTA] 200:10:1. M<sub>n</sub> NMR and conversions calculated by <sup>1</sup>H NMR in CDCl<sub>3</sub>. Samples were measured by SEC (THF) analysis using polystyrene standards.

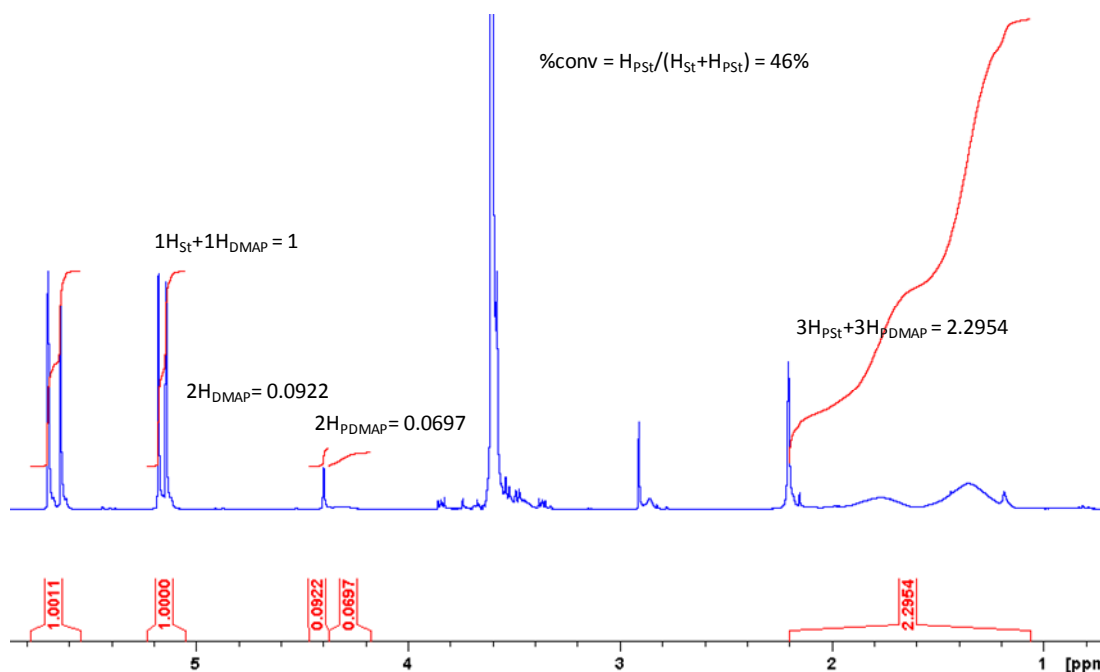


Figure 2.6: Example of a  $^1H$  NMR spectrum in  $CDCl_3$  used to assess conversion for **2.1**/styrene polymerization.

An example of the conversion calculations is shown.

The resultant polymer contained the expected 5 % incorporation of monomer **2.1**. The percentage of **2.1** incorporated in the polymer at different times (calculated by conversion  $^1H$  NMR) remains constant and the polymerization rate is similar to that for styrene suggesting the formation of random copolymers.

In order to confirm that a polymerization is controlled and *pseudo*-living, the plot of  $\ln([M]_0/[M])$  versus polymerization time should be linear, and the molecular weight of the growing polymer should increase linearly with conversion.

Figure 2.8 shows that the kinetic plot was linear until *ca.* 30% conversion, which indicates a controlled radical polymerization is occurring with a constant radical concentration up until this point. No evidence of an induction period was observed.

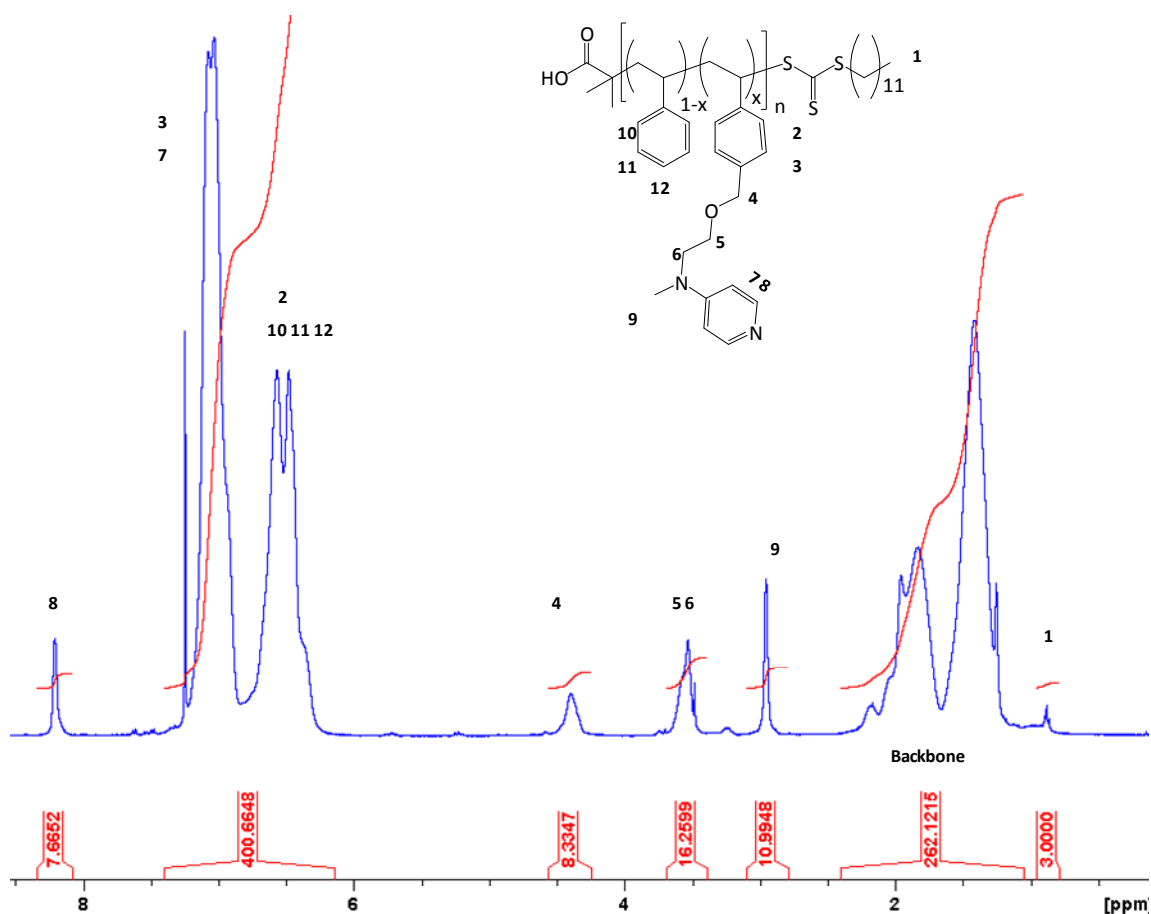


Figure 2.7: Example of a long acquisition  $^1\text{H}$  NMR spectrum in  $\text{CDCl}_3$  to determine the experimental DP and % incorporation of **2.1**.

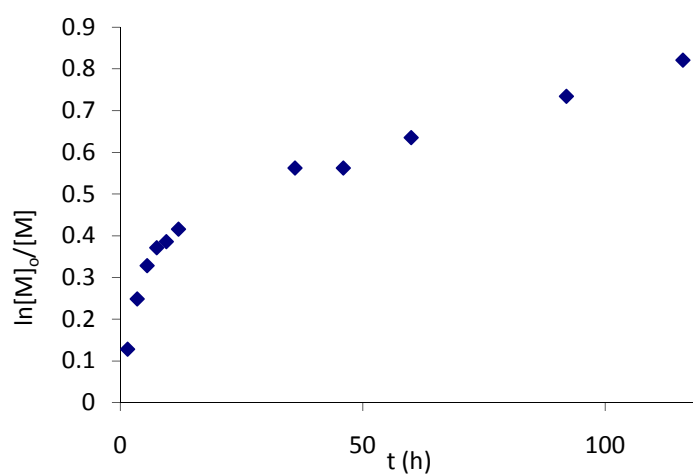


Figure 2.8: Kinetic plot for polymerization of **2.5**

Molecular weights were calculated by conversion  $^1\text{H}$  NMR spectroscopy as shown in previously. The plot of experimental molecular weight *versus* conversion (Figure 2.9) demonstrates the linear dependence of molecular weight with conversion. However, increasing polydispersity indexes with increasing molecular weight and bimodal SEC traces are observed. The different values obtained for the  $M_n$  values calculated by  $^1\text{H}$  NMR spectroscopy (theoretical) and SEC analysis (experimental) might be due to the calibration of the instrument with PS standards; however, bimodal traces were observed after 8 hours reaction (Figure 2.10) at around 30 % conversion which also induces deviations in the  $M_n$  compared to theoretical values.

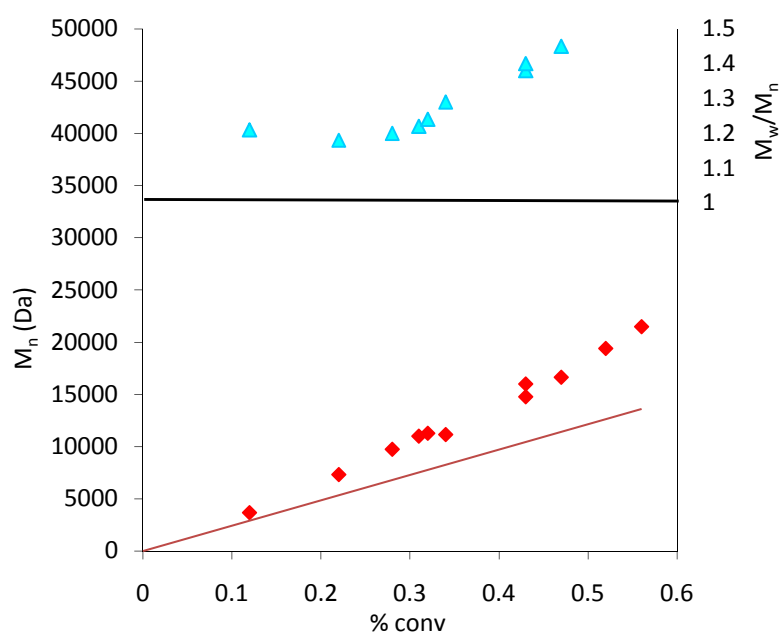


Figure 2.9: Plot of  $M_n$  from SEC data (red squares) versus conversion ( $M_n$  theoretical) from  $^1\text{H}$  NMR spectroscopy (solid line) and Polydispersities for **2.5**.

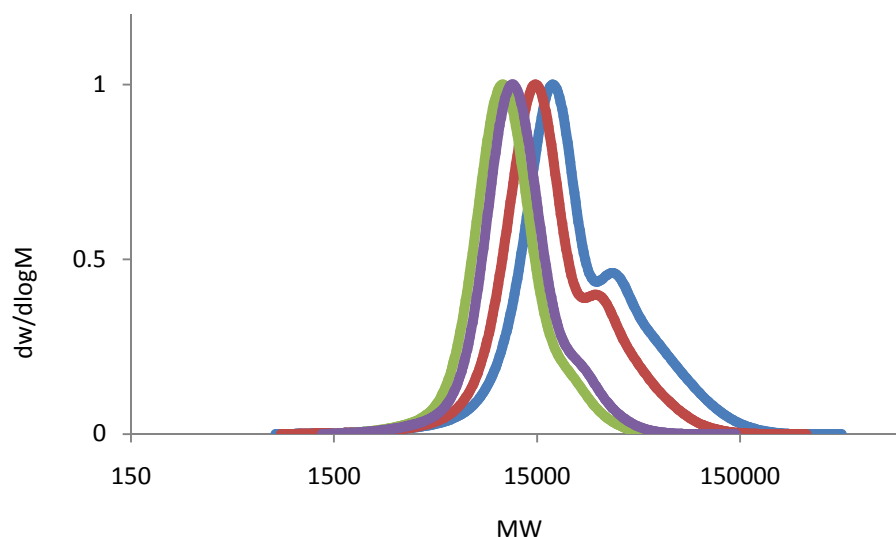


Figure 2.10: From right to left, SEC traces (RI detector) of the different samples of **2.5** taken at 3.5, 5.5, 7.5, 46 and 92 hours.

One of the reasons for a bimodal trace in the SEC could be the loss of the trithiocarbonate end group by radical coupling in some polymer chains. This can be examined by comparing the UV signal with the RI response for the same sample using both detectors in the SEC. The thiocarbonyl group (polymer end group) absorbs at 309 nm in the UV so if the end group is still present, at that wavelength both traces should overlap (Figure 2.11).



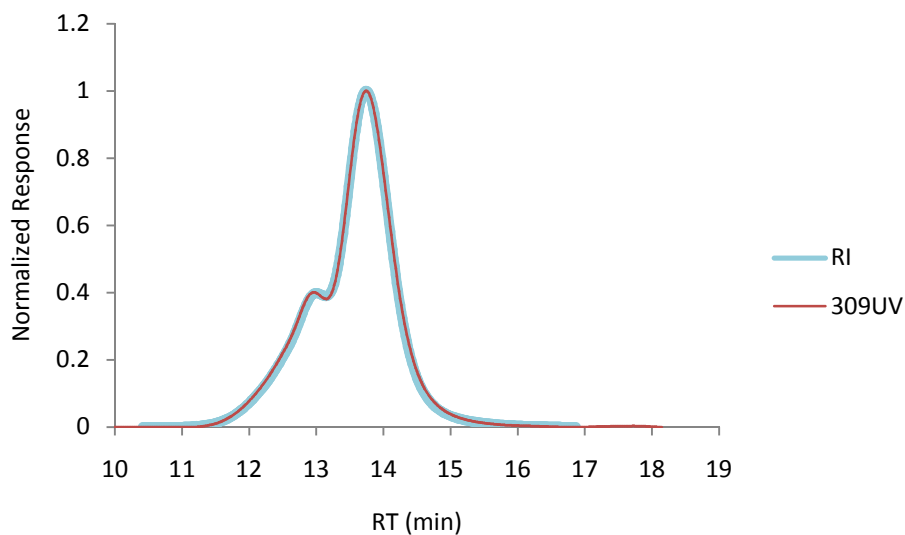
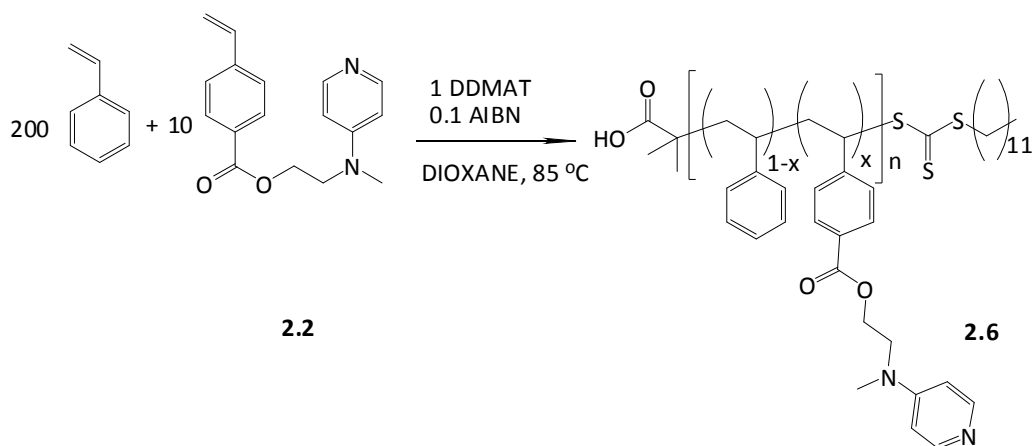


Figure 2.11: Overlay of UV309 (red) and RI (blue) signals from the THF SEC analysis of polymer **2.5** taken at 46 hours.

The overlay of the UV and RI traces proves that the trithiocarbonyl end group is still present in the higher molecular weight polymer (left). Further studies would need to be carried out to be able to explain this data. Given the difficulties found for the polymerization and synthesis of this monomer this route was not further investigated.

*Copolymerization of monomer **2.2** with Styrene:*



Scheme 2.4: Preparation of random copolymer **2.6**.

<b>t (h)</b>	<b>% conv St</b>	<b>% incorp 2.2</b>	<b>M<sub>n</sub> (kDa)</b>	<b>NMR</b>	<b>M<sub>n</sub>SEC (kDa)</b>	<b>M<sub>w</sub>/M<sub>n</sub></b>
1.5	16	9	4.4		4.4	1.18
3.5	25	8	6.9		7.2	1.15
5.5	30	9	8.1		8.6	1.13
7.5	35	8	9.4		9.5	1.12
9.5	36	8	9.6		9.9	1.13
12	40	8	10.6		11.9	1.16
24	46	8	12.0		13.5	1.16
36	48	8	12.6		14.3	1.15
46	53	7	13.7		15.5	1.16
60	55	7	14.1		15.6	1.15
92	63	6	15.9		17.7	1.16

Table 2.2: Data of polymerization kinetics for **2.6**. Polymerization carried out in dioxane. Ratio of

[Styrene]:[**2.2**]:[CTA] 200:10:1. M<sub>n</sub> NMR and conversions calculated by <sup>1</sup>H NMR in CDCl<sub>3</sub>. Samples were measured by SEC (THF) analysis using polystyrene standards.

Kinetic studies of the polymerization of **2.2** with styrene were carried out under the same conditions as **2.1**. Samples were taken from the polymerization ampoule at different times and analyzed by THF SEC and <sup>1</sup>H NMR spectroscopy in CDCl<sub>3</sub> (Table 2.2).

In the same way as for **2.5**, the conversion of the monomers was determined by <sup>1</sup>H NMR by comparing the signals from both monomers with the signals from the resultant polymer as shown in Figure 2.12. Given the higher rate of polymerization for the monomer **2.2** than styrene, there is a higher than predicted incorporation of the functional monomer at low

conversion. Hence, the polymers have a gradient type structure and contain significantly more than the expected 5% of **2.2**.

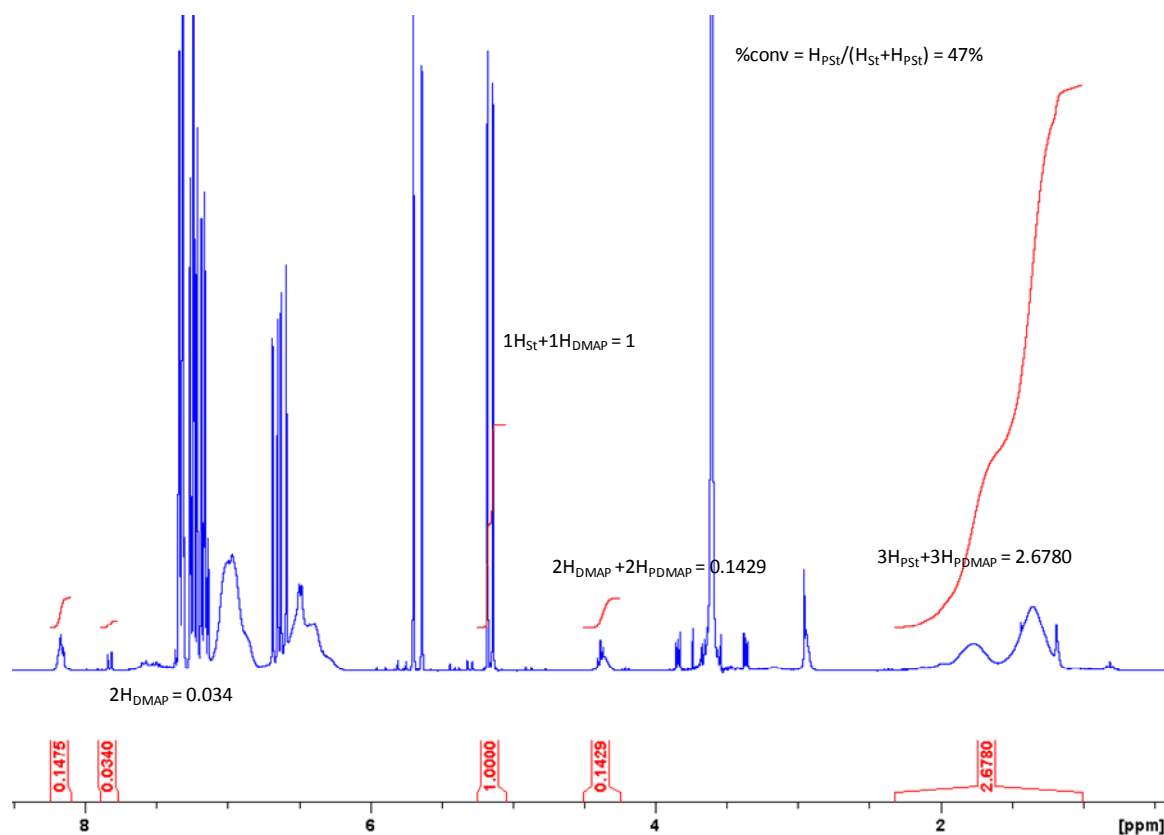


Figure 2.12: Example of a  $^1\text{H}$  NMR spectrum in  $\text{CDCl}_3$  used to calculate conversion for **2.2** /styrene polymerization.

The degree of incorporation of the functional monomer was determined by examination of the long acquisition  $^1\text{H}$  NMR spectrum of the resultant polymer and comparison of the signals attributable to the **2.2** moiety at *ca.* 4.4 ppm (2H) and 8.2 ppm (2H), and the signals for the backbone at *ca.* 1.5 ppm with those for the DDMAT at 0.85 ppm ( $\text{CH}_3$ ) as shown in Figure 2.13. For the example shown a calculated 5 % incorporation of **2.2** was observed.

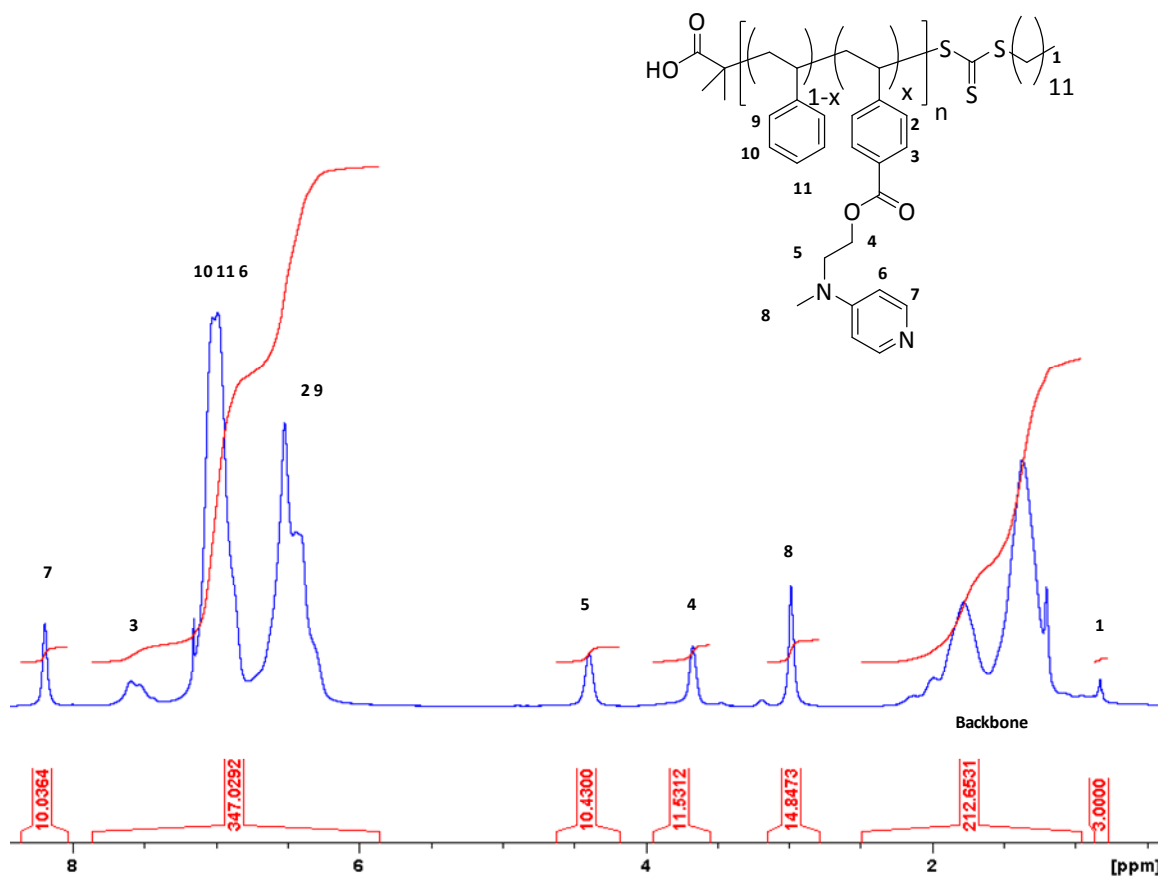


Figure 2.13: Example of a long acquisition  $^1\text{H}$  NMR spectrum in  $\text{CDCl}_3$  to determine the experimental DP and % incorporation of **2.2**

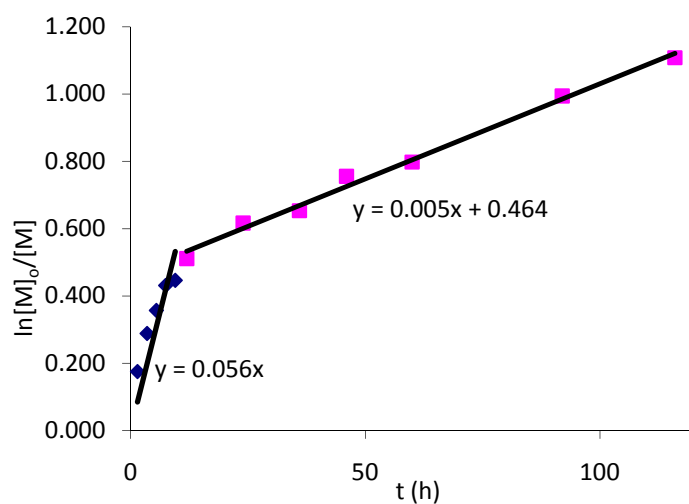


Figure 2.14: Kinetic plot for copolymerization of **2.2** with styrene

As for monomer **2.1**, the kinetic plot was linear until 35% conversion, which indicates a controlled polymerization process is occurring with a constant radical concentration up until this point. Interestingly this polymer was found to have a  $k_p$  of  $0.056 \text{ h}^{-1}$  before 35 % conversion and a different rate constant ( $k_p = 0.0057 \text{ h}^{-1}$ ) was observed after this point (Figure 2.14).  $k_p$  is the propagation ratio constant, and is required to understand how quickly the polymerization is progressing in terms of how quickly new monomers are being added to the growing polymer chain.

The retardation effects found in polymerizations **2.5** and **2.6** have been frequently observed in RAFT polymerizations, although the causes for the retardation effects are still under debate.<sup>58-</sup>

<sup>62</sup> There are two predominant theories on the retardation effects. The theory proposed by Barner-Kowollik *et al.*<sup>63</sup> assumes that the intermediate radical formed in the RAFT polymerization process is relatively stable and long-lived. The authors denote this theory as the slow fragmentation model. The theory of Monteiro *et al.*<sup>64</sup> For retardation of RAFT polymerization suggests that there is significant cross-termination of the intermediate radical with other free radicals existing in solution. The authors denote this theory as the intermediate radical termination model.

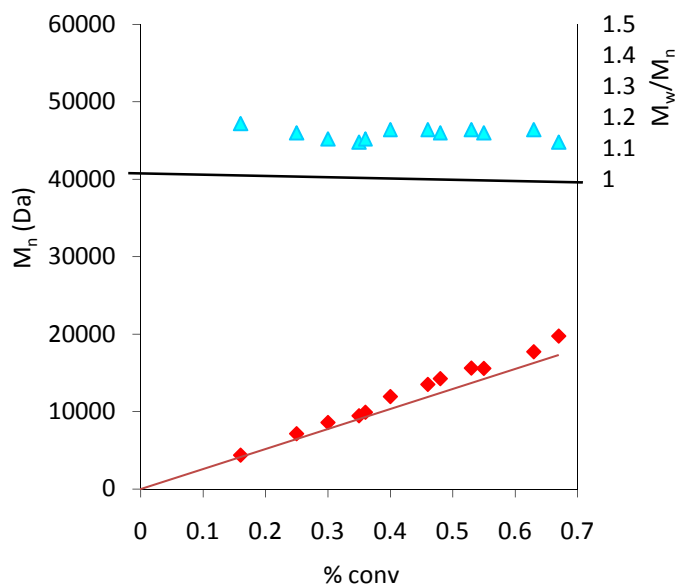


Figure 2.15: Plot of  $M_n$  from SEC data (red squares) versus conversion from  $^1\text{H}$  NMR spectroscopy (solid line) and polydispersities for **2.6**

The same behavior was observed in **2.5**, however in **2.6** the reaction slows but the PDIs remain relatively narrow ( $<1.2$ ) and the molecular weights by SEC (Figure 2.15) correspond closely with the theoretical value calculate by conversion NMR because of the narrow polydispersity (Figure 2.15). The good overlay of the UV trace at 309 nm and the trace from the RI detector suggests good end group fidelity.

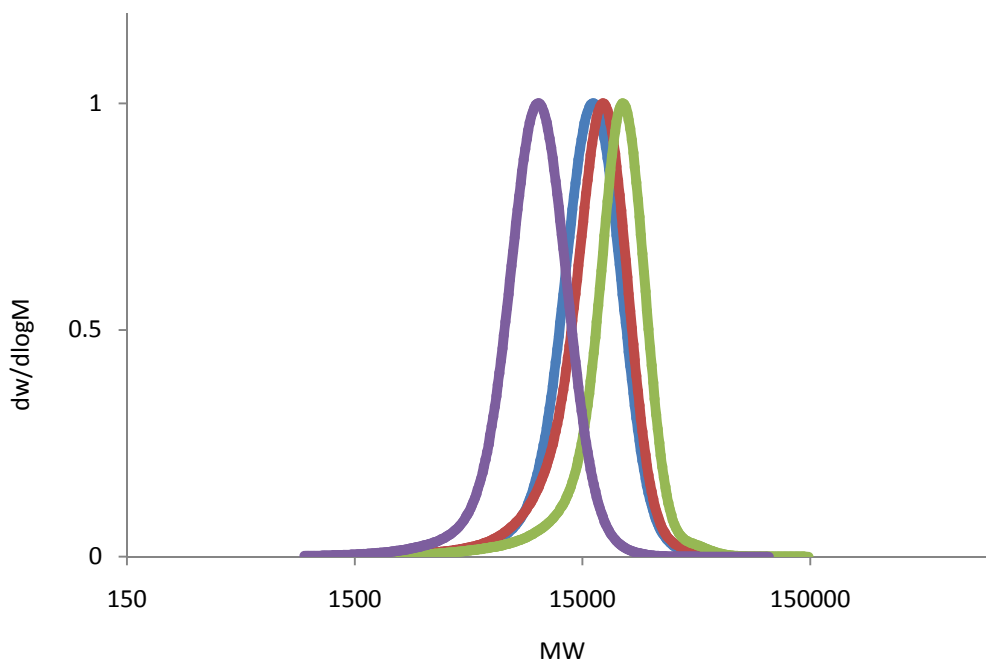
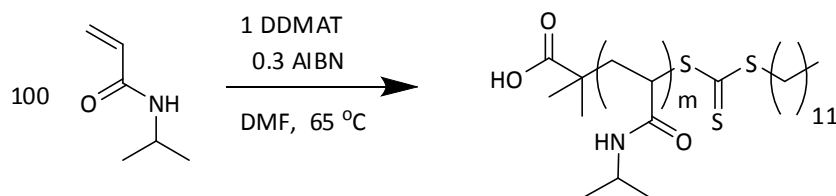


Figure 2.16: From right to left, SEC traces (RI detector) of the different samples of **2.6** taken at 5.5, 7.5, 46 and 92 hours.

### 2.3.3 Formation of amphiphilic block copolymer

For the synthesis of the amphiphilic block copolymer, a strategy was employed which involved the synthesis of a PNIPAM macroinitiator followed by chain extension with DMAP functionalized monomer **2.2** and styrene using established conditions.



Scheme 2.5: Preparation of PNIPAM by RAFT

The homopolymerization of NIPAM has been widely studied in the literature using different initiators and CTAs.<sup>56,65,66</sup> However, the homopolymerization of NIPAM using CTA **2.3** and

AIBN in DMF has not been previously reported so a kinetic study of this reaction was determined to explore its viability (Scheme 2.5).

<b>t(min)</b>	<b>% conv</b>	<b>M<sub>n</sub> SEC (kDa)</b>	<b>M<sub>n</sub> NMR (kDa)</b>	<b>M<sub>w</sub>/M<sub>n</sub></b>
15	10	1.4	1.2	1.35
30	33	7.0	3.8	1.41
45	51	15.6	5.9	1.14
60	60	19.6	7	1.12
75	70	22.4	8.2	1.12
90	74	23.9	8.6	1.12
120	81	31.8	9.5	1.13
180	90	34.2	10.5	1.16
240	93	36.2	10.8	1.13
300	96	37.8	11	1.14

Table 2.3: Data of kinetics for PNIPAM. Polymerization carried out in DMF. Ratio of [NIPAM]:[AIBN]:[**2.3**]

100:0.3:1. M<sub>n</sub> NMR and conversions calculated by <sup>1</sup>H NMR in CDCl<sub>3</sub>. Samples were measured by SEC (DMF)

analysis using PMMA standards.

The conversion of the monomer was determined by <sup>1</sup>H NMR by comparing the signal of the monomer (1H at 4.1 ppm) with the same signal from the resultant polymer at 4 ppm as shown in Figure 2.17. The DP of the resultant polymer can be easily determined by long acquisition <sup>1</sup>H NMR spectroscopy by comparing the signals from the end group (3H<sub>Eg</sub> at 0.85 ppm) with those from the PNIPAM at 4 ppm (1H). (Figure 2.18)



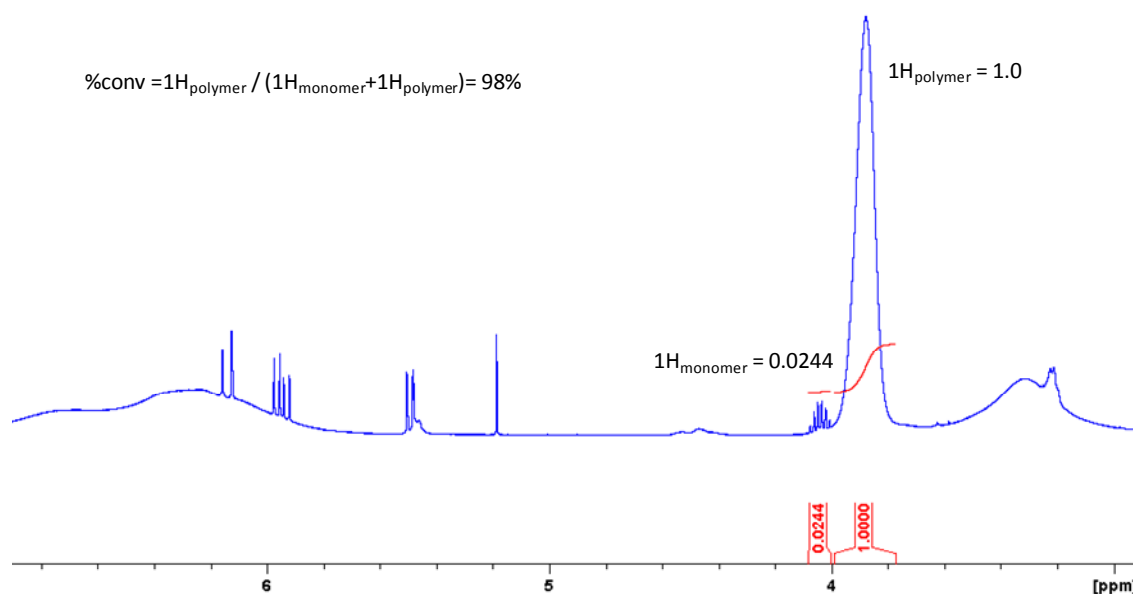


Figure 2.17: Example of a  $^1H$  NMR spectrum in  $CDCl_3$  used to assess conversion for NIPAM polymerization. An example of the conversion calculations is shown.

The kinetic plot was linear until 70 % conversion, which indicates a controlled radical polymerization is occurring with a constant radical concentration up to this point. Although there is evidence of an induction period of around 10 minutes, after this, the molecular weight of PNIPAM increases linearly with conversion (Figure 2.19).

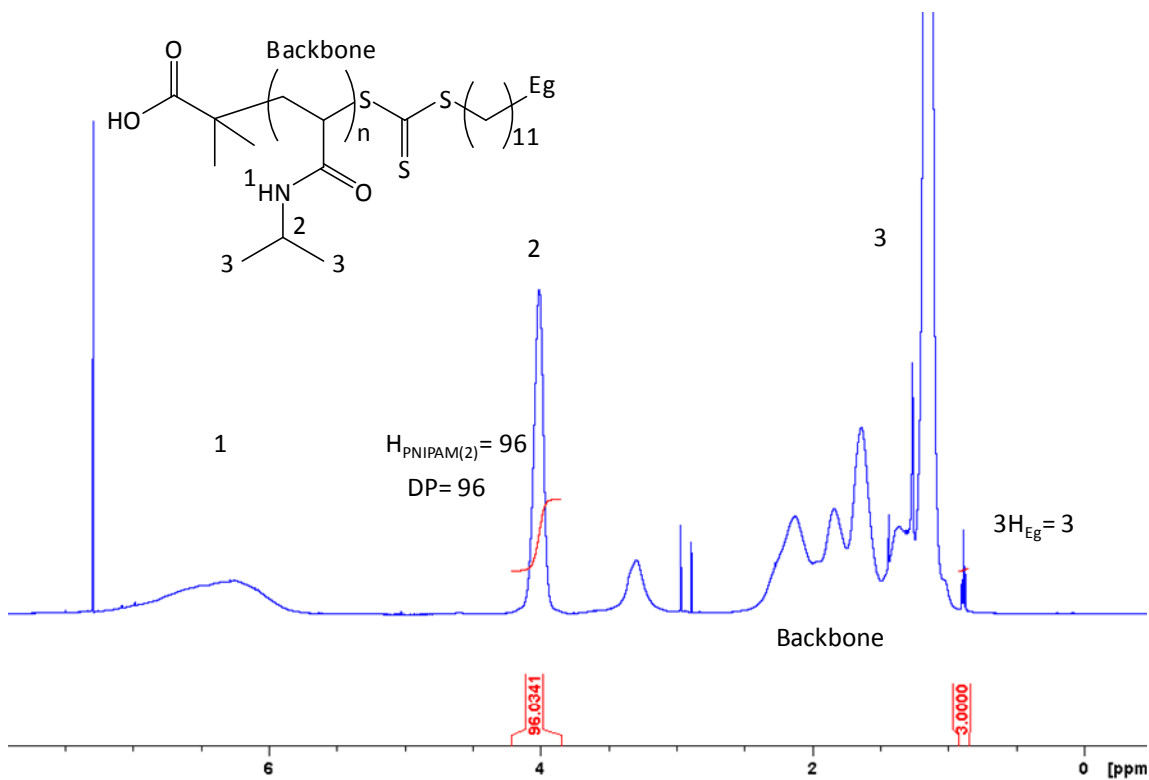


Figure 2.18: Example of a long acquisition  $^1\text{H}$  NMR spectrum in  $\text{CHCl}_3$  to determine the experimental DP of PNIPAM.

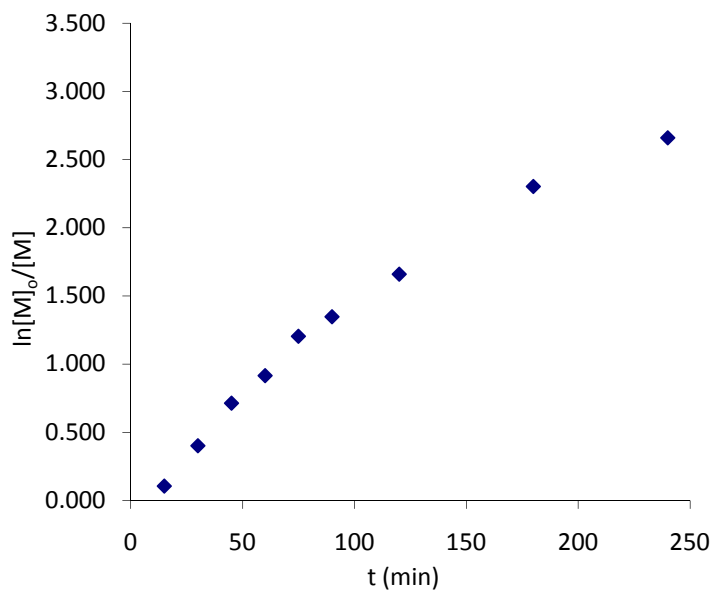


Figure 2.19: Kinetic plot for NIPAM polymerization using **2.3** as a CTA

The experimental molecular weight values calculated by SEC analysis do not fit with the theoretical line by conversion  $^1\text{H}$  NMR (Figure 2.20) because the SEC has been calibrated with PMMA instead of NIPAM. In the literature, a viscometer detector is used to obtain accurate molecular weight data; unfortunately we did not have that equipment available at the time the experiments were performed. The PDIs of the resultant polymers are  $\leq 1.15$  above 33 % conversion. All these data indicate excellent molecular weight control with very low polydispersity for the polymerization of NIPAM using DDMAT.

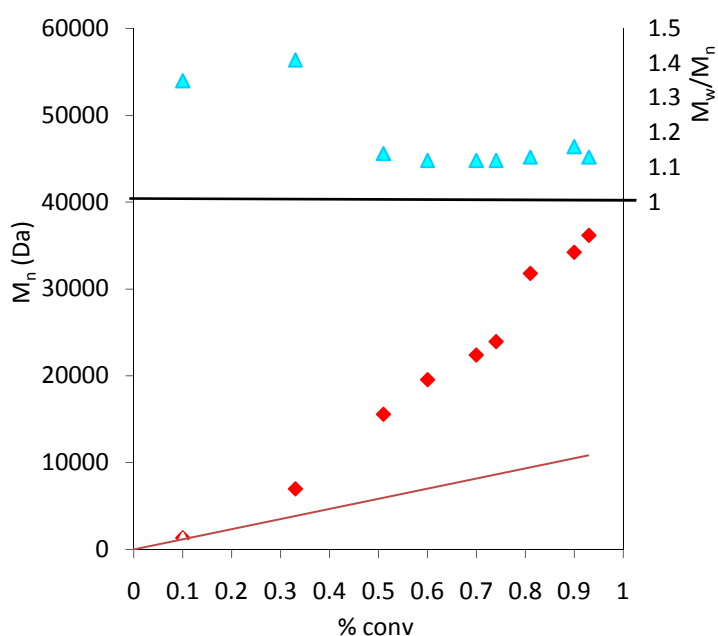


Figure 2.20: Plot of  $M_n$  from SEC data versus conversion from  $^1\text{H}$  NMR spectroscopy and PDIs. The line shows the theoretical  $M_n$  from  $^1\text{H}$  NMR versus conversion.

*Attempted chain extension of PNIPAM with styrene:*

To prove the viability of the chain extension of PNIPAM with a second block of styrene and **2.2**, different attempts to chain extend PNIPAM with 50 equivalents of styrene in DMF were explored (Table 2.4)

Entry	AIBN (eq)	T (°C)	t (h)	M <sub>w</sub> /M <sub>n</sub>	DP <sub>s</sub> (NMR)
1	0	110	18	1.31	10
2	0	110	96	1.13	5
3	0.3	75	96	1.30	38
4	0.1	75	72	1.26	40

Table 2.4: Different conditions used to chain extend PNIPAM with styrene

The starting PNIPAM macro-CTA **2.7** had a DP of 115 calculated by long acquisition <sup>1</sup>H NMR spectroscopy and a polydispersity of 1.08 by DMF SEC calibrated with PMMA standards. Entries 1 and 2 (Table 2.4) show the first attempts to investigate the thermal initiated chain extension of PNIPAM. The resulting polymers were characterized by <sup>1</sup>H NMR spectroscopy and SEC analysis. The NMR spectrum showed broad signals from 6.3 to 7.4 ppm, which indicates the formation of polystyrene, and the integration of these peaks with respect to the PNIPAM proton at 4 ppm suggested chain extension of just *ca.* 10 units of styrene after 96 hours. When analyzing the polymers by SEC, no increase in molecular weight was observed which indicates little or no incorporation of styrene. This suggested that the broad signal in the <sup>1</sup>H NMR spectrum (from 6.3 to 7.4 ppm) corresponded to the thermally self initiated homopolymerization of styrene at 110 °C.

Hence, a new route was explored and the temperature was decreased to 75 °C to investigate the AIBN initiated polymerization (entries 3 and 4 at Table 2.4). As shown in Figure 2.21, using 0.3 equivalents of AIBN, the  $^1\text{H}$  NMR spectrum suggested the incorporation of *ca.* 38 units of styrene.

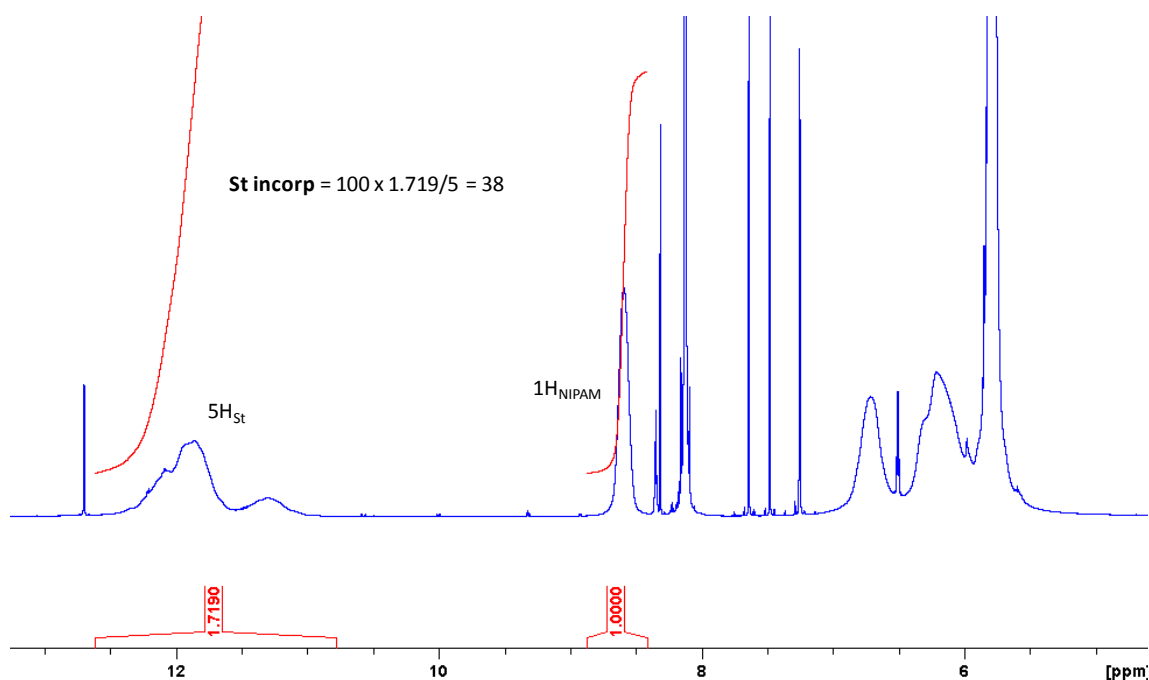


Figure 2.21: Example of a long acquisition  $^1\text{H}$  NMR spectrum in DMSO to determine the incorporation of styrene (Entry 3, Table 2.4)

However, when analyzing the resultant polymer by SEC chromatography both traces were bimodal. When overlaying the RI SEC signals from the starting PNIPAM with the one from the resulting polymer (Figure 2.22) it was observed that only a small fraction of the starting PNIPAM was chain extended evidenced by the high molecular weight shoulder indicating lack of control.

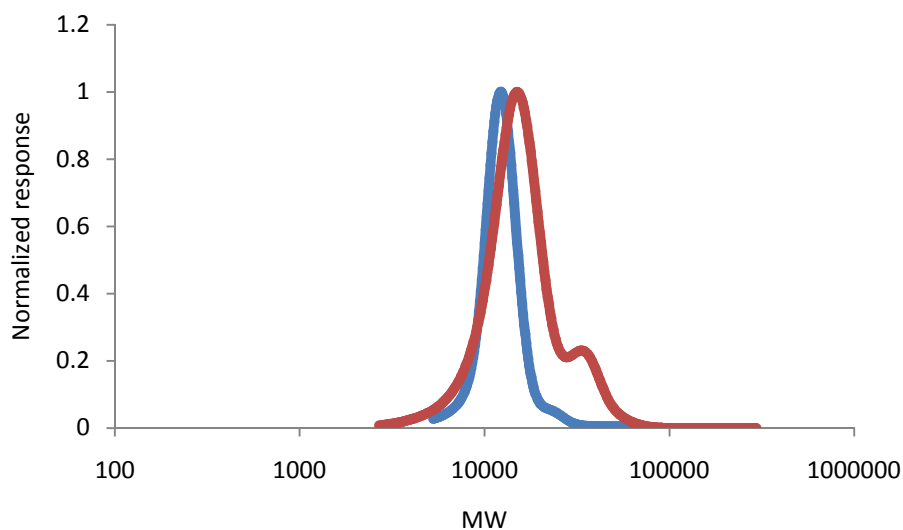


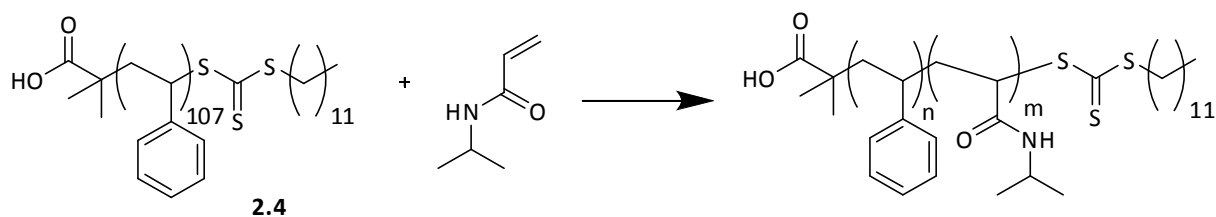
Figure 2.22: Overlay of RI signals from the DMF SEC analysis of PNIPAM (blue) and the new polymer formed (entry 3, Table 2.4) after chain extension with styrene (red).

In order to obtain better control in the polymerization process, the amount of AIBN was reduced to 0.1 equivalents (entry 4, Table 2.4). Unfortunately, when analyzing the NMR and SEC data the results were similar to those found for Entry 3.

This was surprising, as a successful block copolymerization *via* RAFT of styrene and NIPAM has been reported for both monomer addition sequences. Still, as Laschewsky reported recently in the literature, the reported examples used dithioesters, which are known to fragment more easily than analogous trithiocarbonates.<sup>67</sup> Therefore, the change from a growing acrylamide polymer chain to a styrenic one may be difficult.

#### *Chain extension of polystyrene with NIPAM:*

The opposite blocking sequence was investigated as if useful would allow for the preparation of the desired material. Polystyrene has been employed before as a macroRAFT agent for chain extension with NIPAM, using DDMAT as a CTA.<sup>15,68,69</sup>



Entry	NIPAM eq	AIBN eq	Solvent	T °C	t (h)	m
1	50	0.1	DMF	65	19	10
2	50	0.2	DIOXANE	70	24	44
3	50	0.3	DMF	65	21	8

Table 2.5: Different conditions used to chain extend 1 equivalent of polystyrene **2.4** with NIPAM

Three different conditions for the chain extension of polystyrene with NIPAM were investigated which were similar to those reported in the literature (Table 2.5). Very low conversions were obtained for the reactions carried out in DMF with 0.1 and 0.3 equivalents of AIBN (Entries 1 and 3) and the SEC traces (in THF SEC calibrated with polystyrene standards) showed a high molecular weight shoulder after *ca.* 20 hours reaction. However, using dioxane as a solvent at 70 °C polystyrene **2.4** was successfully chain extended with NIPAM (DP = 44) after 24 hours reaction with very good control (**2.8**, Entry 2).

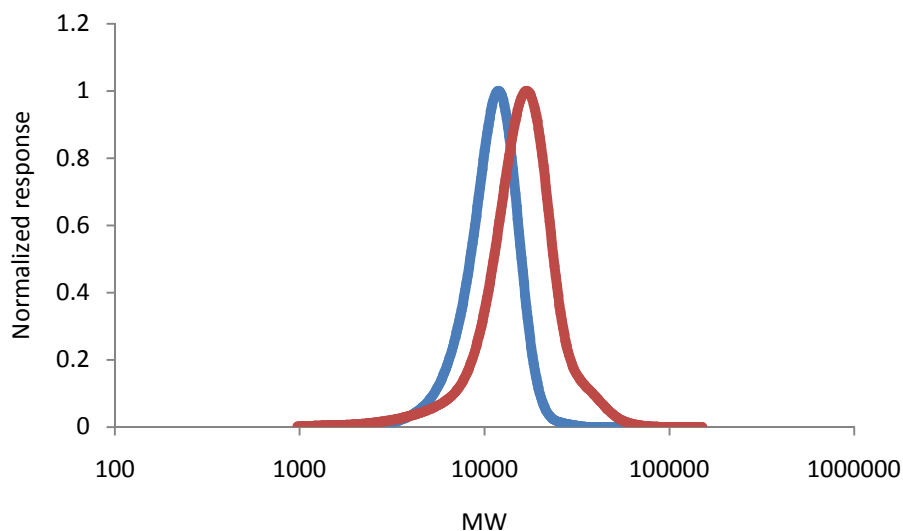


Figure 2.23: Overlay of RI signals from the THF SEC analysis of **2.4** (blue) and the new polymer formed after chain extension with NIPAM, **2.8** (red)

The resultant amphiphilic block copolymer **2.8** had a polydispersity of 1.22 by THF SEC and a molecular weight of 14.3 kDa (Figure 2.23). The DP of the NIPAM block was calculated by long acquisition  $^1\text{H}$  NMR in  $\text{CDCl}_3$  (Figure 2.24) by comparing the aromatic signals of polystyrene at *ca.* 7 ppm with those for the NIPAM at 4 ppm (1H) giving a theoretical molecular weight of 13.0 kDa, which is close to the experimental value obtained by SEC. The difference in molecular weight could be due to the calibration with polystyrene standards, which does not give very accurate data for the PNIPAM block.



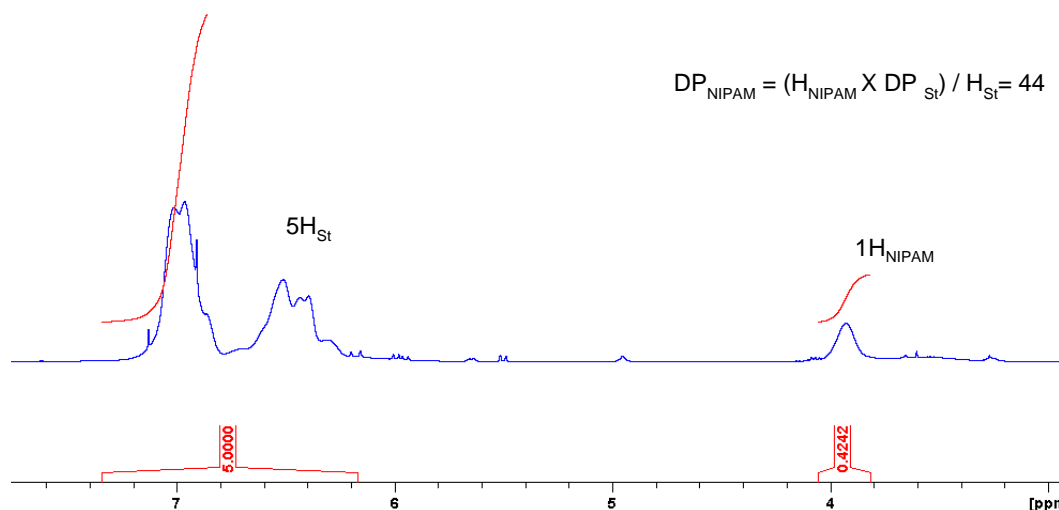
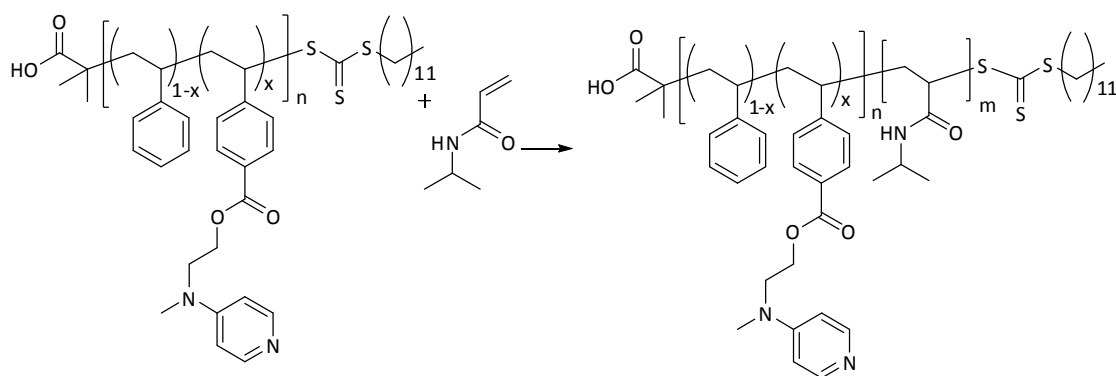


Figure 2.24: Long acquisition  $^1\text{H}$  NMR spectrum in  $\text{CDCl}_3$  of **2.8** to determine the incorporation of NIPAM.

*Attempted chain extension of **2.6** with NIPAM:*

The same conditions as those described in Table 2.5 to chain extend **2.4** with NIPAM were explored to chain extend the DMAP functionalized polystyrene, **2.6** (Table 2.6).

For all the different conditions tried, the  $^1\text{H}$  NMR spectrum showed a broad signal at 4 ppm characteristic for PNIPAM, but when analyzing the SEC data all traces looked bimodal and little or no chain extension was found. In all cases, THF SEC analysis of the resultant polymers gave a molecular weight very close to that expected from the long acquisition  $^1\text{H}$  NMR spectrum. However the overlay of the SEC traces from the starting polymer and the new polymer formed shows a high molecular weight shoulder that indicates that only some of the chains were chain extended with NIPAM. The shoulder could also be explained by the coupling of some chains of the macro-CTA giving a new polymer with higher molecular weight, or could be due to the formation of a new PNIPAM homopolymer without chain extension of the starting polymer. To test this final hypothesis (NIPAM homopolymerization), the resultant polymer was precipitated in water at room temperature.

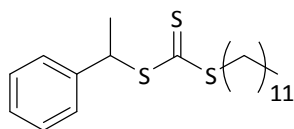


Entry	Macro CTA		NIPAM eq	AIBN eq	Solvent	T °C	t (h)	m
	DP(St/2.2)	M <sub>w</sub> /M <sub>n</sub>						
1	105/5	1.27	50	0.1	DMF	65	19	10
2	80/6	1.21	50	0.2	DIOXANE	70	24	14
3	110/5	1.13	50	0.3	DMF	65	21	40

Table 2.6: Different conditions used to chain extend polystyrene/2.2 copolymers with NIPAM

Under these conditions, PNIPAM would dissolve and the polystyrene based polymer, insoluble in water, would precipitate hence allowing for separation of the second homopolymer. For Entry 3 Table 2.6, when analyzing the precipitated polymer by THF SEC, the results shown a decrease in the polydispersity (from 1.6 to 1.4) and loss of the high molecular weight shoulder. The overlay of the SEC traces of the macro-CTA and the precipitated polymer clearly show that the polymer has not been chain-extended.

Given the difficulties found for the chain extension of these polymers, this route was not further investigated. DDMAT is a functional CTA with a carboxylic acid group, which may interfere in the polymerization process by interacting with the DMAP functionality. A new CTA without acidic functionality was subsequently synthesized as reported in the literature.<sup>70</sup>

Figure 2.25: Structure of dodecyl 1-phenylethyl trithiocarbonate (CTA **2.9**)

The DMAP containing monomer **2.2**, was copolymerized with styrene by RAFT using dodecyl 1-phenylethyl trithiocarbonate (**2.9**, Figure 2.25) as is easy to synthesize and has been proven to be a good chain transfer agent for the polymerization of styrene and styrenic monomers.<sup>57,71</sup> A kinetic study of the copolymerization using **2** was carried out in order to gain further polymerization data regarding the degree of living behavior and rate of polymerization with an intended 5% incorporation of **2.2**, with a view of obtaining an overall target DP of *ca.*50. Samples were taken from the polymerization ampoule at different times and analyzed by SEC (THF eluent) and <sup>1</sup>H NMR spectroscopy in CDCl<sub>3</sub> (Table 2.7).

t(h)	% conv St	% conv <b>2.2</b>	% incorp <b>2.2</b>	M <sub>n</sub> NMR (kDa)	M <sub>n</sub> SEC (kDa)	M <sub>w</sub> /M <sub>n</sub>
1	0.06	0.07	5.5	1.1	0.7	1.25
6	0.20	0.20	4.8	2.6	1.8	1.19
16	0.34	0.60	8.1	4.6	n.d.	n.d.
23	0.40	0.70	8.0	5.3	3.9	1.13
30	0.57	0.84	6.9	7.2	5	1.12

Table 2.7: Data of polymerization kinetics of **2.2**. Polymerizations were carried out in dioxane, with [Styrene]:[**2.2**]:[CTA] ratio of 50:2.5:1. M<sub>n</sub>(NMR) and conversions calculated by <sup>1</sup>H NMR spectroscopy in CDCl<sub>3</sub>. M<sub>n</sub>(SEC) and polydispersities were measured by SEC (THF) analysis using polystyrene standards.

N.d.=not determined.

As shown in Figure 2.26, the kinetic plot is linear, which indicates a controlled polymerization process is occurring with a constant radical concentration. Given the higher rate of polymerization for **2** than St ( $k_p(\text{styrene}) = 0.0262 \text{ min}^{-1}$  and  $k_p(\mathbf{2.2}) = 0.0573 \text{ min}^{-1}$ ), there is a higher than predicted incorporation of the functional monomer at low monomer conversion. Hence, the polymers have a gradient type structure and the resultant polymers contain significantly more than the expected 5% incorporation of monomer **2.2**.

Previous investigations in the group regarding copolymerization of styrene with a styrenic monomer containing an ester linkage in the *para*-position already showed that this type of monomer is preferentially added to the propagating species.<sup>70</sup> This behaviour is not unexpected since the presence of an electron withdrawing group in the *para*-position should activate the double bond and hence enhance reactivity compared to non substituted styrene.

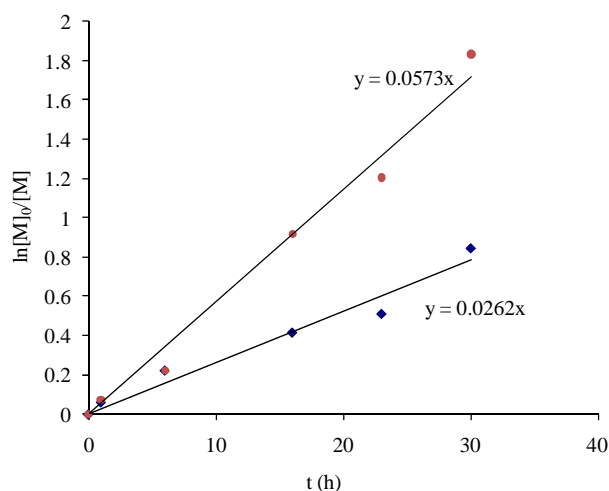


Figure 2.26: Kinetic plot for the copolymerization of styrene (♦) with DMAP monomer **2.2** (●).

A copolymer DMAP-*co*-St, **2.10**, with an overall degree of polymerization of 38, containing 10 % of monomer **2.2** (double than targeted due to fast incorporation) was obtained with

good polymerization control ( $M_n$  (NMR) = 5.1 kDa,  $M_w/M_n$  = 1.11). The degree of incorporation of functional monomer **2.2** was determined by examination of the  $^1\text{H}$  NMR spectrum of the resultant polymer, *via* the comparison of the signals attributable to monomer **2.2** with those for the CTA at 0.85 ppm as explained previously. These calculations assume complete end group fidelity; this was supported by the good overlap of the UV signal at 309 nm (characteristic wavelength for the trithiocarbonate end group) with the RI response for the same sample using both detectors in the SEC (Figure 2.9).

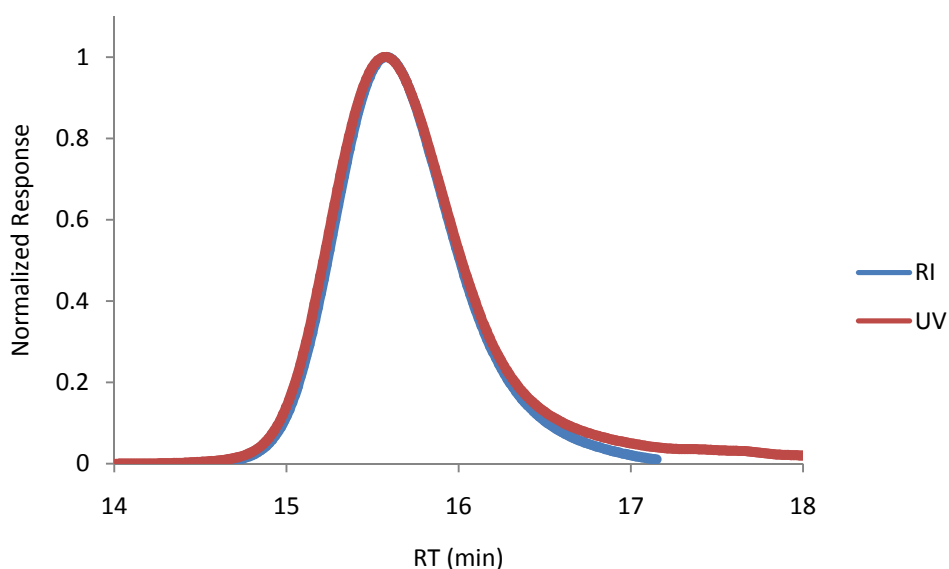


Figure 2.27: Overlay of UV309 (black) and RI (blue) signals from the THF SEC analysis of **2.10**.

For the preparation of the targeted DMAP containing micelles, the macro-CTA **2.10** was chain extended with NIPAM to form a diblock copolymer with a permanently hydrophobic styrenic-DMAP block and a temperature responsive block, which is hydrophilic at room temperature (**2.11**,  $M_n$  (NMR) = 20.5 kDa,  $M_w/M_n$  = 1.42). The degree of polymerization of NIPAM and its molecular weight were determined using the  $^1\text{H}$  NMR spectrum of the resultant polymer by comparing the signals attributable to monomer **2.2** in polymer **2.10** (*ca.*

4.4 ppm and 8.2 ppm) and the signals for the NIPAM proton at *ca.* 4.0 ppm (Figure 2.28). Due to the length of the hydrophilic NIPAM block (degree of polymerization = 140), the hydrophobic chain end of the RAFT CTA was not expected to play an important role in the self-assembly of the polymer. The validity of this assumption was evident from the characterization data showing spherical micelles, which is the morphology predicted based on the packing parameter for the given block lengths.<sup>7</sup>

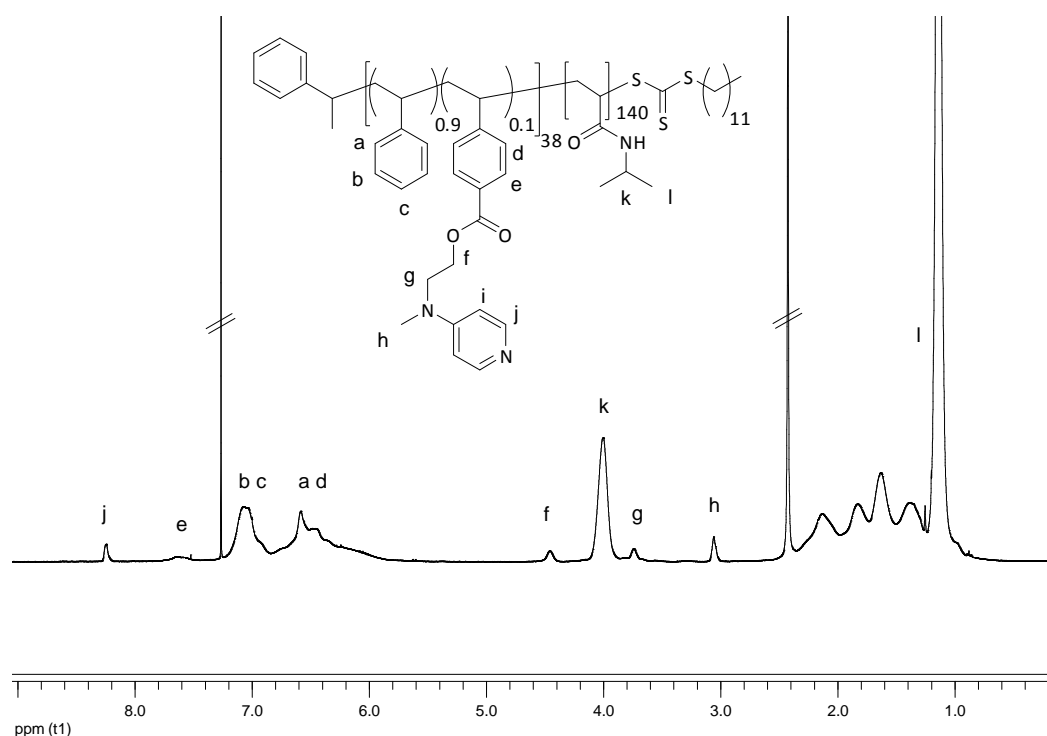


Figure 2.28:  $^1\text{H}$  NMR spectrum of diblock copolymer **2.11** in  $\text{CDCl}_3$ .

#### 2.3.4 Micelle formation

The amphiphilic block copolymer was dissolved in a minimum amount of acetone (at 100 mg/ mL), which is a good solvent for both blocks. Cold water was added dropwise, with stirring, to the polymer solution using a peristaltic pump (rate = 15 mL/h) to form spherical micelles **2.12** following evaporation of the acetone under reduced pressure at low temperature.

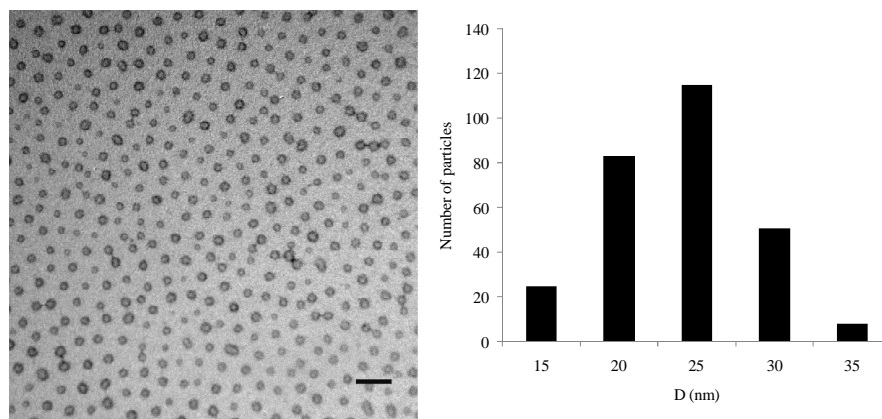


Figure 2.29: Representative TEM micrograph of catalyst **2.12** stained with uranyl acetate (1% solution) and histogram. Scale bar 100nm.

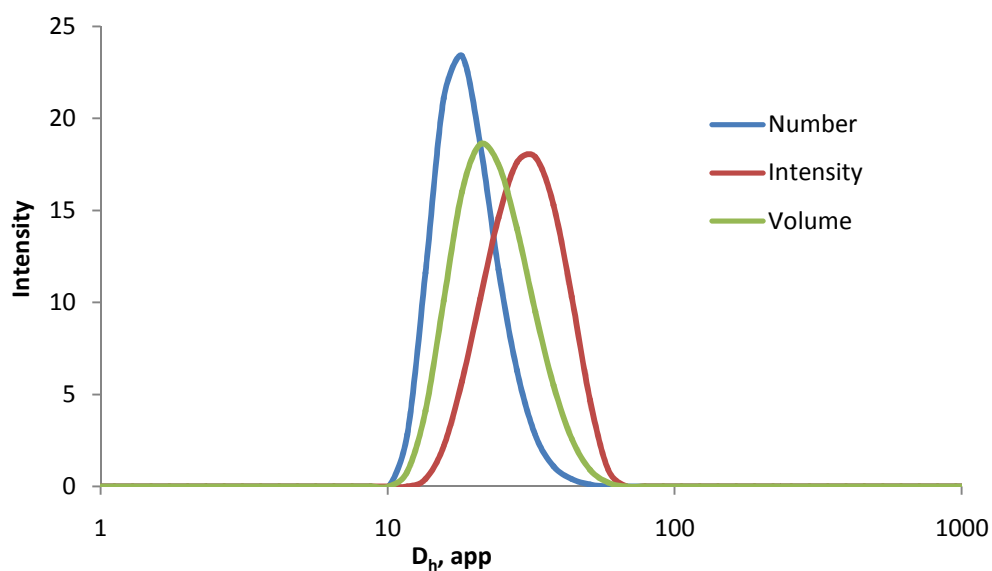


Figure 2.30: Graphical representation of DLS results, showing the size distribution of micelle solution **2.12** (0.1 mg/mL) by number, volume and intensity. ( $D_h = 35.4$  nm, PD = 0.139).

This yielded DMAP-functionalized micelles, **2.12**, at a micellar concentration of *ca.* 6.8 mg/mL. The resulting spherical micelles were found to be *ca.* 25 nm in diameter, determined by both TEM (Figure 2.29,  $D_{av} = 23.8$  nm) and DLS analysis ( $D_h = 35.4$  nm, PD = 0.139, Figure 2.30).

The LCST of micelle solution **2.12** was measured spectrophotometrically by determining the turbidity of the solution at various temperatures (Figure 2.31). It has been previously reported that temperature responsive polymers exhibit lower phase separation temperatures when self-assembled into micelles.<sup>72</sup> Our DMAP containing micelles presented an LCST of 27 °C, which is 5 °C lower than that reported for the PNIPAM homopolymer. The broad hysteresis observed in the cooling process, first observed by Wu *et al.*,<sup>73</sup> indicates that the solution must be cooled below 32 °C to reform the micelles.

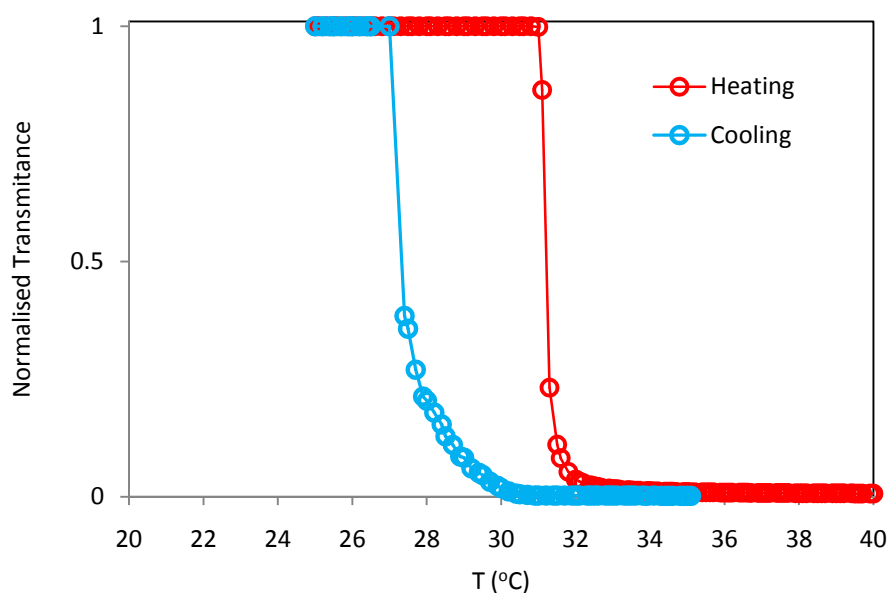


Figure 2.31: Normalized transmittance versus temperature plot for **2.12** at 1 mg/mL in water.

## 2.4 Conclusions

Two different styrenic monomers containing DMAP functionality have been synthesized (**2.1** and **2.2**). The difficulties in synthesizing **2.1** and its poor copolymerization with styrene lead us to abandon this route and instead focus was placed on **2.2**. Monomer **2.2** has been successfully copolymerized with styrene by RAFT using CTA **2.9** giving a gradient-type



polymer with good control over molecular weight and narrow polydispersity. The resultant hydrophobic polymer (**2.10**) has been chain extended with NIPAM to obtain a stimuli-responsive amphiphilic block copolymer with DMAP functionality tethered within the hydrophobic block, **2.11**. This amphiphile has been used to prepare well-defined spherical micelles in water with catalytic functionality in the hydrophobic core, which will be evaluated as nanoreactors to carry out acylation reactions of hydrophobic substrates in aqueous media. Moreover, the temperature responsive properties of this micelles will facilitate the recycling of the catalyst after catalysis.

## 2.5 Experimental Section

### 2.5.1 Materials:

Styrene monomer was filtered through a plug of aluminium oxide prior to use and stored at 4°C. NIPAM and AIBN (2,2'-azo-bis(isobutyronitrile)) were recrystallized from a 9:1 mixture of hexane/acetone and methanol respectively, and stored at 4°C. 4-(*N*-methyl-*N*-(2-hydroxyethyl)amino)pyridine was prepared previously by a member of the group as reported in the literature.<sup>47</sup> All other materials were used as received from Sigma-Aldrich, Fluka, and Acros.

### 2.5.2 Instrumentation:

<sup>1</sup>H NMR and <sup>13</sup>C NMR spectra were recorded with a Bruker DPX-300 spectrometer in CDCl<sub>3</sub> at 25 °C (128 scans). Size exclusion chromatography/gel permeation chromatography (SEC/SEC) measurements were performed with HPLC grade solvents (Fisher), tetrahydrofuran (THF) with 2 % of TEA, at 30 °C or dimethylformamide (DMF) with 1.06 g LiCl per liter at 40 °C as an eluent at a flow rate of 1 mL/min. The molecular weights of the synthesized polymers were calculated relative to polystyrene (PS) or poly methyl methacrylate (PMMA) standards. Lower critical solution temperature (LCST) measurements were analyzed using a Perkin-Elmer UV/vis Spectrometer (Lambda 35) equipped with a Peltier temperature controller at 500 nm with a heating/cooling rate of 1 °C/min. For the characterization of the particles, the micelle solutions were diluted with nanopure water to obtain a final concentration of *ca.* 0.1 mg/mL. TEM images were obtained using a JEOL electron microscope operating at 200 kV equipped with a LaB<sub>6</sub> gun and a Gatan digital camera. To prepare TEM samples, carbon grids were prepared by air plasma treatment to increase the

surface hydrophilicity and then 5  $\mu\text{L}$  of an aqueous solution of micelle was placed on a carbon-coated copper grid for 60s, and the water droplet was removed by a vacuum absorption. Aqueous UA solution (1%) was used to stain the particles using the blotting away method. DLS studies were conducted at 25  $^{\circ}\text{C}$  using a Zetasizer Nano series instrument (Malvern Instruments), at a fixed scattering angle of  $173^{\circ}$ . The data were processed by cumulant analysis of the experimental correlation function and particle diameters were calculated from the computed diffusion coefficients using the Stokes-Einstein equation. Each reported measurement was the average of three runs.

### 2.5.3 Monomer synthesis

#### – Synthesis of monomer **2.1**:

Following a literature procedure,<sup>36</sup> 4-(*N*-methyl-*N*-(2-hydroxyethyl)amino)pyridine (2.1 g, 13.8 mmol) was dissolved in dry DMF (25 mL) in a 100 mL two-necked flask, followed by addition of a solution of sodium hydride (60% dispersion in mineral oil) in dry DMF (10 mL) (0.9 g, 22.7 mmol) under nitrogen atmosphere. After the mixture was stirred for 30 min at RT, a solution of vinylbenzyl chloride (2.5 mL, 16.0 mmol) in dry DMF (10 mL) was added dropwise at 0  $^{\circ}\text{C}$  into the flask with a cannula. After 2 days the solution was filtered and the solvent evaporated under reduced pressure and the orange solid was dissolved in 150 mL of DMF and washed with water (100 mL) and brine (100 mL). The raw product was purified *via* column chromatography (silica gel,  $\text{CHCl}_3$  + 10% MeOH). (1.8 g, 50% yield).

$^1\text{H}$  NMR ( $\text{CDCl}_3$ ):  $\delta$  (ppm) 8.09 (d, 2H,  $J = 6.5$  Hz,  $\text{CHNCH}$ ), 7.42 (d, 2H,  $J = 8$  Hz,  $\text{CCHCHC}$ ), 7.25 (d, 2H,  $J = 8$  Hz,  $\text{CCHCHC}$ ), 6.58 (dd, 1H,  $J = 11$  and 17.5 Hz,  $\text{CH}_2\text{CH}$ ), 6.41 (d, 2H,  $J = 11$  Hz,  $\text{NCHCHC}$ ), 5.65 (d, 1H,  $J = 17.5$  Hz,  $\text{CHH}=\text{H}$ ), 5.20 (d, 1H,  $J = 11$  Hz,

CHH=H), 4.31 (s, 2H, J= 6 Hz, OCH<sub>2</sub>C), 3.60-3.39 (m, 4H, CH<sub>2</sub>CH<sub>2</sub>N), 2.85 (s, 3H, NCH<sub>3</sub>). <sup>13</sup>C NMR (CDCl<sub>3</sub>): δ (ppm) 153.1, 150.3, 137.9, 136.5, 135.9, 126.7, 125.1, 112.6, 106.2, 73.5, 67.6, 50.1, 38.3. *m/z* [ES MS] 269.1 [M+H]<sup>+</sup>; *ν*<sub>max</sub>/cm<sup>-1</sup> 2800-3200 (br), 1593, 1513, 1387, 1352, 1227, 1098, 985, 907, 826, 801.

– *Synthesis of monomer 2.2:*

4-(*N*-methyl-*N*-(2-hydroxyethyl)amino)pyridine<sup>74</sup> (1.13 g, 7.42 mmol), 4-vinyl benzoic acid (1 g, 6.75 mmol) and 1-ethyl-3-(3'-dimethylaminopropyl)carbodiimide, EDCI (2 g, 6.75 mmol) were dissolved in DCM (25 mL) in a 100 mL round bottom flask and stirred at room temperature for 48 h. The white precipitate was filtered off and the white filtrate was washed with brine (2x100 mL) and dried over MgSO<sub>4</sub>. The solvent was evaporated under reduced pressure to afford **2.2** in 60 % yield (1.13 g).

<sup>1</sup>H NMR (CDCl<sub>3</sub>): δ (ppm) 8.02 (d, 2H, J= 6 Hz, CHNCH), 7.70 (d, 2H, J=8 Hz, CCHCHC), 7.24 (d, 2H, J=8 Hz, CCHCHC), 6.52 (dd, 1H, J=11 and 17.5 Hz, CH<sub>2</sub>CH), 6.39 (d, 2H, J=6 Hz, NCHCHC), 5.64 (d, 1H, J=17.5 Hz, CHH=H), 5.17 (d, 1H, J=11 Hz, CHH=H), 4.28 (t, 2H, J=6 Hz, OCH<sub>2</sub>C), 3.57 (t, 2H, J=6 Hz, CH<sub>2</sub>CH<sub>2</sub>N), 2.87 (s, 3H, NCH<sub>3</sub>). <sup>13</sup>C NMR (CDCl<sub>3</sub>): δ (ppm) 149.4, 135.3, 129.3, 125.6, 116.2, 106.1, 61.0, 49.2, 37.3. *m/z* [ES MS] 283.1 [M+H]<sup>+</sup>; *ν*<sub>max</sub>/cm<sup>-1</sup> 2800-2900 (br), 1702, 1598, 1271, 1106, 999, 802, 781, 715.

2.5.4 *Synthesis of the CTA 2.3*<sup>57</sup>

DDMAT was synthesized according with a literature procedure by reaction of dodecanethiol, CS<sub>2</sub>, 2-bromoisobutyric acid and K<sub>3</sub>PO<sub>4</sub> in acetone at room temperature for 2 days (63 % yield).<sup>57</sup>

$^1\text{H}$  NMR ( $\text{CDCl}_3$ ):  $\delta$  (ppm) 11.19 (br s, 1H, COOH), 3.20 (t, 2H,  $J = 7$  Hz,  $\text{SCH}_2$ ), 1.66 (s, 6H,  $\text{C}(\text{CH}_3)_2$ ), 1.60-1.11 (m, 20H,  $\text{CH}_2(\text{CH}_2)_{10}\text{CH}_3$ ), 0.85 (t, 3H,  $J = 7$  Hz,  $(\text{CH}_2)_{10}\text{CH}_3$ )  $^{13}\text{C}$  NMR ( $\text{CDCl}_3$ ):  $\delta$  (ppm) 221.2, 179.3, 56.2, 39.7, 37.5, 32.3, 30.0, 29.7, 29.6, 29.5, 29.4, 28.9, 28.3, 25.6, 23.1, 14.5.  $m/z$  [ES MS] 387.1  $[\text{M}+\text{Na}]^+$ , 365.1  $[\text{M}+\text{H}]^+$   $\nu_{\text{max}}/\text{cm}^{-1}$  2400-3200 (br), 2917, 2849, 1705, 1459, 1280, 1127, 1069, 814, 721, 695.

### 2.5.5 Polymer synthesis

#### – Synthesis of polystyrene **2.4**

DDMAT (**2.3**, 0.017 g, 0.048 mmol) and AIBN (0.8 mg, 0.0048 mmol) were dissolved in styrene (1.1 mL, 9.6 mmol) in an ampoule. The oxygen was removed by three freeze-pump-thaw evacuation cycles. For the last cycle, nitrogen was flushed into the ampoule after thawing. The solution was heated at 85 °C in an oil bath for 21 hours. An aliquot was taken to determine the conversion (which was calculated by  $^1\text{H}$  NMR spectroscopy). The polymer was precipitated twice into a stirred solution of cold MeOH, filtered and placed in the vacuum oven overnight at 40 °C.

$^1\text{H}$  NMR ( $\text{CDCl}_3$ ):  $\delta$  (ppm) = 1.03-2.48 (C-H backbone peaks) 6.32-7.46 (Ar-H), 0.85 (t, 3H, endgroup)  $M_n$  (NMR) = 11.5 kDa, DP = 107,  $M_n$  (SEC, THF) = 10.2 kDa, PDI = 1.12

#### – General procedure for copolymerization of **2.1** and **2.2** using CTA **2.3**

Styrene (1.1 mL, 9.6 mmol), **2.1** or **2.2** (10 eq), DDMAT (**2.3**, 0.012 g, 0.048 mmol), AIBN (0.8 mg, 0.0048 mmol) were dissolved in 1 mL dioxane in an ampoule. The oxygen was removed by three freeze-pump-thaw evacuation cycles. For the last cycle, nitrogen was flushed into the ampoule before thawing. The solution was heated at 85 °C in an oil bath. An aliquot

was taken to determinate the conversion (which was calculated by  $^1\text{H}$  NMR spectroscopy). The polymer was precipitated twice into a stirred solution of cold MeOH, filtered and placed in the vacuum oven overnight at 40 °C.

**2.5:** 116 hours reaction. (styrene/monomer **2.1**)

$^1\text{H}$  NMR ( $\text{CDCl}_3$ ):  $\delta$  (ppm) 8.12 (br d, 2H, CHNCH), 7.43-6.36 (br m, aromatic signals from both monomers), 4.32 (br t, 2H,  $\text{OCH}_2\text{C}$ ), 3.65 (br m, 4H,  $\text{CH}_2\text{CH}_2\text{N}$  and  $\text{CH}_2\text{CH}_2\text{N}$ ), 2.82 (br s, 3H,  $\text{NCH}_3$ ), 1.20-2.25 (br m, backbone), 0.85 (t, 3H end group)  $M_n$  (NMR) = 11.5 kDa,  $m = 99$ ,  $x = 4$ ,  $M_n$  (SEC, THF) = 19.4 kDa,  $M_w / M_n = 1.54$  bimodal

**2.6:** 116 hours reaction. (styrene/monomer **2.2**)

$^1\text{H}$  NMR ( $\text{CDCl}_3$ ):  $\delta$  (ppm) 8.12 (br d, 2H, CHNCH), 7.43-6.40 (br m, aromatic signals from both monomers), 4.32 (br t, 2H,  $\text{CH}_2\text{CH}_2\text{N}$ ), 3.65 (br m, 4H,  $\text{CH}_2\text{CH}_2\text{N}$ ), 2.83 (br s, 3H,  $\text{NCH}_3$ ), 1.21-2.25 (br m, backbone), 0.85 (t, 3H end group)  $M_n$  (NMR) = 13.4 kDa,  $m = 115$ ,  $x = 5$ ,  $M_n$  (SEC, THF) = 20800 Da,  $M_w / M_n = 1.13$

– *General procedure for polymerization of PNIPAM*

NIPAM (1 g, 8.82 mmol), AIBN (4.3 mg, 0.02 mmol) and DDMAT (0.031 g, 0.88 mmol) were dissolved in 1.1 mL of DMF. Then oxygen was removed by three evacuation cycles consisting of freeze-pump-thaw cycles. For the last cycle, nitrogen was flushed into the ampoule after thawing. The solution was heated at 65 °C in an oil bath and samples were collected under nitrogen at different intervals (Table 2.3). The samples were directly analyzed by  $^1\text{H}$  NMR spectroscopy in chloroform (Figure 2.18) and SEC analysis (DMF-PMMA) to determine the molecular weight, polydispersity and conversion.

**2.7:**  $^1\text{H}$  NMR ( $\text{CDCl}_3$ ):  $\delta$  (ppm) 3.98 (br s, 1H, CH), 2.47-0.72 (br m, backbone), 1.23 (br s, 6H,  $\text{CH}_3$ ).), 0.85 (t, 3H, endgroup)  $M_{\text{n}}(\text{NMR}) = 13.3$  kDa,  $n = 115$ ,  $M_{\text{w}} / M_{\text{n}} = 1.08$

– Synthesis of block-copolymer **2.8**

Polystyrene **2.4** (0.1 g, 0.017 mmol), NIPAM (0.12 g, 0.86 mmol), AIBN (0.6 mg, 0.0034 mmol) were dissolved in 1 mL dioxane in an ampoule. The oxygen was removed by three freeze-pump-thaw evacuation cycles. For the last cycle, nitrogen was flushed into the ampoule before thawing. The solution was heated at 70 °C in an oil bath for 24h. An aliquot was taken to determine the conversion (which was calculated by  $^1\text{H}$  NMR spectroscopy). The polymer was precipitated twice into a stirred solution of cold diethylether, filtered and placed in the vacuum oven overnight at 40 °C.

$^1\text{H}$  NMR ( $\text{CDCl}_3$ ):  $\delta$  (ppm) 7.22-5.71 (br m, Ar-H), 3.98 (br s, 1H, CH), 2.47-0.72 (br m, backbone).  $M_{\text{n}}(\text{NMR}) = 16.3$  kDa,  $n = 107$ ,  $m = 44$ ,  $M_{\text{n}}(\text{SEC THF, PMMA}) = 14.3$  kDa,  $M_{\text{w}} / M_{\text{n}}(\text{SEC}) = 1.22$ .

– Synthesis of the CTA **2.9**<sup>70</sup>

Acetone (40 mL) was added to potassium phosphate,  $\text{K}_3\text{PO}_4$  (2.7 g, 6.4 mmol) to form a suspension. To the stirred suspension, 1-dodecanethiol (2.8 mL, 5.8 mmol) was added and stirred for 10 minutes. Subsequently, carbon disulfide,  $\text{CS}_2$  (1.1 mL, 17.5 mmol) was added to the mixture and was stirred for 1 hour after which 1-bromoethyl benzene (1.6 mL, 5.8 mmol) was added. After 5 hours of stirring at room temperature the solvent was removed and the crude product was purified by flash column chromatography (100% petroleum ether) to afford **2.9** in 89% yield (4 g).

$^1\text{H}$  NMR ( $\text{CDCl}_3$ ):  $\delta$  (ppm) 7.22-7.23 (m, 5H, Ar-H), 5.32 (q, 1H,  $J=7$  Hz, CH), 3.31 (t, 2H,  $J=7.5$  Hz,  $\text{CH}_2$ ), 1.74 (d, 3H,  $J=7$  Hz,  $\text{CH}_3$ ), 1.67 (q, 2H,  $J=7.5$  Hz,  $\text{CH}_2$ ), 1.20-1.42 (m, 18H,  $\text{CH}_2$ ), 0.87 (t, 3H,  $J=7.0$  Hz,  $\text{CH}_3$ ).  $^{13}\text{C}$  NMR ( $\text{CDCl}_3$ ):  $\delta$  (ppm) 218.9, 128.0, 127.1, 127.1, 76.8, 76.4, 77.0, 49.4, 36.2, 31.3, 29.0, 28.9, 28.8, 28.7, 28.5, 28.3, 27.3, 22.1, 20.8, 13.3.

– *Synthesis of copolymer 2.10*

Styrene (1 mL, 8.7 mmol), monomer **2.2** (0.13 g, 0.46 mmol) and CTA (**2.9**, 0.035 g, 0.09 mmol) were dissolved in 1 mL DMF in an ampoule. The oxygen was removed by three freeze-pump-thaw evacuation cycles. For the last cycle, nitrogen was flushed into the ampoule before thawing. The solution was put into a preheated oil bath at 110 °C. An aliquot was taken after 24 h to determinate the conversion, which was calculated by  $^1\text{H}$  NMR spectroscopy (St = 45 % conversion, **2.2** = 70 % conversion). The polymer was precipitated twice into a stirred solution of cold MeOH, filtered and placed in the vacuum oven overnight at 40 °C. Molecular weights and polydispersity indices were measured by SEC in THF using polystyrene as narrow standards, and long acquisition  $^1\text{H}$  NMR spectroscopy in  $\text{CDCl}_3$  was used for the determination of percentage incorporation of monomer **2.2** and styrene. Molecular weight by  $^1\text{H}$  NMR spectroscopy was determined by comparing characteristic signals of the styrene (H-Ar) and monomer **2.2** (ca. 4.2 ppm) in the polymer relative to characteristic end group signals.

$^1\text{H}$  NMR ( $\text{CDCl}_3$ ):  $\delta$  (ppm) 8.24 (br d, 2H, CH), 7.61 (br m, 2H, CH), 7.31-6.17 (br m, Ar-H), 4.45 (br t, 2H,  $\text{CH}_2$ ), 3.72 (br t, 2H,  $\text{CH}_2$ ), 3.22 (t, 2H end group,  $\text{CH}_2$ ), 3.02 (br s, 3H,  $\text{CH}_3$ ), 2.45-1.11 (br m, backbone), 0.85 (t, 3H end group,  $\text{CH}_3$ ).  $M_n(\text{NMR}) = 5.1$  kDa,  $n = 38$ ,  $x = 0.9$ ,  $M_n(\text{SEC THF, PS}) = 4.0$  kDa,  $M_w/M_n(\text{SEC}) = 1.11$ .

*Kinetics of the copolymerization of 2.10:*



Styrene (0.34 g, 3.3 mmol), **2.2** (2.5 eq, 0.17 mmol) and CTA (**2.9**, 0.2 g, 0.07 mmol) were dissolved in 0.5 mL DMF in an ampoule. The oxygen was removed by three freeze-pump-thaw evacuation cycles. For the last cycle, nitrogen was flushed into the ampoule before thawing. The solution was put into a preheated oil bath at 110 °C. Aliquots were taken at different times to determinate the conversion, which was calculated by  $^1\text{H}$  NMR spectroscopy.

– *Synthesis of block-copolymer **2.11***

Copolymer **2.10** (0.2 g, 0.04 mmol), NIPAM (0.7 g, 5.8 mmol), AIBN (0.012 g, 0.008 mmol) were dissolved in 3.3 mL of THF in an glass ampoule. The oxygen was removed by three freeze-pump-thaw evacuation cycles. For the last cycle, nitrogen was flushed into the ampoule before thawing. The solution was heated at 65 °C in an oil bath. Following polymerization the polymer was precipitated twice into a stirred solution of cold diethyl ether, filtered and placed in the vacuum oven overnight at 40 °C.

$^1\text{H}$  NMR ( $\text{CDCl}_3$ ):  $\delta$  (ppm) 8.19 (br d, 2H, CH), 7.77-5.61 (br m, Ar-H), 4.40 (br t, 2H,  $\text{CH}_2$ ), 3.94 (br s, 1H, CH), 3.68 (br t, 2H,  $\text{CH}_2$ ), 3.00 (br s, 3H,  $\text{CH}_3$ ), 2.45-0.65 (br m, backbone).  $M_n(\text{NMR}) = 20.5 \text{ kDa}$ ,  $n = 38$ ,  $m = 140$ ,  $M_n(\text{SEC DMF, PMMA}) = 10.3 \text{ kDa}$ ,  $M_w/M_n(\text{SEC}) = 1.42$ .

2.5.6 *Formation of micelles **2.12***

All micellar solutions were obtained by dilution of a stock solution of 6.7 mg/mL of polymer **2.11** in water to obtain the desirable concentration. 670 mg of polymer was dissolved in the minimum amount of acetone (100 mg/mL) in a round bottom flask. The solution was placed in a cold room at 5 °C and 100 mL of water were added dropwise with continuous stirring using a peristaltic pump (drop rate = 15 mL/h). When the addition of water was completed,

the acetone was removed under vacuum keeping the flask in an ice bath. These micelles solutions (6.8 mg/mL) were stored at 5 °C. For each of the esterification reactions, 8 mL of this solution was used (8 mL of solution contains 1.3 mg of DMAP). For the characterization of the particles, the solution **2.12** was diluted with nanopure water to obtain a final concentration of *ca.* 0.1 mg/mL.

## 2.6 References

- (1)Zhang, L. F.; Eisenberg, A. *Science* **1995**, 268, 1728.
- (2)Soo, P. L.; Eisenberg, A. *J. Polym. Sci. Pt. B-Polym. Phys.* **2004**, 42, 923.
- (3)Riess, G. *Prog. Polym. Sci.* **2003**, 28, 1107.
- (4)Jain, S.; Bates, F. S. *Science* **2003**, 300, 460.
- (5)Wooley, K. L. *J. Polym. Sci., Part A: Polym. Chem.* **2000**, 38, 1397.
- (6)Mai, Y.; Eisenberg, A. *Chem. Soc. Rev.* **2012**, 41, 5969.
- (7)Israelachvili, J. N.; Mitchell, D. J.; Ninham, B. W. *J. Chem. Soc., Faraday Trans.* **1976**, 72, 1525.
- (8)Blanazs, A.; Armes, S. P.; Ryan, A. J. *Macromol. Rapid Commun.* **2009**, 30, 267.
- (9)Liu, B.; Perrier, S. J. *Polym. Sci., Part A: Polym. Chem.* **2005**, 43, 3643.
- (10)Eeckman, F.; Moes, A. J.; Amighi, K. *Int. J. Pharm.* **2004**, 273, 109.
- (11)Schild, H. G. *Prog. Polym. Sci.* **1992**, 17, 163.
- (12)Schilli, C. M.; Zhang, M. F.; Rizzardo, E.; Thang, S. H.; Chong, Y. K.; Edwards, K.; Karlsson, G.; Muller, A. H. E. *Macromolecules* **2004**, 37, 7861.
- (13)Arotcarena, M.; Heise, B.; Ishaya, S.; Laschewsky, A. J. *Am. Chem. Soc.* **2002**, 124, 3787.

- (14)Virtanen, J.; Arotcarena, M.; Heise, B.; Ishaya, S.; Laschewsky, A.; Tenhu, H. *Langmuir* **2002**, *18*, 5360.
- (15)Nuopponen, M.; Ojala, J.; Tenhu, H. *Polymer* **2004**, *45*, 3643.
- (16)Hong, C. Y.; You, Y. Z.; Pan, C. Y. *J. Polym. Sci., Part A: Polym. Chem.* **2004**, *42*, 4873.
- (17)Hales, M.; Barner-Kowollik, C.; Davis, T. P.; Stenzel, M. H. *Langmuir* **2004**, *20*, 10809.
- (18)Bergbreiter, D. E.; Case, B. L.; Liu, Y. S.; Caraway, J. W. *Macromolecules* **1998**, *31*, 6053.
- (19)Case, B. L.; Franchina, J. G.; Liu, Y. S.; Bergbreiter, D. E. *Reusable, recoverable, polymeric supports: Applications in homogeneous catalysis*; Marcel Dekker: New York, 1998; Vol. 75.
- (20)Sherrington, D. C. *J. Polym. Sci., Part A: Polym. Chem.* **2001**, *39*, 2364.
- (21)Clapham, B.; Reger, T. S.; Janda, K. D. *Tetrahedron* **2001**, *57*, 4637.
- (22)Shen, Y.; Tang, H.; Ding, S. *Prog. Polym. Sci.* **2004**, *29*, 1053.
- (23)Bergbreiter, D. E.; Tian, J. H.; Hongfa, C. *Chem. Rev.* **2009**, *109*, 530.
- (24)Arumugam, S.; Vutukuri, D. R.; Thayumanavan, S.; Ramamurthy, V. *J. Am. Chem. Soc.* **2005**, *127*, 13200.
- (25)Rossbach, B. M.; Leopold, K.; Weberskirch, R. *Angew. Chem., Int. Ed.* **2006**, *45*, 1309.
- (26)Gall, B.; Bortenschlager, M.; Nuyken, O.; Weberskirch, R. *Macromol. Chem. Phys.* **2008**, *209*, 1152.
- (27)O'Reilly, R. K. *Philos. Trans. R. Soc. A-Math. Phys. Eng. Sci.* **2007**, *365*, 2863.

- (28)Monteiro, M. J. *Macromolecules* **2010**, 43, 1159.
- (29)O'Reilly, R. K.; Joralemon, M. J.; Hawker, C. J.; Wooley, K. L. *Chem.-Eur. J.* **2006**, 12, 6776.
- (30)Ievins, A. D.; Wang, X. F.; Moughton, A. O.; Skey, J.; O'Reilly, R. K. *Macromolecules* **2008**, 41, 2998.
- (31)Steglich, W.; Höfle, G. *Angew. Chem., Int. Ed.* **1969**, 8, 981.
- (32)Höfle, G.; Steglich, W.; Vorbrüggen, H. *Angew. Chem., Int. Ed.* **1978**, 17, 569.
- (33)Xu, S.; Held, I.; Kempf, B.; Mayr, H.; Steglich, W.; Zipse, H. *Chem. Eur. J.* **2005**, 11, 4751.
- (34)Berry, D. J.; Digiovanna, C. V.; Metrick, S. S.; Murugan, R. *Arkivoc* **2001**, 2, 944.
- (35)Helms, B.; Guillaudeu, S. J.; Xie, Y.; McMurdo, M.; Hawker, C. J.; Frechet, J. M. J. *Angew. Chem., Int. Ed.* **2005**, 44, 6384.
- (36)Price, K. E.; Mason, B. P.; Bogdan, A. R.; Broadwater, S. J.; Steinbacher, J. L.; McQuade, D. T. *J. Am. Chem. Soc.* **2006**, 128, 10376.
- (37)Poe, S. L.; Kobaslija, M.; McQuade, D. T. *J. Am. Chem. Soc.* **2006**, 128, 15586.
- (38)Poe, S. L.; Kobaslija, M.; McQuade, D. T. *J. Am. Chem. Soc.* **2007**, 129, 9216.
- (39)Wang, Y.; Wei, G. W.; Zhang, W. Q.; Jiang, X. W.; Zheng, P. W.; Shi, L. Q.; Dong, A. J. *J. Mol. Catal. A: Chem.* **2007**, 266, 233.

- (40)Ge, Z. S.; Xie, D.; Chen, D. Y.; Jiang, X. Z.; Zhang, Y. F.; Liu, H. W.; Liu, S. Y. *Macromolecules* **2007**, *40*, 3538.
- (41)Perrier, S.; Takolpuckdee, P. J. *Polym. Sci. A Polym. Chem.* **2005**, *43*, 5347.
- (42)Chiefari, J.; Chong, Y. K.; Ercole, F.; Krstina, J.; Jeffery, J.; Le, T. P. T.; Mayadunne, R. T. A.; Meijs, G. F.; Moad, C. L.; Moad, G.; Rizzardo, E.; Thang, S. H. *Macromolecules* **1998**, *31*, 5559.
- (43)Moad, G.; Rizzardo, E.; Thang, S. H. *Aust. J. Chem.* **2006**, *59*, 669.
- (44)Moad, G.; Rizzardo, E.; Thang, S. H. *Polymer* **2008**, *49*, 1079.
- (45)Zhang, L.; Eisenberg, A. *Polym. Adv. Technol.* **1998**, *9*, 677.
- (46)Zhang, L.; Eisenberg, A. *Macromolecules* **1999**, *32*, 2239.
- (47)Deratani, A.; Darling, G. D.; Frechet, J. M. J. *Polymer* **1987**, *28*, 825.
- (48)Zhao, B.; Jiang, X. M.; Li, D. J.; Jiang, X. G.; O'Lenick, T. G.; Li, B.; Li, C. Y. *J. Polym. Sci. A Polym. Chem.* **2008**, *46*, 3438.
- (49)Neises, B.; Steglich, W. *Angew. Chem., Int. Ed.* **1978**, *17*, 522.
- (50)Lai, J. T.; Filla, D.; Shea, R. *Macromolecules* **2002**, *35*, 6754.
- (51)Lu, L. C.; Yang, N. F.; Cai, Y. L. *Chem. Commun.* **2005**, 5287.
- (52)Harrisson, S.; Wooley, K. L. *Chem. Commun.* **2005**, 3259.
- (53)Cheng, C.; Sun, G.; Khoshdel, E.; Wooley, K. L. *J. Am. Chem. Soc.* **2007**, *129*, 10086.

- (54)Jiang, X. L.; Schoenmakers, P. J.; van Dongen, J. L. J.; Lou, X. W.; Lima, V.; Brokken-Zijp, J. *Anal. Chem.* **2003**, 75, 5517.
- (55)Llauro, M. F.; Loiseau, J.; Boisson, F.; Delolme, F.; Ladaviere, C.; Claverie, J. J. *Polym. Sci., Part A: Polym. Chem.* **2004**, 42, 5439.
- (56)Convertine, A. J.; Ayres, N.; Scales, C. W.; Lowe, A. B.; McCormick, C. L. *Biomacromolecules* **2004**, 5, 1177.
- (57)Skey, J.; O'Reilly, R. K. *Chem. Commun.* **2008**, 4183.
- (58)Konkolewicz, D.; Hawket, B. S.; Gray-Weale, A.; Perrier, S. *Macromolecules* **2008**, 41, 6400.
- (59)Zhang, Z. B.; Zhu, J.; Cheng, Z. P.; Zhu, X. L. *Polymer* **2007**, 48, 4393.
- (60)Zhou, N.; Lu, L.; Zhu, J.; Yang, X. J.; Wang, X.; Zhu, X. L.; Zhang, Z. B. *J. Appl. Polym. Sci.* **2007**, 105, 2357.
- (61)Zhou, N.; Lu, L.; Zhu, J.; Yang, X.; Wang, X.; Zhu, X.; Zhang, Z. *Polymer* **2007**, 48, 1255.
- (62)Zhou, N. C.; Zhang, Z. B.; Zhu, J.; Cheng, Z. P.; Zhu, X. L. *Macromolecules* **2009**, 42, 3898.
- (63)Barner-Kowollik, C.; Quinn, J. F.; Morsley, D. R.; Davis, T. P. *J. Polym. Sci., Part A: Polym. Chem.* **2001**, 39, 1353.
- (64)Monteiro, M. J.; de Brouwer, H. *Macromolecules* **2001**, 34, 349.
- (65)Housni, A.; Narain, R. *Eur. Polym. J.* **2007**, 43, 4344.

- (66) Ray, B.; Isobe, Y.; Matsumoto, K.; Habaue, S.; Okamoto, Y.; Kamigaito, M.; Sawamoto, M. *Macromolecules* **2004**, *37*, 1702.
- (67) Bivigou-Koumba, A. M.; Kristen, J.; Laschewsky, A.; Muller-Buschbaum, P.; Papadakis, C. *M. Macromol. Chem. Phys.* **2009**, *210*, 565.
- (68) Zhou, X. C.; Ye, X. D.; Zhang, G. Z. *J. Phys. Chem. B* **2007**, *111*, 5111.
- (69) Nykanen, A.; Nuopponen, M.; Laukkanen, A.; Hirvonen, S. P.; Rytela, M.; Turunen, O.; Tenhu, H.; Mezzenga, R.; Ikkala, O.; Ruokolainen, J. *Macromolecules* **2007**, *40*, 5827.
- (70) Lu, A.; Smart, T. P.; Epps, T. H.; Longbottom, D. A.; O'Reilly, R. K. *Macromolecules* **2011**, *44*, 7233.
- (71) Benaglia, M.; Chiefari, J.; Chong, Y. K.; Moad, G.; Rizzardo, E.; Thang, S. H. *J. Am. Chem. Soc.* **2009**, *131*, 6914.
- (72) Jeong, N. S.; Redhead, M.; Bosquillon, C.; Alexander, C.; Kelland, M.; O'Reilly, R. K. *Macromolecules* **2011**, *44*, 886.
- (73) Wang, X.; Qiu, X.; Wu, C. *Macromolecules* **1998**, *31*, 2972.
- (74) Delaney, E. J.; Wood, L. E.; Klotz, I. M. *J. Am. Chem. Soc.* **1982**, *104*, 799.



## **Chapter 3: Molecular recognition driven catalysis using polymeric nanoreactors**

### 3.1 Abstract:

The effect of covalently attaching 4-dimethylaminopyridine (DMAP) functionality to the hydrophobic core of a polymeric micelle in water has been investigated in the context of acylation reactions employing non-water-soluble substrates. For this purpose a novel temperature-responsive polymeric micelle has been synthesized using reversible addition-fragmentation chain transfer (RAFT) polymerization techniques. The reactivity of the tethered organocatalyst within the nanostructure has been found to be extremely high, improving in some cases the acylation rates up to 100 times compared to those for unsupported DMAP in organic solvents. These catalytic nanoreactors have been demonstrated to be capable of reuse up to 6 times whilst maintaining high activity. Furthermore, the exploration of how the properties of this nanoreactor can alter the results obtained with unsupported catalysts has been explored in the context of molecular recognition. Enhancement, inhibition and reversal of reaction selectivity have been achieved by tethering the catalyst in the hydrophobic core of a polymeric micelle, proving the need of kinetically frozen polymeric micelles *versus* surfactants in order to achieve substrate selectivity.

### 3.2 Introduction

The use of water as a solvent for organic reactions has increased in the last decade, as it is the most abundant and cheapest liquid on earth, it is safe, and has shown unique properties such as improving rate and selectivity in some organic reactions.<sup>1-4</sup> However, the use of water for synthetic organic chemistry is restricted because most organic compounds are non-polar and hence insoluble in water. Based on previous results from Breslow and Rideout,<sup>1</sup> in 2005 the

group of Sharpless reported the “on water” protocol where organic substrates were added to water and stirred vigorously forming small droplets of reactants, to allow for effective catalysis and also for easy product isolation by phase separation or filtration.<sup>2</sup> This protocol showed an unexpected increase in rates for several organic reactions using hydrophobic reactants in aqueous solutions compared to those in organic solvents or neat conditions. On the other hand, the environmental and economic assessments of an aqueous reaction are shown to involve a complex set of parameters.<sup>5</sup> Catalysts are often the most expensive component in organic reactions and are usually very toxic, hence there is great interest in the immobilization of catalysts for simplification of product work-up, separation, isolation, and facile recovery of the catalysts.

Specific interactions between biological molecules are essential in nature. Most of the chemical reactions in biological cells are catalyzed by enzymes, which act specifically with one substrate using molecular recognition.<sup>6</sup> The complementarity between the substrates and active site relies on the shape of the molecules, hydrogen bonding, charges, dispersion forces and hydrophobic interactions. Indeed, enzymes generally make use of a compartmentalized hydrophobic cavity surrounded by a hydrophilic outer shell to allow specific catalysis.<sup>7</sup> Inspired by enzymes, several groups have designed a wide range of artificial catalytic systems where the catalyst is isolated from the environment through the use of core-shell structures such as dendrimers and polymeric stars,<sup>8-12</sup> but the cases where these systems allow for efficient catalysis in water are rare. Recent work by Meijer and co-workers reported a compartmentalized catalyst synthesized by supramolecular folding of a single polymer chain that catalyzes carbonyl reductions in water, the authors described this system as an enzyme mimic.<sup>13</sup> Inspired by this work it would be desirable to synthesize a system that combines the

use of water for the reaction of hydrophobic organic substrates, using a hydrophobic environment to improve the reaction rates with advantages of the facile synthesis of amphiphilic diblock copolymer supported catalysts.

The development of new systems to create organic microenvironments in aqueous media using surfactants has been widely investigated.<sup>14,15</sup> These amphiphiles form spherical aggregates with hydrophilic surfaces and hydrophobic cores, the hydrophobic reactants are concentrated within the core resulting in the observed acceleration in reaction rate and introducing selective effects.<sup>16-18</sup> For example, Kobayashi *et al.* carried out dehydration reactions in water using dodecylbenzenesulfonic acid as a surfactant-type catalyst.<sup>16,17</sup> In this system the catalyst enhanced the reaction rate and the hydrophobic interior of the droplets facilitated the exclusion of the water, allowing for the synthesis of esters in high yields for highly hydrophobic substrates. We and others have studied the use of polymeric micelles in order to catalyze organic reactions in aqueous media through incorporation of catalysts into polymeric scaffolds.<sup>19-22</sup> To prepare these materials, functionalized monomers can be covalently incorporated into the hydrophobic domain of a polymeric micelle *via* copolymerization techniques.<sup>23,24</sup> Advantages of these polymeric systems over the extensively studied surfactants are the possibility of facile catalyst recovery and the unique properties originated by the difference in polarity between the shell domain and the very stable hydrophobic pocket created in the core of polymeric nanoreactors compared to more dynamic surfactant systems.<sup>25</sup> Due to the kinetically frozen structure of polymeric micelles, the diffusion of the hydrophobic substrates into the stable hydrophobic core of the micelle is improved,<sup>25</sup> showing unprecedented enhancements of the reaction rates, while the water permeability within the core domain is significantly reduced compared to surfactant based micelles.<sup>22</sup>

In order to explore how the incorporation of the catalyst into the hydrophobic core of a polymeric micelle will affect its catalytic activity, Zhao *et al.* used atom transfer radical polymerization (ATRP) to synthesize a diblock copolymer containing DMAP functionality tethered within the temperature-responsive block which formed the hydrophobic core of the micelle upon heating.<sup>26</sup> They envisioned that if the partition coefficient of the substrate between micelles and water is sufficiently high, the substrates could be concentrated in the core of the micelle, resulting in an enhanced reaction rate. However, contrary to their hypothesis, the DMAP-containing polymer did not accelerate the rate of reaction upon self-assembly. They related this surprising observation to a mass transport limitation of their starting materials from the water to the core of the micelles.

The unique hydrophobic environment created in the core of a polymeric micelle can be tuned by selecting the degree of hydrophobicity of the core block.<sup>27</sup> This has been showed very elegantly by Weck and coworkers who, based on previous work by Weberskirch, designed an optimal polymeric system for the hydrolytic kinetic resolution of epoxides in water.<sup>19,20</sup> In this work, the high local concentration of catalyst in the hydrophobic core of the micelle together with the small amount of water that can penetrate during catalysis were demonstrated to be crucial in achieving higher activity and better enantioselectivity than that obtained under homogeneous conditions in organic media. In addition, the system exhibited outstanding recycling properties.

Several aqueous catalytic systems using surfactants have been reported to achieve substrate selectivity based on hydrophobicity.<sup>17,18,28</sup> However, the use of the unique properties originated by the difference in polarity of the core-shell domains in kinetically frozen polymeric

nanoreactors is still at an early stage in terms of exploitation in the context of molecular recognition. A first approach was recently reported by Weck and co-workers for the selective hydrolytic kinetic resolution of epoxides using shell-crosslinked polymeric nanoreactors in water.<sup>19</sup> Although different reactivities were found for a range of epoxides based on hydrophobicity, only initial experiments were carried out where a competitive reaction of two different substrates of similar reactivities was explored and substrate selectivity was observed based on hydrophobicity.

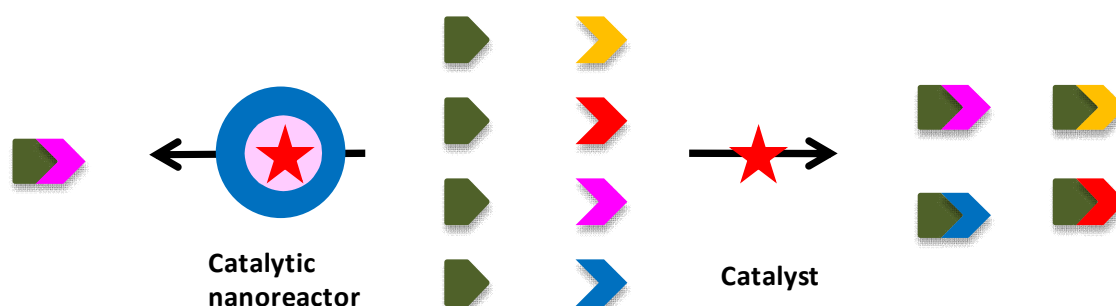


Figure 3.1: Illustration of specific reaction of one substrate (from a pool of 4) using a polymeric nanoreactor as a reaction vessel.

Unfortunately, enzymatic catalysis is much more complex with specific reactions rather than selective ones, enabling distinction between one single target from a mixture of several substrates of different reactivities; therefore, our challenge is to utilize a catalytic polymeric nanostructure as a yocto-litre reaction vessel, whose molecular recognition properties can be utilized to promote a specific reaction from a pool of reactants (Figure 3.1). If the stable polymeric scaffold restricts the permeability such that only the most hydrophobic molecule can diffuse to the core, substrate specificity will be observed. To demonstrate the synthetic utility that this system affords, we have carried out the competitive reaction of different products using kinetically frozen catalytic nanoreactors in aqueous media. Our results clearly

indicate that by tethering the catalyst in a confined hydrophobic environment, specific molecular recognition is achieved in the presence of several substrates and the reactivity can be significantly enhanced compared to that for unsupported catalysis and surfactant based systems.

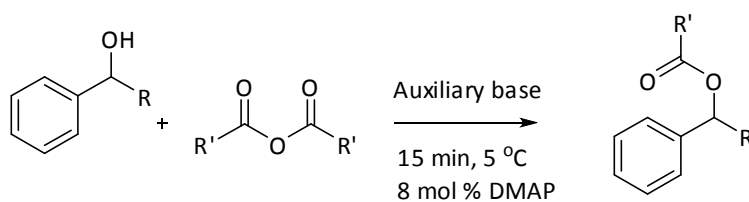
### 3.3 Results and discussion

#### 3.3.1 *Acylation Reactions:*

In order to probe the effects of encapsulating a catalyst in a hydrophobic environment in an overall aqueous medium the well-established DMAP catalyzed acylation reaction of an alcohol was investigated as a model system. The previously synthesized DMAP-containing micelles **2.12** in water were tested as catalytic nanoreactors for different substrates as indicated in Table 3.1. In homogeneous systems this reaction is generally carried out in anhydrous conditions (since the anhydride slowly hydrolyzes upon contact with water) and preferentially in bulk or less-polar solvents to facilitate the recycling of the catalyst.<sup>29</sup> Similar conditions to those reported by Fréchet for the acylation of alcohols using DMAP-containing dendrimers were targeted.<sup>30</sup> All catalytic reactions were carried out with stirring at 5 °C to ensure polyNIPAM was completely dissolved. Aliquots were taken from the reaction mixture at different times and the conversion was determined by HPLC analysis. All reactions were performed in triplicate. In these reactions 8 mol % of DMAP was employed, taking into account that each polymer chain contains an average of 4 units of the catalytically active DMAP moiety.

In the first approach (Entry 1, Table 3.1) the acylation reaction was carried out using 1 equivalent of 1-phenylethanol (0.02 M) with 3 equivalents of anhydride and 1.5 equivalents of TEA in the aqueous micelle solution **2.12** (at 8 mol % DMAP loading). When using acetic anhydride as the substrate the reaction reached 26 % conversion in 15 minutes and then appeared to stop.





Entry	R	R'	% conv	% conv
			(15 min)	(24 h)
1	CH <sub>3</sub>	CH <sub>3</sub>	26	32
2	CH <sub>2</sub> CH <sub>3</sub>	CH <sub>3</sub>	28	29
3	CH <sub>3</sub>	CH <sub>2</sub> CH <sub>2</sub> C <sub>3</sub>	47	53
4*	CH <sub>3</sub>	CH <sub>2</sub> CH <sub>2</sub> CH <sub>3</sub>	65	66
5*	CH <sub>2</sub> CH <sub>3</sub>	CH <sub>2</sub> CH <sub>2</sub> CH <sub>3</sub>	94	98

Table 3.1: Data showing conversions after 15 minutes and 24 hours for acylation reactions in the micelles, **2.12**.

All reactions contained 8 mol % DMAP, [OH] = 0.02 M, 1.5 equivalents of auxiliary base (TEA), 1 equivalent of alcohol and 3 equivalents of anhydride. Conversions determined by HPLC measurements with mesitylene as the internal standard. \*N,N-Diisopropylethylamine (DIPEA) was used as auxiliary base instead of TEA.

The drastic decrease in the reaction rate after achieving approximately 25% conversion may be attributed to a mass transport limitation as predicted by Zhao and co-workers.<sup>26</sup> If the hydrophobicity of the reactants is the driving force of the reaction, when the product is more hydrophobic than the substrates the nanoreactor will eventually become saturated, preventing the starting materials in the water from moving into the reactive hydrophobic core and hence stopping the reaction. This hypothesis was investigated by adding a new batch of starting materials (alcohol, anhydride and auxiliary base) to the micellar solution after reaching this point. As expected, only 25% of this additional batch was acylated and the reaction stopped when the ratio of reactants-products reached the equilibrium between the hydrophobic core of

the reactor and the water. The addition of fresh starting materials was repeated 4 times and the results observed were reproducible; the acylation reached equilibrium and in all cases only 25 % conversion was observed 15 minutes after each addition (see section 3.5.6).

The addition of a 5<sup>th</sup> batch ( $[\text{OH}] = 0.10 \text{ M}$ ) resulted in the partial precipitation of the polymer. This observation gave us an indication about the concentration limits of our micellar system. While the lower limit ( $[\text{OH}] = 0.02 \text{ M}$ ) is determined by the detection limit of the method of analysis (HPLC), the higher limit appears to be dependent on the amount of hydrophobic materials that the nanoreactor can house inside the hydrophobic core domain.

### 3.3.2 *Effect of substituents on the equilibrium position:*

In order to overcome the above mentioned mass transport limitation and achieve higher acylation conversion, further experiments were carried out using different alcohol and anhydride substrates (Entries 2 to 5, Table 3.1). We expect that the use of more hydrophobic starting materials will favor the diffusion of reactants to the core and hence increase the reaction conversions before equilibrium is reached. In all cases the acylation reaction of different substrates in the aqueous solution containing DMAP micelles **2.12** reached the equilibrium position after 15 minutes. Initially, a less water-soluble alcohol (R = ethyl *versus* methyl) was targeted but unfortunately the hydrophobicity of the alcohol did not show any significant contribution to the reaction rate at this point (Entry 2, Table 3.1).

Studies by Steglich *et al.* based on kinetic measurements of the DMAP-catalyzed acylation of alcohols concluded that the rate-determining step of esterification reactions of this type is the reaction of the N-acylpyridinium carboxylate with the alcohol.<sup>31</sup> Neither DMAP nor the

auxiliary base enters the kinetic equation. Hence, in our micellar system the use of a more hydrophobic anhydride seems to be key, as suggested by the reaction mechanism (Figure 4).

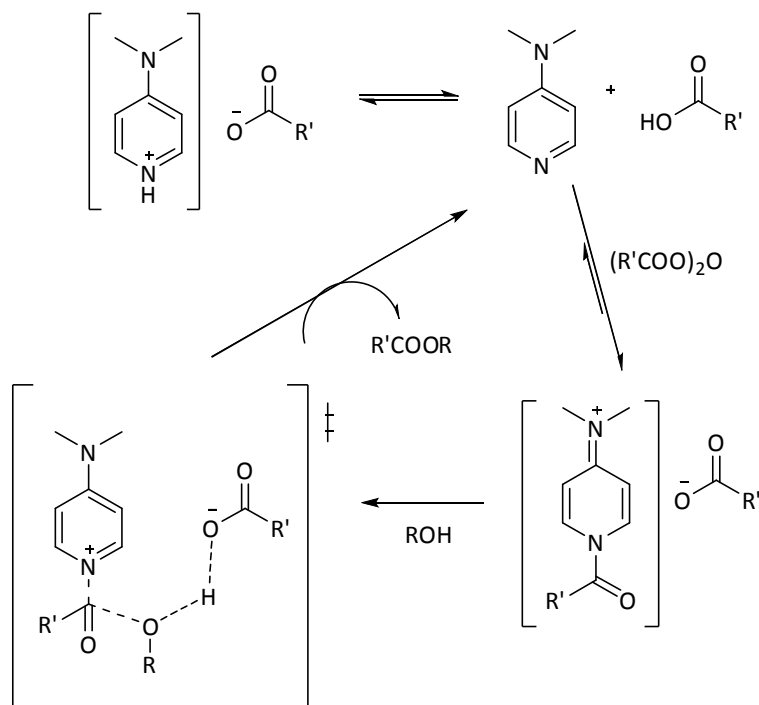


Figure 3.2: Proposed mechanism for the DMAP-catalyzed acylation.<sup>29,31</sup>

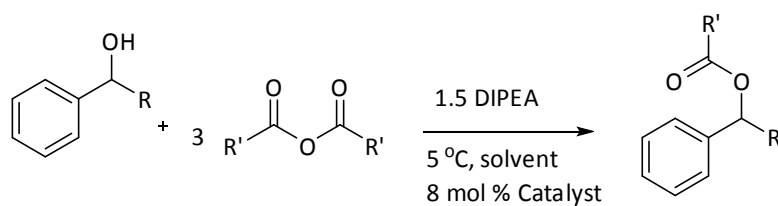
When using the more hydrophobic butyric anhydride under exactly the same conditions as previously discussed (Entry 3, Table 3.1) the conversion of the esterification reaction increased, obtaining an acceptable 47 % after 15 minutes. This promising result was slightly improved by introducing a more hydrophobic auxiliary amine, *N,N*-diisopropylethylamine (DIPEA), which increased the conversion to 65 % over the same time period (Entry 4, Table 3.1). However, when a more hydrophobic alcohol, anhydride and auxiliary amine were used, the acylation reaction was completed within 15 minute (Entry 5, Table 3.1). It is not unexpected that the use of longer alkyl chains on the starting materials afforded higher conversions due to improved partitioning and concentration within the catalytically active micellar core. On the other hand, when the reactions were carried out in THF using

unsupported DMAP as a catalyst, the use of more hydrophobic substrates did not significantly affect the reaction rates (see section 3.5.6). These results emphasize the importance of the hydrophobicity of the substrates to allow for high activity and conversion in our micellar systems.

### 3.3.3 *Comparison with organic solvents and bulk:*

To obtain further data about how the environment created inside the micelle affects the rates of reaction, the acylation of 1-phenylpropanol with butyric anhydride was carried out in different solvents and in neat conditions using unsupported DMAP as the catalyst. The reaction proceeded very fast in less polar solvents (hexane) and solvent free conditions compared to more polar solvents such as THF or water (Entries 1 to 4, Table 3.2). This behaviour has previously been reported by Ishihara and co-workers for the acylation reactions of a range of alcohols under different conditions.<sup>29</sup> The use of less polar solvents aids the regeneration of the DMAP catalyst which results in higher reactivities, while polar solvents cause the formation of ammonium salts and lead to a decrease in reactivity.

For this reason it is not surprising that the acylation in water only achieved 8 % conversion when non-supported DMAP was used (Entry 1, Table 3.2). It is noteworthy that, although the reactions in bulk and in the micellar system (Entries 4 and 6) yielded the same conversion at the equilibrium position, the reaction in the aqueous micelles is 8 times faster than that in hexane, which can be attributed to the “concentrator effect” observed by Fréchet and co-workers.<sup>30</sup>



Entry	Catalyst	Solvent	% conv.	% conv.
			(15 min)	(24 h)
1	DMAP*	Water	2	8
2	DMAP*	THF	13	87
3	DMAP*	Hexane	85	86
4	DMAP*	Bulk	58	96
5	DMAP*	<b>3.2**</b>	0	3
6	<b>2.11</b>	<b>2.12**</b>	94	98
7	<b>2.11</b>	THF	2	60

Table 3.2: Data showing reaction conversion after 15 minutes and 24 hours for the acylation reactions in different solvent conditions. All reactions were carried out with 8 mol % DMAP,  $[\text{OH}] = 0.02\text{ M}$ , 1.5 equivalents of auxiliary base, 1 equivalent of alcohol and 3 equivalents of anhydride. Conversions were determined by HPLC measurements, with mesitylene as the internal standard.  $\text{R} = \text{CH}_2\text{CH}_3$ ,  $\text{R}' = \text{CH}_2\text{CH}_2\text{CH}_3$ . \* Unsupported DMAP was used as a catalyst. \*\*Micelle in water.

On the other hand, the higher conversions for the polymer-supported DMAP catalyst **2.12** compared to the acylations in bulk (Entries 4 and 6, Table 3.2) agree with the polarity effects observed by Ishihara *et al.*<sup>29</sup> The substrates themselves are a more polar solvent than hexane resulting in a deceleration of the acylation under solvent free conditions. These reactions confirm that the micelles create a more favorable environment for the acylation to occur in pure water similar to that created in organic solvent or neat conditions.

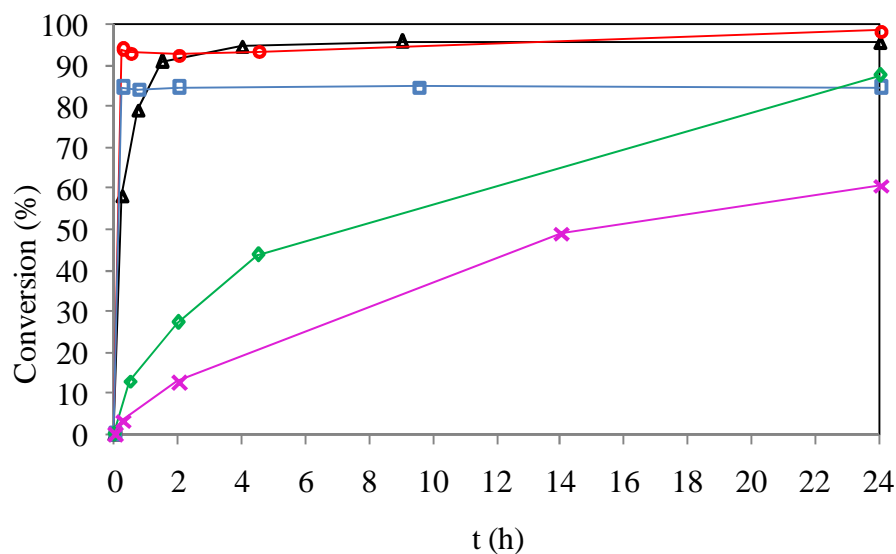


Figure 3.3: Conversions *vs* reaction times for DMAP catalyzed acylation reactions in Table 3.2: Entry 2 (◇), Entry 3 (□), Entry 4 (Δ), Entry 6 (○) and Entry 7 (×), R = CH<sub>2</sub>CH<sub>3</sub>, R' = CH<sub>2</sub>CH<sub>2</sub>CH<sub>3</sub>.

We were also interested in whether simple addition of DMAP to a non-functionalized micellar system would allow for similar catalyst activities. Hence, we next explored the requirement of tethering the catalyst in the hydrophobic environment of a micelle compared to simple addition of DMAP to a micellar system. For this purpose a new block copolymer PS<sub>38</sub>-*b*-PNIPAM<sub>140</sub> (**3.1**,  $M_n$  (NMR) = 19.2 kDa,  $M_w/M_n$  (GPC) = 1.29, which contained no DMAP functionality) was synthesized and self assembled into micelles **3.2**, *via* the procedure described for the DMAP nanoreactors. DLS and TEM studies show that the unfunctionalized micelles **3.2** were of similar size to the DMAP containing micelles **2.12** ( $D_{av}$  = 23.1 nm,  $D_h$  = 35.4 nm, see 3.5.4). DMAP small molecule (8 mol % loading) was added to micellar solution **3.2** and stirred for 1 hour before addition of the alcohol, anhydride and DIPEA. The aliquots taken from the reaction after 24 hours showed that the acylation does not occur in water if the DMAP functionality is not covalently attached within the hydrophobic environment. We

attribute this important observation to two different factors: unlike the starting materials, DMAP is water soluble, and given the small amount added to the solution (1.3 mg in 8 mL of water) it is unlikely that the organic substrates find any DMAP in the hydrophobic core. Secondly, it is likely that the DMAP catalyst is poisoned by protonation from the acid created by the excess of anhydride hydrolyzed in the aqueous media.

The rate of acylation using polymer-supported DMAP **2.11** in THF is lower and less efficient than the non-supported DMAP (Entries 2 and 7, Table 3.2). THF is a good solvent for both blocks of the amphiphilic polymer, hence self-assembly into micelles does not occur and the acylation will proceed as a conventional “polymer supported” catalyzed reaction, where unlike the non-supported catalyst, the DMAP functionality is more sterically hindered. These results demonstrate the advantages of tethering the catalyst into the interior pocket of a polymeric nanoreactor rather than just onto a simple polymer support. The high local concentration of catalyst within the core domain leads to enhanced activity similar to that for organic solvents or neat conditions and the hydrophobic core creates a hydrophobic non-polar environment preventing DMAP protonation.

#### 3.3.4 Catalyst loading:

To further investigate the potential of our DMAP-containing micelles, the amount of catalyst was reduced to 0.8 and 0.08 mol %. When the most efficient esterification reaction (Entry 5, Table 3.1) was repeated with the catalyst loading lowered by 10 fold only a 10 % drop in conversion was observed, and similarly the equilibrium point was reached in 15 minutes. However, lowering the catalyst 100 times lead to a significant decrease in conversion, achieving *ca.* 50 % of the acylation product at the equilibrium position after 6 hours (Figure 3.4).

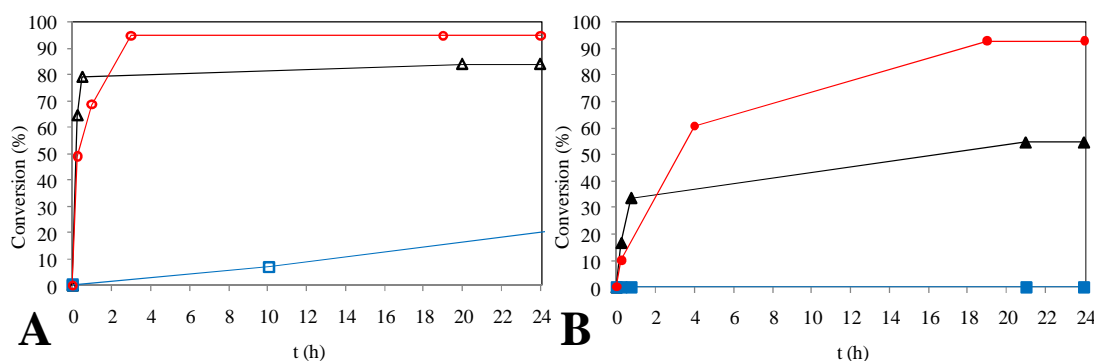


Figure 3.4: Acylation reactions using 0.8 % (A) and 0.08 % (B) DMAP catalyst in the micelles (triangle) compared to the small molecule reaction in THF (square) or hexane (circle) for conditions shown in Table 3.2.

To provide a direct comparison the acylation was explored under the same conditions with small molecule DMAP in THF and hexane (Figure 3.4). The reduction of the catalyst content in the THF homogeneous system induced a drastic decrease in reaction rates compared to those for the DMAP-containing micelles. By reducing the non-supported catalyst to 0.8 mol % (Figure 3.4a), the conversion decreased more than 50 %, and furthermore, no reaction was observed after 24 hours when the amount of catalyst was reduced to 0.08 % (Figure 3.4b). When homogeneous catalysis was carried out in hexane, the reaction rates decreased compared to those for the same conditions using 8 % catalyst, however both reactions (0.8 and 0.08 % catalyst) achieved more than 95 % conversion in 24 hours.

In our experiments with lower catalyst loading the micelle solution **2.12** was diluted to the desired concentration, however given the kinetically frozen nature of our micelles we hypothesize that this essentially resulted in a reduction in the total number of micelles in the solution and hence less “catalytic pumps” to catalyze the reaction. For this reason we believe that the equilibrium of the substrates between water and the micelles is reached faster leading to lower conversions compared to those for hexane. We postulate that the synthesis of a new



polymer containing lower DMAP loadings but retaining the same block lengths as **2.11** will allow us to reduce the catalyst loading whilst maintaining the same number of “hydrophobic pockets” and hence potentially reaching higher conversions.

### 3.3.5 *Recycling experiments:*

One of the main advantages of tethering the catalyst to a polymeric support over the widely studied catalysis using surfactants is the facile recovery of the polymer for recycling. In our recycling experiments 0.8 mol % DMAP-supported catalysts from a diluted solution of **2.12** was employed to catalyze the acylation reaction of 1-phenyl propanol with 3 equivalents of butyric anhydride and 1.5 equivalents of DIPEA as auxiliary base. The reactants together with a known amount of mesitylene (as an internal standard) were added to the micelle solution at 5 °C and after 1 hour a sample was taken and analyzed by HPLC to determine the conversion. The product was then extracted with diethyl ether and the same aqueous solution was reused in a new acylation reaction by addition of a second batch of reactants. The catalyst was reused with little or no change in reaction rate or conversion 5 times (80%, 74 %, 83 %, 70% and 79 % respectively after 1 hour). However, after this point it was noted that the reaction mixture became brown due to the excess of water soluble auxiliary base in solution, which was not removed by organic extraction.

Hence, a new recycling route was investigated using the stimulus-responsive properties of our system. After extraction of the synthesized product with diethyl ether, the aqueous phase containing the micellar catalyst was heated to a temperature above 50 °C. At this temperature, the polymer exists as a fine powder and was collected by centrifugation. The recovered catalyst was reused in another reaction cycle using the same amount of reactants and water to keep the

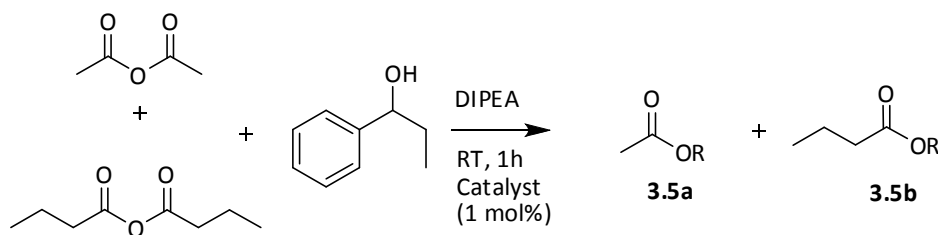
concentration of reactants the same as in a fresh cycle, and this experiment achieved 85 % conversion after 1 hour of reaction. The product was then extracted with diethyl ether after the 6 recycling cycles and the aqueous solution was freeze-dried in order to analyze the solid residue by  $^1\text{H}$  NMR spectroscopy. Integration of the characteristic DMAP peak at *ca.* 4.4 ppm confirms that the DMAP functionality is present and still attached to the polymer backbone following recycling.

Alternatively, the polymer can be purified to be used in a different reaction by heating the micellar solution above the lower critical solution temperature (LCST) of the micelles. The precipitated polymer can then be recovered by filtration and washed with ethyl acetate in order to remove all organics. A  $^1\text{H}$  NMR spectrum of the clean polymer after reaction can be found in the supporting information (see section 3.5.7).

Given the low LCST of the micelles synthesized in the previous chapter **2.12** all initial reactions were carried out in the fridge, hence a new polymer was synthesized by chain extension of the DMAP containing polymer **2.10** with 190 units of NIPAM giving a new polymer with a longer hydrophilic chain **3.3**. The polymer was self-assembled into water as described in Chapter 1. The new spherical micelles **3.4** were found to be *ca.* 24 nm in diameter as determined by TEM analysis (see section 3.5.7)

### 3.3.6 *Molecular recognition:*

In order to investigate selective esterification reactions in this system, the competitive reaction between two different anhydrides with 1-phenylpropanol in the presence of auxiliary base were studied (Table 3.3).

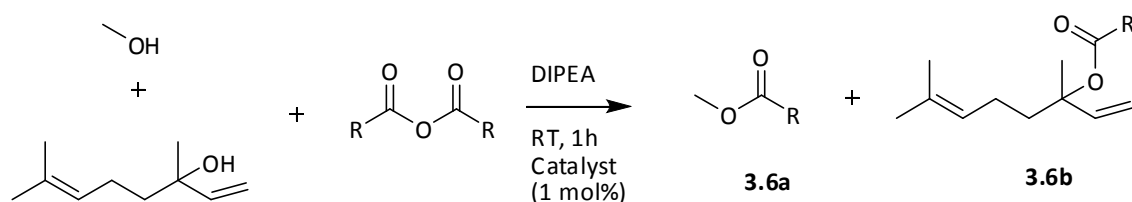


Catalyst	% Conversion ( <b>3.5a</b> + <b>3.5b</b> )
<b>3.4</b>	83 (22+61)
DMAP	92 (52+40)
<b>2.2</b> /SDS	26 (2+24)

Table 3.3: Reaction contained 1 mol % of catalyst, 1 equivalent alcohol, 1.5 equivalents of auxiliary base (DIPEA) and 1.5 equivalents of each anhydride. Conversions determined by HPLC analysis with mesitylene as the internal standard. R= CH(C<sub>6</sub>H<sub>5</sub>)C<sub>2</sub>H<sub>5</sub>

When a 1:1 mixture of acetic anhydride and butyric anhydride was added to the reaction mixture using unsupported DMAP in neat conditions, 12% less of the ester from the bulkier anhydride **3.5b** was obtained (**3.5a**/**3.5b** = 1.3), probably due to steric effects. On the other hand, when micelles **3.4** was used as a catalyst in aqueous media, the selectivity of the reaction was reversed and **3.5b** was formed preferentially (**3.5a**/**3.5b** = 0.4). As observed by Weck, the increase of the length of the carbon chain resulted in a remarkable increase in its reactivity within the micelle. Although both reactions reached high conversions, as predicted, this first experiment clearly indicates that just the micellar system **3.4** exhibits molecular recognition based on hydrophobicity (the more hydrophobic, the more reactive) and independent of steric effects. Similar results were obtained in the competitive acylation of 1-phenyl-1-propanol with acetic and valeric anhydrides (see 3.5.8).

To obtain further data about how the environment created inside the polymeric micelle **3.4** affects selectivity and reaction rates, the same reaction was explored using sodium dodecyl sulfate (SDS) as the surfactant and a modified DMAP with high hydrophobicity (the previously synthesized styrenic monomer **2.2**). Although this new system also shows selectivity based on hydrophobicity, the acylation reaction was more than 3 times slower, achieving just 26% conversion after 1 hour compared to the 83% obtained for the polymeric system **3.4**.



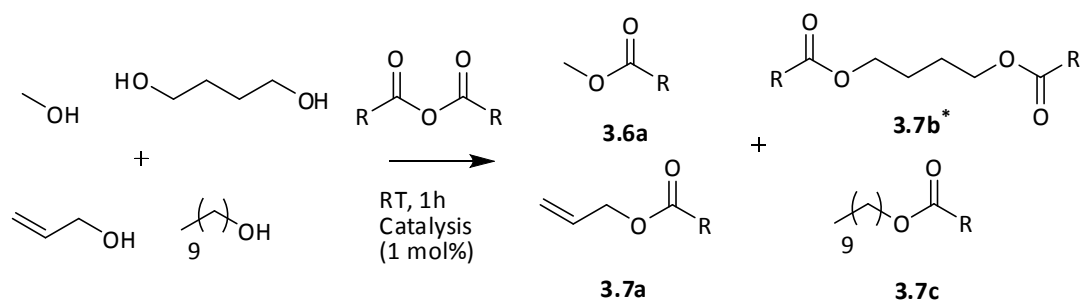
Catalyst	% Conversion (3.6a+3.6b)
<b>3.4</b>	60 (0+60)
DMAP	>99 (>99+0)
<b>2.2</b> /SDS	65 (45+20)

Table 3.4: Reaction contained 1 mol % of catalyst, 1 equivalent of each alcohol, 1.5 equivalents of auxiliary base (DIPEA) and 3 equivalents of anhydride. Conversions determined by GC analysis with mesitylene as the internal standard. R= CH<sub>2</sub>CH<sub>2</sub>CH<sub>3</sub>

To further explore the selectivity of this system, **3.4** was used in the 1:1 competition reaction of linalool and completely water-soluble methanol. Linalool is a compound present in many flowers and plants and its acylated products are commonly used as a scent for hygiene products and cleaning agents.<sup>32</sup> However, ordinary methods of acylation cannot be used with linalool due to its unreactive nature and its tendency to cyclize upon heating. Despite this, in the case of

the polymeric micelles **3.4**, 60% conversion was reached after 1 hour compared to 2% conversion for unsupported DMAP during the same period (Table 3.4).

Given the reactivity and hydrophilic nature of methanol, it is not surprising that its acylation was complete after 1 hour in the homogeneous system, but interestingly no conversion was observed in the nanoreactor, where the unique product formed was the less reactive acylated linalool **3.6b**. This new observation suggests that the encapsulation of the catalyst in the core of a polymeric micelle not only reverses selectivity based on hydrophobicity but facilitates the reaction of otherwise non-reactive alcohols by bringing the substrate in closer proximity to the catalyst. To our knowledge, this is the first example where the selectivity of the reaction is reversed and specificity is achieved by encapsulating the catalyst in a synthetic hydrophobic pocket, facilitating the reaction of otherwise non-reactive substrates while inhibiting the formation of the otherwise most favourable product. On the other hand, when the reaction was carried out in the presence of SDS using **2.2** as a catalyst, 45% of the methanol had reacted after 1 hour and only 20% of the product from the less reactive linalool was formed. As hypothesized, these control experiments confirm that the tethering of the catalyst in the hydrophobic core of a kinetically frozen polymeric micelle creates a unique hydrophobic environment able to completely inhibit the reaction of hydrophilic substrates and extraordinarily enhance the reactivity of hydrophobic substrates compared to that of the less stable surfactant-based systems.



Product	DMAP (bulk)	DMAP micelles (3.4)
3.6a	>99	trace
3.7a	32	trace
3.7b*	>99	trace
3.7c	75	>99

Table 3.5: Reactions contained 1 mol % of catalyst, 1 equivalent of each alcohol, 1.5 equivalents of auxiliary base (DIPEA) and 4 equivalents of anhydride. Conversions determined by GC analysis with mesitylene as the internal standard. \*Mixture of the mono- and di-alkylated products observed. R= CH<sub>2</sub>CH<sub>2</sub>CH<sub>3</sub>

As a proof-of-principle that polymeric micelles can act as nano-vessels for specific molecular recognition in the presence of multiple substrates, we investigated how the presence of the polymeric micelles **3.4** affected the substrate selectivity in a one pot acylation reaction of four different alcohols with similar reactivities. Preliminary experiments showed that, when equimolar amounts of two different alcohols were tested under these conditions, the ratio of products obtained was highly dependent on the hydrophobicity of the alcohols (see experimental section). Following these initial experiments, the competitive DMAP-catalyzed acylation between four primary alcohols (methanol, allyl alcohol, 1,4-butanediol and 1-decanol) with butyric anhydride in the presence of auxiliary base was studied. Initially a mixture of one equivalent of each alcohol was butyrylated using unsupported DMAP in neat conditions (Table 3.5).

As expected, the conversions obtained for the different alcohols simply depend on their reactivity. The primary alcohols were efficiently acylated and only the less reactive allyl alcohol and the bulkier 1-decanol were still present after 1 hour. When the same reaction was tested in the micellar system **3.4**, just the hydrophobic 1-decanol formed the acylated product (**3.7c**) quantitatively in the same time. These results highlight the specific acylation of one alcohol in the presence of several closely related substrates allow for significant expansion of the utility of our organocatalytic nanoreactor system.

### 3.4 Conclusions

The catalytic activity for the acylation of hydrophobic substrates in aqueous media of the DMAP-functionalized nanoreactors synthesized in Chapter 1 has been determined and compared to that of unsupported DMAP in organic solvents. The data indicate that the high local concentration of catalyst and the hydrophobic environment created in the core of the nanoreactors are crucial to achieving high acylation reactivities. The reaction rates in the aqueous micellar system are comparable and in some instances greater than those for homogeneous reactions in organic media. Moreover, the polymeric catalyst was reused in 6 consecutive cycles without loss of activity and the stimulus-responsive properties were utilized to assist in the recovery of the active polymer. The applicability of the system has been shown to be very dependent on mass transport limitations of reagents, products and regenerative species and a deep mechanistic understanding of the reaction catalyzed is necessary.

The synthesized polymeric nanoreactors show specific substrate recognition able to drastically modify the selectivity of the reactions based on the simple concept of hydrophobicity and the hydrophobic core-substrate attraction, induced by the unique nature of the polymeric micelle,

which creates a concentrated catalytic environment that allows for reaction of otherwise non-reactive species. These results demonstrate a significant improvement of the effects observed for surfactant-based systems. This is the first example of a catalytic polymeric nanoreactor capable of effectively distinguishing from a pool of substrates of similar or different reactivities and where specificity is achieved based on substrate hydrophobicity. We see these results as first step towards the design and development of new enzyme mimics for organic reactions in water.

### 3.5 Experimental Section

#### 3.5.1 *Materials:*

Styrene monomer was filtered through a plug of aluminum oxide prior to use and stored at 4°C. NIPAM and AIBN (2,2'-azo-bis(isobutyronitrile)) were recrystallized from a 9:1 mixture of hexane/acetone and methanol respectively, and stored at 4°C. 4-(N-methyl-N-(2-hydroxyethyl)amino)pyridine was prepared previously by a member of the group as reported in the literature.<sup>33</sup> All other materials were used as received from Sigma-Aldrich, Fluka, and Acros.

#### 3.5.2 *Instrumentation:*

<sup>1</sup>H NMR spectra were recorded with a Bruker DPX-300 spectrometer in CDCl<sub>3</sub> at 25 °C (128 scans). Chemical shifts are given in ppm downfield from an internal reference of TMS. Size exclusion chromatography (SEC) measurements were performed with HPLC grade solvents (Fisher), tetrahydrofuran (THF) with 2 % of TEA, at 30 °C or dimethylformamide (DMF) 1.06 g LiCl per liter at 40 °C as an eluent at a flow rate of 1 mL/min. The molecular weights of



the synthesized polymers were calculated relative to polystyrene (PS) or poly methyl methacrylate (PMMA) standards. Lower critical solution temperature (LCST) measurements were analyzed using a Perkin-Elmer UV/vis Spectrometer (Lambda 35) equipped with a Peltier temperature controller at 500 nm with a heating/cooling rate of 1 °C/min. For the characterization of the particles, the micelle solution was diluted with nanopure water to obtain a final concentration of *ca.* 0.1 mg/mL. TEM images were obtained using a JEOL electron microscope operating at 200 kV equipped with a LaB6 gun and a Gatan digital camera. To prepare TEM samples, carbon grids were prepared by oxygen plasma treatment to increase the surface hydrophilicity and then 5 µL of an aqueous solution of micelle was placed on a carbon-coated copper grid for 60 s, and the water droplet was removed by vacuum absorption. Aqueous uranyl acetate (UA) solution (1%) was used to stain the particles. DLS studies were conducted at 25°C using a Zetasizer Nano series instrument (Malvern Instruments), at a fixed scattering angle of 173°. The data were processed by cumulants analysis of the experimental correlation function and particle diameters were calculated from the computed diffusion coefficients using the Stokes-Einstein equation. Each reported measurement was the average of three runs. For the HPLC measurements, the aliquots taken were analyzed on a reversed-phase Discovery C18 HPLC column, using a gradient method going from 95:5 water:methanol to 5:95 water:methanol over a 12 minute time period, at 2.0 mL/min using a PDA detector and mesitylene was used as a standard ( $t_R = 8.25$  min) or over a 15 minutes time period ( $t_R = 10.31$  min). For the GC measurements, the aliquots taken were analyzed on chiral capillary column (Varian CP-Chirasil-DEX fused WCOT, 25m x 0.25mm, with Hydrogen, 1 kPa), using a gradient of temperature from 40 to 200 °C over a 9 minutes

period, 2 mL/min, in combination with an FID detector. Mesitylene was used as a standard ( $t_R$  = 4.50 min).

### 3.5.3 Polymers synthesis

#### – Styrene homopolymerization

Styrene (4 mL, 35 mmol) and CTA **2.9** (0.13 g, 0.3 mmol) were dissolved in 4 mL of DMF in an ampoule. The oxygen was removed by three freeze-pump-thaw evacuation cycles. For the last cycle, nitrogen was flushed into the ampoule before thawing. The solution was heated at 110 °C in an oil bath. An aliquot was taken after 30 hours to determine the conversion by  $^1\text{H}$  NMR spectroscopy (43 %). The polymer was precipitated twice into a stirred solution of cold  $\text{CH}_3\text{OH}$ , filtered and placed in the vacuum oven overnight at 40 °C.

$^1\text{H}$  NMR (400 MHz,  $\text{CDCl}_3$ ):  $\delta$  (ppm) 7.37-6.23 (br m, Ar-H), 3.25 (t, 2H end group), 2.45-1.12 (br m, backbone), 0.85 (t, 3H end group).  $M_n(\text{NMR}) = 4.4$  kDa,  $n = 38$ ,  $M_n(\text{SEC THF, PS}) = 4.3$  kDa,  $M_w / M_n(\text{SEC}) = 1.09$ .

#### – Chain extension of polystyrene with NIPAM (3.1)

Polystyrene (0.3 g, 0.07 mmol), NIPAM (1.6 g, 14 mmol), AIBN (2.4 mg, 0.014 mmol) were dissolved in 7 mL of THF in an ampoule. The oxygen was removed by three freeze-pump-thaw evacuation cycles. For the last cycle, nitrogen was flushed into the ampoule before thawing. The solution was heated at 65 °C in an oil bath. After 7 hours (72 % conversion by  $^1\text{H}$  NMR spectroscopy), the polymer was precipitated twice into a stirred solution of cold diethyl ether, filtered and placed in the vacuum oven overnight at 40 °C.

$^1\text{H}$  NMR ( $\text{CDCl}_3$ ):  $\delta$  (ppm) 7.22-5.71 (br m, Ar-H), 3.98 (br s, 1H, CH), 2.47-0.72 (br m, backbone).  $M_{\text{n}}(\text{NMR}) = 19.2$  kDa,  $n = 38$ ,  $m = 140$ ,  $M_{\text{n}}(\text{SEC DMF, PMMA}) = 10.8$  kDa,  $M_{\text{w}} / M_{\text{n}}(\text{SEC}) = 1.29$

– Chain extension of **2.10** with NIPAM (**3.3**):

The synthesis of the DMAP containing monomer and its copolymerization with styrene has been reported in Chapter 1.

**2.10:**  $M_{\text{n}}(\text{NMR}) = 5.1$  kDa,  $n = 38$ ,  $x = 0.9$ ,  $M_{\text{n}}(\text{SEC THF, PS}) = 4.0$  kDa,  $M_{\text{w}}/M_{\text{n}} = 1.11$ .

The previously synthesized DMAP containing polymer (**2.10**, 0.1 g, 0.02 mmol), NIPAM (0.45 g, 4 mmol), AIBN (0.6 mg, 0.004 mmol) was dissolved in 2.2 mL of THF in a glass ampoule. The oxygen was removed by three freeze-pump-thaw evacuation cycles. For the last cycle, nitrogen was flushed into the ampoule before thawing. The solution was heated at 65 °C in an oil bath. Following polymerization, the polymer was precipitated twice into a stirred solution of cold diethyl ether, filtered and placed in the vacuum oven overnight at 40 °C.

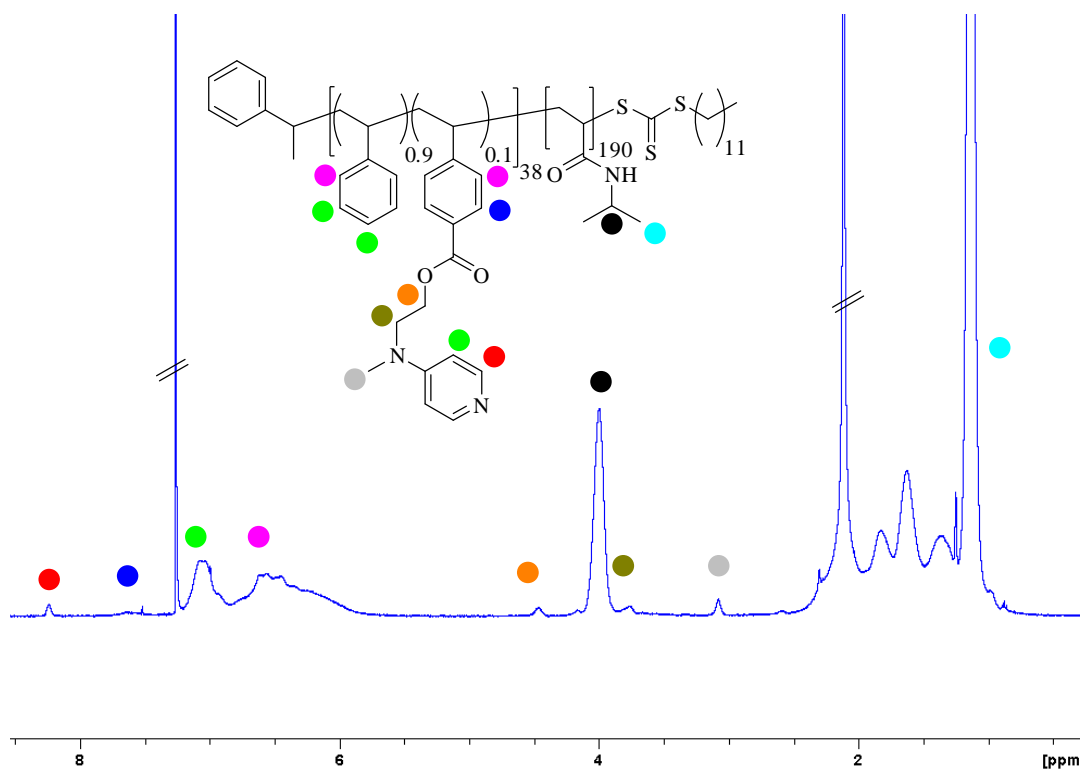


Figure 3.5:  $^1\text{H}$  NMR spectrum of DMAP containing amphiphilic block copolymer in  $\text{CDCl}_3$ .

$^1\text{H}$  NMR ( $\text{CDCl}_3$ ):  $\delta$  (ppm) 8.19 (br d, 2H, CH), 7.77-5.61 (br m, Ar-H), 4.40 (br t, 2H,  $\text{CH}_2$ ), 3.94 (br s, 1H, CH), 3.68 (br t, 2H,  $\text{CH}_2$ ), 3.00 (br s, 3H,  $\text{CH}_3$ ), 2.45-0.65 (br m, backbone).  $M_n(\text{NMR}) = 26.4 \text{ kDa}$ ,  $n = 38$ ,  $m = 190$ ,  $M_n(\text{SEC DMF, PMMA}) = 8.7 \text{ kDa}$ ,  $M_w/M_n = 1.63$ .

#### 3.5.4 Formation of micelles 3.2

The micellar solution was obtained by dilution of a stock solution of 6.7 mg / mL of polymer **3.1** in nanopure water to obtain the desired concentration. 670 mg of polymer was dissolved in the minimum amount of acetone (100 mg/mL) in a round bottom flask. The solution was placed in a cold room at 5 °C and 100 mL of water was added dropwise with continuous stirring using a peristaltic pump (rate = 15 mL/h). When the addition of water was completed, the acetone was removed under vacuum keeping the flask in an ice bath. The micelle solution (6.7 mg / mL) was stored at 5 °C. For the esterification reaction, 8 mL of this solution was

used. For the characterization of the particles, the solution **3.2** was diluted with nanopure water to obtain a final concentration of 0.1 mg/mL.

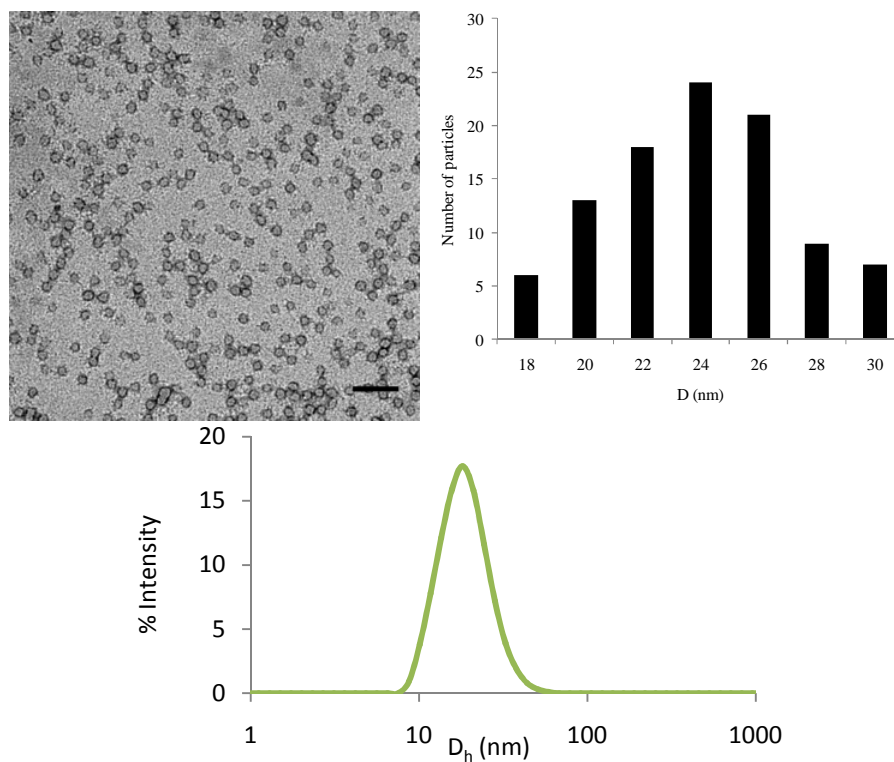


Figure 3.6: Representative TEM micrograph and histogram of micelles **3.2** stained with uranyl acetate (1%),  $D_{av}$  = 23 nm. Scale bar = 100 nm. DLS results, showing the size of micelles **3.2** (0.1 mg/mL) by number. ( $D_h$  = 31.2 nm, PD = 0.234)

### 3.5.5 Formation of DMAP containing micelles **3.4**

500 mg of polymer **3.3** was dissolved in the minimum amount of acetone (100 mg/mL) in a round bottom flask. The solution was placed in a cold room at 5 °C and 100 mL of water were added dropwise with continuous stirring using a peristaltic pump (drop rate = 15 mL/h). When the addition of water was completed, the acetone was removed under vacuum keeping the flask in an ice bath. These micelles solutions (5 mg/mL) were stored at 5 °C. For each of the esterification reactions, 2 mL of this solution was used (1.3 mg of DMAP). For the

characterization of the particles, the solution **3.4** was diluted with nanopure water to obtain a final concentration of 0.1 mg/mL.

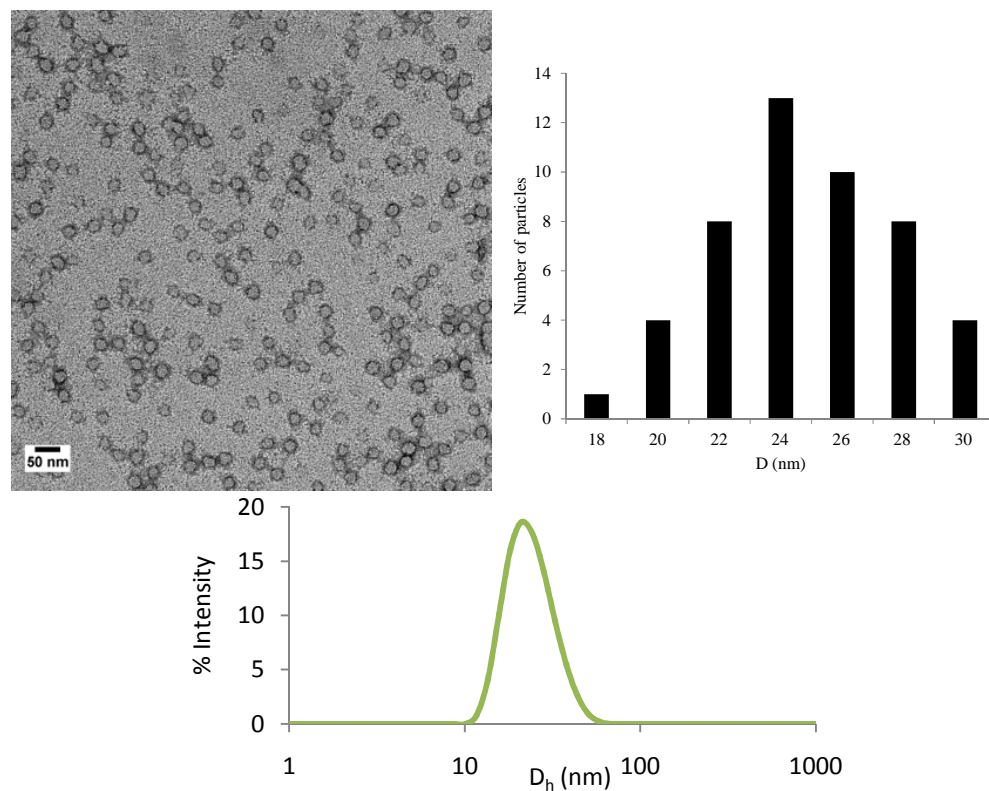


Figure 3.7: Representative TEM micrograph and histogram of micelles **3.4** ( $D_{av} = 24\text{nm}$ ) stained with uranyl acetate (1% solution). Scale bar = 50 nm. (0.1 mg/mL) DLS showing a  $D_{h,number} = 31.0\text{ nm}$ , PD = 0.263

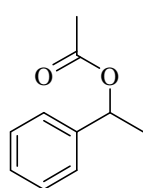
### 3.5.6 General protocol for the acylation reaction of 1 alcohol with 1 anhydride:

In the micelle **3.4**

1 equivalent of the corresponding alcohol (0.02 M), 1.5 equivalents of the auxiliary base and 3 equivalents of the anhydride were added together to 8 mL of solution **4** with a known amount of mesitylene as the internal standard. Samples of 0.2 mL were taken at different times, dissolved in 1 mL of THF and filtered through a plug of silica for HPLC analysis. Mesitylene was used as a standard ( $t_R = 8.25\text{ min}$ ). The reaction mixture was extracted twice with diethyl

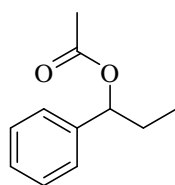
ether (2 x 3 mL). The organic layer was purified by flash column chromatography (100 % chloroform) and characterized by  $^{13}\text{C}$  and  $^1\text{H}$  NMR spectroscopy and high resolution mass spectroscopy. All the esterification products from Table 1 are known compounds and have been confirmed by  $^1\text{H}$  and  $^{13}\text{C}$  NMR spectroscopy and high resolution mass spectrometry (HR-ESI).

1-phenylethyl acetate (commercially available):



$^1\text{H}$  NMR ( $\text{CDCl}_3$ ):  $\delta$  (ppm) 7.32 (m, 5H, Ar-H), 5.90 (q, 1H,  $J=6.5$  Hz, CH), 2.05 (s, 3H,  $\text{CH}_3$ ), 1.53 (d, 3H,  $J=6.5$  Hz,  $\text{CH}_3$ ),  $^{13}\text{C}$  NMR ( $\text{CDCl}_3$ ):  $\delta$  (ppm) 172.9, 141.9, 128.5, 127.8, 126.1, 72.0, 22.3, 9.9.

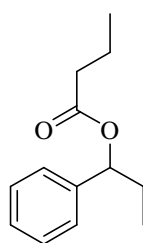
1-phenylpropyl acetate<sup>34</sup>



$^1\text{H}$  NMR ( $\text{CDCl}_3$ ):  $\delta$  (ppm) 7.35 (m, 5H, Ar-H), 5.66 (t, 1H,  $J=6.5$  Hz, CH), 2.06 (s, 3H,  $\text{CH}_3$ ), 1.87 (m, 2H,  $J=7.5$  Hz,  $\text{CH}_2$ ), 0.88 (t, 3H,  $J=7.5$  Hz,  $\text{CH}_3$ )  $^{13}\text{C}$  NMR ( $\text{CDCl}_3$ ):  $\delta$  (ppm) 170.4, 140.6, 128.4, 127.8, 126.6,

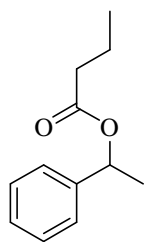
77.4, 29.3, 21.3, 9.9. (HR-ESI): 178.0996 (Calcd),  $[\text{M}+\text{Na}]^+$  201.0893 (Found)].

1-phenylethyl butyrate<sup>35</sup>



$^1\text{H}$  NMR ( $\text{CDCl}_3$ ):  $\delta$  (ppm) 7.28 (m, 5H, Ar-H), 5.66 (t, 1H,  $J=7.5$  Hz, CH), 2.32 (t, 2H,  $J=7.5$  Hz,  $\text{CH}_2$ ), 1.86 (m, 2H,  $J=7.5$  Hz,  $\text{CH}_2$ ), 1.65 (q, 2H,  $J=7.5$  Hz,  $\text{CH}_2$ ), 0.92 (m, 6H,  $J=7.5$  Hz,  $2\times\text{CH}_3$ )  $^{13}\text{C}$  NMR ( $\text{CDCl}_3$ ):  $\delta$  (ppm) 173.0, 140.7, 128.3, 127.8, 126.5, 77.1, 36.5, 29.4, 18.5, 13.7, 9.9. (HR-ESI): 206.1305

(Calcd),  $[\text{M}+\text{Na}]^+$  229.1202 (Found)].

1-phenylpropyl butyrate<sup>36</sup>

<sup>1</sup>H NMR (CDCl<sub>3</sub>): δ (ppm) 7.20 (m, 5H, Ar-H), 5.80 (q, 1H, J=6.5 Hz, CH), 2.21 (t, 2H, J=7.5 Hz, CH<sub>2</sub>), 1.55 (q, 2H, J=7.5 Hz, CH<sub>2</sub>), 1.43 (d, 3H, J=6.5 Hz, CH<sub>3</sub>), 0.83 (t, 3H, J=7.5 Hz, CH<sub>3</sub>), <sup>13</sup>C NMR (CDCl<sub>3</sub>): δ (ppm) 172.9, 141.9, 128.5, 127.8, 126.1, 72.0, 36.5, 22.3, 18.5, 13.7. (HR-ESI): 192.1148

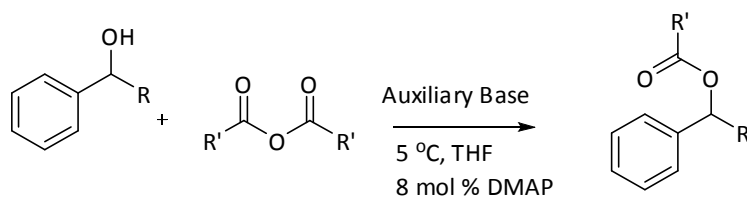
(Calcd), [M+Na]<sup>+</sup> 215.1042 (Found)].

*Small molecule reaction (DMAP)*

To a solution of 8 mL of solvent (water, THF or hexane) and 1.3 mg of DMAP (8 mol %) at 5 °C, 1 equivalent of the corresponding alcohol, 1.5 equivalents of the auxiliary base and 1.5 or 3 equivalents of the anhydride were added, together with a known amount of mesitylene as the internal standard for HPLC analysis. Samples of 0.2 mL were taken at different times and diluted in THF for HPLC analysis. The solvent was removed under vacuum and the resulting residue was purified by column chromatography in 100 % chloroform and characterized by <sup>1</sup>H NMR spectroscopy.



*Acylation reactions in THF using unsupported DMAP:*



Entry	R	R'	% Conv
1*	CH <sub>3</sub>	CH <sub>3</sub>	26
2	CH <sub>3</sub>	CH <sub>2</sub> CH <sub>2</sub> CH <sub>3</sub>	65
3	CH <sub>2</sub> CH <sub>3</sub>	CH <sub>2</sub> CH <sub>2</sub> CH <sub>3</sub>	94

Table 3.6: Data showing conversion at 24 h for acylation reactions in THF. All reactions contained 8 mol % DMAP, [OH] = 0.02 M, 1.5 equivalents of auxiliary base (DIPEA), 1 equivalent of alcohol and 3 equivalents of anhydride. Conversions determined by HPLC measurements using mesitylene as the internal standard. \* TEA used as auxiliary base instead of DIPEA.

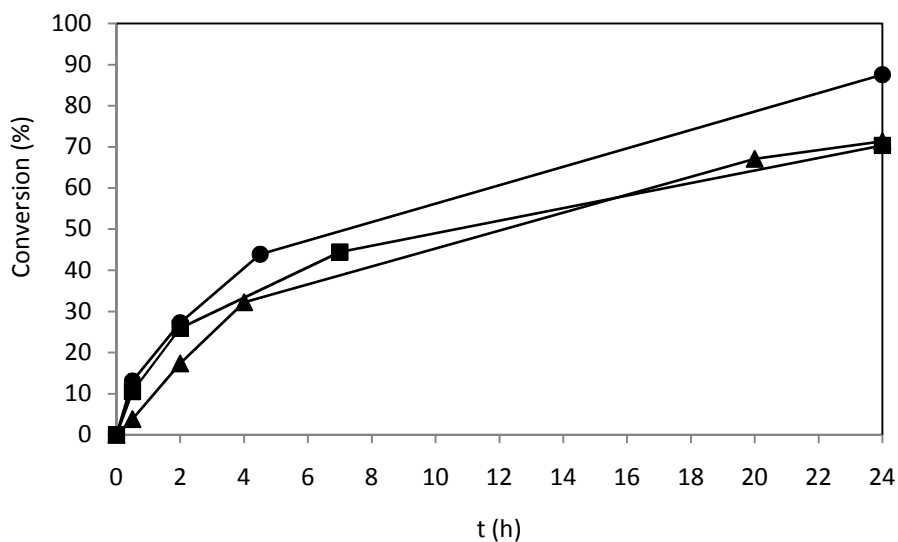


Figure 3.8: Unsupported DMAP catalyzed acylation reactions in THF for entries 1 (■), 2 (▲) and 3 (●) (Table 3.6) under the same conditions used for entries 1, 4 and 5 in Table 3.1.

*Continuous addition of starting materials:*

To 8 mL solution (micelles **2.12** or THF), 1 equivalent of the 1-phenylethanol, 1.5 equivalents of TEA and 3 equivalents butyric anhydride were added together with a known amount of mesitylene. The solutions contained 8 mol % DMAP catalysts (unsupported DMAP in the case of THF or polymer-supported in the case of solution **2.12**). After 24 hours reaction a fresh batch of starting materials (TEA, alcohol and anhydride) were added to the reaction mixture. The same procedure was repeated 4 times and samples were taken every 15 minutes and 24 hours after each addition and analyzed by HPLC as explained previously.

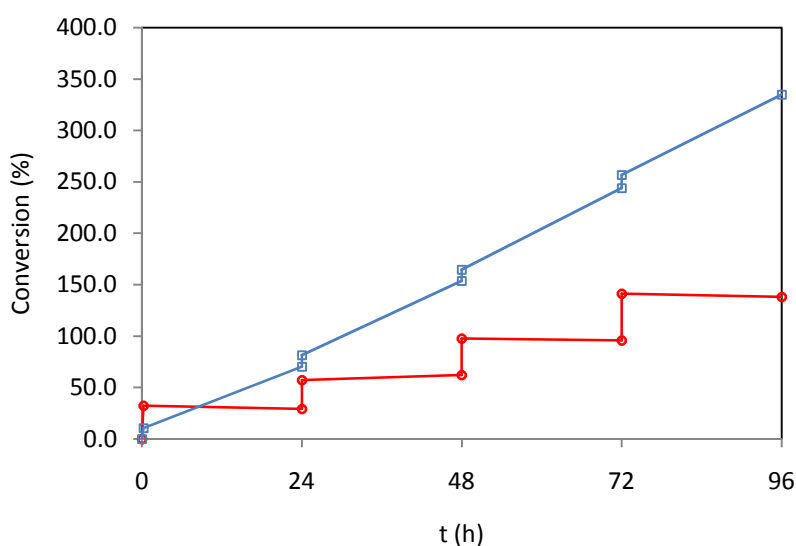
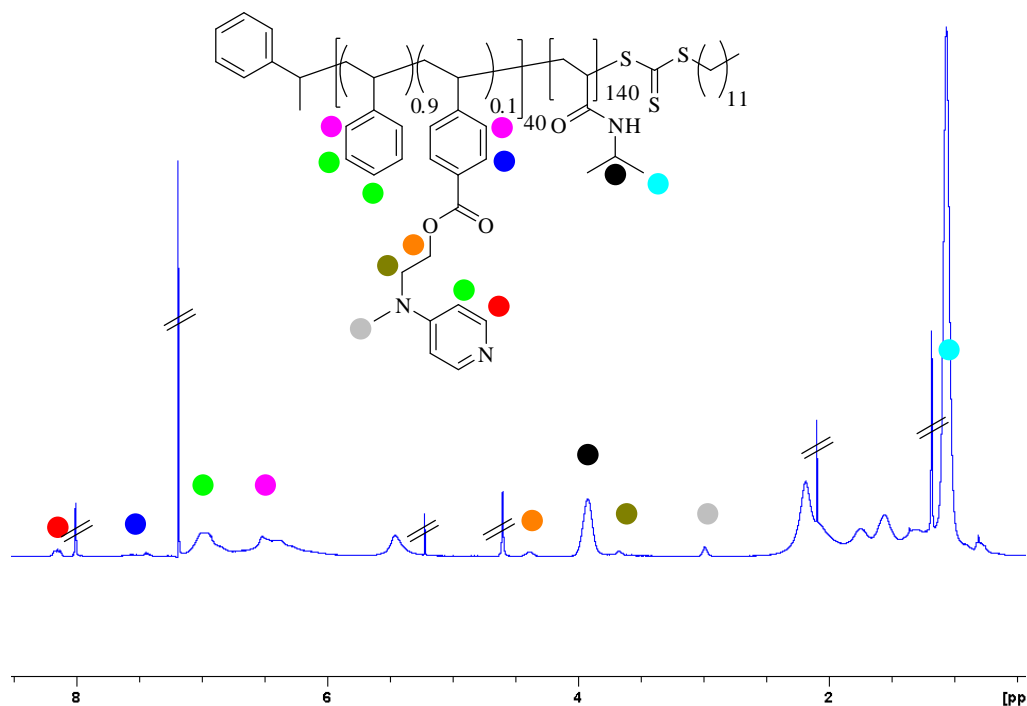


Figure 3.9: Kinetics for the acylation reactions of the addition every 24 hours of 1 equivalent of 1-phenyl ethanol, 3 equivalents of butyric anhydride and 1.5 equivalents of TEA to a solution initially containing 8 % DMAP catalyst in the micelles **2.12** (red circles) compared to the small molecule reaction in THF (blue squares).

## 3.5.7 Recycling experiments

Figure 3.10:  $^1\text{H}$  NMR spectrum of block-copolymer **2.11** in  $\text{CDCl}_3$  after recycling

## 3.5.8 General protocol for the selective acylation reaction of 1-phenylpropanol

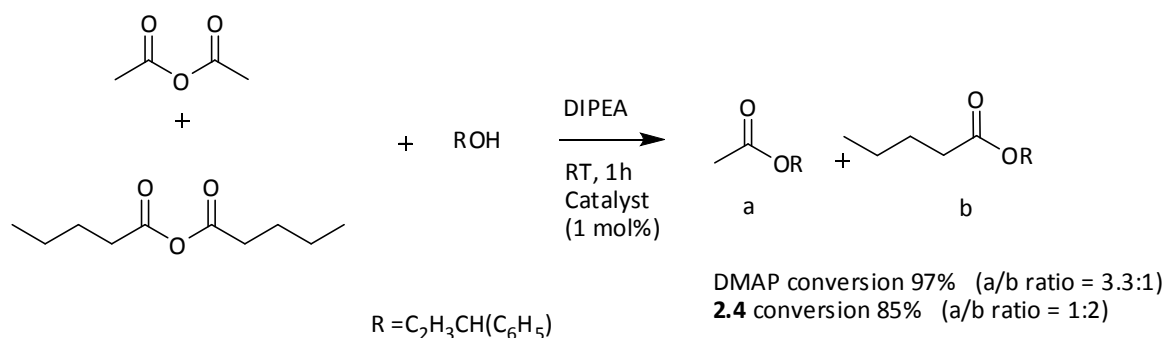
– *In the micelle (3.4):*

1 equivalent (0.115 mmol) of alcohol (0.06 M), 1.5 equivalents of the auxiliary base, 1.5 equivalents of butyric anhydride and 1.5 equivalents of acetic anhydride were added together to 2 mL of M-DMAP solution (10 mg of polymer = 0.14 mg of DMAP). A sample of 0.1 mL was taken after 1 hour, dissolved in 1 mL of THF with a known amount of mesitylene as the internal standard and filtered through a plug of silica prior to HPLC analysis.  $t_R(\mathbf{1a}) = 7.71$  minutes,  $t_R(\mathbf{1b}) = 9.64$  minutes.

– *In the bulk (DMAP):*

1 equivalent (1.15 mmol) of alcohol, 1.5 equivalents of the auxiliary base, 1.5 equivalents of butyric anhydride and 1.5 equivalents of acetic anhydride were mixed together to 0.14 mg of unsupported DMAP (1 mol %). Samples of 0.005 mL were taken at different times, dissolved in 1 mL of THF with a known amount of mesitylene as the internal standard and analyzed by HPLC.  $t_R(\mathbf{a}) = 7.71$  minutes,  $t_R(\mathbf{b}) = 11.13$  minutes.

*Competitive reactions between acetic anhydride and valeric anhydride:* 1 mol % (DMAP or **3.4**) of catalyst, 1.5 equivalent of each anhydride, 1.5 equivalents of auxiliary base (DIPEA) and 1 equivalents of 1-phenylpropanol. Conversions determined by HPLC analysis with mesitylene as the internal standard.



### 3.5.9 One pot selective acylation of different alcohols with butyric anhydride:

– *In the micelle (**3.4**):*

1 equivalent (0.115 mmol) of each alcohol (0.06 M), 1.5 equivalents of DIPEA, and 3 or 4 equivalents of butyric anhydride were added together to 2 mL of **3.4** solution (10 mg of polymer = 0.14 mg of DMAP). Samples of 0.1 mL were taken after 1 hour, dissolved in 1 mL of dioxane with a known amount of mesitylene as the internal standard and analyzed by GC.

Samples were also taken at  $t = 0$  (before addition of anhydride) to calculate the conversions by the disappearance of the alcohol peak compared to the reference.

$t_R$  (Mesitylene)= 4.50 min,  $t_R$  (methanol)= 1.27 min,  $t_R$  (allyl alcohol)= 2.39 min,  $t_R$  (1,4-butandiol)= 5.9 min,  $t_R$  (1-decanol)= 6.50 min,  $t_R$  (linalool)= 5.81 min.

– *In the bulk (DMAP):*

1 equivalent (1.15 mmol) of alcohol, 1.5 equivalents of the auxiliary base and 3 or 4 equivalents of butyric anhydride were mixed together to 0.14 mg of unsupported DMAP (1 mol %). Samples of 0.005 mL were taken after 1 hour, dissolved in 1 mL of dioxane with a known amount of mesitylene as the internal standard and analyzed by GC. Samples were also taken at  $t = 0$  (before addition of anhydride) to calculate the conversions by the disappearance of the alcohol peak compared to the reference.

Other competitive reactions between 2 alcohols:

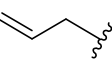
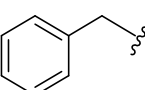
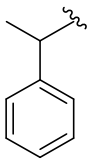
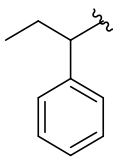
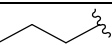
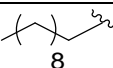
$\left\{ \begin{array}{c} R_1OH \\ + \\ R_2OH \end{array} \right\} + \begin{array}{c} \text{O} \quad \text{O} \\ \parallel \quad \parallel \\ R - \text{C} - \text{O} - \text{C} - R \\ R = nPr \end{array} \xrightarrow[\text{RT, 1h}]{\text{DIPEA}} \begin{array}{c} R_1 - \text{O} - \text{C}(=\text{O}) - R \\ \text{a} \end{array} + \begin{array}{c} R_2 - \text{O} - \text{C}(=\text{O}) - R \\ \text{b} \end{array}$ <p style="text-align: center;">Catalyst (1 mol%)</p>			
Catalyst	R <sub>1</sub>	R <sub>2</sub>	a/b
DMAP			1:1
<b>3.4</b>			0.5:1
DMAP			1:1
<b>3.4</b>			0.8:1
DMAP			1:1
<b>3.4</b>			0.6:1

Table 3.7: Reactions contained 1 mol % (DMAP or DMAP micelles **3.4**) of catalyst, 1 equivalent of each alcohol,

1.5 equivalents of auxiliary base (DIPEA) and 3 equivalents of anhydride. Conversions determined by GC

analysis with mesitylene as the internal standard.

### 3.6 References

- (1) Rideout, D. C.; Breslow, R. *J. Am. Chem. Soc.* **1980**, *102*, 7816.
- (2) Narayan, S.; Muldoon, J.; Finn, M. G.; Fokin, V. V.; Kolb, H. C.; Sharpless, K. B. *Angew. Chem., Int. Ed.* **2005**, *44*, 3275.
- (3) Gruttadauria, M.; Giacalone, F.; Noto, R. *Adv. Synth. Catal.* **2009**, *351*, 33.
- (4) Scroggins, S. T.; Chi, Y.; Fréchet, J. M. J. *Angew. Chem., Int. Ed.* **2010**, *49*, 2393.
- (5) Blackmond, D. G.; Armstrong, A.; Coombe, V.; Wells, A. *Angew. Chem., Int. Ed.* **2007**, *46*, 3798.
- (6) Garcia-Viloca, M.; Gao, J.; Karplus, M.; Truhlar, D. G. *Science* **2004**, *303*, 186.
- (7) Malisi, C.; Kohlbacher, O.; Höcker, B. *Proteins: Struct., Funct., Bioinf.* **2009**, *77*, 74.
- (8) Helms, B.; Guillaudeau, S. J.; Xie, Y.; McMurdo, M.; Hawker, C. J.; Frechet, J. M. J. *Angew. Chem., Int. Ed.* **2005**, *44*, 6384.
- (9) Helms, B.; Fréchet, J. M. J. *Adv. Synth. Catal.* **2006**, *348*, 1125.
- (10) Chi, Y. G.; Scroggins, S. T.; Frechet, J. M. J. *J. Am. Chem. Soc.* **2008**, *130*, 6322.
- (11) Terashima, T.; Kamigaito, M.; Baek, K.-Y.; Ando, T.; Sawamoto, M. *J. Am. Chem. Soc.* **2003**, *125*, 5288.
- (12) Terashima, T.; Ouchi, M.; Ando, T.; Sawamoto, M. *J. Polym. Sci., Part A: Polym. Chem.* **2010**, *48*, 373.

- (13) Terashima, T.; Mes, T.; De Greef, T. F. A.; Gillissen, M. A. J.; Besenius, P.; Palmans, A. R. A.; Meijer, E. W. *J. Am. Chem. Soc.* **2011**, *133*, 4742.
- (14) Dwars, T.; Paetzold, E.; Oehme, G. *Angew. Chem., Int. Ed.* **2005**, *44*, 7174.
- (15) Wang, Y.; Xu, H.; Ma, N.; Wang, Z.; Zhang, X.; Liu, J.; Shen, J. *Langmuir* **2006**, *22*, 5552.
- (16) Manabe, K.; Sun, X.-M.; Kobayashi, S. *J. Am. Chem. Soc.* **2001**, *123*, 10101.
- (17) Manabe, K.; Iimura, S.; Sun, X.-M.; Kobayashi, S. *J. Am. Chem. Soc.* **2002**, *124*, 11971.
- (18) Kunishima, M.; Kikuchi, K.; Kawai, Y.; Hioki, K. *Angew. Chem., Int. Ed.* **2012**, *51*, 2080.
- (19) Liu, Y.; Wang, Y.; Wang, Y.; Lu, J.; Piñón, V.; Weck, M. *J. Am. Chem. Soc.* **2011**, *133*, 14260.
- (20) Rossbach, B. M.; Leopold, K.; Weberskirch, R. *Angew. Chem., Int. Ed.* **2006**, *45*, 1309.
- (21) Ge, Z. S.; Xie, D.; Chen, D. Y.; Jiang, X. Z.; Zhang, Y. F.; Liu, H. W.; Liu, S. Y. *Macromolecules* **2007**, *40*, 3538.
- (22) Cotanda, P.; Lu, A.; Patterson, J. P.; Petzetakis, N.; O'Reilly, R. K. *Macromolecules* **2012**, *45*, 2377.
- (23) Lu, A.; Smart, T. P.; Epps, T. H.; Longbottom, D. A.; O'Reilly, R. K. *Macromolecules* **2011**, *44*, 7233.
- (24) Ievins, A. D.; Wang, X. F.; Moughton, A. O.; Skey, J.; O'Reilly, R. K. *Macromolecules* **2008**, *41*, 2998.



- (25) Arumugam, S.; Vutukuri, D. R.; Thayumanavan, S.; Ramamurthy, V. *J. Am. Chem. Soc.* **2005**, *127*, 13200.
- (26) O'Lenick, T. G.; Jiang, X.; Zhao, B. *Polymer* **2009**, *50*, 4363.
- (27) Lejeune, E.; Drechsler, M.; Jestin, J.; Müller, A. H. E.; Chassenieux, C.; Colombani, O. *Macromolecules* **2010**, *43*, 2667.
- (28) Trentin, F.; Scarso, A.; Strukul, G. *Tetrahedron Lett.* **2011**, *52*, 6978.
- (29) Sakakura, A.; Kawajiri, K.; Ohkubo, T.; Kosugi, Y.; Ishihara, K. *J. Am. Chem. Soc.* **2007**, *129*, 14775.
- (30) Helms, B.; Liang, C. O.; Hawker, C. J.; Fréchet, J. M. J. *Macromolecules* **2005**, *38*, 5411.
- (31) Xu, S.; Held, I.; Kempf, B.; Mayr, H.; Steglich, W.; Zipse, H. *Chem. Eur. J.* **2005**, *11*, 4751.
- (32) Letizia, C. S.; Cocchiara, J.; Lalko, J.; Api, A. M. *Food Chem. Toxicol.* **2003**, *41*, 965.
- (33) Deratani, A.; Darling, G. D.; Frechet, J. M. J. *Polymer* **1987**, *28*, 825.
- (34) Chakraborti, A. K.; Shivani *J. Org. Chem.* **2006**, *71*, 5785.
- (35) Castillo, B.; Delgado, Y.; Barletta, G.; Griebenow, K. *Tetrahedron* **2010**, *66*, 2175.
- (36) Sim, Y. K.; Jung, S.; Lim, J. Y.; Kim, J.; Kim, S.-H.; Song, B. K.; Kim, B. T.; Lee, H.; Park, S. *Tetrahedron Lett.* **2011**, *52*, 1041.

## **Chapter 4: Design of amino polymers via RAFT**

**polymerization for the synthesis of polyurethane foams**

## 4.1 Abstract

Polyurethane (PU/PUR) foams are prepared by the step-growth polymerization of polyols and polyisocyanates. Commercially these reactions are catalyzed by tertiary amines. The nature (electronic and steric properties) of the amine determines the ultimate properties of the foams by influencing the degree of gelling *versus* blowing. However, the use of amine catalysts have associated hazards so it would be important to protect/tether these and release at will. To effectively control the properties of the polyurethane produced, we have studied the preparation of novel amino functionalized polymers for the application in the polyurethane reaction. Four novel mono- and multi-dentate amino monomers have been synthesized. These monomers have been homopolymerized and/or copolymerized with a non-reactive monomer by RAFT. The new monomers and functional polymers have been tested as supported catalysts for the polyurethane foam reaction between a polyol and isocyanate.

The ultimate goal of this project is to synthesize a core-shell catalytic polymeric particle where the amino motifs are protected from the reaction environment by an inert shell for controlled release.

## 4.2 Introduction

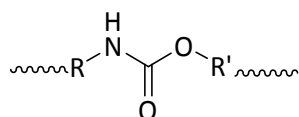
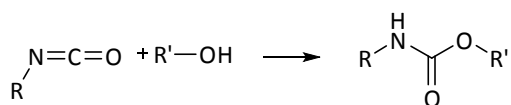


Figure 4.1: Urethane link

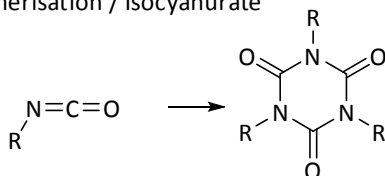
Polyurethane (PUR or PU) is any polymer consisting of a chain of organic units joined by urethane (carbamate) links (Figure 4.1).

PU foams are formed through step-growth polymerization by mixing of a polyol with water, a catalyst, a surfactant, a chain extender, and a physical blowing agent in the first stage. In the second stage, the blended polyol is mixed with a diisocyanate to react.<sup>1</sup> The reactions between polyol premixtures and isocyanates to form PU foams have been the subject of many investigations.<sup>2</sup> The dominating reactions are the formation of urethane, urea and isocyanurate chain linkages (Scheme 4.1). The catalyst ultimately controls to what extent these three reactions occur establishing the mechanism of formation of the PU foam and the physical properties of the product polymer. Various combinations of catalysts can be used in order to establish an optimum balance between the chain propagation (isocyanate with hydroxyl) reaction and the blowing reaction (isocyanate with water). The polymer formation rate and gas formation rate must be balanced so that the gas is entrapped efficiently in the gelling polymer and the cell-walls develop sufficient strength to maintain their structure without collapse or shrinkage. Catalysts are also important for assuring completeness of reaction or “cure” in the finished foam.

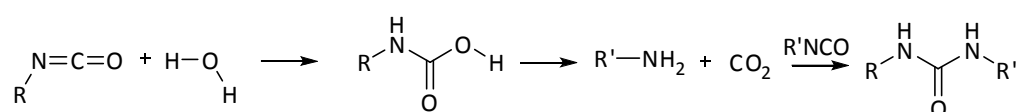
Gelling / Urethane



Trimerisation / Isocyanurate



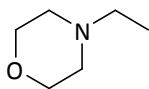
Blowing / Urea



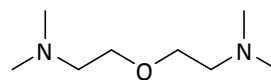
Scheme 4.1: Dominating reactions in PU foam formation

The selection of a catalyst system for a particular grade of foam is a complex task requiring small-scale experimentation and further refinement for production-scale. The kinetic rate of reactions of PU foam formation mainly depends on the rates of the blowing and gelling reaction, controlled by an amine catalyst, an organo-catalyst, or a combination of the two. Organometallic catalysts promote the gelling reaction between the isocyanate and a polyol. Of the many metals available, tin compounds are the most widely used. Because of the high aquatic toxicity of some organotin compounds, there has been an attempt to ban organotin compounds from all coating applications.<sup>2,3</sup> Currently, tertiary amines are the most commonly used polyurethane foam catalysts. Most tertiary amine catalysts will catalyze all three reactions to some extent and their molecular structure gives some idea about the most favorable reaction.<sup>1</sup>

- Blowing catalysts: generally have an ether linkage two carbons away from tertiary nitrogen.

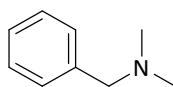


N-ethylmorpholine

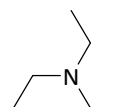


Bis (2-dimethylamino) ether

- Gelling catalysts: Strong gel catalysts contain alkyl-substituted nitrogens (triethylamine, pentamethyldiethylenetriamine) while the weak ones generally contain ring-substituted nitrogens (benzyl dimethylamine).

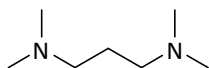


benzyl dimethylamine

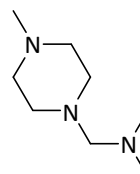


triethylamine

- Balanced catalysts: Usually sterically unhindered molecules that allow equal competition between isocyanate and polyol for the active centers of the catalyst molecules.



tetramethylpropylene diamine



dimethylaminoethylmethyl piperazine

The catalytic activity of amines is due to the presence of a free electron pair on the nitrogen atom. Steric hindrance about the nitrogen atom and the electronic effects of substituent groups are the main factors influencing the relative catalytic activity of various amines. In some foam systems, combinations of various amines are used in an attempt to balance the gelling and blowing reactions so that the foaming process can be adequately controlled.

Polyurethane formulations cover an extremely wide range of stiffness, hardness, and densities.

- Low-density flexible foam used in seating
- Low-density rigid foam used for thermal insulation and molding

- Soft solid elastomers used for gel pads and print rollers
- Low density elastomers used in footwear
- Hard solid plastics used as electronic instrument bezels and structural parts
- Flexible plastics used as straps and bands

Some amines impart a residual odor to the foam, which may limit their use in applications such as bedding and upholstered furniture. The use of the more volatile amines may reduce odor in the final product but may also reduce cure due to rapid loss of the catalyst. However, high volatility often results in low flash points, high vapor pressures and handling problems. Many catalyst suppliers have introduced catalysts containing an isocyanate reactive group to help tie the molecule into the polymer network. Unfortunately, this process generally decreases the catalytic activity of the molecule.

In this direction, the ultimate goal of this project is to develop new polymer supported catalytic particles with stimuli-responsive properties based on amino functionalities that have been selectively supported onto polymeric materials to control the polyurethane foam reaction (Figure 4.2). These nanostructures will have the amino functionality protected within the central core domain until a stimulus is applied to effectively release the catalyst and minimize the hazards associated to handling problems.

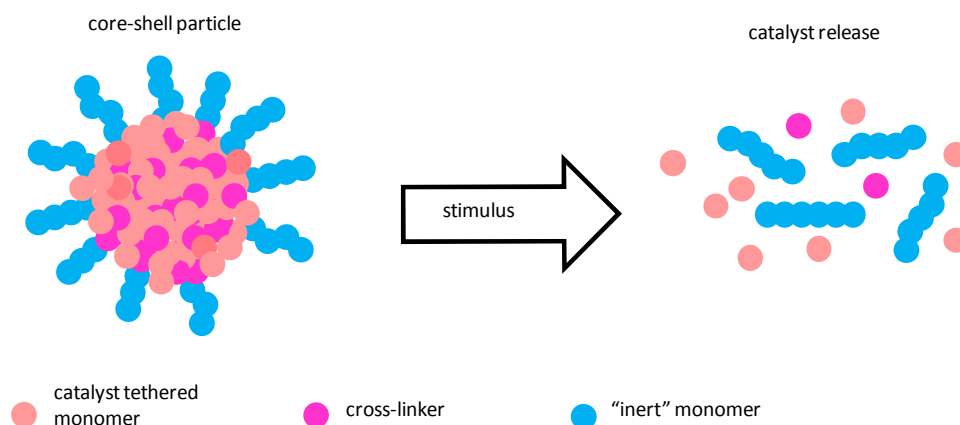


Figure 4.2: Schematic representation of the project strategy

We are interested in using reversible addition-fragmentation chain transfer (RAFT) polymerization to develop a highly effective means for the incorporation of tertiary amino motifs into polymeric species in a highly tolerable and tunable manner.<sup>4,5</sup> RAFT is highly tolerant of functional groups and is proposed to enable a controlled radical polymerization of functionalized monomers to afford well-defined, functional polymers with unique properties and capabilities.<sup>6-12</sup>

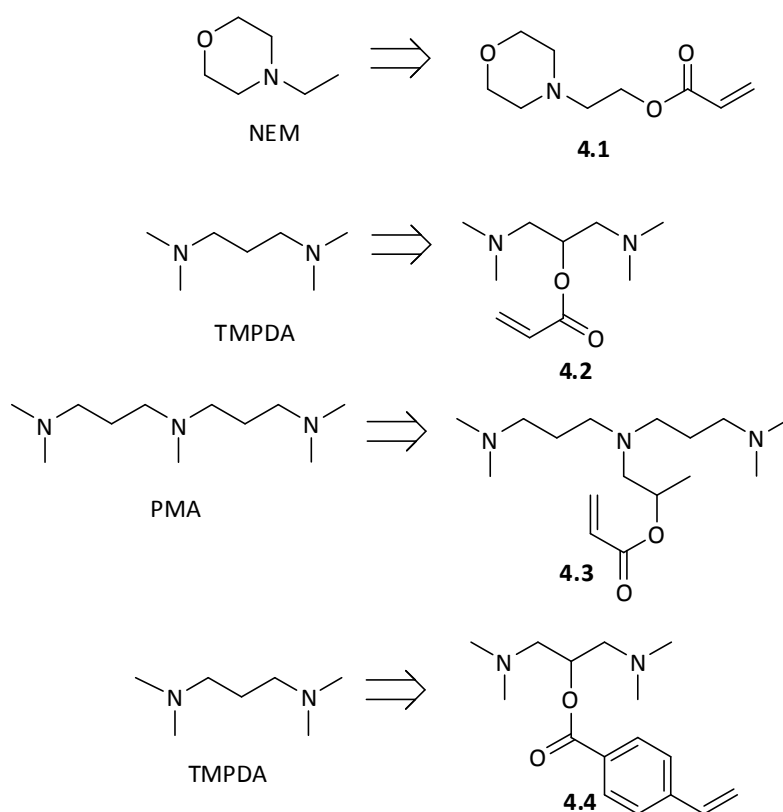
Much of the work in the area of multidentate supported polymers has been towards the preparation of supported ATRP ligands. However most of this work has utilized a post polymerization modification approach.<sup>13-20</sup> In our case, the preparation of novel amino functionalized polymers as catalysts in the polyurethane reaction have been explored by direct polymerization using RAFT, which enables the preparation of well-defined functional block copolymers without the need of protecting groups. This will allow the catalyst to be tethered to a polymer scaffold in order to effectively control the properties of the polyurethane produced.



### 4.3 Results

#### 4.3.1 Synthesis of multidentate amino monomers

A number of amino catalysts used in the formation of PU foams were targeted and incorporated in to a monomer in order to explore their polymerization using RAFT techniques. Tetramethylpropylenediamine (TMPDA) catalyst is currently being used to manufacture polyurethane foams. Studies carried out by AWE gave the basis of catalyst that may be possible replacements for the TMPDA catalyst.

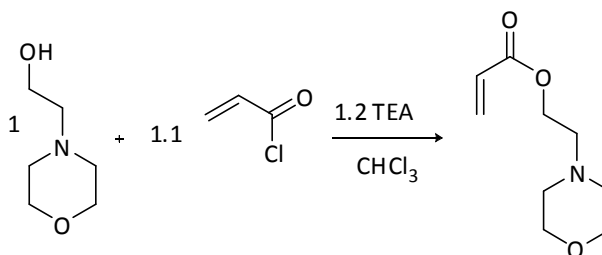


Scheme 4.2: Structure of the monomers containing 3 different amino functionalities

Initial work focused on the synthesis of the monomers **4.1**, **4.2** and **4.3** to form the acrylate versions of three tertiary amines catalyst proposed by AWE, N- ethyl morpholine (NEM), Pentamethyldipropylenetriamine (PMA), and the currently used TMPDA. These 3

monomers were synthesized from commercially available alcohols by reaction with acryloyl chloride.

The synthesis of the methacrylate version of morpholine has been previously reported in the literature.<sup>21-23</sup>



Scheme 4.3: Synthesis of NEM monomer **4.1**

Using a similar strategy to that reported in the literature (Scheme 4.3), monomer **4.1** was synthesized by the reaction of commercially available acryloyl chloride and 4-(2-hydroxyethyl)morpholine in the presence of triethylamine (TEA) and  $\text{CHCl}_3$  as a solvent. After 16 hours reaction, the signal at ca. 3.5 ppm ( $\text{CH}_2\text{OH}$  in the starting material) shifted to 4.2 ppm indicates that the reaction has gone to completion. **4.1** was washed with 1 M NaOH and isolated as a yellow liquid in a 77 % yield. The monomer was characterized by  $^{13}\text{C}$  and  $^1\text{H}$  NMR spectroscopy in  $\text{CDCl}_3$  as shown in Figure 4.3 .

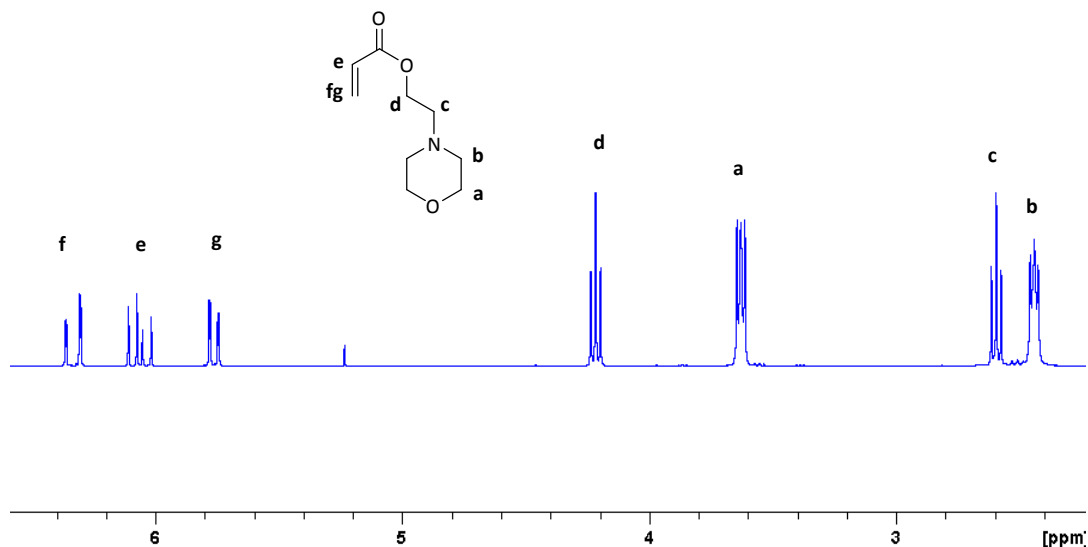
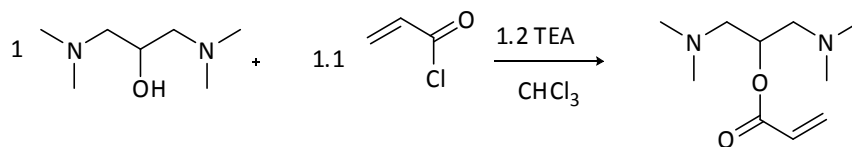


Figure 4.3:  $^1\text{H}$  NMR spectrum of **4.1** in  $\text{CDCl}_3$  (at 5.30 ppm residual DCM)

When scaling up the reaction under the same reaction conditions, the increase in the amount of starting alcohol from 1 to 5 and then 10 mL resulted in a decrease of the yield from 77 to 65 to 36 %. The conversion  $^1\text{H}$  NMR showed complete reaction of the starting alcohol in all cases which indicates that the product is lost in the work up due to the partial solubility of the product in the basic aqueous phase during extraction.

Following the same procedure as for monomer **4.1**, TMPDA monomer **4.2** was synthesized by the reaction of acryloyl chloride and commercially available 1,3-bis dimethylamino-2-propanol in presence of 1.2 equivalents of TEA (Scheme 4.4).



Scheme 4.4: Synthesis of TMPDA monomer **4.2**

After 15 hours the reaction achieved *ca.* 100 % conversion, calculated by analyzing a sample of the reaction mixture by  $^1\text{H}$  NMR in  $\text{CDCl}_3$  by comparing the CH signal from the starting alcohol at 3.7 ppm with the signal from the same proton in the monomer at 5.2 ppm. The reaction mixture was washed with 1 M NaOH, the solvent was evaporated and the product was dissolved in EtOAc and passed through a plug of neutral alumina to remove the remaining salts. The pure monomer was isolated as a pale yellow liquid in a 65 % yield and characterized by  $^{13}\text{C}$ ,  $^1\text{H}$  NMR spectroscopy (Figure 4.4) in  $\text{CDCl}_3$  and mass spectrometry.

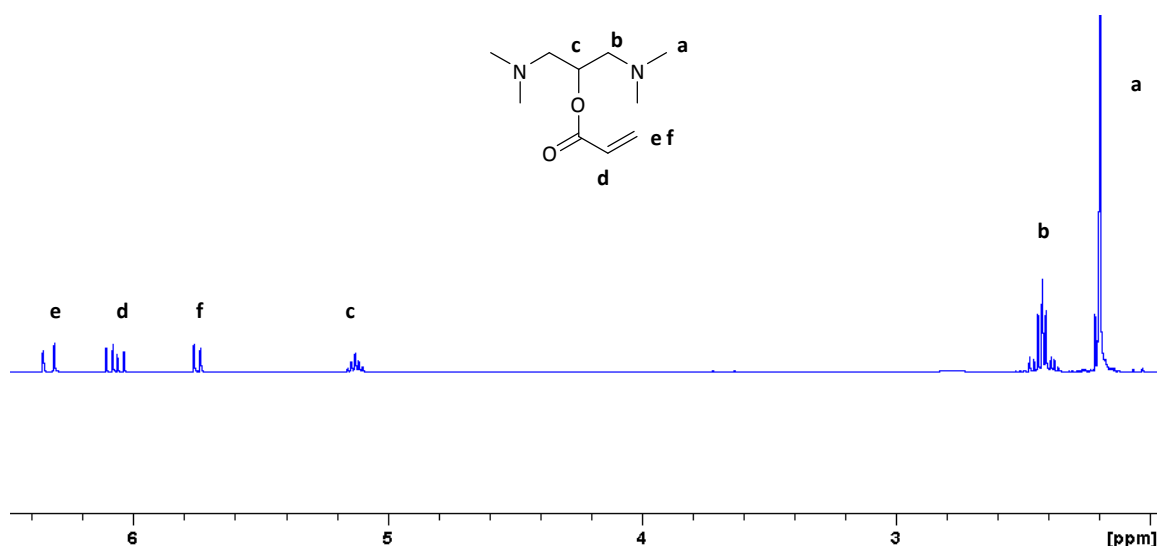
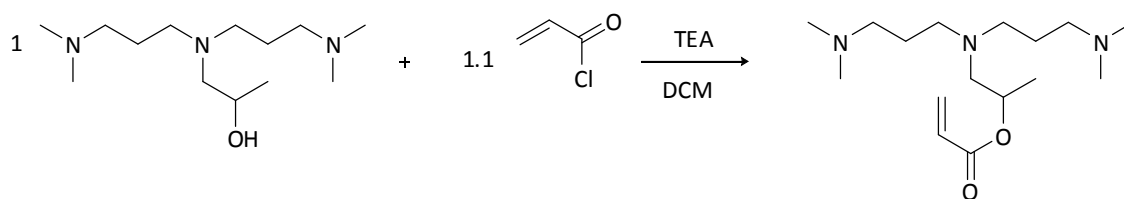


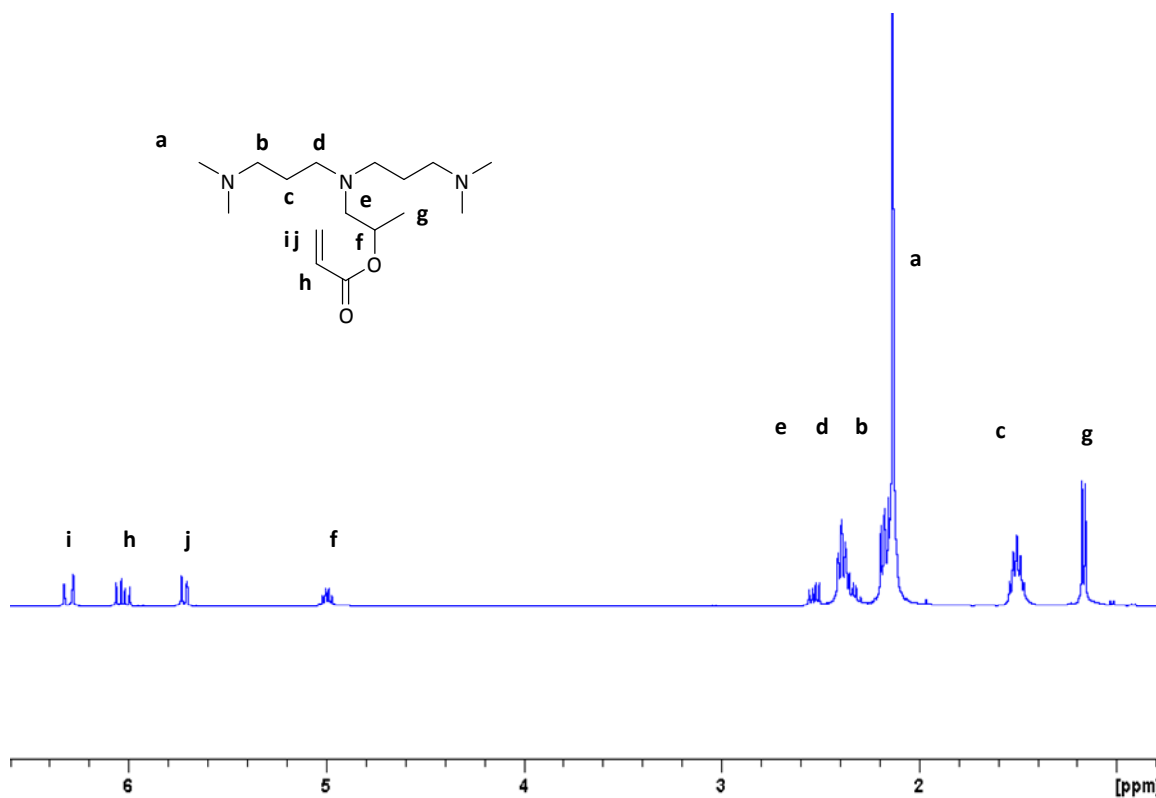
Figure 4.4:  $^1\text{H}$  NMR spectrum of monomer **4.2** in  $\text{CDCl}_3$

In order to incorporate the PMA motif into a polymer, monomer **4.3** was initially synthesized following the same procedure as above (Scheme 4.5). Although the conversion of the reaction was high (88 % after 1 day, calculated by  $^1\text{H}$  NMR comparing the CH signal from the starting alcohol at 3.7 ppm with the same proton in the resultant monomer at 5.0 ppm), many difficulties were found to remove the TEA from the monomer synthesized.

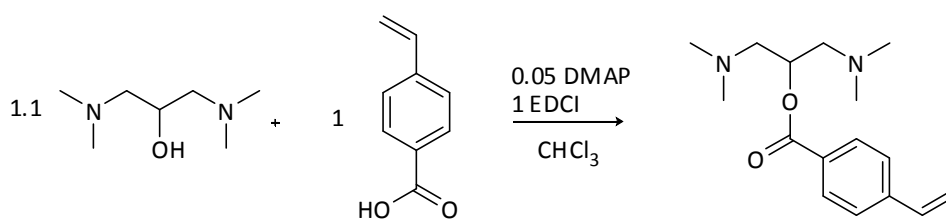


Scheme 4.5: Synthesis of monomer 4.3

PMA itself incorporates tertiary amine functionality to the mixture; therefore, the reaction was carried out in absence of TEA under the same conditions reported above. After washing with 1 M NaOH and drying with Na<sub>2</sub>SO<sub>4</sub>, the monomer was isolated as a brown liquid in a 36% yield. The low yield may be attributed to the precipitation of the monomer after formation of salts with the Cl<sup>-</sup> (from the acryloyl chloride) due to the absence of TEA removed by aqueous basic washing, reducing the overall yield. In order to avoid this problem in subsequent reactions, Na<sub>2</sub>CO<sub>3</sub> was added to the reaction mixture before extraction, stirred for 1 hour and filtered to deprotonate the tertiary amine before washing with 1 M NaOH. The organic phase was dried with Na<sub>2</sub>SO<sub>4</sub> and filtered. The solvent was evaporated under reduced pressure at room temperature and left under vacuum overnight. The clean monomer was obtained as an amber viscous liquid in a 91 % yield and characterized by mass spectrometry, <sup>13</sup>C and <sup>1</sup>H NMR spectroscopy in CDCl<sub>3</sub> (Figure 4.5).

Figure 4.5:  $^1\text{H}$  NMR spectrum of monomer **4.3** in  $\text{CDCl}_3$ 

A second monomer containing TMPDA functionality was synthesized (compound **4.4**). By comparing the catalytic activity of the polymer formed with monomer **4.2** (acrylate) to the one from the styrenic version of TMPDA, **4.4**, the effect of the backbone on the catalytic activity of the amino polymers can be investigated. The styrenic monomer **4.4** was synthesized from commercially available vinyl benzoic acid and 1,3-bis dimethylamino-2-propanol at room temperature by established procedures using Steglich esterification route.<sup>24</sup>

Scheme 4.6: Synthesis of styrenic TMPDA monomer **4.4**.

The conversion of the reaction can be followed by  $^1\text{H}$  NMR by comparing the CH peak at 3.7 ppm from the starting material shifting to 5.3 ppm when forming the ester. After 2 days, the reaction mixture was washed with 1 M NaOH, water and brine and purified by column chromatography using neutral alumina as a stationary phase and EtOAc as a solvent. The pure monomer was isolated as a very pale yellow liquid in a 44% yield and characterized by  $^1\text{H}$  and  $^{13}\text{C}$  NMR and mass spectroscopy (Figure 4.6).

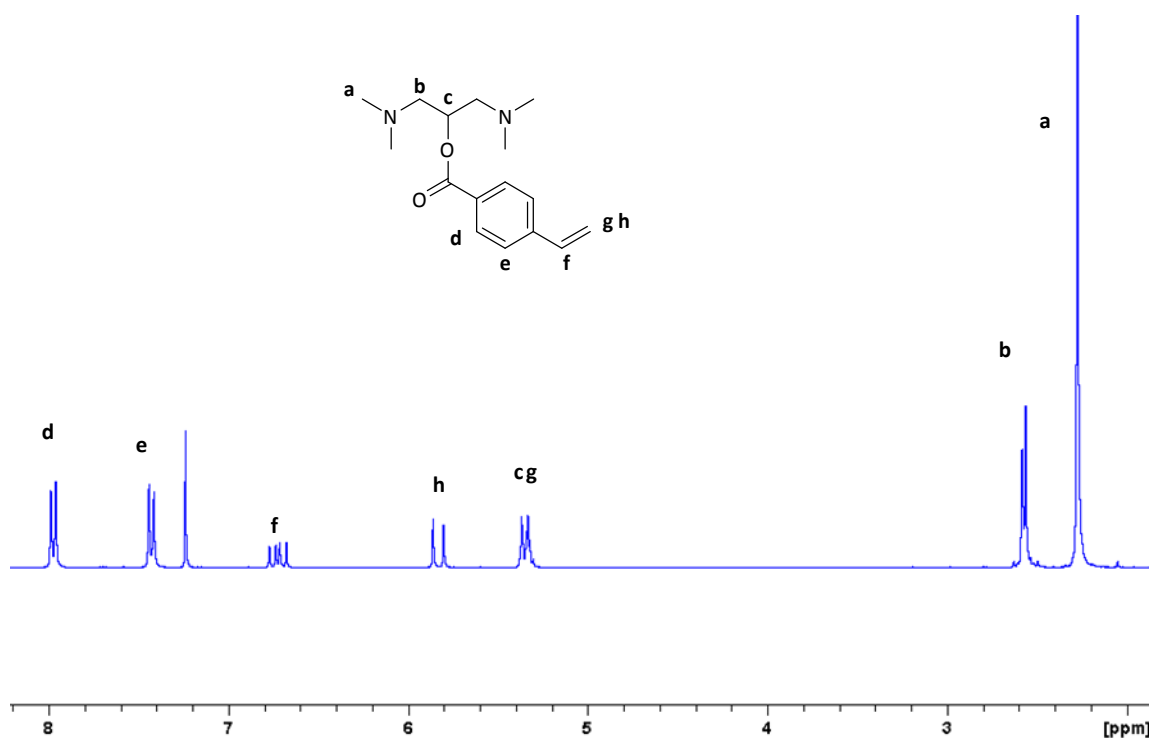


Figure 4.6:  $^1\text{H}$  NMR spectrum of **4.4** in  $\text{CDCl}_3$

#### 4.3.2 Direct homopolymerization by RAFT

The preparation of amino functionalized polymers by RAFT was explored using the new multidentate monomers **4.1**, **4.2**, **4.3** and **4.4**. This will allow for the exploration of the effect of tethering the catalyst into a polymer support on the rate and properties of the PU foam produced.

– *Synthesis of the chain transfer agent 4.5:*

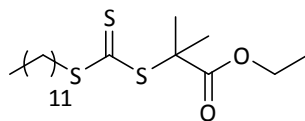


Figure 4.7: Structure of DDMEAT (**4.5**)

DDMAT (**2.3**) is a commonly used RAFT agent, easy to synthesize, which has been demonstrated to mediate the polymerization of a wide range of monomers including acrylates and styrenes.<sup>25,26</sup> However, the acid group in CTA **2.3** could interact with the amino functionality from the monomers slowing down the polymerization. Therefore, a new CTA without acid functionality was prepared. The homopolymerization of the monomers was explored using S-1-dodecyl-S'-( $\alpha,\alpha'$ -dimethyl- $\alpha''$ -ethyl acetate) trithiocarbonate DDMEAT (**4.5**, Figure 4.7).<sup>27</sup>

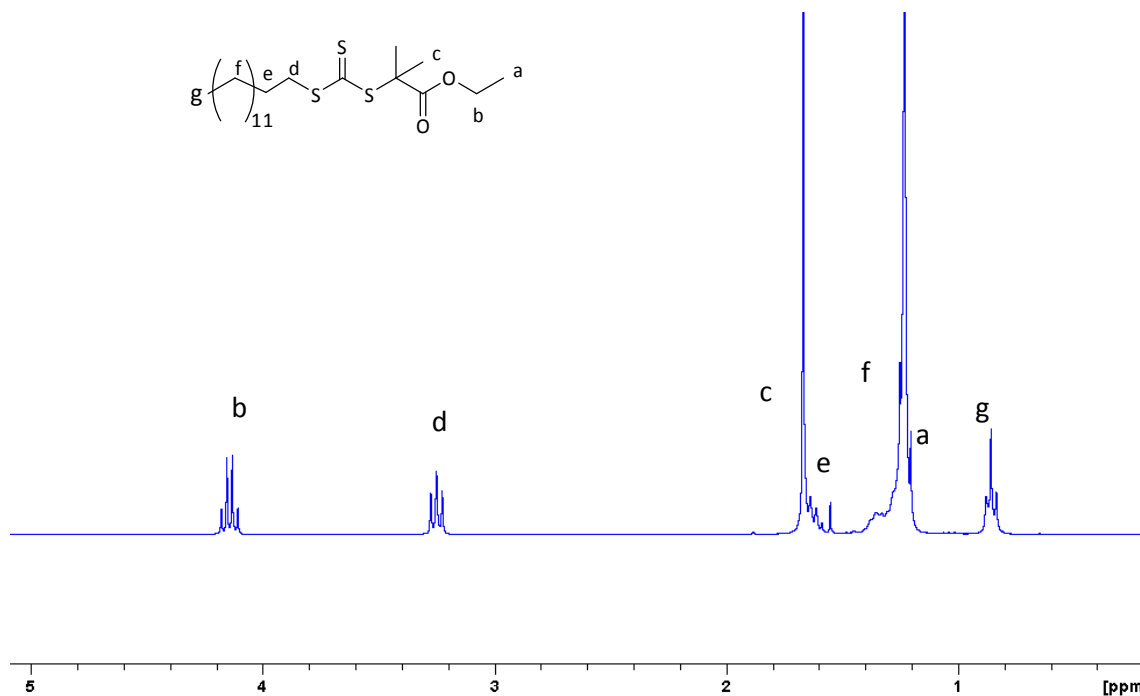
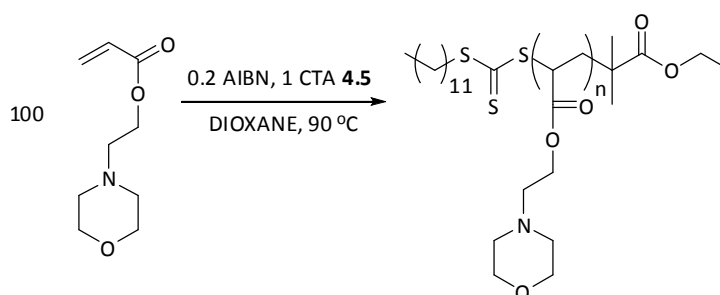


Figure 4.8:  $^1\text{H}$  NMR spectrum of CTA **4.5** in  $\text{CDCl}_3$



DDMEAT is the ester-analogue of the commonly used RAFT agent DDMAT (**2.4**). CTA **4.5** was prepared by esterification reaction of DDMAT with ethanol to avoid the undesirable acid-base reaction of the acidic group from CTA **2.4** with the basic amines. After 20 hours reaction the product obtained was purified by column chromatography using DCM. The clean product was isolated as a yellow liquid in a 78 % yield (Figure 4.8).

– Homopolymerization of NEM monomer **4.1** to afford polymer **4.6**



Scheme 4.7 : Polymerization of monomer **4.1** using CTA **4.5**

The polymerization of **4.1** was explored by RAFT using DDMEAT (**4.5**) as a chain transfer agent (Scheme 4.7). To our knowledge, monomer **4.1** has never been polymerized by RAFT before; hence, standard conditions for the polymerization of acrylates were used.<sup>28</sup> After 15 hours at 90 °C the reaction went to 60 % conversion, calculated by <sup>1</sup>H NMR comparing the vinyl peaks from the monomer at *ca.* 6 ppm (3x1H) with the backbone peaks from the polymer at *ca.* 1.5 ppm (3H).

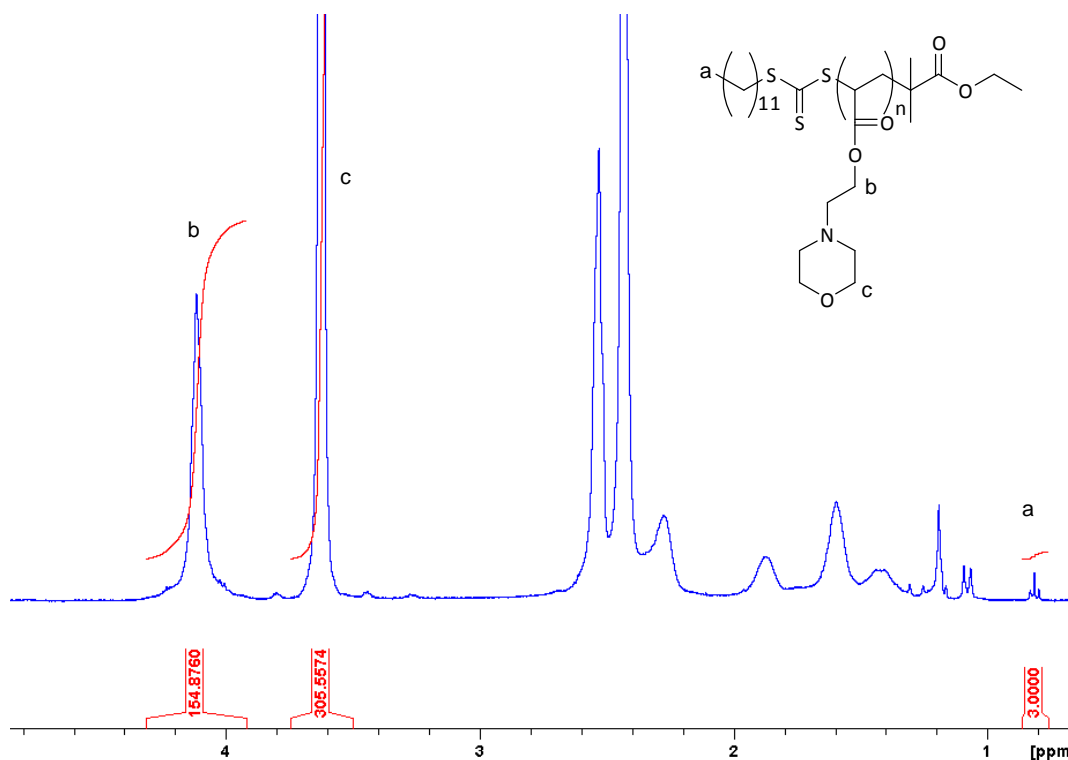


Figure 4.9: Extended  $^1\text{H}$  NMR spectrum in  $\text{CDCl}_3$  to determine the experimental DP of polymer **4.6**.

After purification by precipitation in cold hexane, the polymer obtained **4.6** had a DP of 76 ( $M_n = 14.4$  kDa), calculated by extended  $^1\text{H}$  NMR in  $\text{CDCl}_3$  comparing the integration of the CTA protons (3H at 0.85 ppm) to the integration of the polymer protons (2H at 4.2 and 2.6 ppm and 4H at 3.6 and 2.4 ppm) (Figure 4.9). The polydispersity of the resultant polymer was 1.47 by THF SEC calibrated with PMMA standards. The overlay of the RI and UV trace at 309 nm suggests the majority of the RAFT endgroups are present in the polymer chains (Figure 4.10).<sup>i</sup>

<sup>i</sup> End group fidelity by  $^1\text{H}$  NMR and SEC: The degree of polymerization of the polymer could be very easily determined by examination of the extended  $^1\text{H}$  NMR spectrum of the resultant polymer and comparison of the signals attributable to the CTA with those for the polymer. The match of the DP of the polymer with the theoretical value calculated by conversion NMR can be considered a proof of end group fidelity. On the other hand, the thiocarbonyl group (polymer end group) absorbs at 309 nm. By comparing the signal from the UV detector at 309 nm with the RI response for the same sample using both detectors in the SEC, if the end group is present through the polymer, at that wavelength both traces should overlap.

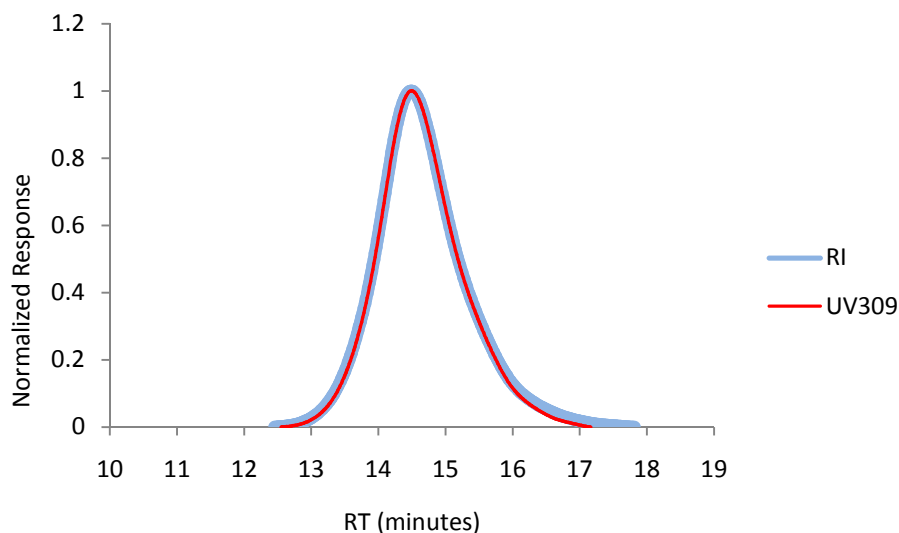
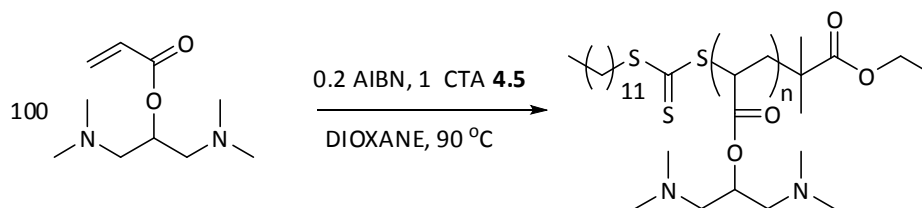


Figure 4.10: Overlay of the RI and UV<sub>309</sub> traces from the THF SEC for NEM homopolymer.

– *TMPDA homopolymer 4.7*



Scheme 4.8: Polymerization of TMPDA monomer **4.2** using CTA **4.5**.

Using similar conditions as reported for polymer **4.6**, the homopolymerization of monomer **4.2** by RAFT using CTA **4.5** was performed (Scheme 4.8). After 18 hours reaction at 90 °C the reaction achieved 47 % conversion, calculated by <sup>1</sup>H NMR in CDCl<sub>3</sub>. Different solvents were investigated in order to purify the polymer by precipitation (DMF, DCM, THF, acetone, hexane, dioxane, ethyl acetate, diethyl ether, H<sub>2</sub>O, basic water, acidic water). Unfortunately the polymer formed, as well as the monomer was soluble in all the solvents and hence they could not be separated.

The reaction mixture was dialyzed in water using a membrane with a pore size of 3.5 kDa in order to remove all the small molecules. After 2 days, the sample was freeze dried but it was not soluble in any available deuterated solvent. Several solubility tests were carried out and the sample could only be solubilized in acidic D<sub>2</sub>O. However, the <sup>1</sup>H NMR spectrum showed new unexpected peaks, so this purification route was also abandoned.<sup>ii</sup>

The reaction was repeated under the same conditions. In this case, in order to remove the unreacted starting monomer after polymerization the sample was dissolved in dioxane and freeze dried. Unfortunately, after 2 days only 10 % of the monomer was evaporated (Figure 4.11) and the SEC trace was bimodal, probably due to the coupling between polymer chains due to the extended polymerization times.

In order to reduce polymerization times, the reaction was carried out in the bulk at 75 °C. After 15 h the reaction achieved 50% conversion and 20% of the remaining unreacted monomer was removed by freeze drying the reaction mixture from dioxane. This time the SEC trace shows one single distribution with a polydispersity of 1.57 (Figure 4.12). Given the problems found in purification, the calculation of the molecular weight of the polymer by end group analysis was not possible. Moreover, the SEC analysis does not provide an accurate value for amine polymers since it is calibrated with PMMA or PS standards. Hence, the molecular weight was estimated from the conversion <sup>1</sup>H NMR spectrum being *ca.* 10.3 kDa.

---

<sup>ii</sup> Experiments carried out in next chapter for other amino monomers suggest that this new signals may be attributed to the amino catalyze self-hydrolysis of the ester bond.

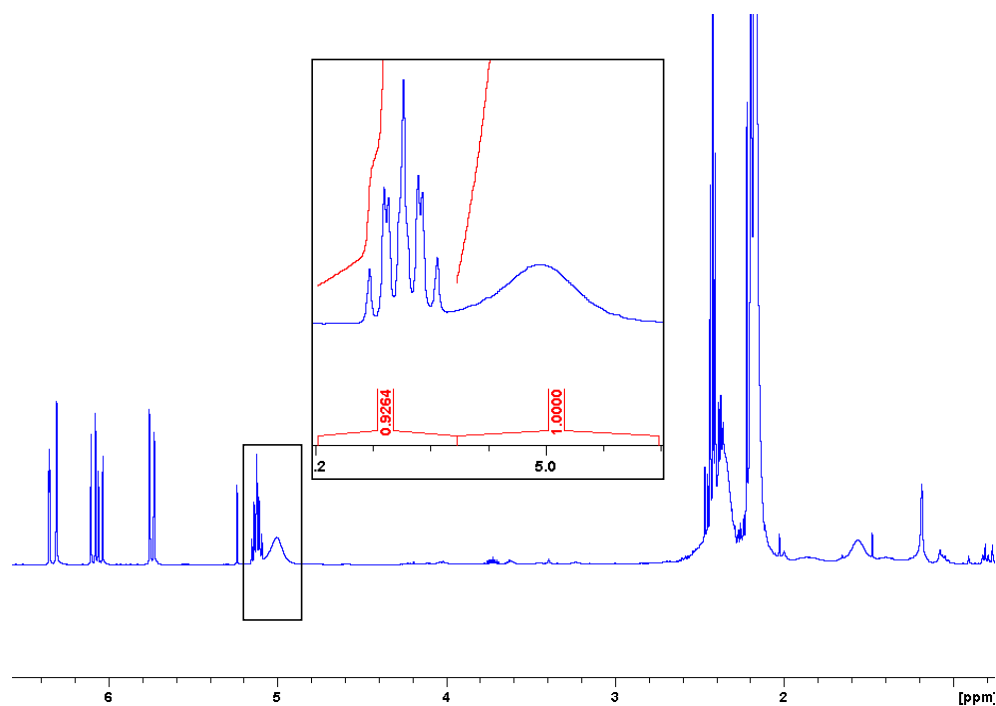


Figure 4.11:  $^1\text{H}$  NMR spectrum in  $\text{CDCl}_3$  of **4.7** with 47 % of monomer present after freeze-drying  
 $(0.9264 \times 100 / 1 + 0.9264 = 47 \%)$

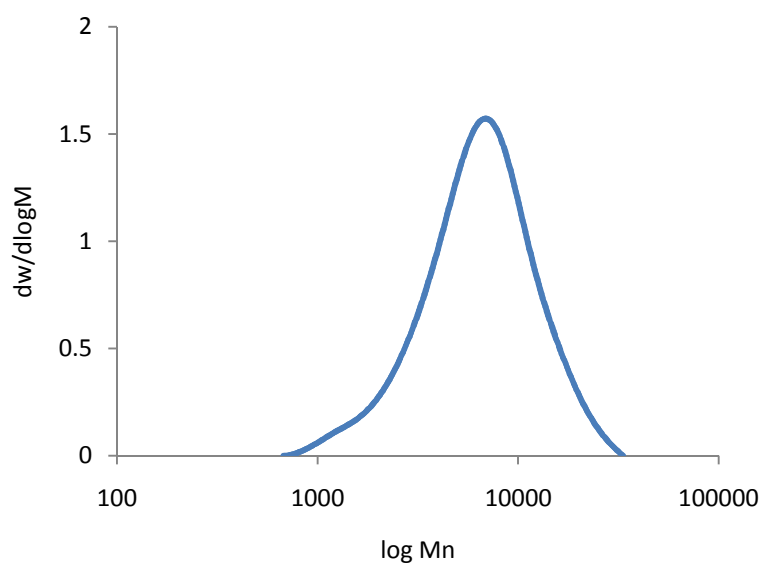
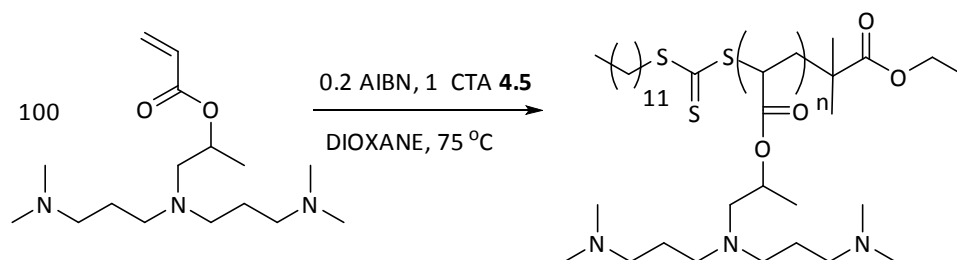


Figure 4.12: THF SEC trace from the RI detector for polymer **4.7**.

– Attempted homopolymerization of PMA monomer **4.3**: polymer **4.8**



Scheme 4.9: Homopolymerization of **4.3** using CTA **4.5**.

100 equivalents of monomer **4.3** were dissolved in double the volume of dioxane with 1 equivalent of CTA **4.5** and 0.2 equivalents of AIBN as a radical initiator (Scheme 4.9). After removing the oxygen the reaction ampoule was heated at 75 °C for 15 hours. After this time, an aliquot was taken to calculate the conversion by  $^1\text{H}$  NMR, but no signals attributable to the formation of polymer were observed.

Due to the high viscosity of the PMA monomer, the polymerization conditions were modified by increasing the amount of solvent in order to improve solubility of the new formed polymer (4:1 and 10:1 volume compared to monomer) using **2.9** as a CTA (synthesized in Chapter 2) and AIBN as radical initiator. Different aliquots were taken to follow the reaction, but after 24 hours no conversion was observed by  $^1\text{H}$  NMR spectroscopy in any of both reactions. Therefore, in a final attempt, 100 equivalents of monomer **4.3** were introduced in an ampoule in bulk solvent with 0.2 equivalents of AIBN and CTA **2.9**. After removing the oxygen, the reaction mixture was heated at 65 °C for 12 hours. The  $^1\text{H}$  NMR analysis of the sample taken showed that no polymerization occurred.

Given the difficulties to polymerize monomer **4.3** with CTAs **2.9** and **4.5**, a new commercially available CTA was tested. 2-cyano-2-propyl dodecyl trithiocarbonate (Figure 4.13) has been

proved to be a good CTA for a wide range of monomer including methacrylates.<sup>29</sup>

Unfortunately, in our case no polymer was formed after 24 hours.

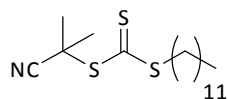
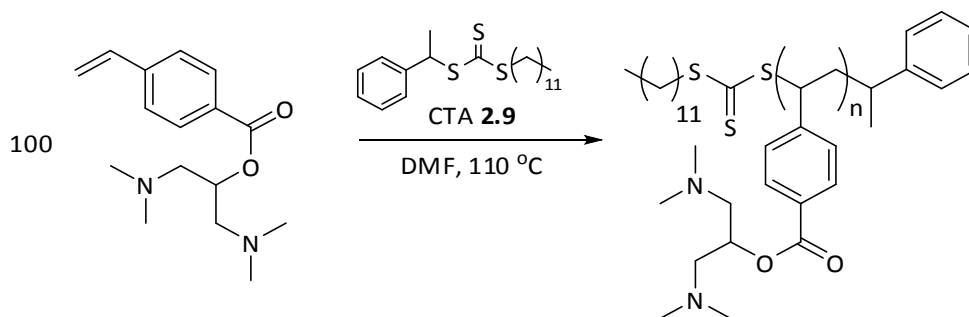


Figure 4.13: Structure of 2-cyano-2-propyl dodecyl trithiocarbonate.

Given the size and structure of the monomer, it is perhaps not surprising that the homopolymerization of **4.3** could be inhibited due to steric hindrance. Five different concentrations and 3 different CTAs have been tested in order to homopolymerize **4.3** without success, what lead to abandon this route and focus in the copolymerization with a non reactive monomer to form a functional PMA polymeric scaffold.

#### Styrenic TMPDA homopolymer **4.9**



Scheme 4.10: Homopolymerization of styrenic TMPDA **4.4** using CTA **2.9**

The styrenic TMPDA containing monomer, **4.4**, was polymerized by RAFT using dodecyl 1-phenylethyl trithiocarbonate (**2.9**) as this trithiocarbonate is known to be good chain transfer agents for the polymerization of styrene and styrenic monomers as seen in Chapter 2. 100

equivalents of **4.4** were introduced in a polymerization ampoule with 1 equivalent of CTA **2.9** in DMF (2:1 monomer:solvent). After removing the oxygen by 3 cycles of freeze-pump-thaw the ampoule was filled with nitrogen, sealed and heated at 110 °C. Different samples were taken at different times to calculate the conversion by  $^1\text{H}$  NMR spectroscopy (Figure 4.14).

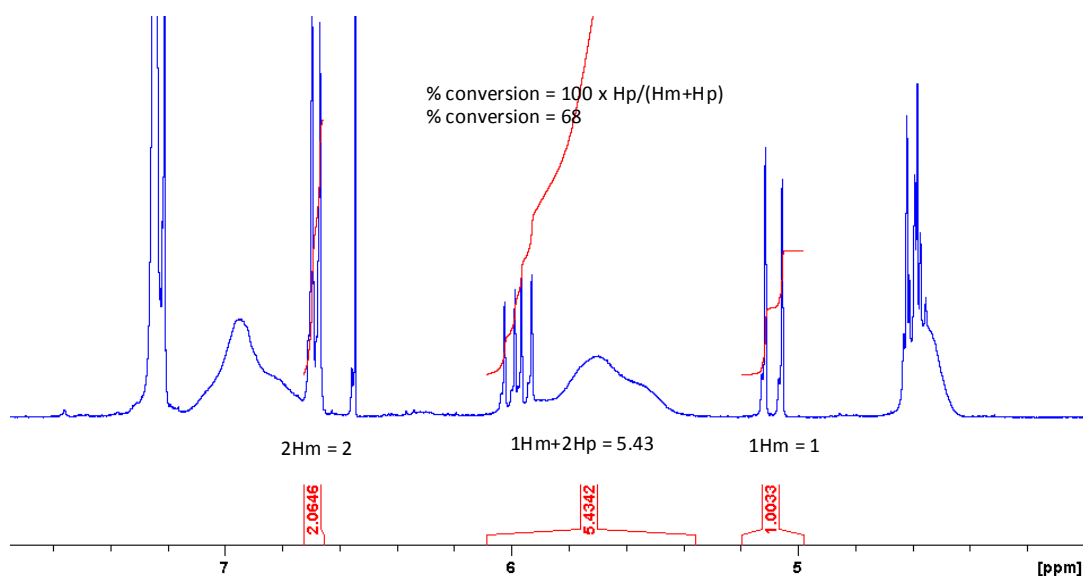


Figure 4.14: Example of a  $^1\text{H}$  NMR spectrum in  $\text{CDCl}_3$  used to calculate conversion for polymer **4.9**. An example of the conversion calculations is shown.

After 35 hours reaction the analysis of the crude by  $^1\text{H}$  NMR spectroscopy showed that 80 % of the monomer had polymerized. The resultant polymer was purified by precipitation in hexane and dried in a vacuum oven. By introducing the TMPDA motif into a styrenic monomer the synthesis and purification of the TMPDA containing polymer has improved compared to that for the acrylate counterpart (**4.7**). The SEC analysis of the clean polymer gave a Gaussian distribution with a  $M_w/M_n$  of 1.43. The overlay of the  $\text{UV}_{309}$  and RI signals proves the good trithiocarbonate end group fidelity, as shown in Figure 4.15.



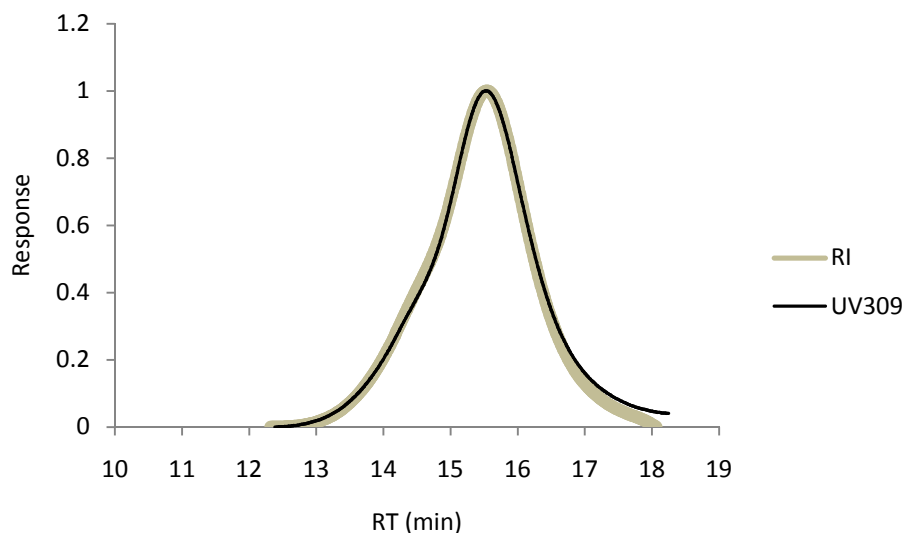


Figure 4.15: Overlay of UV<sub>309</sub> and RI signals from the THF SEC analysis of **4.9**

The molecular weight of the polymer was obtained by extended  $^1\text{H}$  NMR in  $\text{CDCl}_3$  by careful integration of the signals corresponding to the end group at 0.85 ppm (3H) with respect to the polymer peaks ( $M_{\text{nNMR}} = 24.5$  kDa).

#### 1.1.1 Copolymerization

By copolymerizing the amino monomers with a non reactive monomer the physical properties of the polymer will change as well as its catalytic properties. Introducing the new motif in to the polymer chain, the distance in between amines will increase, which has been proved to play an important role in the polyurethane foam formation.<sup>30</sup>

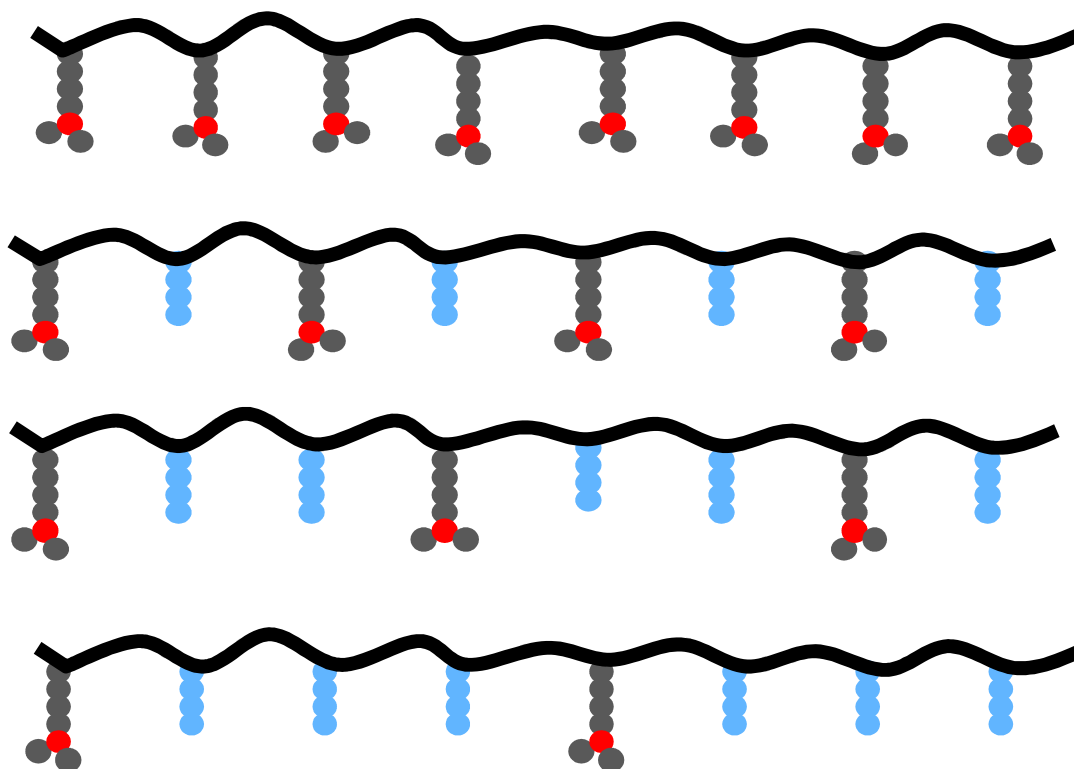


Figure 4.16: Schematic representation of separation between amino monomers prepared *via* copolymerization route.

Moreover, given the difficulties found in purifying some of the polymers due to their high solubility, the introduction of a less soluble co-monomer is expected to facilitate their purification. The monomer chosen for the copolymerization is commercially available methyl acrylate (MA, Figure 4.17).

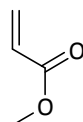


Figure 4.17: Structure of methyl acrylate (MA)

The choice of co-monomer is based on a number of different factors. Firstly, besides being commercially available, MA is non hindered and is chemically “inert” in the PU foam formation in order to avoid undesired side reactions taking place together with the amino

catalysis. Secondly, MA is a non activated acrylate; hence, it is expected to have similar reactivities to the synthesized acrylate amino monomers, which should favor the copolymerization of both monomers at the same rate, giving copolymers with homogeneous distribution of both monomers along the backbone. At the same time, the shorter alkane chain in the MA compared to the amino monomers synthesized should minimize the steric hindrance during catalysis.

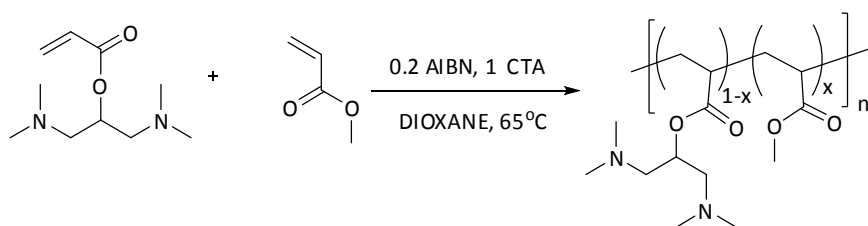
To be able to scale up the reactions for testing in industry, the synthesis of the CTA needs to be fast and efficient. The synthesis of DDEMAT (**4.5**) takes at least 3 days and after 2 work ups gives an overall yield of ca. 50%; therefore the synthesis of the amino polymers using CTA **2.9** was also investigated. Dodecyl 1-phenylethyl carbonotrithioate (**2.9**) can be synthesized based on a literature procedure and, as explained in Chapter 2,<sup>25</sup> after 5 hours reaction and a simple purification step **2.9** can be obtained as a purified yellow liquid in a 90% yield.<sup>iii</sup>

– *MA-co-TMPDA copolymers*

Given the difficulties found for the purification of the homopolymer **4.7**, the copolymerization with the less soluble monomer MA was investigated. The copolymerization of monomer **4.2** with methyl acrylate was studied in detail using dioxane as a solvent and AIBN as a radical initiator (Scheme 4.11).

---

<sup>iii</sup> The kinetics studies carried out in next chapter provide evidence that both **4.5** and **2.9** can readily polymerize amino containing polymers. Given this result from now on both CTAs will be used depending on availability.

Scheme 4.11: Copolymerization of **4.2** with methyl acrylate using either CTA **2.9** or **4.5**

The monomer **4.2** was polymerized with MA in 4 different ratios with **4.5**, aiming for 5, 25, 50 and 75 % incorporation of amino monomer into the polymer chain (Table 4.1).

Entry	MA (eq)	<b>4.2</b> (eq)	t (h)	Conv MA (%)	Conv <b>4.2</b> (%)	$M_w/M_n$	DP <sub>th</sub>	DP <sub>NMR</sub>	x
<b>4.10</b>	25	75	8	83	76	1.34	78	35	0.28
<b>4.11</b>	50	50	8	97	85	1.46	91	63	0.57
<b>4.12</b>	75	25	9	85	86	1.56	85	65	0.63
<b>4.13*</b>	95	5	15	82	72	1.16	82	112	0.96

Table 4.1: Summary of polymerization conditions for polymers **4.10** to **4.13**. All polymerizations carried out with 0.2 equivalents of AIBN and 1 equivalent of **4.5**. Conversions calculated by  $^1\text{H}$  NMR in  $\text{CDCl}_3$ , DP calculated by  $^1\text{H}$  extended NMR in  $\text{CDCl}_3$ ,  $M_w/M_n$  calculated by SEC (DMF) analysis using PMMA standards. DP<sub>th</sub> calculated by conversion NMR. \***2.9** was used as the CTA

The polymerizations were quenched by adding a minimum amount of DCM and precipitating into a large excess of the appropriate cold solvent. Due to the larger amount of amine in polymer **4.10** and **4.11**, these polymers were precipitated in cold heptanes while the polymers with more MA in their composition (**4.12** and **4.13**) were precipitated in cold diethyl ether. After decanting the solvent, the sticky yellow polymers were collected from the bottom of the flask by dissolving in DCM and precipitating again.  $^1\text{H}$  NMR spectroscopy was used to

calculate the conversion of the monomers by comparing the integration of the signals from the monomers with the signals from the resultant polymer (Figure 4.18).

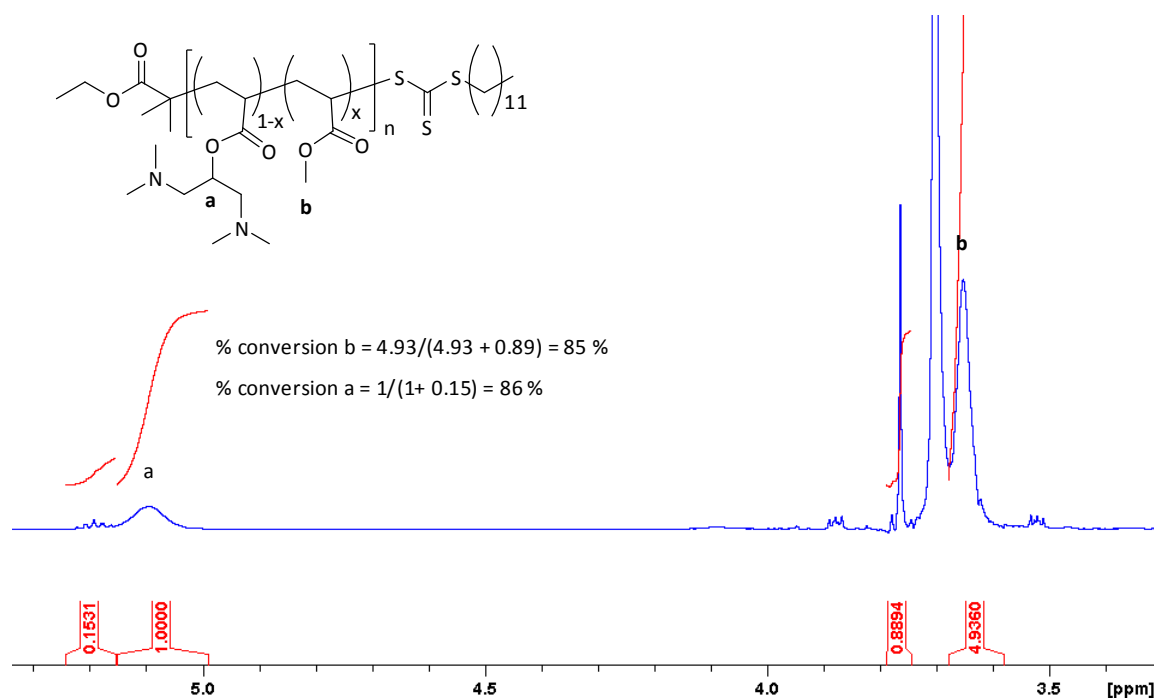


Figure 4.18: Example of a  $^1\text{H}$  NMR spectrum in  $\text{CDCl}_3$  used to calculate conversion for **4.2**/MA polymerization.

An example of the conversion calculations for **4.10** is shown.

Although the conversions were high after 8 or 9 hours and the final incorporation of **4.2** match the initial loadings, the overall DP of the polymer is much lower than expected. This may be explained by the method used to calculate each value. All 3 values (conversion, incorporation and DP) are calculated by careful integration of the signals from the  $^1\text{H}$  NMR spectra in  $\text{CDCl}_3$  (Figure 4.19). However, the calculation of the conversions and the incorporation of monomer do not take in account the integration of the end groups. As explained previously, the conversions are obtained from the ratio of the peaks monomer/polymer and the final incorporations are calculated by the ratio of the peaks of both monomers in the polymer chain. In contrast, the calculation of the final DP requires the integration of the end groups with

respect to the polymer signals. End group analysis by  $^1\text{H}$  NMR is a very sensitive technique. Any impurities in the polymer can lead to over integrate the signals from the end group which will result in an underestimation of the final DP. The polymers synthesized are gluey and difficult to purify because the impurities maybe hard to remove, so this can be the reason for the unexpected DPs for polymers **4.10**, **4.11** and **4.12**.

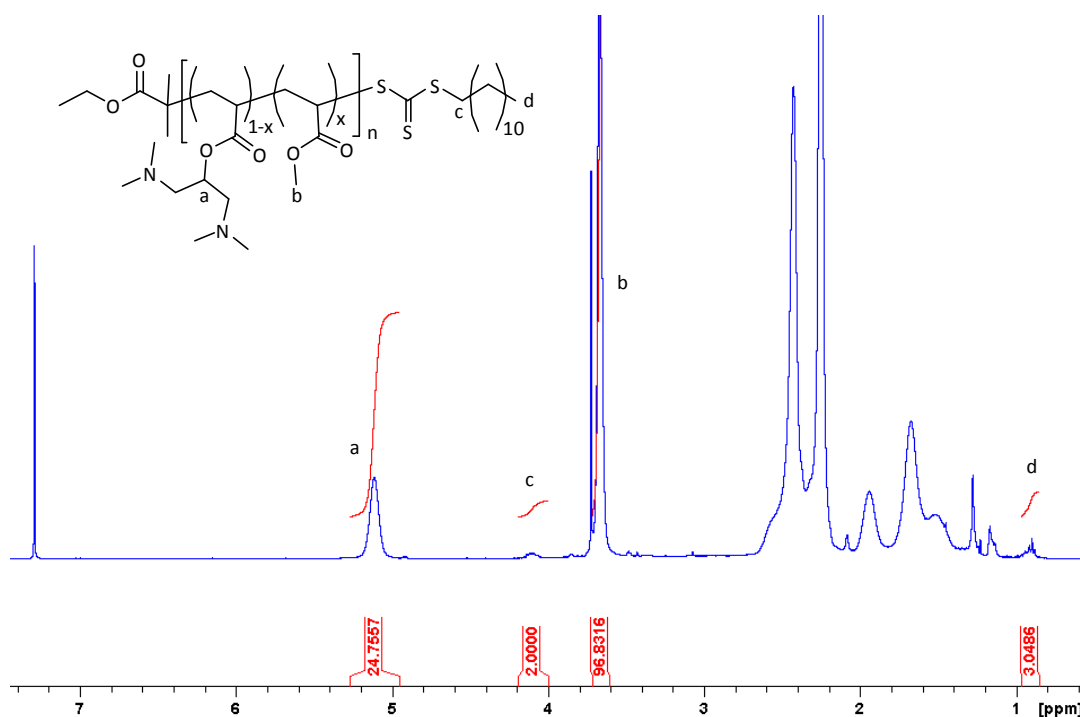


Figure 4.19: Example of an extended  $^1\text{H}$  NMR spectrum in  $\text{CDCl}_3$  to determine the experimental DP of **4.2**/MA copolymers.

In the case of **4.13**, the end group analysis by  $^1\text{H}$  NMR over estimates the theoretical DP suggesting lack of end group fidelity. This hypothesis was confirmed by SEC analysis of the traces given by the RI and UV detector at 309 nm. An example of the overlay is represented in Figure 4.20. The overlay of both traces is not perfect suggesting that not all end groups are present in each polymer chain. In order to obtain more information about the

copolymerization of these monomers kinetics studies and reactivity ratios would need to be investigated.

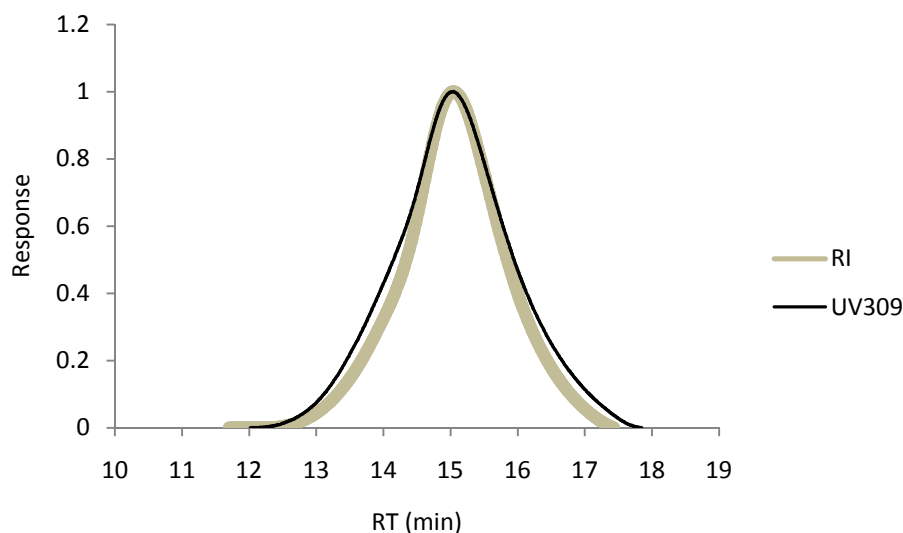


Figure 4.20: Overlay of UV<sub>309</sub> and RI signals from the DMF SEC analysis of **4.12**.

– *PMA-co-MA copolymer: 4.14*



Scheme 4.12: Copolymerization of monomer **4.3** with MA by RAFT

In the first attempt, 95 equivalents of MA were mixed with 5 equivalents of monomer **4.3** in dioxane with **2.9** as a CTA and AIBN as a radical initiator, aiming 5% incorporation of the amino monomer. After 15 hours at 65 °C very high conversion was observed by <sup>1</sup>H NMR spectroscopy for both monomers, so the polymer was precipitated in diethyl ether giving dark orange oil. The resultant polymer was characterized by extended <sup>1</sup>H NMR showing an overall

DP of 220 with 3% incorporation of **4.3** as shown in Figure 4.21. The reason for the degree of polymerization value is double than expected could be the lost of the end group and coupling reactions occurring between polymer chains. This theory is supported by the presence of a high molecular weight shoulder in the trace obtained for the polymer using DMF SEC analysis (Figure 4.22).

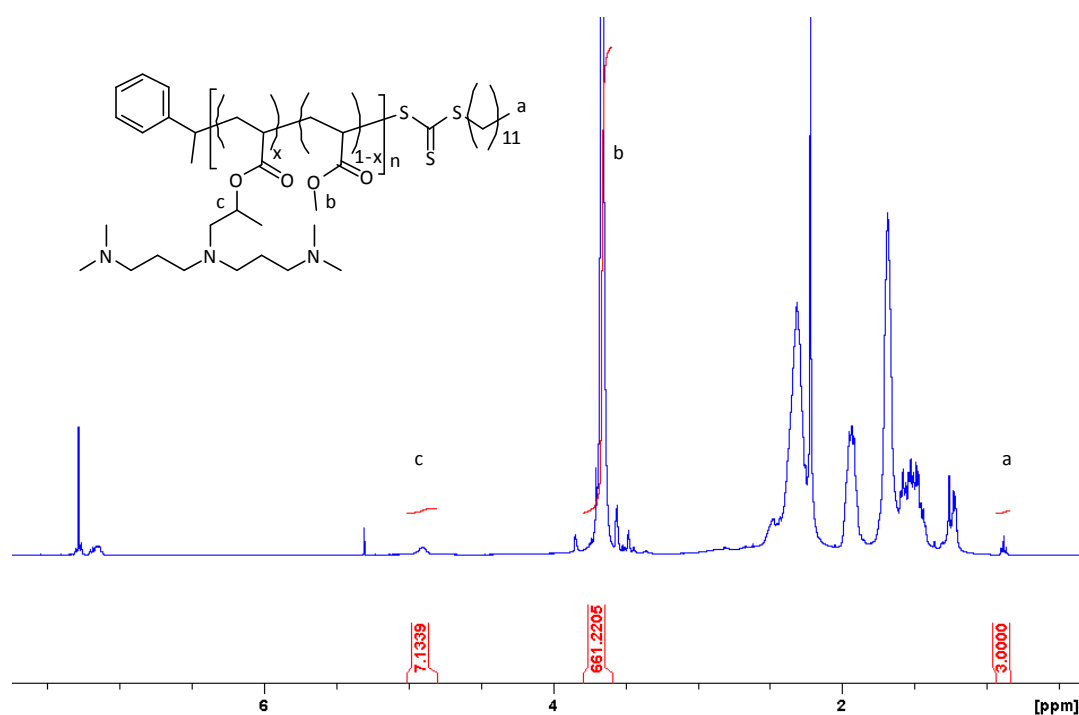


Figure 4.21: Example of an extended  $^1\text{H}$  NMR spectrum in  $\text{CDCl}_3$  to determine the experimental DP of **4.3**/MA copolymers.

Hence, decreasing the polymerization time was explored. Using the same conditions as mentioned above, the copolymerization of MA with **4.3** was explored using **4.5** as a **CTA**. After 8 hours reaction, an aliquot was taken to calculate the conversion by  $^1\text{H}$  NMR, and was precipitated in hexane as brown oil and dissolved in dioxane to eliminate the remaining monomer by freeze drying. The resultant polymer was characterized by extended  $^1\text{H}$  NMR showing an overall DP of 80 ( $M_n = 7.8$  kDa) with 4 % incorporation of **4.3** (Figure 4.21). The



analysis by DMF SEC gave a narrower  $M_w/M_n = 1.21$  however a small molecular weight shoulder was still present (Figure 4.22).

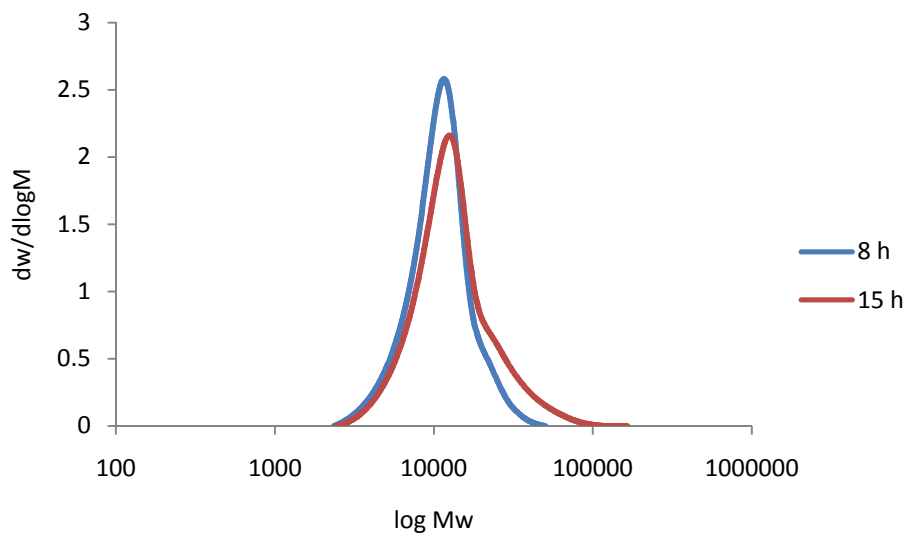
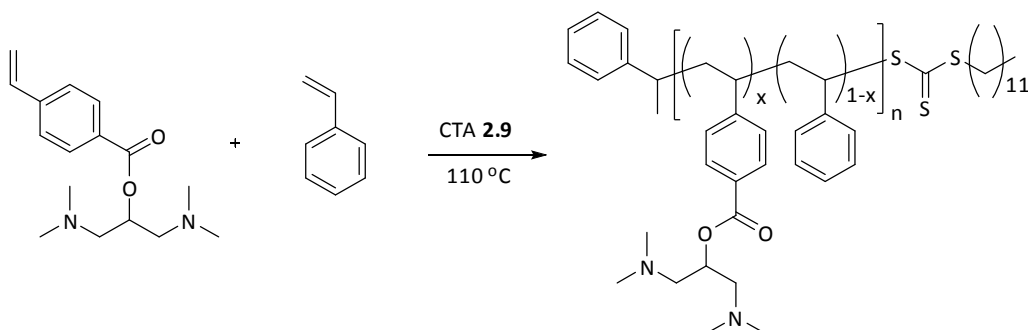


Figure 4.22: Overlay of RI signals from the DMF SEC analysis of polymer **4.14** after polymerization for 8 and 15 h.

Different attempts were carried out in order to increase the incorporation of **4.3** in the polymer, using the same conditions described above. Unfortunately, the copolymerization of **4.3** with MA was unsuccessful for higher loadings than 5%.

– Copolymerization of styrenic TMPDA **4.4** with styrene to afford polymer **4.15**



Scheme 4.13: Copolymerization of **4.4** with styrene.

The polymerization of **4.4** with styrene was studied, aiming for 5% incorporation of amino monomer. The monomers were polymerized in absence of oxygen using **2.9** as a CTA. The solution was heated at 110 °C in an oil bath. An aliquot was taken to determine the conversion (which was calculated by  $^1\text{H}$  NMR spectroscopy). The polymer was precipitated into a stirred solution of cold methanol, filtered and placed in the vacuum oven overnight at 40 °C. The resultant polymer showed a molecular weight of 5.4 kDa ( $\text{DP} = 46$ ) with 7% incorporation of **4.4** calculated by extended  $^1\text{H}$  NMR and a  $M_w/M_n$  of 1.27 obtained by SEC using THF as a solvent. As shown in Figure 4.23, the overlay of the  $\text{UV}_{309}$  and RI signals proves the good trithiocarbonate end group fidelity of the resultant polymer.

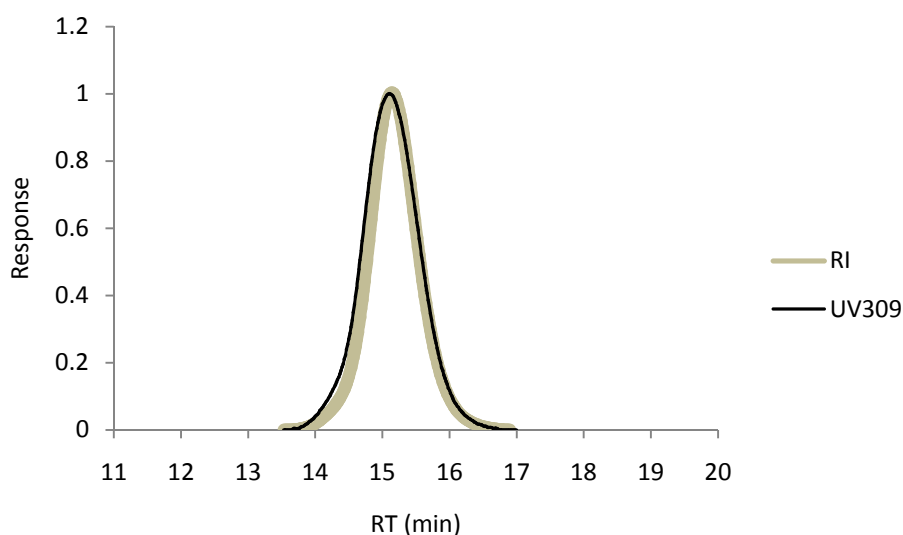


Figure 4.23: Overlay of  $\text{UV}_{309}$  and RI signals from the DMF SEC analysis of **4.15**

### 1.1.2 Polyurethane foam tests

Polymers and monomers synthesized were tested by AWE as catalysts for the formation of polyurethane foams. Initially, the catalytic activity of all monomers synthesized was investigated by comparing the percentage of foam rise *versus* time with the currently used

TMPDA catalyst (Figure 4.24). Although all monomers perform better than without catalyst, unfortunately none of the synthesized monomers achieves similar rate in the foam rise compared to that for the currently used TMPDA catalyst. Given the better performance of TMPDA (**4.2**) and NEM (**4.1**) acrylates compared to that for the styrenic version of TMPDA (**4.4**), new experiments were performed in order to assess their catalytic activity when tethered in a polymer (Figure 4.25)

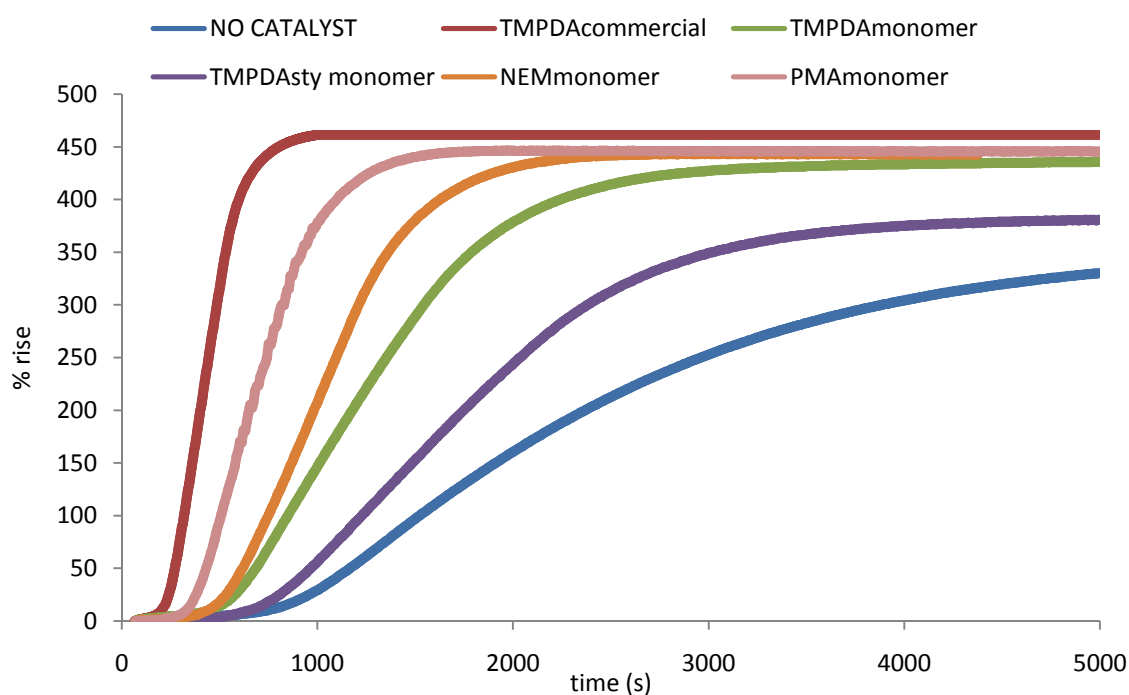


Figure 4.24: PU foam formation rise profile for the different monomers synthesized in this Chapter.

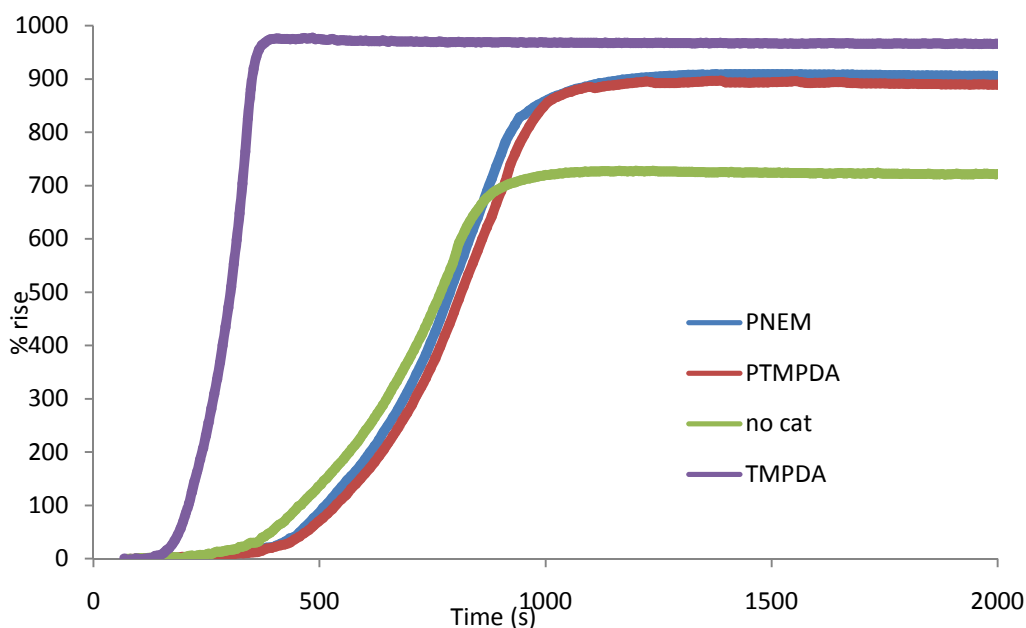


Figure 4.25: Percentage of rise *versus* time for the polyurethane foams synthesized using polymers **4.6** (PNEM) and **4.7** (PTMPDA) as a catalyst.

Unfortunately, the experimental data reveals that polymers **4.6** and **4.7** cannot be used as a substitute for TMPDA for the catalysis of PU foams. Although the increase of rise in the foam is higher than without catalyst, the catalytic activity of both monomers is reduced compared to that for the currently used TMPDA catalysts. Given the poor results obtained for the foam reaction catalyzed by the synthesized monomers, a new route was explored.

– *Commercially available catalyst*

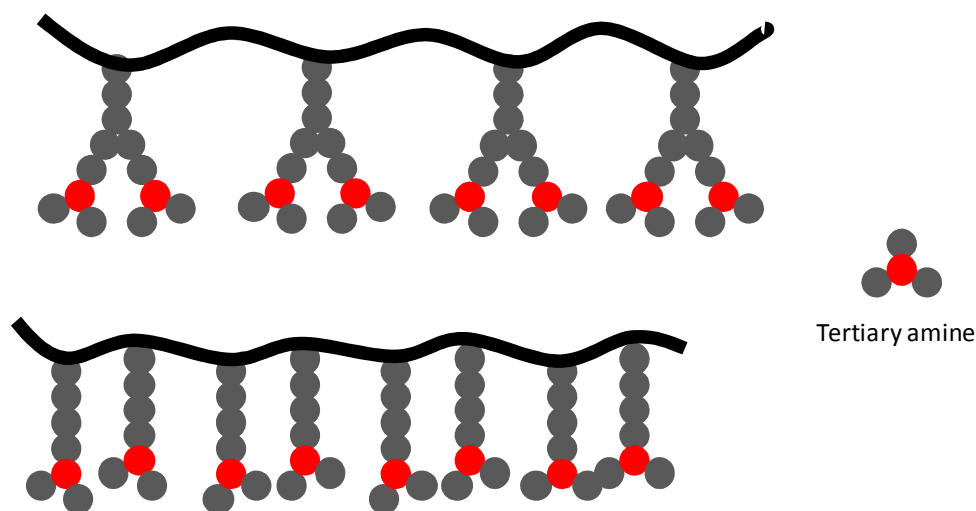


Figure 4.26: Schematic representation of multidentate versus monodentate amino polymers.

In order to mimic the multidentate character of the previously synthesized monomers, DMAEA homopolymer was investigated as a catalyst for the PU foam formation (Figure 4.26). This monomer contains the tertiary amine motif present in the currently used amino catalysts and could be easily copolymerized with a non-reactive monomer to modify the distance between active nitrogen, which has been proved to play an important role in the physical properties of the polyurethane foam.<sup>1,30</sup>

PDMAEA synthesized in Chapter 5 (5.1) was tested by AWE as a catalyst for the formation of PU foams (Figure 4.27). The foams catalyzed by PDMAEA showed a very similar performance in terms of overall percentage of rise and rise rate to the currently used commercially available TMPDA; hence, this polymer was selected in order to synthesize core-shell particles.

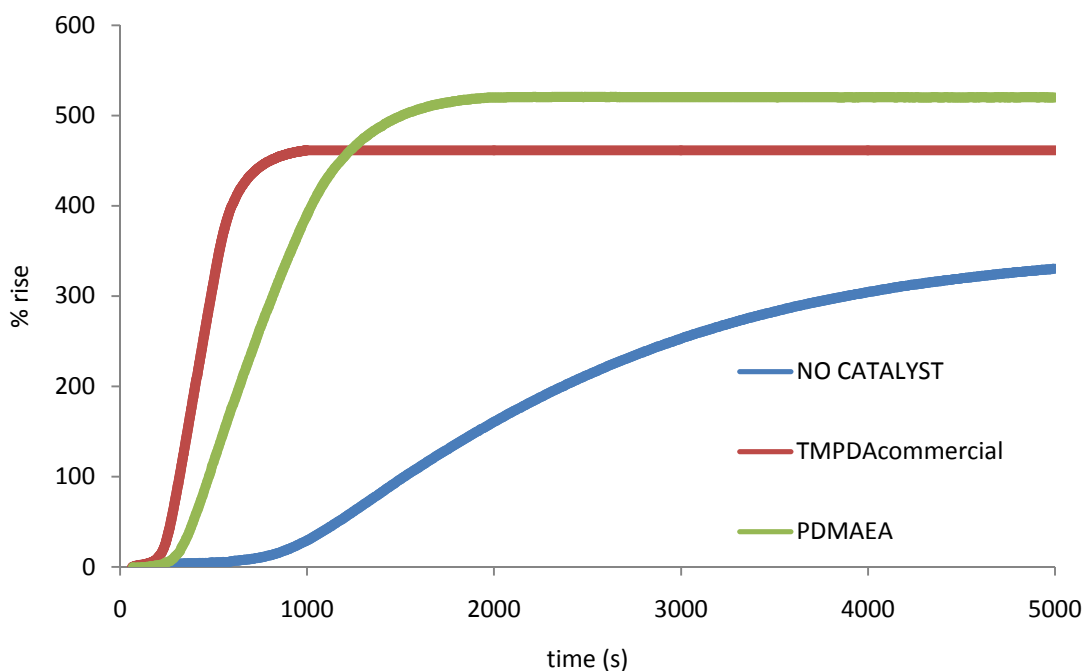


Figure 4.27: Rise profile for the PU foam formation using PDMAEA as a catalyst, compared to that for the reaction using commercially available TMPDA and with no catalyst.

### 1.1.3 Particle formation (*Future work*)

As described in Chapter 5, DMAEA can be readily polymerized by RAFT but, moreover, its degradation properties could be used as a “release” mechanism upon heating. The amine obtained from the degradation of the polymer (dimethylaminoethanol), has been already tested by AWE and has shown very good catalytic properties for the formation of PU foams. Further work will be focus in the synthesis of cross-linked particles protected by an inert polymeric shell. This will involve the formation of polymeric stars, with a core formed by copolymerization of the amino-monomers with a reversible crosslinker protected by a polyalcohol shell (Figure 4.28).

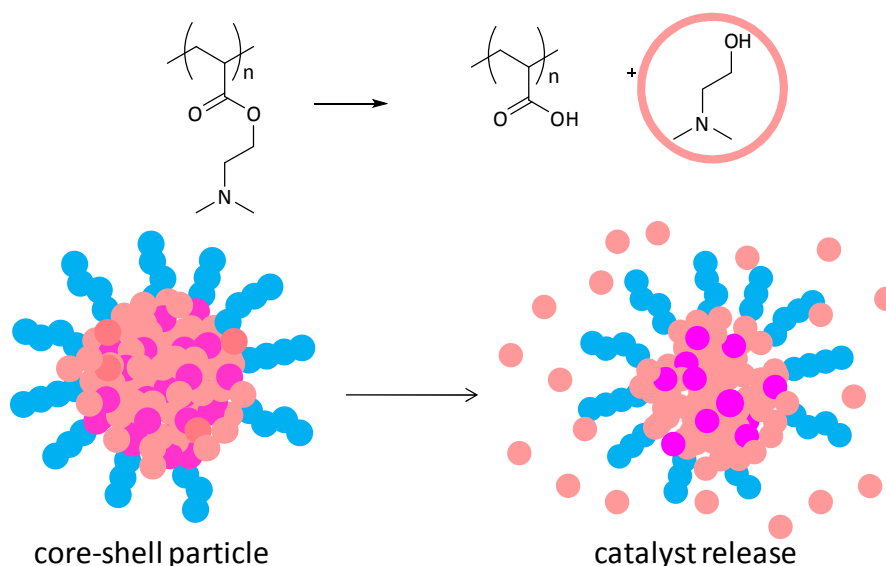


Figure 4.28: Schematic representation of the strategy to synthesize amino-containing core-shell particle for controlled release.

#### 4.4 Conclusions

Four different monomers have been synthesized with structures analogous to the currently used amino catalysts for polyurethane production. Three of which have been homopolymerized by RAFT with good control without the need of protecting groups. The monomers have been also copolymerized with a non reactive monomer in order to study how the separation between amino motives affects the properties of the catalyst. These new monomers and functional polymers were tested as supported catalysts for the polyurethane foam reaction between a polyol and isocyanate. Unfortunately, the performance of these new synthesized polymers was poor when compared to that for the currently used commercially available amines and new polymeric catalyst must be designed and tested in order to obtain a valuable polymeric substitute.

To improve reaction control, these monomers will be incorporated into a polymeric structure that responds to an increase of temperature by releasing the amino functionality. These structures will be synthesized by copolymerization of the monomers with a temperature responsive crosslinkable monomer to form crosslinked polymer aggregates which will release the amino functionality as single polymer chains by breaking the crosslink upon heating.



## 4.5 Experimental

### 4.5.1 Materials

Styrene and methyl acrylate monomers were filtered through a plug of silica prior to use and stored at 4 °C. AIBN (2,2'-azo-bis(isobutyronitrile)) was recrystallized from ethyl acetate and stored at 4 °C. All other materials were used as received from Aldrich, Fluka, and Acros.

### 4.5.2 Instrumentation:

<sup>1</sup>H NMR and <sup>13</sup>C NMR spectra were recorded with a Bruker DPX-300 spectrometer in CDCl<sub>3</sub> unless otherwise specified. Extended <sup>1</sup>H and <sup>13</sup>C NMR spectra were recorded on a Bruker DPX-400 spectrometer at 25 °C (128 scans). Size exclusion chromatography (SEC) measurements were performed with HPLC grade solvents (Fisher), tetrahydrofuran (with 2 % of TEA) at 30 °C or DMF (1.06 g LiCl per litre) at 40 °C as an eluent at a flow rate of 1 mL/min. The molecular weights of polymers were calculated relative to polystyrene or PMMA standards.

### 4.5.3 Synthesis of *S*-1-dodecyl-*S'*-( $\alpha,\alpha'$ -dimethyl- $\alpha''$ -methyl acetate) trithiocarbonate (**4.5**, DDMEAT)

DDMEAT (**4.5**) was prepared by esterification reaction of **2.4** with ethanol following a literature procedure.<sup>27</sup> A mixture of 1 equivalent of **2.4** (0.5 g), 1.1 equivalents of 1-ethyl-3-(3-dimethylaminopropyl) carbodiimide (3.7 g, EDCI) and 0.1 equivalents of DMAP (0.16 g) in EtOH (40mL EtOH / 1g **2.4**) was stirred at room temperature for 20 hours. The EtOH was evaporated and the reaction mixture was dissolved in DCM and filtered to remove the salts.

The product was purified by passing thorough a plug of silica dissolved in a mixture of hexane and DCM (1:4) and the clean product was isolated as a yellow liquid in a 78 % yield (0.37 g).

**4.5;**  $^1\text{H}$  NMR ( $\text{CDCl}_3$ ):  $\delta$  (ppm) 4.12 (q, 2H,  $J = 7.5$  Hz,  $\text{CH}_3\text{CH}_2\text{O}$ ), 3.25 (t, 2H,  $J = 7.5$  Hz,  $\text{SCH}_2$ ), 1.66 (s, 6H,  $\text{C}(\text{CH}_3)_2$ ), 1.60-1.11 (m, 20H,  $\text{CH}_2(\text{CH}_2)_{10}\text{CH}_3$ ), 0.85 (t, 3H,  $J = 7.5$  Hz,  $(\text{CH}_2)_{10}\text{CH}_3$ )  $^{13}\text{C}$  NMR ( $\text{CDCl}_3$ ):  $\delta$  (ppm) 211.8, 173.0, 62.4, 55.7, 36.9, 31.9, 29.2, 25.5, 22.7, 14.1

#### 4.5.4 Monomer synthesis

##### – NEM monomer, **4.1**

Following a literature procedure,<sup>21</sup> a mixture of 1 equivalent of 4-(2-hydroxyethyl)morpholine (1 mL, 8.26 mmol) and 1.1 equivalents of triethylamine (TEA, 1.2 mL) in  $\text{CHCl}_3$  (10 mL  $\text{CHCl}_3$  / 1 mL amine) was stirred at room temperature under nitrogen for 30 min. The mixture was cooled to 0 °C and a solution of 1.2 equivalents (0.86 mL) of acryloyl chloride in 2 mL  $\text{CHCl}_3$  was added dropwise and warmed at room temperature overnight. The solvent was evaporated and the solid residue was dissolved in DCM and filtered to remove the salts, washed with 1 M NaOH and dried with sodium sulfate. The  $\text{CHCl}_3$  was removed with the rotary evaporator (at room temperature). The yield of the reaction was 77 % (1.17 g).

**4.1;**  $^1\text{H}$  NMR ( $\text{CDCl}_3$ ):  $\delta$  (ppm) 6.33 (dd, 1H,  $J = 1.5$  and 17.5 Hz,  $\text{CHH}=\text{CH}$ ), 6.11 (dd, 1H,  $J = 10.5$  and 17.5 Hz,  $\text{CH}_2=\text{CH}$ ), 5.78 (dd, 1H,  $J = 1.5$  and 10.5 Hz,  $\text{CHH}=\text{CH}$ ), 4.21 (t, 4H,  $J = 6$  Hz,  $\text{CH}_2\text{OCH}_2$ ), 3.63 (t, 4H,  $J = 4.5$  Hz,  $\text{OCH}_2\text{CH}_2$ ), 2.61 (t, 2H,  $J = 6$  Hz,  $\text{CH}_2\text{CH}_2\text{O}$ ), 2.45 (t, 2H,  $J = 4.5$  Hz,  $\text{CH}_2\text{CH}_2\text{N}$ )  $^{13}\text{C}$  NMR ( $\text{CDCl}_3$ ):  $\delta$  (ppm) 166.5, 131.0, 128.3, 67.3, 61.8, 57.3, 54.0.

– *TMPDA monomer, 4.2*

Using a similar procedure as reported for **4.1**, a mixture of 1 equivalent of 1,3-bis dimethylamino-2-propanol (5 mL, 29.5 mmol) and 1.1 equivalents (4.5 mL) of triethylamine (TEA) in  $\text{CHCl}_3$  (10 mL  $\text{CHCl}_3$  / 1 mL amine) was stirred at room temperature under nitrogen for 30 min. The mixture was cooled to 0 °C and a solution of 1.1 equivalents (3 mL) of acryloyl chloride in  $\text{CHCl}_3$  was added dropwise and left at room temperature for 15 hours.

The reaction mixture was filtered to remove the salts, and washed with 1 M NaOH and dried over sodium sulfate. After evaporating the  $\text{CHCl}_3$  the reaction mixture was dissolved in EtOAc and passed through a plug of neutral alumina to remove the remaining salts. The solvent was removed with the rotary evaporator (at room temperature). The yield of the reaction was 65 % (3.9 g).

**4.2;**  $^1\text{H}$  NMR ( $\text{CDCl}_3$ ):  $\delta$  (ppm) 6.37 (dd, 1H,  $J = 1.5$  and 17.5 Hz,  $\text{CHH}=\text{H}$ ), 6.11 (dd, 1H,  $J = 10.5$  and 17.5 Hz  $\text{CH}_2\text{CH}$ ), 5.80 (dd, 1H,  $J = 1.5$  and 10.5 Hz  $\text{CHH}=\text{H}$ ), 5.16 (m, 1H,  $\text{CH}_2\text{CHCH}_2$ ), 2.46 (m, 4H,  $\text{NCH}_2\text{CHCH}_2\text{N}$ ), 2.22 (s, 12H,  $\text{CH}_3\text{N}$ ),  $^{13}\text{C}$  NMR ( $\text{CDCl}_3$ ):  $\delta$  (ppm) 165.0, 130.1, 128.3, 69.7, 61.1, 45.6  $m/z$  [ES MS] 201.2  $[\text{M}+\text{H}]^+$

– *PMA monomer, 4.3*

1 equivalent (18.1 mmol) of 1-[bis[3-(dimethylamino)propyl]amino]-2-propanol in  $\text{CHCl}_3$  (10 mL  $\text{CHCl}_3$  / 1 ML amine) was stirred at room temperature under nitrogen for 30 min. The mixture was cooled to 0 °C and a solution of 1.1 equivalents of acryloyl chloride in  $\text{CHCl}_3$  was added dropwise and warmed to room temperature and stirred overnight.

$\text{Na}_2\text{CO}_3$  was added to the reaction mixture and stirred for 1 hour. The solution was filtered, washed with 1 M NaOH and dried over sodium sulfate. The mixture was filtered and the  $\text{CHCl}_3$  was removed with the rotary evaporator (at room temperature) and dried under vacuum overnight. The yield of the reaction was 91 %.

**4.3;**  $^1\text{H}$  NMR ( $\text{CDCl}_3$ ):  $\delta$  (ppm) 6.35 (dd, 1H,  $J = 1.5$  and  $17.5$  Hz,  $\text{CHH}=\text{H}$ ), 6.05 (dd, 1H,  $J = 10.5$  and  $17.5$  Hz,  $\text{CH}_2\text{CH}$ ), 5.75 (dd, 1H,  $J = 10.5$  and  $17.5$  Hz,  $\text{CHH}=\text{H}$ ), 5.05 (m, 1H,  $\text{CH}_2\text{CH}(\text{CH}_3)\text{OH}$ ), 2.57 (dd, 1H,  $J = 13.5$  Hz,  $\text{NCHHCH}(\text{CH}_3)\text{O}$ ), 2.43 (m, 5H,  $\text{CH}_2\text{NCH}_2\text{CH}_2$  and  $\text{NCHHCH}(\text{CH}_3)\text{O}$ ), 2.18 (m, 14H,  $\text{CH}_3\text{N}$  and  $(\text{CH}_3)_2\text{NCH}_2\text{CH}_2$ ), 1.55 (q, 4H,  $J = 7$  Hz,  $\text{CH}_2\text{CH}_2\text{CH}_2$ ), 1.21 (d, 3H,  $J = 6.5$  Hz,  $\text{CH}_3\text{CH}$ )  $^{13}\text{C}$  NMR ( $\text{CDCl}_3$ ):  $\delta$  (ppm) 165.5, 130.0, 129.1, 69.3, 59.2, 57.5, 52.7, 45.6, 25.8, 18.6  $m/z$  [ES MS] 300.2  $[\text{M}+\text{H}]^+$

– *TMPDA styrenic monomer, 4.4*

4-vinyl benzoic acid (1 eq, 5.3 mmol) was dissolved in 15 mL of DCM in a 100 mL two-necked flask, followed by addition of DMAP (0.05 eq, 0.26 mmol) and EDCI (1 eq, 5.3 mmol) under nitrogen atmosphere. After the mixture was stirred for 30 minutes at room temperature, 1,3-bisdimethylamino-2-propanol (1.1 eq, 5.9 mmol) was added into the flask. After 5 days reaction the solution was filtered and washed with NaOH (100 mL), water (100 mL) and brine (100 mL) and purified by column chromatography using neutral alumina with EtOAc as a solvent. 44% yield.

**4.4;**  $^1\text{H}$  NMR ( $\text{CDCl}_3$ ):  $\delta$  (ppm) 8.00 (d, 2H,  $J = 8.5$  Hz,  $\text{CH}=\text{CCHCH}_2$ ), 7.43 (d, 2H,  $J = 8.5$  Hz,  $\text{CH}=\text{CCO}$ ), 6.70 (dd, 1H,  $J = 11$  and  $17.5$  Hz,  $\text{CH}_2=\text{CHC}$ ), 5.83 (d, 1H,  $J = 17.5$  Hz,  $\text{CCHH}=\text{CH}_2$ ), 5.37 (m, 2H,  $\text{CCHH}=\text{CH}$  and  $\text{COOCH}$ ), 2.59 (d, 4H,  $J = 6$  Hz,

$\text{CH}_2\text{N}(\text{CH}_3)_2$ , 2.27 (s, 12H,  $\text{CH}_3\text{N}$ )  $^{13}\text{C}$  NMR ( $\text{CDCl}_3$ ):  $\delta$  (ppm) 154.3, 136.2, 130, 126.5, 116.4, 71.3, 61.9, 46.0  $m/z$  [ES MS] 277.2  $[\text{M}+\text{Na}]^+$ , 295.2  $[\text{M}+\text{H}]^+$

#### 4.5.5 Polymer Synthesis

##### – NEM homopolymer; 4.6

100 equivalents of **4.1** 0.2 equivalents of AIBN and 1 equivalent of **2.4** where dissolved in dioxane (2 mL dioxane/1 g of monomer) and heated at 90 °C after 3 freeze-pump-thaw cycles to remove the oxygen. After 2 days reaction (60 % conversion) polymer was precipitated 3 times in cold hexane and dried under vacuum.  $M_{\text{nNMR}} = 14.4$  kDa,  $n = 76$ ,  $M_w/M_n$  (THF, PMMA standards) = 1.47.  $^1\text{H}$  NMR (400 MHz,  $\text{CDCl}_3$ ):  $\delta$  (ppm) 4.11 (br t, 2H,  $\text{CH}_2\text{OCH}_2$ ), 3.62 (br t, 4H,  $\text{OCH}_2\text{CH}_2$ ), 2.52 (br t, 2H,  $\text{CH}_2\text{CH}_2\text{O}$ ), 2.43 (br t, 4H,  $\text{CH}_2\text{CH}_2\text{N}$ ), 1.25-2.10 (br m, backbone), 0.85 (t, 3H end group)

##### – TMPDA homopolymer; 4.7

100 equivalents of **4.2**, 0.2 equivalents of AIBN and 1 equivalent of DDMEAT where heated at 75 °C after 3 cycles of freeze-pump-thaw to remove the oxygen. After 15 h reaction (50% conversion) the mixture was dissolved in dioxane and freeze-dried to remove the unreacted monomer.  $M_{\text{nNMR}} = 10$  kDa (by conversion),  $n = 50$  (by conversion),  $M_w/M_n$  (THF, PMMA standards) = 1.57.  $^1\text{H}$  NMR (400 MHz,  $\text{CDCl}_3$ ):  $\delta$  (ppm) 5.01 (br q, 1H,  $\text{CH}_2\text{CHCH}_2$ ), 2.36 (br q, 4H,  $\text{NCH}_2\text{CHCH}_2\text{N}$ ), 2.17 (br s, 12H,  $\text{CH}_3\text{N}$ ), 1.25-2.10 (br m, backbone), 0.85 (t, 3H end group)

– Styrenic TMPDA homopolymer; 4.9

100 equivalents of **4.4** (7.2 mmol) were introduced in a polymerization ampoule with 1 equivalent of **2.9** and 0.2 equivalents of AIBN in DMF (1:2 volume compare to monomer). After removing the oxygen by 3 freeze-pump-thaw cycles the ampoule was filled with nitrogen, sealed and heated at 110 °C. After 35 hours reaction the analysis of the crude by <sup>1</sup>H NMR showed that 80 % of the monomer had polymerized. The polymer was precipitated twice in hexane and dried in the vacuum oven at 40 °C overnight.  $M_{n,NMR} = 24.5$  kDa,  $n = 88$ ,  $M_w/M_n$  (THF, PS standards) = 1.43. <sup>1</sup>H NMR (400 MHz, CDCl<sub>3</sub>): 7.71 (br d, 2H, CH=CCHCH<sub>2</sub>), 7.11 (m, 5H end group), 6.48 (br d, 2H, CH=CCO), 5.34 (br m, 1H, COOCH), 2.58 (br d, 4H, CH<sub>2</sub>N(CH<sub>3</sub>)<sub>2</sub>), 2.25 (br s, 12H, CH<sub>3</sub>N) 2.80-0.8 (br m, backbone),

– General procedure for copolymerization

A solution of 100 equivalents of a combination of the 2 monomers, 0.2 equivalents of AIBN and 1 equivalent of CTA in dioxane (1/3 volume compare to monomer) were added to a dry ampoule containing a stirrer bar. The solution was degassed using at least 3 freeze-pump-thaw cycles (until no oxygen bubbles are seen), back filled with nitrogen gas, sealed and placed in a pre-heated oil bath at the required temperature. After a certain amount of time, an aliquot was removed for <sup>1</sup>H NMR analysis in CDCl<sub>3</sub> to determine the conversion. The polymerization is quenched by adding a small amount of DCM and precipitating the reaction mixture dropwise into stirred cold solvent to produce liquid/viscous polymer. The solvent was decanted and the polymer was dissolved in the minimum amount of DCM and precipitated again. After 2 or 3 precipitations, the DCM was removed in the rotary evaporator and the resultant polymer was dried in a vacuum oven at 40 °C overnight. Molecular weights and polydispersity indices were

measured by DMF or THF SEC measurements using PMMA as narrow standards and  $^1\text{H}$  NMR spectroscopy in  $\text{CDCl}_3$  were used for the determination of polymerization conversion, using a crude sample of the polymerization reaction mixture before workup by careful integration of polymer peak to monomer signals. Extended  $^1\text{H}$  NMR spectroscopy in  $\text{CDCl}_3$  was used for the determination of end group functionality and molecular weight by careful integration of the polymer backbone and characteristic functional monomer peaks to the end group signals.

– *Copolymerization of **4.2** with MA: **4.10**, **4.11**, **4.12**, **4.13***

A solution of “x” equivalents of MA, “100-x” equivalents of **4.2**, 0.2 equivalents of AIBN and 1 equivalent of CTA (**4.5** or **2.9**) in dioxane (1:3 volume compare to monomer) was added to a dry ampoule containing a stirrer bar. The solution was degassed using at least 3 freeze-pump-thaw cycles and filled with nitrogen, sealed and placed in an oil bath at 65 °C. After a certain amount of time, an aliquot was removed for  $^1\text{H}$  NMR analysis to determine the conversion. The polymerization is quenched by the addition of a minimal amount of DCM and precipitated dropwise into stirred cold diethyl ether or heptanes (x2) to produce a gluey amber polymer that was dried in a vacuum oven at 40 °C overnight.

$^1\text{H}$  NMR (400 MHz,  $\text{CDCl}_3$ ):  $\delta$  (ppm) 5.01 (br q, 1H,  $\text{CH}_2\text{CHCH}_2$ ), 3.66 (br s, 3H,  $\text{CH}_3\text{O}$ ), 2.36 (br q, 4H,  $\text{NCH}_2\text{CHCH}_2\text{N}$ ), 2.17 (br s, 12H,  $\text{CH}_3\text{N}$ ), 1.25-2.10 (br m, backbone), 0.85 (t, 3H end group)

– *Copolymerization of **4.3** with MA*

A solution of 95 equivalents of MA, 5 equivalents of **4.3**, **4.5** was added to a dry ampoule containing a dry stirrer bar. The solution was degassed using at least 3 freeze-pump-thaw cycles

and filled with nitrogen, sealed and placed in an oil bath at 65 °C. After a certain amount of time, an aliquot was removed for NMR analysis to determine the conversion. The polymerization is quenched by the addition of a minimal amount of DCM and precipitated drop wise into stirred cold diethyl ether (x2) and freeze dried from dioxane to produce a viscous dark yellow polymer that was dried in a vacuum oven at 40 °C overnight.  $M_{n,NMR} = 7.8$  kDa,  $n = 80$ ,  $x = 0.04$ ,  $M_w/M_n$  (DMF, PMMA standards) = 1.21.  $^1H$  NMR ( $CDCl_3$ ):  $\delta$  (ppm) 4.84 (br m, 1H,  $CH_2CH(CH_3)OH$ ), 3.66 (br s, 3H,  $CH_3O$ ), 2.18 (br s, 12H,  $CH_3N$ ), 1.91 (br q, 4H,  $CH_2CH_2CH_2$ ), 1.25-2.10 (br m, backbone), 0.85 (t, 3H end group)

– *Copolymerization of 4.4 with styrene*

Styrene (95 eq, 26.2 mmol), **1.1** (5 eq), **2.9** (1 eq, 0.028 mmol), were put in an ampoule. The oxygen was removed by three freeze-pump-thaw evacuation cycles. For the last cycle, nitrogen was flushed into the ampoule before thawing. The solution was heated at 110 °C in an oil bath. An aliquot was taken to determine the conversion by  $^1H$  NMR spectroscopy in  $CDCl_3$  after 15 h reaction (61 %). The polymer was precipitated twice into a stirred solution of cold MeOH. The yellow powder was filtered and placed in the vacuum oven overnight at 40 °C.  $M_{n,NMR} = 5$  kDa,  $n = 46$ ,  $x = 0.07$ ,  $M_w/M_n$  (THF, PS standards) = 1.12.  $^1H$  NMR (400 MHz,  $CDCl_3$ ): 7.71 (br d, 2H,  $CH=CCHCH_2$ ), 7.35-6.25 (br m, 7H Aromatics), 5.34 (br m, 1H,  $COOCH$ ), 3.92 (m, 1H, end group), 2.58 (br d, 4H,  $CH_2N(CH_3)_2$ ), 2.25 (br s, 12H,  $CH_3N$ ) 2.30-0.8 (br m, backbone), 0.85 (t, 3H end group).



## 4.6 References

- (1)Malwitz, N.; Wong, S.-W.; Frisch, K. C.; Manis, P. A. *J. Cell. Plast.* **1987**, 23, 461.
- (2)Singh, H.; Sharma, T. P.; Jain, A. K. *J. Appl. Polym. Sci.* **2007**, 106, 1014.
- (3)Blank, W. J.; He, Z. A.; Hessel, E. T. *Prog. Org. Coat.* **1999**, 35, 19.
- (4)Chiefari, J.; Chong, Y. K.; Ercole, F.; Krstina, J.; Jeffery, J.; Le, T. P. T.; Mayadunne, R. T. A.; Meijs, G. F.; Moad, C. L.; Moad, G.; Rizzardo, E.; Thang, S. H. *Macromolecules* **1998**, 31, 5559.
- (5)Lokitz, B. S.; Convertine, A. J.; Ezell, R. G.; Heidenreich, A.; Li, Y.; McCormick, C. L. *Macromolecules* **2006**, 39, 8594.
- (6)Mori, H.; Iwaya, H.; Nagai, A.; Endo, T. *Chem. Commun.* **2005**, 4872.
- (7)Akimoto, J.; Nakayama, M.; Sakai, K.; Okano, T. *J. Polym. Sci., Part A: Polym. Chem.* **2008**, 46, 7127.
- (8)Becer, C. R.; Hahn, S.; Fijten, M. W. M.; Thijs, H. M. L.; Hoogenboom, R.; Schubert, U. S. *J. Polym. Sci., Part A: Polym. Chem.* **2008**, 46, 7138.
- (9)Gujraty, K. V.; Yanjarappa, M. J.; Saraph, A.; Joshi, A.; Mogridge, J.; Kane, R. S. *J. Polym. Sci., Part A: Polym. Chem.* **2008**, 46, 7249.
- (10)Theato, P. *J. Polym. Sci., Part A: Polym. Chem.* **2008**, 46, 6677.

- (11) Evans, A. C.; Skey, J.; Wright, M.; Qu, W.; Ondeck, C.; Longbottom, D. A.; O'Reilly, R. K. *J. Polym. Sci., Part A: Polym. Chem.* **2009**, 47, 6814.
- (12) Vestberg, R.; Piekarski, A. M.; Pressly, E. D.; Van Berkel, K. Y.; Malkoch, M.; Gerbac, J.; Ueno, N.; Hawker, C. J. *J. Polym. Sci., Part A: Polym. Chem.* **2009**, 47, 1237.
- (13) Shen, Y.; Tang, H.; Ding, S. *Prog. Polym. Sci.* **2004**, 29, 1053.
- (14) Grignard, B.; Jerome, C.; Calberg, C.; Jerome, R.; Detrembleur, C. *Eur. Polym. J.* **2008**, 44, 861.
- (15) Grignard, B.; Calberg, C.; Jerome, C.; Wang, W.; Howdle, S.; Detrembleur, C. *Chem. Commun.* **2008**, 5803.
- (16) Grignard, B.; Jerome, C.; Calberg, C.; Jerome, R.; Wang, W.; Howdle, S. M.; Detrembleur, C. *Chem. Commun.* **2008**, 314.
- (17) Grignard, B.; Jérôme, C.; Calberg, C.; Jérôme, R.; Detrembleur, C. *Eur. Polym. J.* **2008**, 44, 861.
- (18) Grignard, B.; Jerome, C.; Calberg, C.; Detrembleur, C.; Jerome, R. *J. Polym. Sci., Part A: Polym. Chem.* **2007**, 45, 1499.
- (19) Kumar, K. R.; Kizhakkedathu, J. N.; Brooks, D. E. *Macromol. Chem. Phys.* **2004**, 205, 567.
- (20) Faucher, S.; Zhu, S. *J. Polym. Sci., Part A: Polym. Chem.* **2007**, 45, 553.
- (21) Velasco, D.; Elvira, C.; Roman, J. S. *J. Mater. Sci.: Mater. Med.* **2008**, 19, 1453.
- (22) Wang, D.; Wu, T.; Wan, X. J.; Wang, X. F.; Liu, S. Y. *Langmuir* **2007**, 23, 11866.

- (23) Bütün, V.; Sönmez, S.; Yarlğan, S.; Taktak, F. F.; Atay, A.; Bütün, S. *Polymer* **2008**, *49*, 4057.
- (24) Neises, B.; Steglich, W. *Angew. Chem., Int. Ed.* **1978**, *17*, 522.
- (25) Skey, J.; O'Reilly, R. K. *Chem. Commun.* **2008**, 4183.
- (26) Lai, J. T.; Filla, D.; Shea, R. *Macromolecules* **2002**, *35*, 6754.
- (27) Ma, J.; Cheng, C.; Sun, G. R.; Wooley, K. L. *Macromolecules* **2008**, *41*, 9080.
- (28) Moad, G.; Rizzardo, E.; Thang, S. H. *Aust. J. Chem.* **2012**, *65*, 985.
- (29) Chong, Y. K.; Moad, G.; Rizzardo, E.; Thang, S. H. *Macromolecules* **2007**, *40*, 4446.
- (30) AWE In *confidential report* 2010.

## **Chapter 5: Stimuli-responsive properties of DMAEA containing polymers**

## 5.1 Abstract

Reversible addition-fragmentation chain transfer (RAFT) copolymerization of dimethylaminoethyl acrylate (DMAEA) and methyl acrylate (MA) has been performed with good control over molecular weight and polydispersity. A screening in composition of P(DMAEA-*co*-MA) copolymers was elaborated from 0% to 75% of MA. The behavior of the pH and temperature-sensitive copolymers was studied in aqueous solution by measuring the lower critical solution temperatures (LCST) and the acid dissociation constants ( $pK_a$ ). The higher incorporation of MA in the co-polymer resulted in an increase in the  $pK_a$  values due to the larger distance between charges facilitating the protonation of adjacent nitrogens.

The LCST behavior of the copolymers was studied in pure water and in aqueous solution buffered at pH 8. The LCST values were irreproducible and were highly influenced by the self-hydrolysis of DMAEA. Hence, kinetic studies have been performed in order to quantify the degree of self-hydrolysis at different temperatures and polymer concentrations in order to investigate new applications for these polymers.

## 5.2 Introduction

Polymers from *N*-substituted (meth)acrylates are of increasing interest for many applications (biosensors, membranes, drug delivery systems, substrates for cell culture, isolation of biomolecules, and enzyme activity control) because they show specific solution properties, such as micellization, thermosensitivity, and pH sensitivity.<sup>1,2</sup> In many of these applications, the usefulness of polyamines is closely related to their ability to possess cationic charges due to the

protonation of the amine nitrogens, typically under low pH conditions.<sup>3</sup> Therefore, in selecting optimal polyamine materials for specific applications, one of the key parameters that needs to be considered is the pH-dependent charge characteristics of the polymers.<sup>1</sup> Different studies have shown that the connectivity and tight spacing between amine groups in a polyamine chain causes a retardation of the protonation of amine groups relative to the same compounds in their monomeric state.<sup>1,4</sup>

Typical examples are the polymers of dimethylaminoethyl methacrylate (DMAEMA). These polymers also show lower critical solution temperatures (LCST) around body temperature, and therefore, their exploitation as biomaterials and polymer electrolytes have been extensively investigated.<sup>1,5,6</sup> DMAEMA homopolymer (PDMAEA) has a  $pK_a$  of *ca.* 7.0 and therefore behaves as a weak polybase at higher pH values, whereas at lower pH values, the amine groups are protonated, and the polymer behaves as a cationic polyelectrolyte. At room temperature, PDMAEMA is water-soluble over a wide pH range.<sup>7</sup> PDMAEMA also exhibits inverse temperature solubility behavior and precipitates out of neutral or basic aqueous solution between 32 and 53 °C, depending on its molecular weight.<sup>8</sup> It is nontoxic and can be absorbed *via* endocytosis; hence, can be used as a nonviral DNA vector.<sup>5,9</sup> In addition, is an attractive system for biological applications, having antibacterial and anticancer activities.<sup>6</sup>

Many polymerization techniques have been described to synthesize PDMAEMA, which is a pH- and temperature-sensitive polymer, including anionic polymerization or group transfer polymerization. Controlled radical polymerizations (CRP) techniques such as atom transfer radical polymerization (ATRP) have been investigated to afford relatively well-defined PDMAEMA polymers, even if the copper catalyst was complexed by amino groups in both

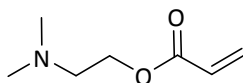
monomer and polymer.<sup>10</sup> Furthermore, well-defined PDMAEMA synthesized *via* reversible addition–fragmentation chain transfer (RAFT) polymerizations without the need of additives or special conditions has also been reported.<sup>11–13</sup>

The incorporation of a co-monomer in the polymer should provide a change in the properties of the polymer, and indeed, the stimuli-responsive properties are strongly dependent on many parameters, such as the molecular weight and polydispersity index. It has been demonstrated that well-defined polymers synthesized by CRP techniques exhibit a much sharper LCST transition compared to ill-defined polymers that have been prepared by free radical polymerization.<sup>14</sup> The monomer composition in the polymer also influences the temperature and pH responsiveness as the hydrophilicity/hydrophobicity balance in the polymer is of crucial importance. In this way, DMAEMA has been copolymerized with many co-monomers to provide materials with different LCSTs. Methacrylates, N-isopropylacrylamide (NIPAM) and styrene have been successfully copolymerized with DMAEMA.<sup>15,16</sup>

Fewer studies have been carried out using the acrylate version, DMAEA, and this chapter will explore this monomer further and highlight some important differences between this monomer and its methacrylate counterpart.

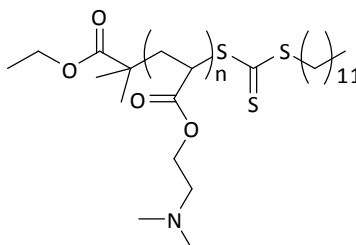
### 5.3 Results and discussion

#### 5.3.1 Homopolymerization of DMAEA



Scheme 5.1: Structure of the commercially available DMAEA

A summary of the polymerization conditions for the homopolymerization of DMAEA using CTA **4.5** is reported in Table 5.1. In a first attempt, following a literature procedure DMAEA was polymerized using RAFT in dioxane (1:3 volume compared to monomer) at 80 °C (Table 5.1, Entry 1).<sup>17</sup> The conversion of the monomer was determined by <sup>1</sup>H NMR spectroscopy in CDCl<sub>3</sub> by comparing the signal of the monomer (2H at 4.3 ppm) with the same signal from the resultant polymer at 4.1 ppm. The polymer was purified by repeated precipitation in cold heptane.



Entry	T (°C)	t (h)	Conv <sup>a</sup> %	M <sub>n</sub> <sup>SEC</sup> (kDa)	M <sub>n</sub> <sup>NMR</sup> (kDa)	DP <sup>b</sup>	M <sub>w</sub> /M <sub>n</sub> <sup>c</sup>
<b>1</b>	80	3	97	12.0	n.d.	n.d.	1.65
<b>2<sup>d</sup></b>	65	16/40	40/77	11.1	n.d.	n.d.	1.27
<b>3 (5.1)</b>	65	5	88	11.0	13	91	1.39

Table 5.1: Summary of polymerization conditions for homopolymerization of DMAEA. All polymerizations carried out with 0.2 equivalents of AIBN, 100 equivalents of monomer and 1 equivalent of CTA **4.5** in dioxane (1:3 volume compared to monomer). <sup>a</sup> Conversions calculated by <sup>1</sup>H NMR spectroscopy in CDCl<sub>3</sub>. <sup>b</sup> Degree of polymerization (DP) calculated by <sup>1</sup>H long acquisition NMR in CDCl<sub>3</sub> (n.d. = not determined). <sup>c</sup> Calculated by SEC (THF) analysis using PMMA standards. <sup>d</sup> In toluene 50 % volume and DMF SEC using PMMA standards.



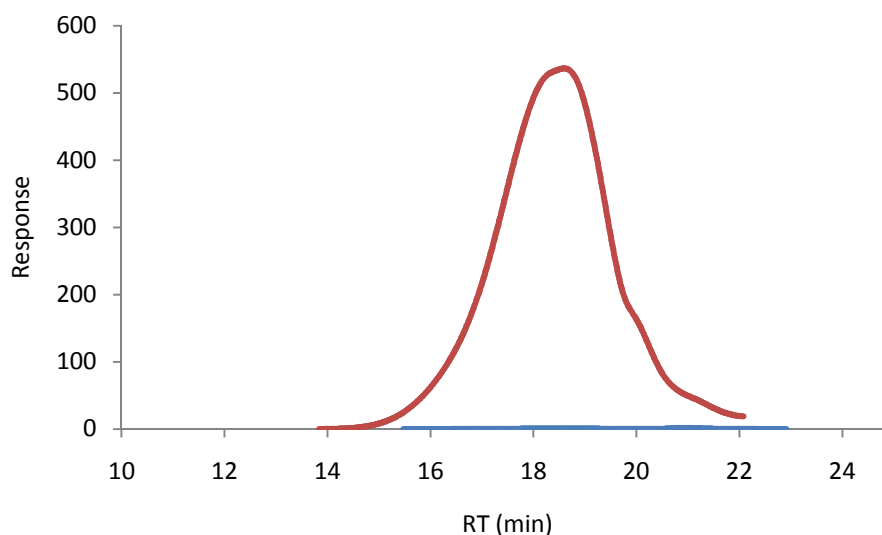


Figure 5.1: RI (red) and UV (blue) signals from the THF SEC analysis of polymer obtained under conditions reported in Table 5.1, Entry 1

The SEC trace of a representative polymer is shown in Figure 5.1. No end group was found for this polymer either by  $^1\text{H}$  NMR or  $\text{UV}_{309}$  SEC analysis. The lack of end group fidelity was proposed to be due to the high temperatures employed for the polymerization.<sup>18</sup> Following a different literature procedure DMAEA was polymerized using RAFT in toluene (1:1 volume compared to monomer) at 65 °C (Table 5.1, entry 2).<sup>19</sup> An aliquot of the reaction mixture was taken at different times to calculate the conversion by  $^1\text{H}$  NMR by comparing the signal of the monomer (2H at 4.3 ppm) with the same signal from the resultant polymer at 4.1 ppm. After 16 h only a 53 % of the monomer had reacted so the reaction was left for a total of 40 h giving 77 % conversion. The polydispersity of the resultant polymer was determined to be 1.27, calculated by SEC using THF as a solvent (PMMA standards). Although the polydispersity index was narrow compared to previous polymerizations, the analysis of the polymer by long acquisition  $^1\text{H}$  NMR spectroscopy proved that the polymer again did not have a RAFT end

group, determined by the absence of CTA signals; this may be explained by the long polymerization time required to achieve high conversions.

This hypothesis was investigated by slightly changing the polymerization conditions; using dioxane as a solvent (1:3 volume compared to monomer, Table 5.1, Entry 3) at 65 °C, and indeed 80 % conversion was achieved after 3 hours. Although the polydispersity was broader (1.27 *vs* 1.39), good end group fidelity was achieved, as confirmed by <sup>1</sup>H NMR and SEC analysis. The resultant polymer DP was determined to be 91 (**5.1**) by long acquisition <sup>1</sup>H NMR in CDCl<sub>3</sub> (Figure 5.2).

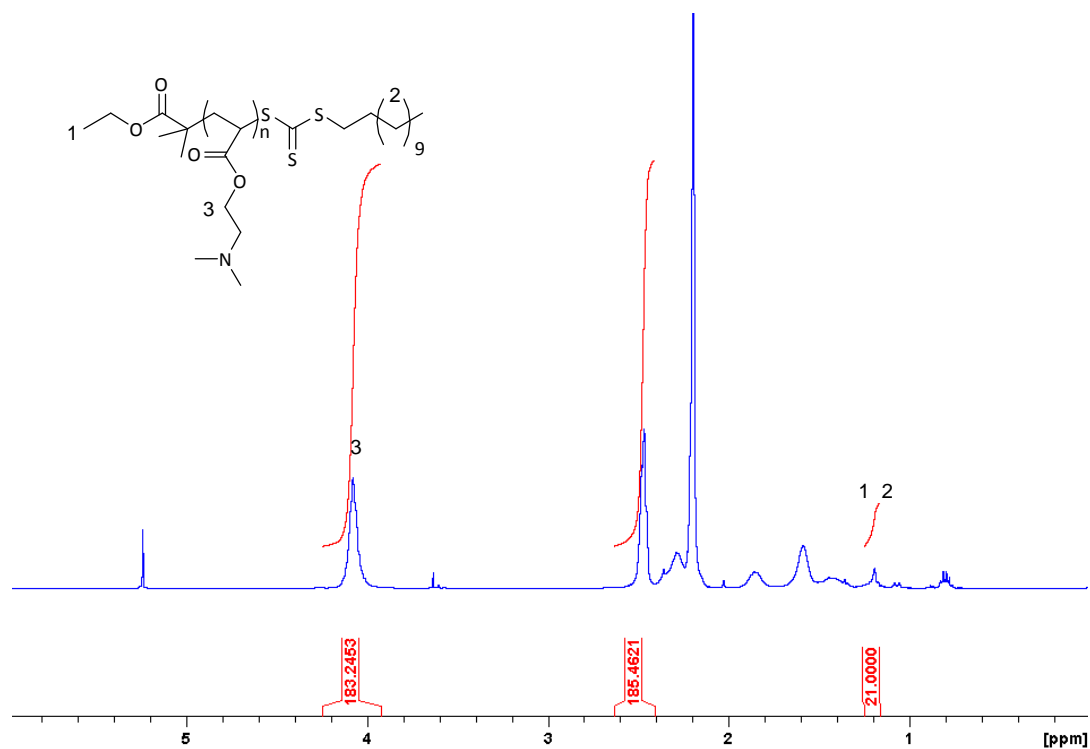


Figure 5.2: Long acquisition <sup>1</sup>H NMR spectrum in CDCl<sub>3</sub> of DMAEA homopolymer **5.1**.

As discussed in the previous chapter, the need to scale up the reactions requires the synthesis of CTA to be fast and efficient.

Figure 5.3: Structure of CTAs **2.9** and **4.5**

The synthesis of DDEMAT (**4.5**) requires 3 days and 2 work ups to achieve an overall yield of *ca.* 50%; while dodecyl 1-phenylethyl carbonotrithioate (**2.9**) can be synthesized in just 5 hours with a simple purification step giving a yield of 90% (Figure 5.3). To compare the efficiency of both CTAs in the polymerization of PDMAEA, kinetic studies of the homopolymerization of DMAEA were carried out using the above optimized conditions (Table 5.2). Given that both CTAs have the same Z group, very similar behavior is expected.<sup>20</sup>

Entry	t (min)	% conversion	% conversion	M <sub>n</sub> NMR	M <sub>n</sub> NMR	M <sub>w</sub> /M <sub>n</sub>	M <sub>w</sub> /M <sub>n</sub>
		4.5	2.9	4.5	2.9	4.5	2.9
				(kDa)	(kDa)		
1	45	20	20	3.2	3.2	1.16	1.19
2	90	23	20	3.7	3.2	1.17	1.18
3	135	46	44	7.0	6.8	1.29	1.34
4	195	64	59	9.5	8.8	1.42	1.39
5	255	73	70	11.0	10.4	1.45	1.52

Table 5.2: Kinetic data of polymerization of DMAEA with 2 different CTAs. Conversions calculated by <sup>1</sup>H NMR

in CDCl<sub>3</sub>. Samples were measured by SEC (THF) analysis using PMMA standards.

The conversion of the reaction was determined by <sup>1</sup>H NMR by comparing the signal of the monomer (2H at 4.2 ppm) with the same signal from the resultant polymer at 4.1 ppm. The

DP of the resultant polymer was determined by long acquisition  $^1\text{H}$  NMR spectroscopy by comparing in both cases, the signals from the end group functionalities (see Figure 5.2).

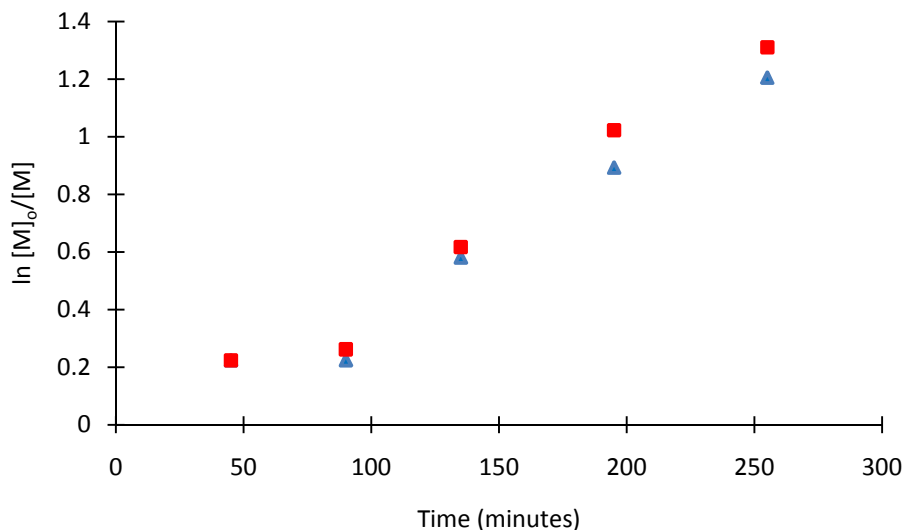


Figure 5.4: Kinetic data for the polymerization of DMAEA with 4.5 ( $\blacktriangle$ ) and 2.9 ( $\blacksquare$ )

The kinetic plot was linear in both cases indicating a controlled radical polymerization with a constant radical concentration. Although there is evidence of an induction period of about 60 minutes, the molecular weight of the polymer increased linearly with conversion at the same rate for both CTA's.

The SEC analysis gives inaccurate molecular weight data due to the interactions of the amino functional group with the SEC analytical columns (Figure 5.5 and Figure 5.6). The  $M_w/M_n$  values increase with polymerization time (Table 5.2) which can be explained by the larger amount of amino groups in the polymer at higher conversions, thus increasing interactions with the columns and resulting in the observed broadening of the trace.

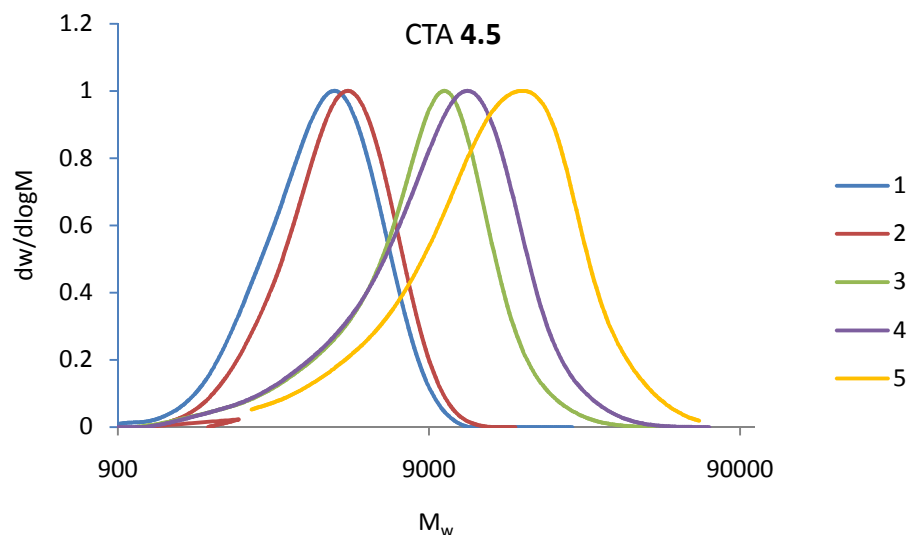


Figure 5.5: From left to right, SEC traces (RI) of the different PDMAEA samples using CTA 4.5 taken at 45, 90, 135, 195 and 255 minutes (Table 5.2)

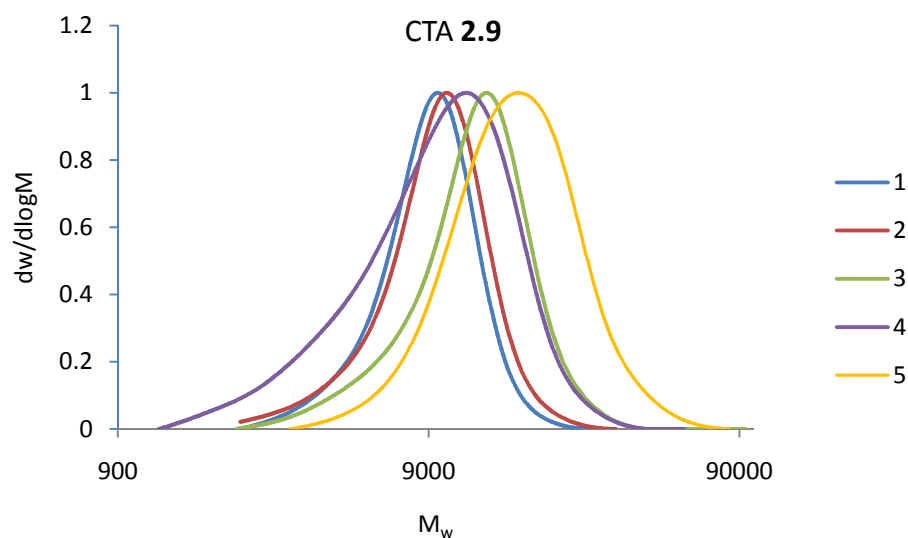


Figure 5.6: From left to right, SEC traces (RI) of the different PDMAEA samples using CTA 2.9 taken at 45, 90, 135, 195 and 255 minutes (Table 5.2).

The overlay of the SEC traces from the IR and UV detector at 309 indicates very good end group fidelity was achieved in both cases. Figure 5.7 also confirms **4.5** and **2.9** give polymers with very similar polydispersities, end group fidelity and molecular weights.

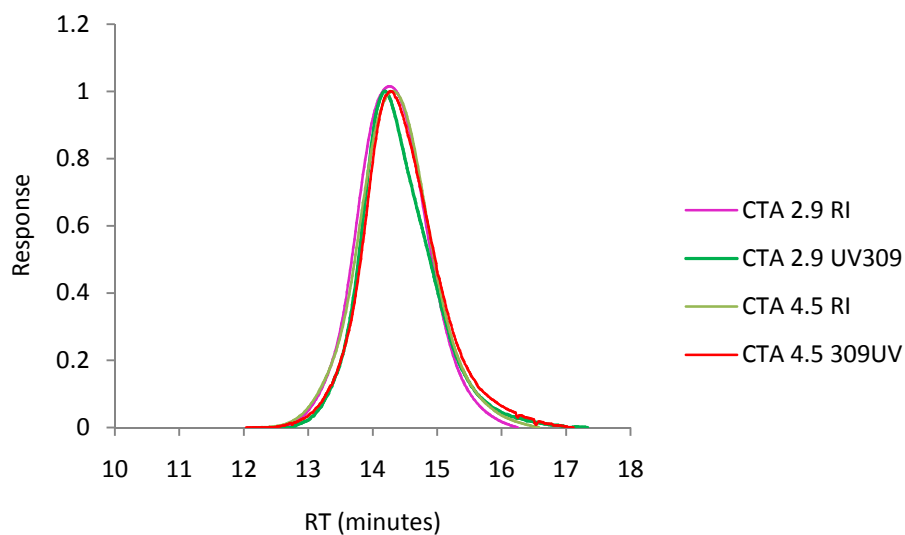


Figure 5.7: Overlay of UV<sub>309</sub> and RI normalized signals from the THF SEC analysis of PDMAEA using **4.5** and **2.9**.

The kinetics studies carried out provided evidence that both **4.5** and **2.9** can readily polymerize amine-containing polymers. Given this result, from now on both CTAs will be used depending on their availability.

### 5.3.2 Copolymerizations

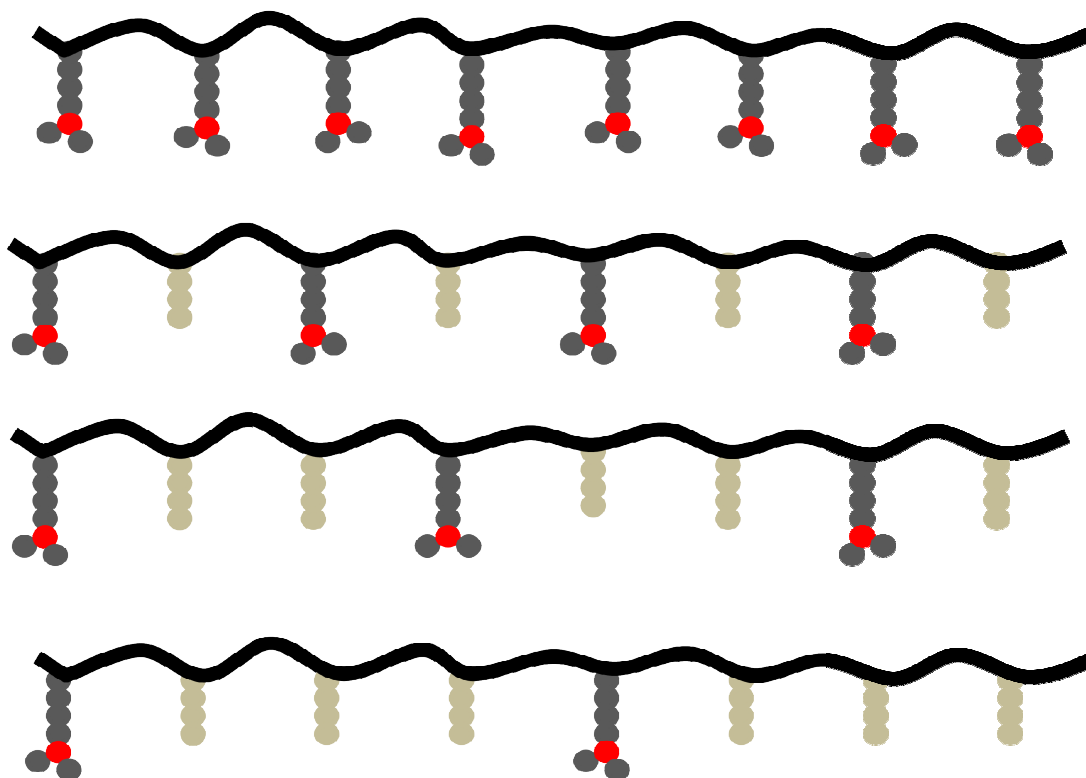


Figure 5.8: Schematic representation of separation between amino monomers prepared *via* a copolymerization route. (PDMAEA, and PDMAEA-*co*-MA at 75, 50 and 25% amine loading)

The monomer chosen for the copolymerization is commercially available methyl acrylate (MA, Figure 5.9).

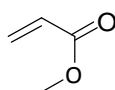
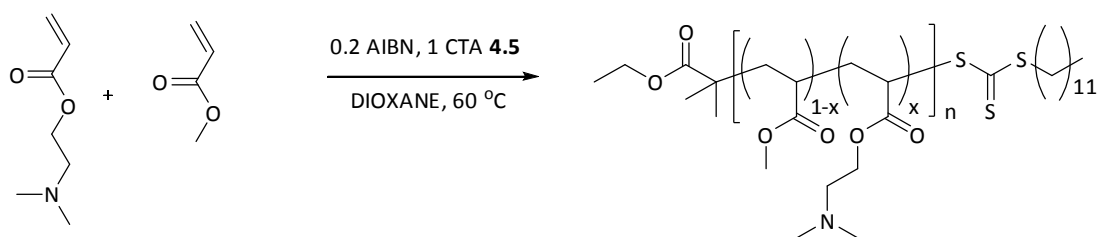


Figure 5.9: Structure of methyl acrylate (MA).

The choice of co-monomer is based on a number of different factors. Firstly, it must be chemically “inert” (no LCST or pH responsive properties) in order to avoid undesirable side interactions taking place in solution. Secondly, MA is a non-hindered acrylate with similar

structure to DMAEA, which should favor the copolymerization of both monomers at a similar rate, giving copolymers with homogeneous distribution of both monomers along the backbone. At the same time, the shorter alkane chain in the MA compared to DMAEA should minimize steric hindrance around the amino centers.

### 5.3.3 Copolymerization of DMAEA with MA



Scheme 5.2: General preparation of MA/DMAEA random copolymers with CTA **4.5**

Using the same conditions as reported for the homopolymerization of DMAEA (Scheme 5.2), five different copolymers were synthesized containing different loadings of amine functionality (DMAEA) from 5 to 75% (Table 5.3).

Polymer	DMAEA eq	%conv MA	%conv DMAEA	$M_w/M_n$	DP MA	DP DMAEA	x
<b>5.2</b>	5	93	96	1.17	62	4	<b>0.93</b>
<b>5.3</b>	10	92	91	1.18	80	10	<b>0.88</b>
<b>5.4</b>	25	82	89	1.19	104	38	<b>0.73</b>
<b>5.5</b>	50	80	80	1.28	50	50	<b>0.50</b>
<b>5.6</b>	75	78	78	1.26	22	77	<b>0.23</b>

Table 5.3: Data for the copolymerization of MA-*co*-DMAEA at different loadings using **4.5**. Conversions and DP calculated by  $^1\text{H}$  NMR in  $\text{CDCl}_3$ . Samples were measured by SEC (DMF) analysis using PMMA standards.



The conversion of the two monomers was determined by  $^1\text{H}$  NMR by comparing the signals from both monomers with the signals from the resultant polymer as demonstrated in Figure 5.10 for the copolymerization of MA with 25 % of DMAEA (**5.4**, Table 5.3).

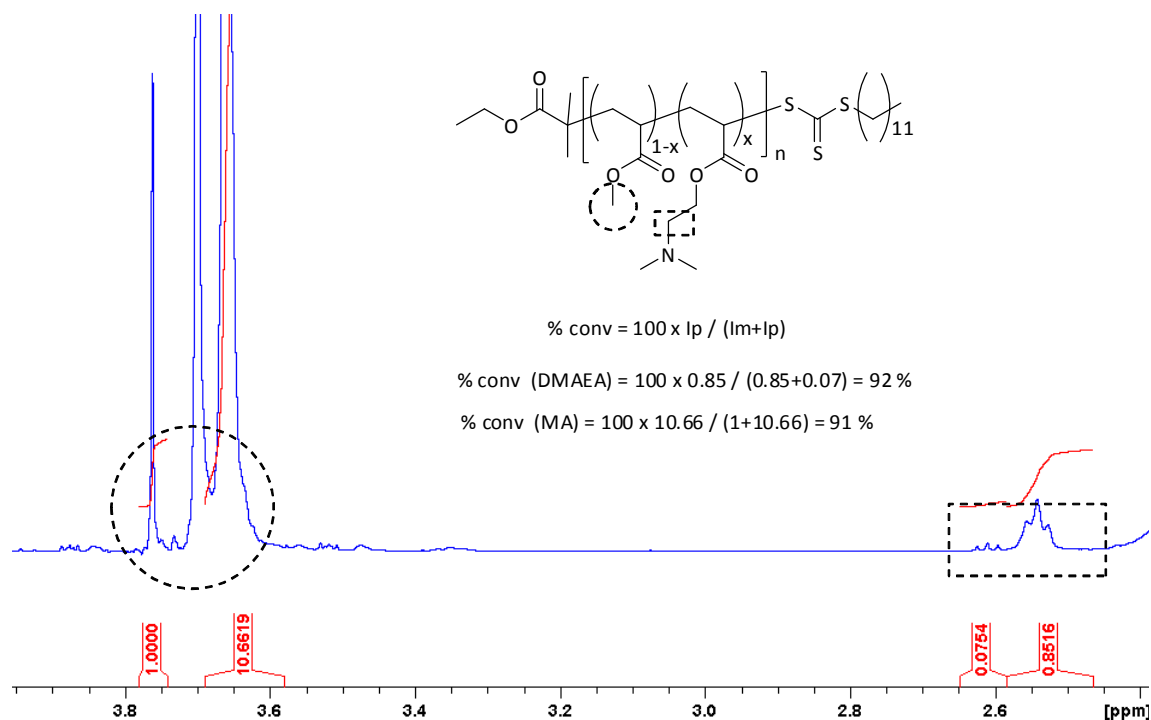
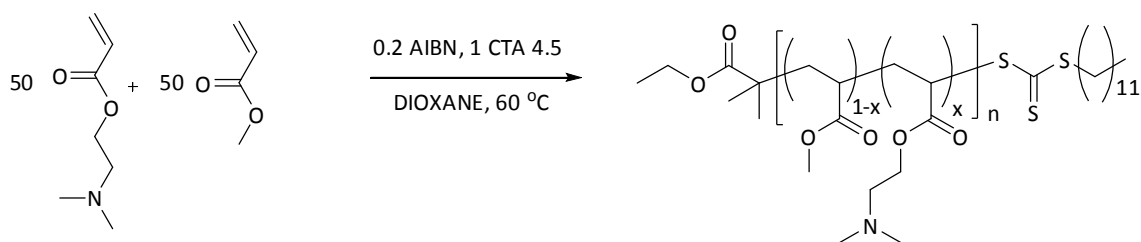


Figure 5.10: Example of a  $^1\text{H}$  NMR spectrum in  $\text{CDCl}_3$  used to calculate conversion for DMAEA/MA copolymerization. An example of the conversion calculations is shown for **5.4**, Table 5.3. ( $I_p$  = intensity polymer peak,  $I_m$  = intensity monomer peak)

The polymers were quenched and purified by precipitation in cold heptane after 4 hours of reaction giving the targeted polymers with controlled molecular weights and relatively narrow polydispersities. The polydispersity was observed to increase with increasing the DMAEA loading, due to increasing interactions of the amine functionalities with the SEC columns.

Scheme 5.3: Preparation of polymer **5.5** with CTA **4.5**

To study the copolymerization of DMAEA with MA by RAFT, kinetic studies of the copolymerization were carried out by taking aliquots from the reaction of 50 equivalents of DMAEA with 50 equivalents of MA in dioxane at different times, with the conversion of both monomers determined by  $^1\text{H}$  NMR spectroscopy.

<b>t(min)</b>	<b>%conv DMAEA</b>	<b>%conv MA</b>	<b><math>M_{n\text{NMR}}</math> kDa</b>	<b><math>M_w/M_n</math></b>
<b>60</b>	50	50	11.4	1.36
<b>120</b>	64	64	14.7	1.46
<b>180</b>	74	72	16.8	1.57
<b>240</b>	80	80	18.2	1.78

Table 5.4: Kinetic data of copolymerization of DMAEA with MA using CTA **4.5**. Polymerization carried out in dioxane. Ratio of  $[\text{DMAEA}]:[\text{MA}]:[\text{4.5}]$  50:50:1. Conversions calculated by  $^1\text{H}$  NMR in  $\text{CDCl}_3$ . THF SEC (PMMA standards)

The plot of  $\ln([M]_0/[M])$  versus polymerization time (Figure 5.11) highlights the similarity in rate of polymerization of the two monomers, as shown by the overlapping points in the kinetic plot. It should be noted that polydispersity values are higher than the previously reported ones due to the unavailability of the DMF SEC. Given the interactions of the amino motifs with the SEC columns, THF is a less ideal solvent.

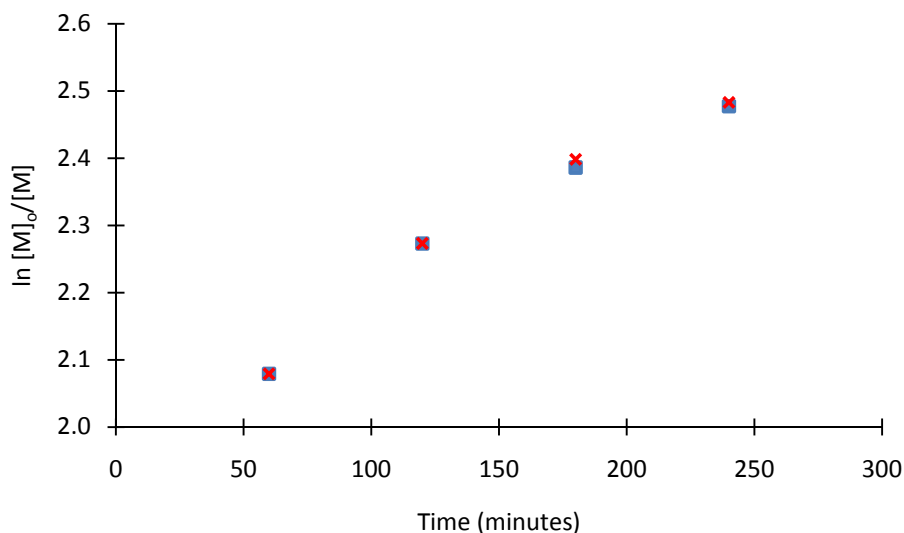
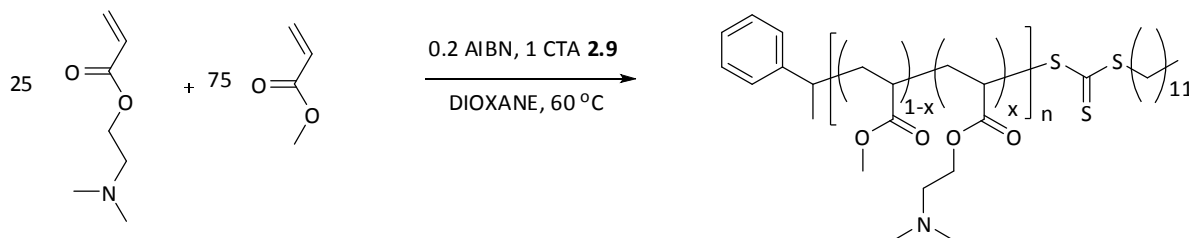


Figure 5.11: Kinetic data for the copolymerization at 1:1 ratio of DMAEA (X) with MA (■).

The copolymerization of 25 equivalents of DMAEA with 75 equivalents of MA was studied in detail using CTA **2.9**.



Scheme 5.4: Preparation of DMAEA-*co*-MA random copolymer with **2.9**.

Aliquots were taken at different times to calculate the conversion of the monomers as explained previously. The samples were dissolved in  $\text{CDCl}_3$  for the  $^1\text{H}$  NMR analysis and subsequently dried and then re-dissolved in THF for SEC analysis. Results are summarized in Table 5.5 and an example calculation of the incorporation of each monomer is illustrated in Figure 5.12.

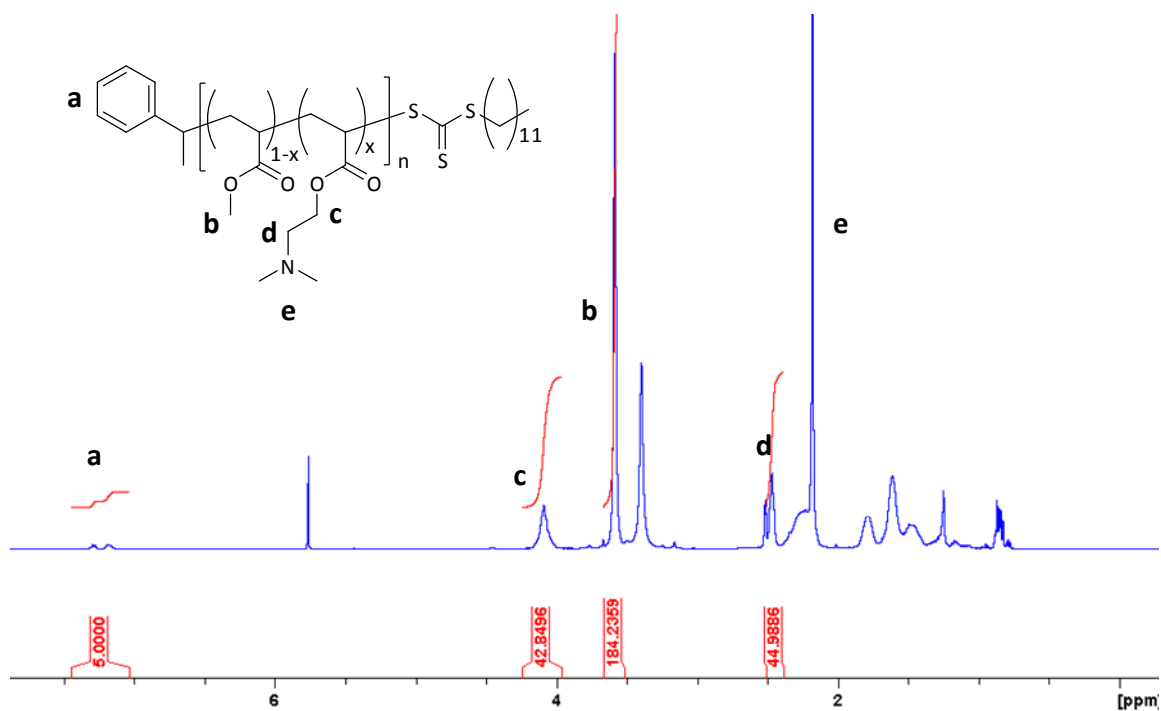


Figure 5.12: Example of a  $^1\text{H}$  NMR spectrum in  $d_6$ -DMSO used to assess conversion for MA/DMAEA

copolymerization (CTA **2.9**) showing a polymer with  $x = 0.25$  and  $n = 42 + (184/3) = 103$ .

$t(\text{min})$	%conv DMAEA	%conv MA	$M_{n\text{SEC}}$ kDa	$M_{n\text{NMR}}$ kDa	$M_w/M_n$
30	4	7	2.0	1.2	1.13
60	22	16	2.5	4.5	1.11
120	42	40	5.3	9.4	1.09
180	57	58	7.2	13.1	1.10
240	65	67	8.2	15.0	1.13
300	77	80	-	17.9	-

Table 5.5: Kinetic data of copolymerization of DMAEA with MA using **2.9**. Polymerization carried out in dioxane. Ratio of [DMAEA]: [MA]: [**2.9**] 25:75:1. Conversions calculated by  $^1\text{H}$  NMR in  $\text{CDCl}_3$

In order to confirm that a polymerization is controlled and pseudo-living, the plot of  $\ln([M]_0/[M])$  versus polymerization time should be linear, and the molecular weight of the growing polymer should increase linearly with conversion (Figure 5.13). The different values obtained for the theoretical  $M_n$  calculated by conversion ( $^1\text{H}$  NMR spectrometry) and the experimental  $M_n$  obtained by SEC analysis can be attributed to the use of PMMA standards to calibrate the SEC, which provides inaccurate estimation for the molecular weight of PDMAEA.

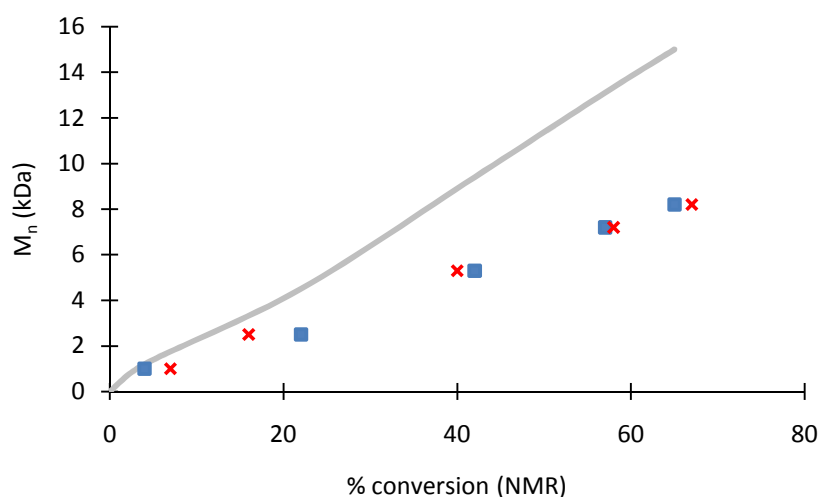


Figure 5.13: Plot of  $M_n$  from SEC data (DMAEA x, MA ■) versus conversion from  $^1\text{H}$  NMR spectroscopy (solid line) for the copolymerization of DMAEA-co-MA (25:75) with CTA **2.9**.

Figure 5.14 shows that this copolymerization possesses *pseudo*-living behavior and a constant radical concentration throughout the polymerization with a short induction period of around 15 minutes. In addition, this figure confirms that the rate of polymerization of DMAEA is very similar to that of MA.

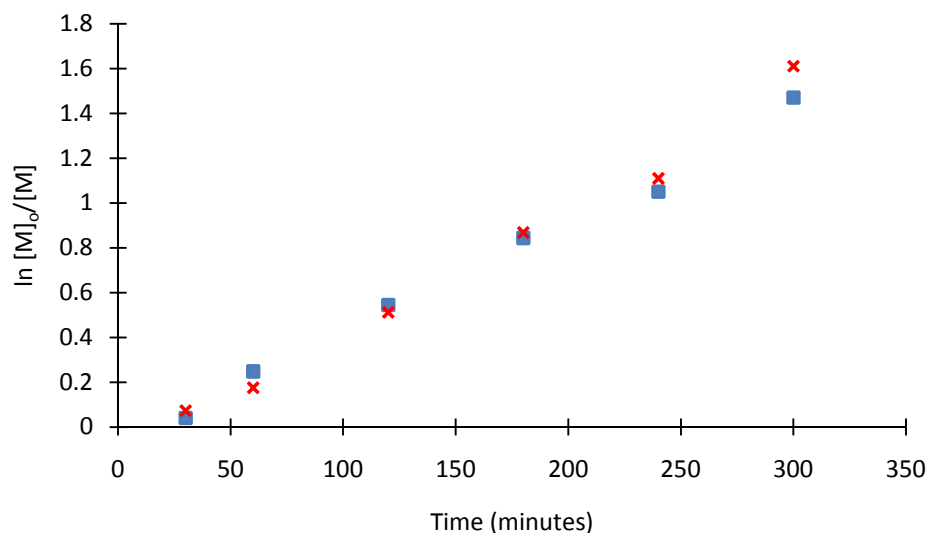
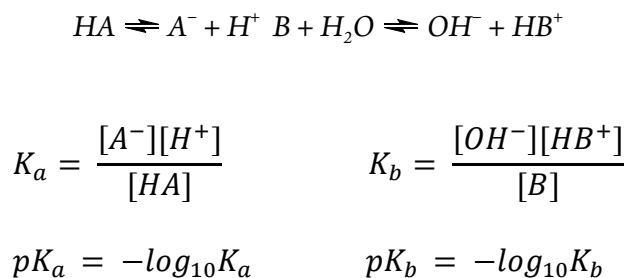


Figure 5.14: Kinetic data for the copolymerization of DMAEA-co-MA (25:75) with CTA **2.9** (DMAEA x, MA ■)

From the kinetic studies of the copolymerization of DMAEA with MA at different ratios and CTAs, it can be asserted that both monomers polymerize at very similar rates. Hence, random copolymers will be obtained with regular distribution of both monomers along the polymer backbone. To further confirm this, reactivity ratios should be calculated.<sup>16</sup>

#### 5.3.4 pH-responsive dilute solution behavior

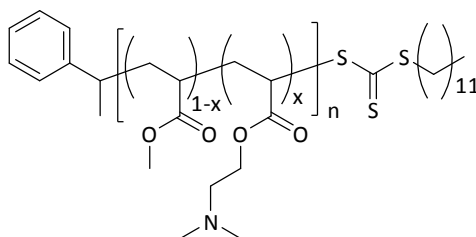
A characteristic property of polymers bearing tertiary amine motifs is the pH-responsive solution behavior attributed to the weak basicity of the amino group.<sup>2</sup> The acid dissociation constant,  $K_a$ , is a quantitative measure of the strength of an acid in solution. It is the equilibrium constant for the dissociation reaction in the context of acid-base reactions. The equilibrium can be written symbolically as shown in Scheme 5.5. HA represents a generic acid that dissociates into the conjugate base of the acid ( $A^-$ ), and the hydrogen ion or proton ( $H^+$ ). Due to the many orders of magnitude, a logarithmic measure of  $K_a$  is commonly used ( $pK_a$ ).



Scheme 5.5: Symbolic representation of the acid-base equilibrium.

The equilibrium constant  $K_b$  for a base can be defined as the association constant for protonation of the base, B, to form the conjugate acid,  $HB^+$  (Scheme 5.5).  $K_b$  is related to  $K_a$  for the conjugate acid. In water, the concentration of the hydroxide ion,  $[OH^-]$ , is related to the concentration of the hydrogen ion by  $K_w = [H^+][OH^-]$ . When  $K_a$ ,  $K_b$  and  $K_w$  are determined under the same temperature and ionic strength conditions,  $pK_b = pK_w - pK_a$ . In aqueous solutions, at 25 °C  $pK_w$  is 13.99, so  $pK_b \sim 14 - pK_a$ . In effect there is no need to define  $pK_b$  separately from  $pK_a$ , although  $pK_b$  values can be found in some of the older literature. The higher the value of  $pK_a$ , the lower the extent of dissociation. The stronger the base, the weaker the conjugated acid and the higher the  $pK_a$ .

In order to calculate the  $pK_a$  values, fresh aqueous solutions of the synthesized polymers were prepared using nanopure water. The polymers were synthesized as reported above using CTA **2.9** and the characterization data is reported in Table 5.6. The DMAEA homopolymer (**5.10**) and the random co-polymers containing *ca.* 75 and 50 % DMAEA dissolved spontaneously in non-buffered water ( $pH > 9$ ) while the copolymer containing 25 % DMAEA was insoluble at this pH. We propose this is due to the high loading of hydrophobic MA and the behavior of this polymer will not be further discussed herein.



Polymer	x	DP <sub>NMR</sub>	M <sub>nNMR</sub>	M <sub>w</sub> /M <sub>n</sub>	pK <sub>a</sub>
<b>5.7</b>	1	75	10.7	1.19	6.2
<b>5.8</b>	0.78	80	10.8	1.22	6.4
<b>5.9</b>	0.5	67	8.1	1.19	6.7
<b>DMAEA</b>	-	-	-	-	8.4

Table 5.6: Characterization data for the synthesized DMAEA/MA copolymers and DMAEA monomer.

The fresh solutions were titrated with HCl 0.1 M, using an automated titrator and the pK<sub>a</sub> values were determined from the second derivative of the titration curve as shown in Figure 5.15.<sup>21</sup> The pK<sub>a</sub> values obtained for the polymers are around 2 units lower than the pK<sub>a</sub> of the DMAEA monomer. This surprising but expected result can be explained by the fact that, in the absence of salt, the positive charges created upon protonation of some amine units makes the subsequent deprotonation of the other amine units more and more difficult as observed by Colombani *et al.* for polyacrylic acid.<sup>4</sup>



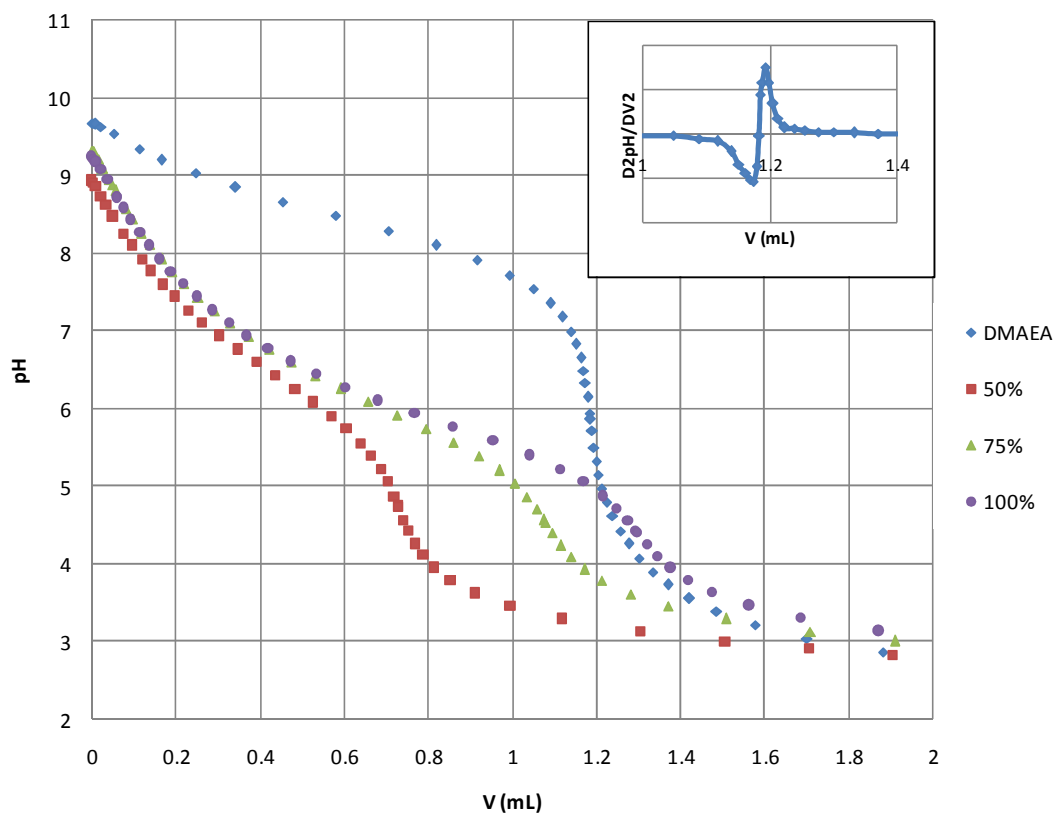


Figure 5.15: Titration curves for the DMAEA monomer and the three polymers **5.7**, **5.8** and **5.9** (Table 5.6).

Inset is the second derivative of the curve for DMAEA.

The titration of the DMAEA-MA copolymers shows that a decrease in amine loading ( $x$ , from *ca.* 100%, **5.7**, to 50%, **5.9**) resulted in an increase in the  $pK_a$  values (from 6.2 to 6.7). This behavior is expected based on the theory that these copolymers have reduced steric hindrance of protonated units due to the larger distance between the amino motifs and hence a higher  $pK_a$  value (Figure 5.16).

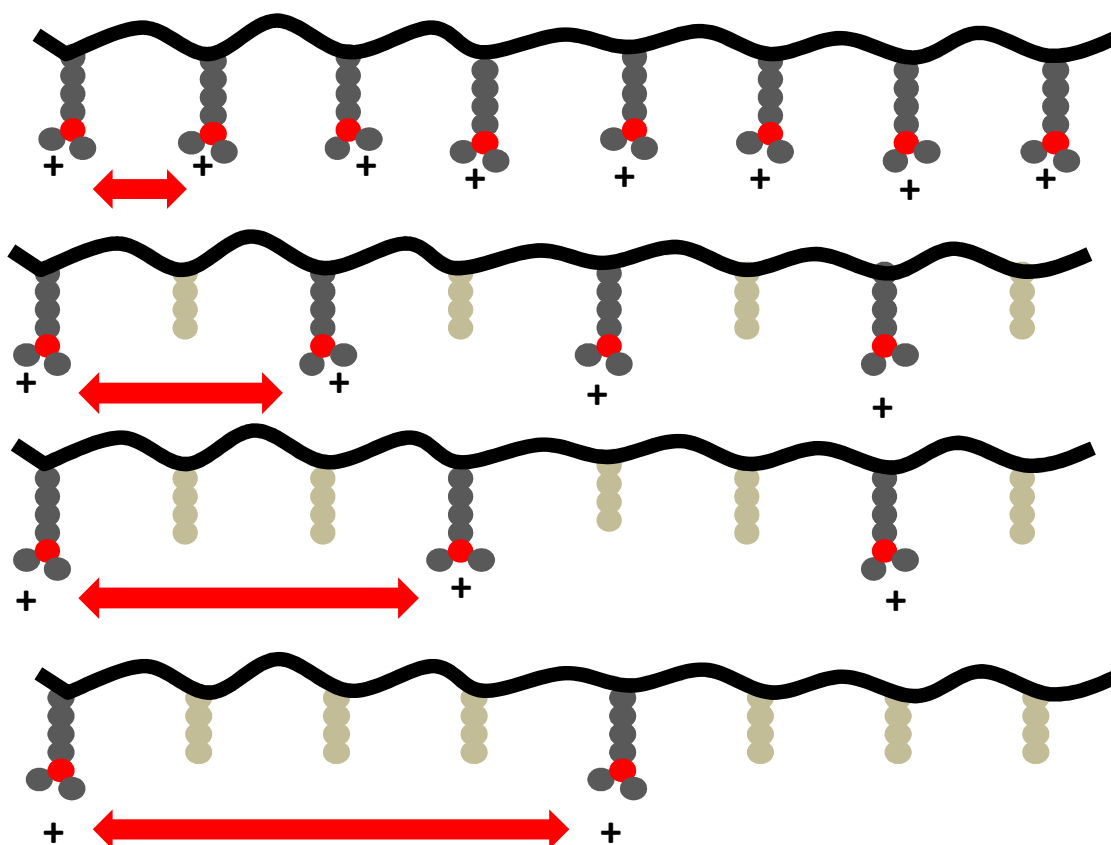


Figure 5.16: Schematic representation of the increasing distance between charges by the increased co-monomer incorporation.

These results are clear evidence that the acid-base properties of a polyelectrolyte can be tuned by introducing an inert monomer between the charges, facilitating the protonation (or deprotonation) of adjacent motifs by spacing out the already charges species.

### 5.3.5 Temperature responsive properties

The phase transition observed in thermosensitive polymers in aqueous solutions is attributed to a change in the hydrophilic-hydrophobic balance of the polymer with respect to the hydrogen bonding interaction between the polymer and water.<sup>22</sup> Therefore, increasing the hydrophobicity of the polymer should induce a decrease in its LCST. This behavior has been observed for copolymers of stimuli-responsive DMAEMA with the hydrophobic *n*-butyl

methacrylate.<sup>23</sup> The LCST of PDMAEMA has been reported to be around 30-37 °C;<sup>24</sup> as DMAEMA is the methacrylate version of DMAEA (more hydrophobic) a higher LCST is expected for the DMAEA homopolymer. Fresh solutions of the copolymers containing *ca.* 50 (**5.9**) and 75% DMAEA (**5.8**) as well as PDMAEA homopolymer (**5.7**) were prepared at different concentrations in nanopure water (from 0.5 to 2 mg/mL). All solutions contained the same amount of amine (in mass) in order to achieve the same pH = 9.1. Determination of the LCSTs was carried out by UV/vis spectroscopy at 500 nm where heating ramp was fixed to 1 °C/min (Figure 5.17).

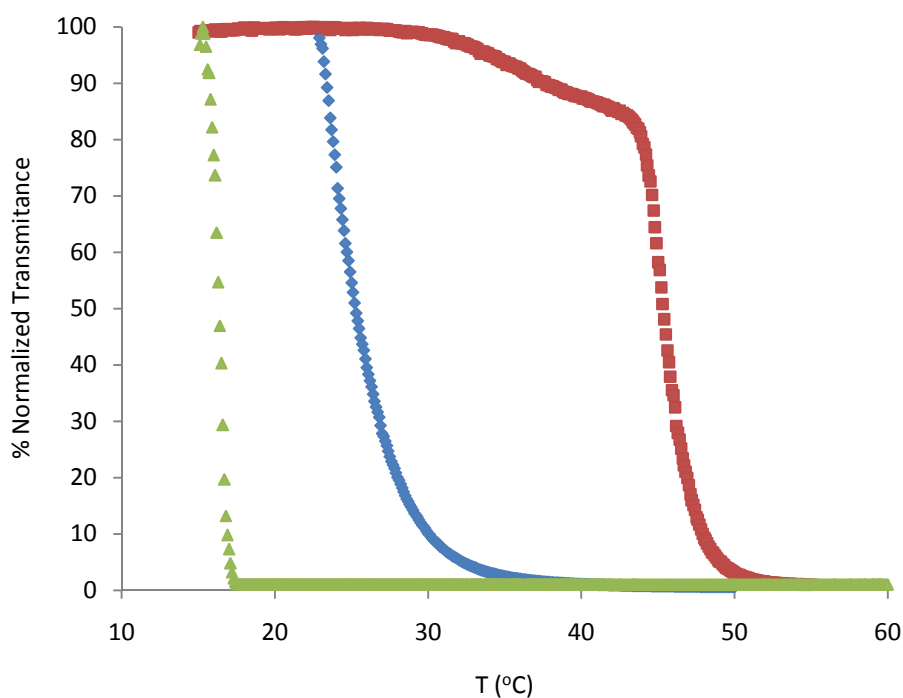


Figure 5.17: Phase transitions of the three polymers **5.7**(green), **5.8** (red) and **5.9** (blue) in nanopure water as measured by UV/vis spectroscopy at 500 nm (cloud points from left to right were determined as 16, 25 and 45 °C)

Contrary to our hypothesis, the presence of a less hydrophobic backbone (methacrylate to acrylate) induced a decrease in the LCST of PDMAEA compared to PDMAEMA (16 *versus ca.* 32 °C). On the other hand, as mentioned above, the incorporation of a hydrophobic comonomer is expected to induce a decrease in the LCST. However, in our case by increasing the amount of MA in the polymer, the LCST moves to higher temperatures (from 16 to 45 °C). This effect (the increase in LCST) has been reported for the copolymerization of the temperature responsive oligo(ethylene glycol) methacrylate with the hydrophilic methacrylic acid.<sup>11</sup> Moreover, it must be pointed out that the incorporation of 25 % of MA in the polymer chain increases LCST of the polymer by 29 °C compared to the homopolymer, while the incorporation of 50 % of the hydrophobic MA results in just a 9 °C increase.

In order to further understand these unexpected results, the LCST curves of the subsequent heat-cool cycles were investigated. Figure 5.18 a) and b) show the LCST behavior of PDMAEA **5.7** and the copolymer containing 25 % of MA **5.8**. In both cases it can be appreciated that the polymers do not present LCSTs after the first cycle, suggesting that the temperature responsive properties are not reversible. Graph c) (Figure 5.18) shows the LCSTs of the copolymer containing 50% DMAEA **5.9**. In this case different LCSTs are recorded in each heating cycle: 25, 18, 24, 33, 41 and 34 °C. Due to the unexpected results, the LCST measurements were repeated using a buffered solution at pH = 8 (tris(hydroxymethyl)aminomethane, TRIS). Since DMAEA is expected to be pH and temperature responsive, by keeping the pH constant we will obtain information only related to the temperature changes in the solution.

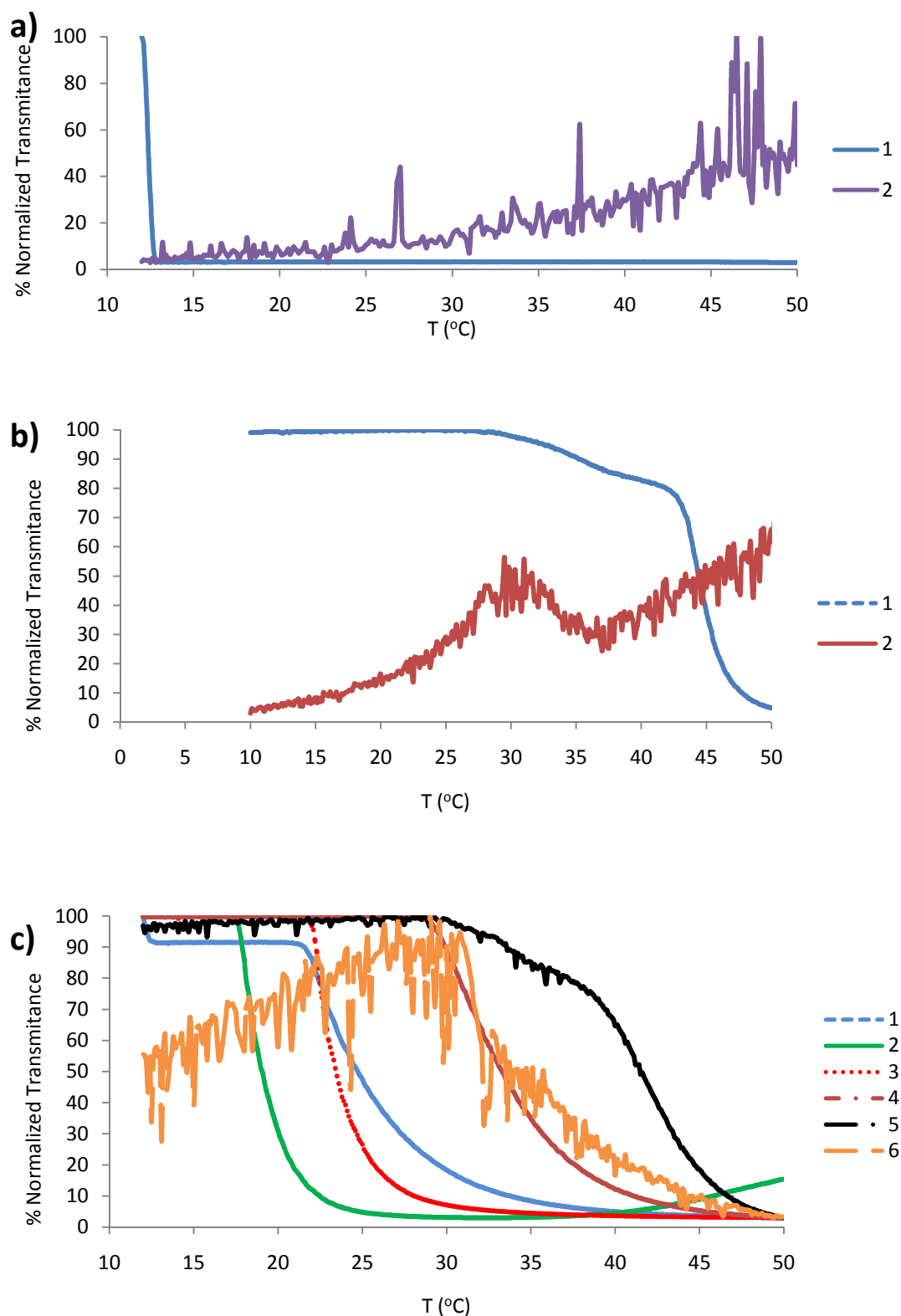


Figure 5.18: Different heating cycles showing the phase transitions of the three polymers a) 5.7, b) 5.8 and c) 5.9

in nanopure water as measured by UV/vis spectroscopy at 500 nm.

The polymers were dissolved in a buffered solution at pH 8 at the same concentrations as utilized above. By decreasing the pH (in non-buffered solution the pH was 9.1), the degree of protonation is increased and hence the LCST of the polymers should move to higher temperatures (Figure 5.19). Again, unexpected results were observed, showing no LCST behavior for any of the polymers, independent of the amine loading at this pH.

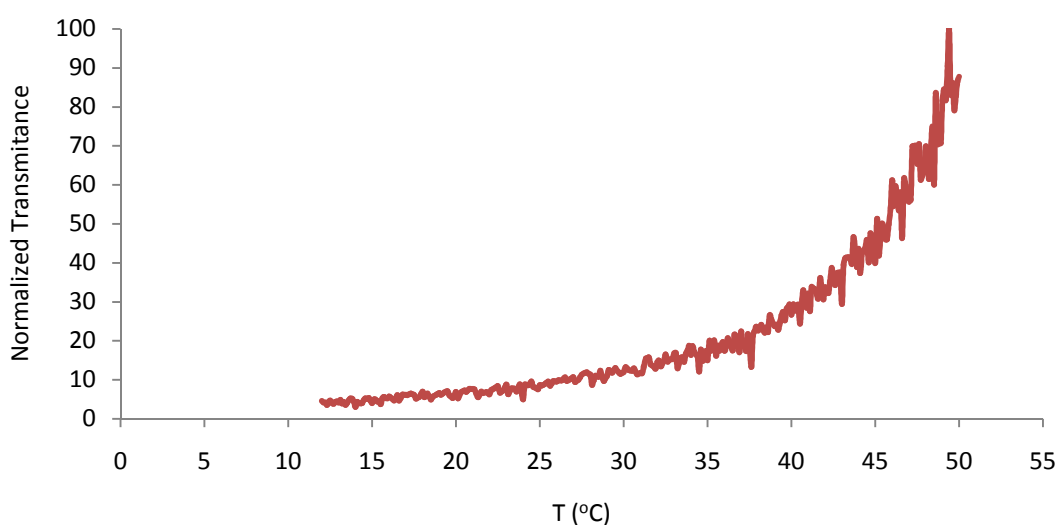


Figure 5.19: Example of the first heating cycle of polymer **5.9** in buffered solution (pH = 8) showing the absence of an LCST.

Given this inexplicable trend in LCST behavior, the samples were freeze dried after the LCST measurements, dissolved in D<sub>2</sub>O and analyzed by <sup>1</sup>H NMR spectroscopy. As shown in Figure 5.20 for polymer **5.7**, some new sharp peaks appeared at *ca.* 3.7, 2.8 and 2.5 ppm, which gave clear evidence of some alteration in the polymer structure following the heating cycles used for the LCST measurements.

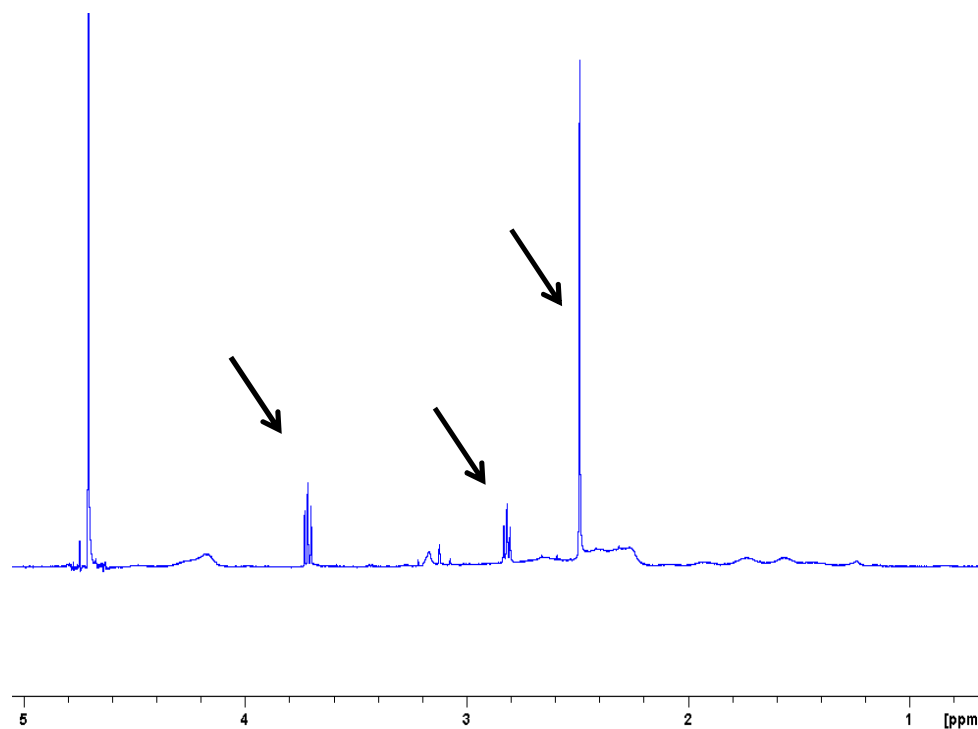
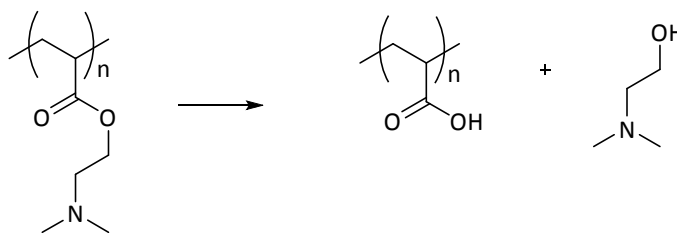


Figure 5.20:  $^1\text{H}$  NMR spectrum in  $\text{D}_2\text{O}$  of polymer **5.7** after the measurement of LCST (after 3 cooling/heating cycles).

### 5.3.6 Self-catalyzed hydrolysis in water<sup>25</sup>

The sharpness of the signals observed in the  $^1\text{H}$  NMR spectrum of PDMAEA **5.7** and the irreproducible LCST results suggested it was possible that the ester bond had been hydrolyzed. Indeed, a few reports in literature can be found describing the self hydrolysis of PDMAEA in aqueous environment giving polyacrylic acid and *N,N*-dimethylethanolamine (Scheme 5.6).<sup>25,26</sup> The rate of hydrolysis is reported to be very slow at room temperature (*ca.* 5% after 1 hour) and independent of the solution pH or the molecular weight of the polymer.



Scheme 5.6: Schematic representation of the hydrolysis of PDMAEA giving polyacrylic acid and *N,N*-dimethylethanolamine.

However, to our knowledge there are no reports on how the self-hydrolysis of PDMAEA can be affected by changes in temperature and/or concentration. These two parameters are key in order to explain our non reproducible LCST results; therefore we decided to investigate how temperature and concentration affect the rate of hydrolysis.

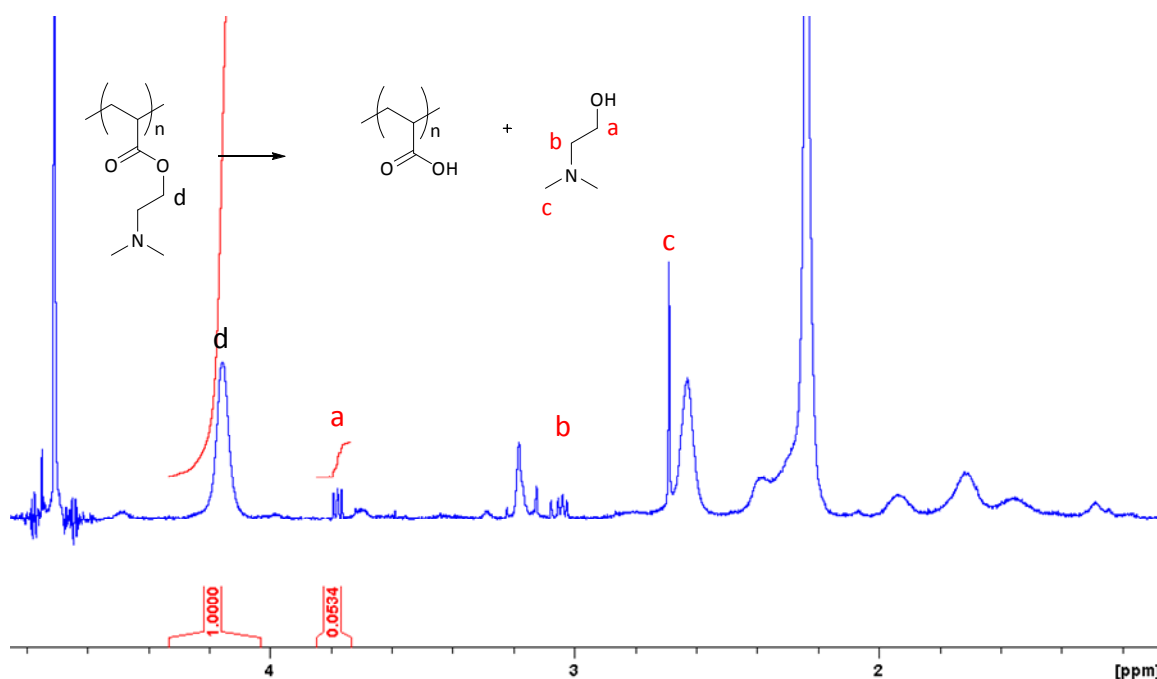


Figure 5.21:  $^1\text{H}$  NMR spectrum in  $\text{D}_2\text{O}$  showing PDMAEA degradation of 5 %.

Studies by Monteiro and co-workers report PDMAEA degradation rates at room temperature at concentrations of 30 mg/mL.<sup>25</sup> In their studies, 30% of the polymer is hydrolyzed to PAA at



room temperature in 24 hours and *ca.* 60 % after 150 hours, calculated by  $^1\text{H}$  NMR spectrometry in  $\text{D}_2\text{O}$  by comparing the integration of the PDMAEA peaks at 4.16 ppm to that for the *N,N*-dimethylethanolamine at 3.79 ppm (Figure 5.21).

Since our LCST measurements are taken at a concentration of 10 mg/mL, the kinetics of the reaction by  $^1\text{H}$  NMR spectroscopy was investigated at this concentration in order to evaluate how the concentration influences the rate of degradation (Figure 5.22).

The analysis of the  $^1\text{H}$  NMR spectrum by integration of the signals as shown in Figure 5.21 indicates that the rate of degradation is independent of concentration. Degradation studies were carried out with a solution of PDMAEA **5.7** at a concentration of 2 mg/mL confirms this hypothesis (Figure 5.23).

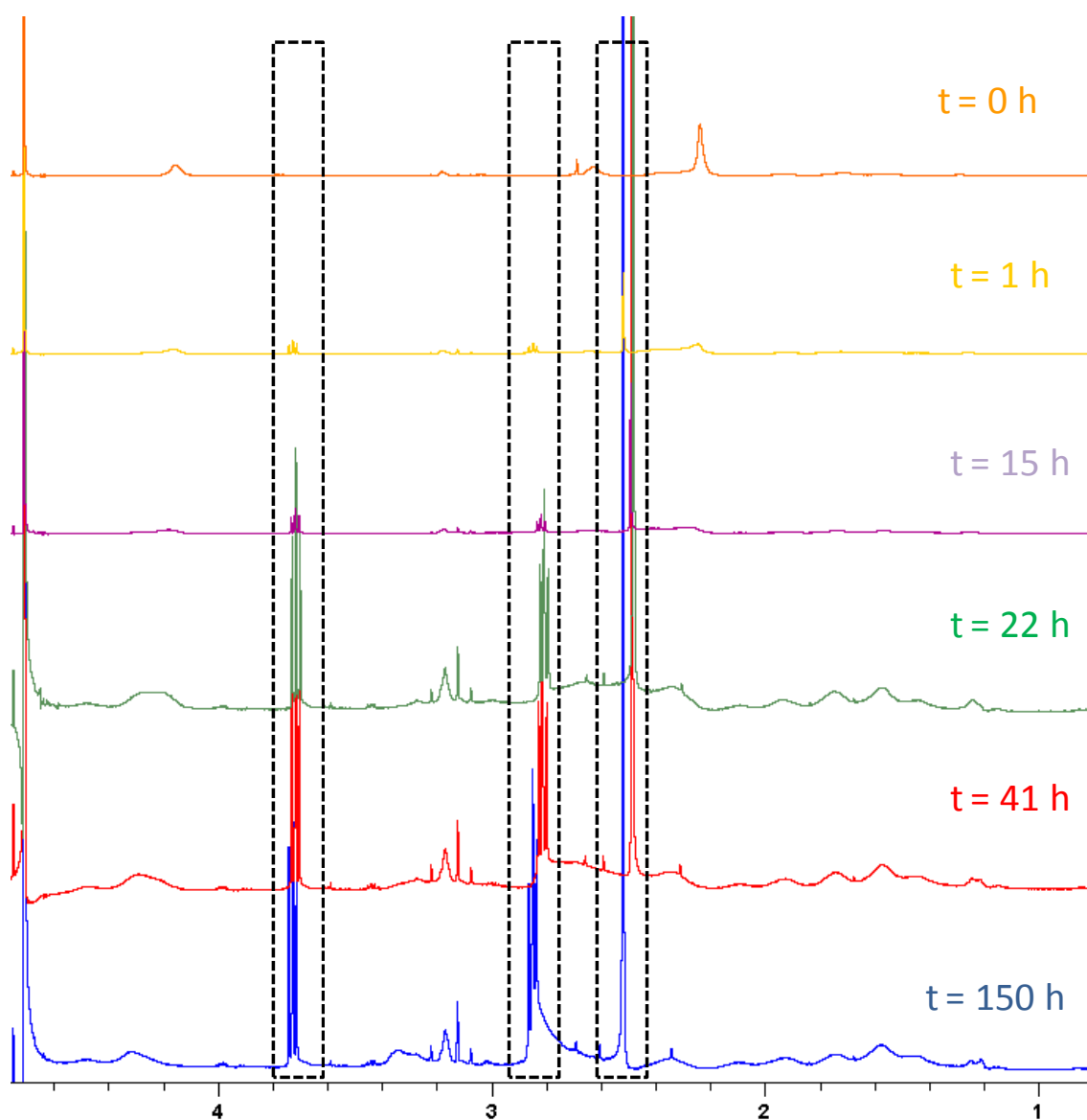


Figure S.22:  $^1\text{H}$  NMR spectrum in  $\text{D}_2\text{O}$  showing the degradation of a 10 mg/mL solution of PDMAEA at room temperature.

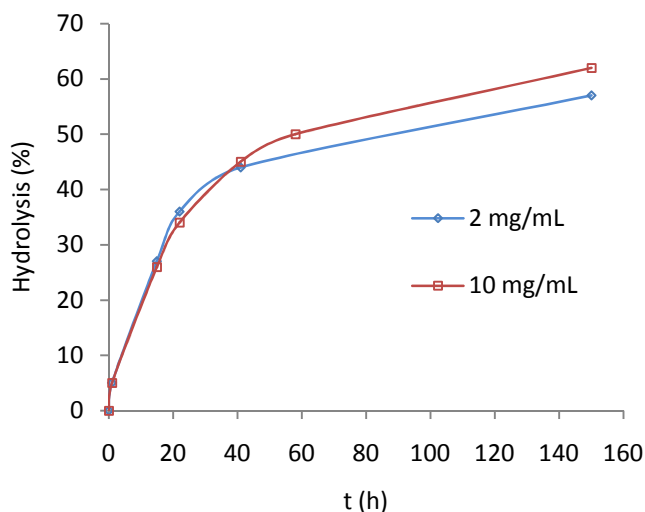


Figure 5.23: Hydrolysis kinetics of PDMAEA at different concentrations.

During the LCST measurements, the temperature is ramped from 10 °C to 60 °C at 1 °C/minute in consecutive heating/cooling cycles. These conditions were reproduced during the  $^1\text{H}$  NMR measurements by heating and cooling the sample in *ca.* 1 hour cycles. Since the polymers containing different incorporations of MA along the backbone have given different results in the  $\text{pK}_a$  measurements, the behavior of polymers **5.7**, **5.8**, and **5.9** was investigated at the same temperature range as LCST measurements. This was done in order to study how the rate of hydrolysis is affected by the distance between amino motifs. The  $^1\text{H}$  NMR studies for the degradation of polymers containing *ca.* 50, 75 and 100% DMAEA (polymers **5.9**, **5.8** and **5.7** respectively) reveal that there is no influence on the spacing of the amino motifs on the degradation of the polymer (Figure 5.24). The small difference observed between the different polymers after 3 consecutive cooling/heating cycles is not significant and can be attributed to the method of calculation of the percentage of hydrolysis.

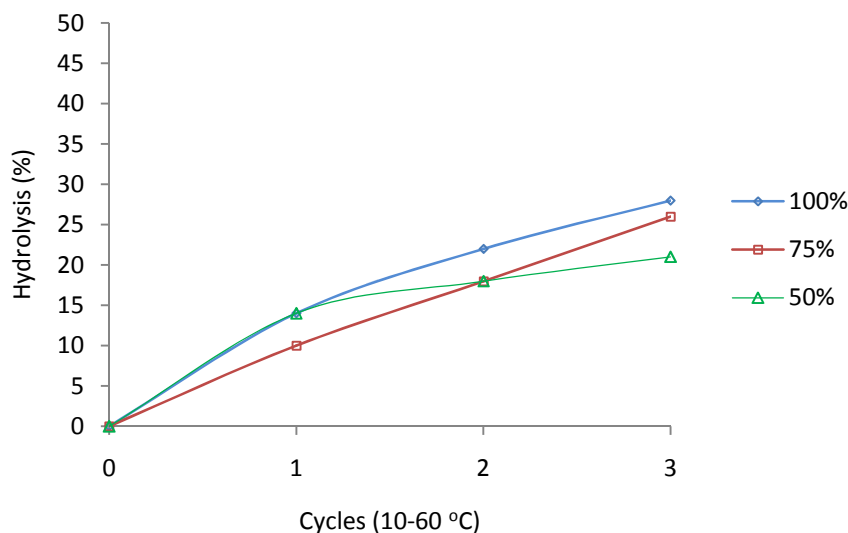


Figure 5.24: Hydrolysis kinetics of polymers 5.7, 5.8 and 5.9 through 3 heating/cooling cycles.

Due to its auto-degradable character, PDMAEA could be used as a “single LCST” or “non-reversible LCST” polymer. Indeed, Monteiro and co-workers have reported the use of PDMAEA as a delivery carrier suitable for DNA or siRNA using its ability to auto-degradable and its low toxicity.<sup>25</sup>

We propose that PDMAEA could be use as a novel protected version of polyacrylic acid. With the exception of RAFT, no other CRP technique can directly polymerize acrylic acid (AA).<sup>27,28</sup> Moreover, PAA characterization (especially by SEC) is an overall challenge due to of its polyelectrolyte character. Therefore, protected monomers are often used for the preparation of well-defined polymers by CRPs to achieve fully characterized polymers.<sup>29-31</sup> Typical examples of protected molecules used as masked acrylic acid monomers are tert-butyl acrylate (t-BuA),<sup>32,33</sup> tert-butyl methacrylate (t-BuMA),<sup>34</sup> trimethylsilyl methacrylate (TMSMA),<sup>35</sup> 2-tetrahydropyranyl methacrylate (THPMA),<sup>36</sup> p-nitrophenyl methacrylate (*p*-NPMA)<sup>37</sup> as well as *N*-(acryloyloxy)succinimide (NAS)<sup>38</sup> and tetrahydropyranyl acrylate (THPA).<sup>39</sup> The

deprotection of these monomers are generally carried out *via* hydrolysis under acidic/thermal conditions.<sup>40</sup>

The fact that this polymer self-hydrolyzes in the presence of water without the need of any additives, at any pH or concentration, makes it extremely suitable when its deprotection is desired in the presence of other functionalities susceptible to hydrolysis. In order to achieve a complete hydrolysis in a short period of time, the polymer in aqueous solution can be heated at 60 °C, achieving a full deprotection in less than 2 hours.

#### 5.4 Conclusions

Four different polymers and MA copolymers containing different incorporations of DMAEA have been synthesized by RAFT with good control. The pH responsiveness of these polymers has been evaluated by  $pK_a$  measurements. The results indicate that, by spacing out the amino motifs with a non-responsive co-monomer, the  $pK_a$  of the copolymers can be increased which can be explained by the larger distance between charges facilitating the protonation of adjacent nitrogens.

The methacrylate version of DMAEA, DMAEMA has been extensively reported as it forms water soluble polymers with various interesting properties as mentioned in the introduction to this chapter. For this reason, PDMAEA was expected to present similar properties to those reported for PDMAEMA such as temperature responsiveness. However, PDMAEA self-catalyzes the hydrolysis of the ester bond at any given pH or concentration, which give this polymer some unique potential applications compared to its more popular methacrylate counterpart.

## 5.5 Experimental

### 5.5.1 Materials

Monomers were filtered through a plug of silica prior to use and stored at 4 °C. AIBN (2,2'-azobis(isobutyronitrile)) was recrystallized from ethyl acetate and stored at 4 °C. All other materials were used as received from Aldrich, Fluka, and Acros.

### 5.5.2 Instrumentation:

$^1\text{H}$  NMR and  $^{13}\text{C}$  NMR spectra were recorded with a Bruker DPX-300 spectrometer in  $\text{CDCl}_3$  unless otherwise specified. Long acquisition  $^1\text{H}$  and  $^{13}\text{C}$  NMR spectra were recorded on a Bruker DPX-400 spectrometer at different temperatures (128 scans). Size exclusion chromatography (SEC) measurements were performed with HPLC grade solvents (Fisher), tetrahydrofuran (with 2 % of TEA) at 30 °C or DMF (1.06 g LiCl per litre) at 40 °C as an eluent at a flow rate of 1 mL/min. The molecular weights of polymers were calculated relative to polystyrene or PMMA standards. Lower critical solution temperature (LCST) measurements were analyzed using a Perkin-Elmer UV/vis Spectrometer (Lambda 35) equipped with a Peltier temperature controller at 500 nm with a heating/cooling rate of 1 °C/min.

### 5.5.3 Hydrogen ion titration

40 mL of solution was used for each potentiometric titration experiment. Potentiometric titration was performed at room temperature with an automatic titrator (Mettler Toledo G20) controlled by LabX software. To determine the  $\text{pK}_a$  values of the both the amine polymers and monomers a 10 mg/mL solution of the respective monomer or

polymer was titrated using 0.1 M HCl solution. Raw data given is plotted to produce pH against titrant volume. The second derivative is calculated using the equation;

$$\text{Second derivative} = \Delta (\Delta \text{pH} / \Delta V) / \Delta V$$

For each data point the second derivative was calculated, this was then plotted against titrant volume and  $\text{pK}_a$  is taken at the pH value that where the second derivative is equal to zero.

#### 5.5.4 General procedure for homopolymerization of DMAEA:

100 equivalents of DMAEA, 0.2 equivalents of AIBN and 1 equivalent of CTA (**2.9** or **4.5**) were dissolved in dioxane or toluene and heated at 80 or 65 °C after 3 freeze-pump-thaw cycles to remove oxygen. After a time, an aliquot was taken to calculate the conversion by  $^1\text{H}$  NMR in  $\text{CDCl}_3$ . The polymer was purified by precipitation in cold heptane, re-dissolved in DCM and re-precipitated 3 times. The viscous yellow polymer was dried overnight in a vacuum oven at 40 °C and analyzed by long acquisition  $^1\text{H}$  NMR in  $\text{CDCl}_3$  and THF SEC or DMF SEC using PMMA standards.  $^1\text{H}$  NMR (400 MHz,  $\text{CDCl}_3$ ):  $\delta$  (ppm) 4.08 (br t, 2H,  $\text{OCH}_2\text{CH}_2\text{N}$ ), 2.47 (br t, 2H,  $\text{OCH}_2\text{CH}_2\text{N}$ ), 2.20 (br s, 6H,  $\text{CH}_3\text{N}$ ), 1.19 (s, 12H, end group), 1.00-2.00 (br m, backbone) 0.85 (t, 3H end group).

(See text for molecular weight data)

#### 5.5.5 General procedure for copolymerization of MA with DMAEA

A solution of 100 equivalents of a combination of the 2 monomers (MA= x, DMAEA = 100-x), 0.2 equivalents of AIBN and 1 equivalent of CTA in dioxane (1:3 volume compare to monomer) were added to a dry ampoule containing a stirrer bar. The solution was degassed using at least 3 freeze-pump-thaw cycles (until no oxygen bubbles were seen), back filled with

nitrogen gas, sealed and placed in a pre-heated oil bath at the required temperature. After a certain amount of time, an aliquot was removed for  $^1\text{H}$  NMR analysis in  $\text{CDCl}_3$  to determine the conversion. The polymerization is quenched by adding a small amount of DCM and precipitated dropwise into stirred cold solvent to give liquid/viscous polymer. The solvent was decanted and the polymer was dissolved in the minimum amount of DCM and precipitated again. After 2 or 3 precipitations, the DCM was removed in the rotary evaporator and the resultant polymer was dried in a vacuum oven at  $40\text{ }^\circ\text{C}$  overnight. Molecular weights and polydispersity indices were measured by DMF or THF SEC measurements using PMMA as narrow standards and  $^1\text{H}$  NMR spectroscopy in  $\text{CDCl}_3$  was used for the determination of polymerization conversion, using a crude sample of the polymerization reaction mixture before workup by careful integration of polymer peak to monomer signals. Long acquisition  $^1\text{H}$  NMR spectroscopy in  $\text{CDCl}_3$  was used for the determination of end group functionality and molecular weight by careful integration of the polymer backbone and characteristic functional monomer peaks to the end group signals.

$^1\text{H}$  NMR (400 MHz,  $\text{CDCl}_3$ ):  $\delta$  (ppm) 4.08 (br t, 2H,  $\text{OCH}_2\text{CH}_2\text{N}$ ), 3.66 (br s, 3H,  $\text{CH}_3\text{O}$ ), 2.47 (br t, 2H,  $\text{OCH}_2\text{CH}_2\text{N}$ ), 2.20 (br s, 6H,  $\text{CH}_3\text{N}$ ), 1.19 (s, 12H, end group), 1.00-2.00 (br m, backbone) 0.85 (t, 3H end group).

(See text for molecular weight data)



## 5.6 References

- (1) Lee, H.; Son, S. H.; Sharma, R.; Won, Y.-Y. *J. Phys. Chem. B* **2011**, *115*, 844.
- (2) Bütün, V.; Armes, S. P.; Billingham, N. C. *Polymer* **2001**, *42*, 5993.
- (3) Samal, S. K.; Dash, M.; Van Vlierberghe, S.; Kaplan, D. L.; Chiellini, E.; van Blitterswijk, C.; Moroni, L.; Dubruel, P. *Chem. Soc. Rev.* **2012**.
- (4) Colombani, O.; Ruppel, M.; Schubert, F.; Zettl, H.; Pergushov, D. V.; Müller, A. H. E. *Macromolecules* **2007**, *40*, 4338.
- (5) van Steenis, J. H.; van Maarseveen, E. M.; Verbaan, F. J.; Verrijk, R.; Crommelin, D. J. A.; Storm, G.; Hennink, W. E. *J. Control. Release* **2003**, *87*, 167.
- (6) Yancheva, E.; Paneva, D.; Danchev, D.; Mespouille, L.; Dubois, P.; Manolova, N.; Rashkov, I. *Macromol. Biosci.* **2007**, *7*, 940.
- (7) Karanikolopoulos, N.; Zamurovic, M.; Pitsikalis, M.; Hadjichristidis, N. *Biomacromolecules* **2009**, *11*, 430.
- (8) Liu, S. Y.; Weaver, J. V. M.; Tang, Y. Q.; Billingham, N. C.; Armes, S. P.; Tribe, K. *Macromolecules* **2002**, *35*, 6121.
- (9) Dincer, S.; Turk, M.; Piskin, E. *Gene Ther.* **2005**, *12*, 139.
- (10) Zhang, X.; Xia, J.; Matyjaszewski, K. *Macromolecules* **1998**, *31*, 5167.

- (11) Becer, C. R.; Hahn, S.; Fijten, M. W. M.; Thijs, H. M. L.; Hoogenboom, R.; Schubert, U. S. *J. Polym. Sci., Part A: Polym. Chem.* **2008**, *46*, 7138.
- (12) Hoogenboom, R.; Schubert, U. S.; Van Camp, W.; Du Prez, F. E. *Macromolecules* **2005**, *38*, 7653.
- (13) Sahnoun, M.; Charreyre, M.-T.; Veron, L.; Delair, T.; D'Agosto, F. *J. Polym. Sci., Part A: Polym. Chem.* **2005**, *43*, 3551.
- (14) Mori, H.; Iwaya, H.; Nagai, A.; Endo, T. *Chem. Commun.* **2005**, 4872.
- (15) Creutz, S.; Teyssié, P.; Jérôme, R. *Macromolecules* **1997**, *30*, 6.
- (16) Fournier, D.; Hoogenboom, R.; Thijs, H. M. L.; Paulus, R. M.; Schubert, U. S. *Macromolecules* **2007**, *40*, 915.
- (17) Du, J.; O'Reilly, R. K. *Macromol. Chem. Phys.* **2010**, *211*, 1530.
- (18) Zhong, M.; Matyjaszewski, K. *Macromolecules* **2011**,
- (19) Rowe, M. D.; Chang, C.-C.; Thamm, D. H.; Kraft, S. L.; Harmon, J. F.; Vogt, A. P.; Sumerlin, B. S.; Boyes, S. G. *Langmuir* **2009**, *25*, 9487.
- (20) Lowe, A. B.; McCormick, C. L. *Prog. Polym. Sci.* **2007**, *32*, 283.
- (21) Qiang, Z.; Adams, C. *Water Res.* **2004**, *38*, 2874.
- (22) Liu, R.; Fraylich, M.; Saunders, B. *Colloid Polym. Sci.* **2009**, *287*, 627.
- (23) Lee, S. B.; Russell, A. J.; Matyjaszewski, K. *Biomacromolecules* **2003**, *4*, 1386.

- (24)Plamper, F. A.; Ruppel, M.; Schmalz, A.; Borisov, O.; Ballauff, M.; Müller, A. H. E. *Macromolecules* **2007**, *40*, 8361.
- (25)Truong, N. P.; Jia, Z.; Burges, M.; McMillan, N. A. J.; Monteiro, M. J. *Biomacromolecules* **2011**, *12*, 1876.
- (26)McCool, M. B.; Senogles, E. *Eur. Polym. J.* **1989**, *25*, 857.
- (27)Mori, H.; Müller, A. H. E. *Prog. Polym. Sci.* **2003**, *28*, 1403.
- (28)Chiefari, J.; Chong, Y. K.; Ercole, F.; Krstina, J.; Jeffery, J.; Le, T. P. T.; Mayadunne, R. T. A.; Meijs, G. F.; Moad, C. L.; Moad, G.; Rizzardo, E.; Thang, S. H. *Macromolecules* **1998**, *31*, 5559.
- (29)Davis, K. A.; Matyjaszewski, K. *Macromolecules* **2000**, *33*, 4039.
- (30)Davis, K. A.; Charleux, B.; Matyjaszewski, K. *J. Polym. Sci., Part A: Polym. Chem.* **2000**, *38*, 2274.
- (31)Hawker, C. J.; Bosman, A. W.; Harth, E. *Chem. Rev.* **2001**, *101*, 3661.
- (32)Zhang, L.; Shen, H.; Eisenberg, A. *Macromolecules* **1997**, *30*, 1001.
- (33)Burguière, C.; Pascual, S.; Bui, C.; Vairon, J.-P.; Charleux, B.; Davis, K. A.; Matyjaszewski, K.; Bétremieux, I. *Macromolecules* **2001**, *34*, 4439.
- (34)Lowe, A. B.; Billingham, N. C.; Armes, S. P. *Macromolecules* **1998**, *31*, 5991.
- (35)Sanji, T.; Nakatsuka, Y.; Kitayama, F.; Sakurai, H. *Chem. Commun.* **1999**, 2201.

- (36) Lu, S.; Fan, Q.-L.; Liu, S.-Y.; Chua, S.-J.; Huang, W. *Macromolecules* **2002**, 35, 9875.
- (37) Liu, Y.; Wang, L.; Pan, C. *Macromolecules* **1999**, 32, 8301.
- (38) Samarajeewa, S.; Shrestha, R.; Li, Y.; Wooley, K. L. *J. Am. Chem. Soc.* **2012**, 134, 1235.
- (39) Bütün, V.; Vamvakaki, M.; Billingham, N. C.; Armes, S. P. *Polymer* **2000**, 41, 3173.
- (40) Patrickios, C. S.; Hertler, W. R.; Abbott, N. L.; Hatton, T. A. *Macromolecules* **1994**, 27, 2364.

## Conclusions

Although supported catalysis has been a popular subject for many years, the study of polymeric nanostructures in order to catalyze organic reactions has received increasing interest in the last decade and is still in an early stage. However, the recent advances in CRP techniques may provide a very versatile route to synthesize well defined functional structures and hence facilitate further research in this area. Indeed, responsive properties and functionalities can now be introduced in the nanoreactors without the need of protecting groups or stringent conditions. By tethering the catalysts into a polymeric support the catalyst can be easily recovered but, moreover, the protected and confined environment provided by the polymeric nanoreactor can act as a yocto-litre reaction vessel concentrating reactants into the core in a confined environment where solvophobic products can be protected from degradation, the solubility of the catalyst can be modified and the rate of reaction can be enhanced compared to that for homogeneous systems.

The field of nanoreactors will benefit by further advances in the field of polymer synthesis which in turn will give access to nanoreactors with higher degree of molecular and compositional homogeneity. Fine control over the sequence and polydispersity of BCPs will open new avenues to mimic the structural complexity and hence precise and elegant function achieved in natural systems.

However, the synthesis of polymeric nanoreactors must be further simplified to also allow its commercial exploitation and application. Next generation nanoreactors should be prepared from cheap starting materials in a one pot synthesis that will enable for versatile

functionalization and will have robust structural characteristics. We see star polymeric nanoreactors as a very promising approach towards this direction.